INFRARED ABSORPTION ASSOCIATED WITH STRONG HYDROGEN BONDS

Thesis by

Norman Edward Albert

In Partial Fulfillment of the Requirements

For the Degree of

Doctor of Philosophy

California Institute of Technology

Pasadena, California

1961

Acknowledgments

I would like to express my deepest appreciation to Professor Richard M. Badger for his continued encouragement, guidance and criticisms throughout the course of this research as well as my tenure as a graduate student in the Division of Chemistry and Chemical Engineering at the California Institute of Technology. It is hoped the experience gained while working under his direction will have a lasting influence on the author.

I am deeply indebted to the California Institute of Technology, the E. I. duPont de Nemours Company, and the Dow Chemical Company for financial assistance which enabled me to undertake graduate work in the field of Chemistry.

Finally, I wish to express my appreciation to the number of graduate students in the Molecular Structure and Physical Chemistry groups for the invaluable discussions and pleasant companionship during my stay at the Institute.

"But where shall wisdom be found?, and where is the place of understanding?" Job 28: 12.

Abstract

The hydrogen bond systems in potassium hydrogen fluoride, acetamide hemihydrochloride, nickel dimethylglyoxime, potassium hydrogen bis-phenylacetate and maleic acid were studied via infrared spectroscopy between 5000 cm^{-1} and 400 cm^{-1}. Each compound was studied in detail by the potassium bromide pressed disc technique.

The infrared active fundamentals of the bifluoride ion were found to be shifted from the values reported for the pure, crystalline compound. Integral absorption intensities of the two infrared active fundamentals in the KBr solid solution were evaluated and interpreted in terms of the effective charge motion.

Spectra of acetamide hemihydrochloride, nickel dimethylglyoxime and potassium hydrogen bis-phenylacetate exhibited unusual features: an intense, extremely broad background absorption between 2000 cm^{-1} and 400 cm^{-1} and a deep "window" in the broad background. Maleic acid, however, was found to give a normal, well-behaved spectrum. These unusual features have been interpreted in terms of the symmetry of the hydrogen bond and the complexity of the hydrogen bonded molecules. The broad background is regarded as the superposition of several hydrogen bond vibrational modes, each of which is anharmonically coupled with low frequency intermolecular vibrational modes. The "windows" have been explained on the basis of a special perturbation between certain vibrational energy levels of the hydrogen bond modes and the molecular group modes in a small fraction of the molecules; in a majority of the molecules the perturbation is

either absent or is very weak. It is suggested that these features are characteristic of short. symmetric hydrogen bonds in complex molecules.

Table of Contents

Part I

A Review of Hydrogen Bonding

Introduction:

Although the hydrogen bond is not a particularly strong bond it has great significance in determining the properties of substances. Because of its small bond energy and the small activation energy involved in its formation and dissociation the hydrogen bond is expected to play an important part in reactions occuring at normal temperatures. For example, the hydrogen bond is believed to be responsible for the retention of the native configuration of protein molecules. Since it plays such an important role in a number of different phenomena much work has been carried out in recent years with the hope of the eventual elucidation of the nature of the hydrogen bond.

Over the years several excellent reviews have been published covering different aspects of hydrogen bonding.[1-5] The recent publication of the papers and discussions presented at the Symposium on Hydrogen Bonding at Ljubljana, Yugoslavia during the summer of 1957 are of interest though almost two years old.[6] This section will, therefore, be a condensation and consolidation of the more important aspects of hydrogen bonding scattered among the numerous publications as well as a brief review for those not entirely familiar with the field.

Structure and Strength of Hydrogen Bonds:

For well over thirty years it has been recognized that when a hydrogen atom is attached to a highly electronegative

atom it has an affinity for a second electronegative atom, so strongly at times that it may be considered as a bond between them.[7] Schematically such a bond may be represented as X-H---Y, where the hydrogen atom, H, is directly bonded to the electronegative atom X and weakly bonded to the second electronegative atom Y, which has either a lone-pair of electrons or, more rarely, a group with π electrons. In general the coordination number of the hydrogen in the hydrogen bond does not exceed two.[7]

Only the more electronegative atoms tend to form hydrogen bonds, and the strength of the bond increases with an increase in the electronegativity of the two bonded atoms. With reference to the various scales of electronegativity,[8] fluorine, oxygen, nitrogen and chlorine fulfill the requirement. Experimentally, fluorine forms very strong hydrogen bonds, oxygen weaker ones, nitrogen still weaker and chlorine, although it has the same electronegativity as nitrogen, only very weak hydrogen bonds. Though extremely weak, evidence of C-H hydrogen bonding has been found for polyhalogenated methane and ethane with donor solvents.[2, 9, 10, 11] By comparison, the energies of hydrogen bonds are much less than the energies of conventional bonds, see Table I-1. Therefore, one must not confuse this type of "bond" with the more conventional chemical bond.[4] More complete tables of hydrogen bond energies may be found[12, 13, 14] for those interested in a particular type of hydrogen bond.

A direct comparison of relative hydrogen bond strengths from the measured bond energies is not always possible because they are so markedly affected by the structure of the molecules and the environmental conditions. For example, the O-H---O bond energy for benzoic acid and salicylic acid in benzene solution is 4.4 kcal/ mole and 2.8 kcal/ mole, respectively. Moreover, the values differ for the same acids in different solvents; reported to be 2.8 and 3.85 kcal/ mole and 4.4 and 4.2 kcal/ mole for salicylic acid and benzoic acid in benzene and chloroform solutions, in that order.(14) It is apparent that the hydrogen bonds formed are not entirely the same. One must, therefore, consider the possible location and arrangement of the atoms in the hydrogen bond with respect to the molecule or molecules involved in its formation.

Table I - 1

Energy Values for Some Hydrogen Bonds and Single-Bonds

Hydrogen Bond Type	Energy(a) (kcal/mole)	Single-Bond	Energy(b) (kcal/mole)
N-H---O	2.3	----	----
C-H---O	2.6	C-H	87.3
O-H---N	4.7	----	----
N-H---N	6	N-H	83.7
O-H---O	6	O-H	110.2
F-H---F	7	H-4	147.2

(a) Values taken from paper by Coulson (Research 10, 150(1957).
(b) Values taken from Pauling, The Nature of the Chemical Bond, 2nd. Ed., Cornell University Press, Ithica, New York(1948), p. 53.

To a first approximation hydrogen bonds may be classified as either intramolecular or intermolecular, that is, whether the bonding takes place between atoms in the same molecule or between atoms of neighboring molecules. Succinic acid[15] and salicylic acid[16] are examples of these bonds, see Figures I - 1(a) and I - 1(b). The former is commonly referred to as association and the latter as chelation. Unfortunately, this simplified classification is not always possible as many compounds possess both types of hydrogen bonds in varying degrees at the same time. This is particularly true for crystalline substances of which salicylic acid is an excellent example, Figure I - 1(b), bonds labelled (1) and (2).

The general geometry of hydrogen bonding should be considered as a guiding principle in the classification of this type of bond. In most cases the hydrogen atom lies along, or very close to, the line joining the other two nuclei, so that the bond is straight. This is the case of many intermolecular hydrogen bonds as exhibited by succinic acid, Figure I - 1(a), and bond (2) in salicylic acid, Figure I - 1(b). There are, however, many examples where the hydrogen atom does not lie on the line joining the two nuclei but is considerably displaced from it. This is the bent hydrogen bond and may be examplified by the intramolecular hydrogen bond in salicylic acid, bond (1) in Figure I - 1(b), and the intermolecular hydrogen bond in α-resorcinol,[17] Figure I - 1(c). More rarely, the hydrogen atom is attracted about equally by two electronegative atoms on

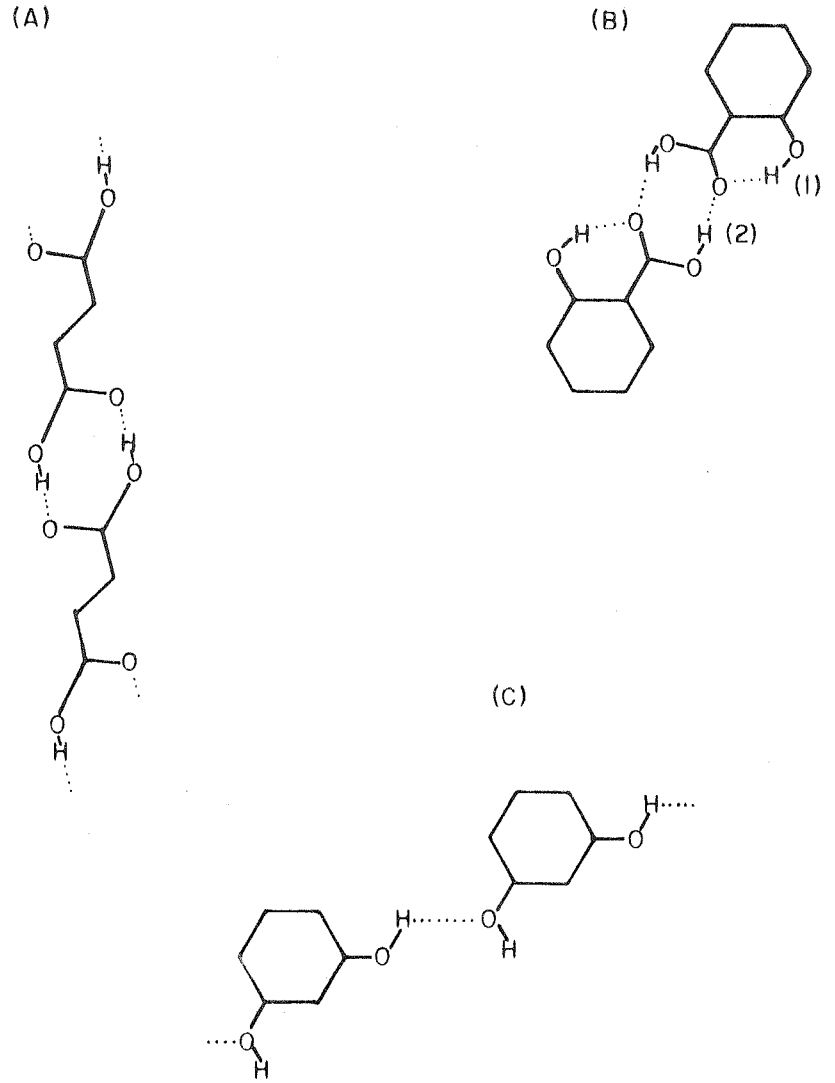

FIGURE I-1

Types of Hydrogen Bonds

(A) SUCCINIC ACID: linear or straight, unsymmetric, intermolecular type.

(B) SALICYCLIC ACID: bond (1) bent, unsymmetric, intramolecular; bond (2) almost linear, unsymmetric, intermolecular.

(C) α-RESORCINAL: bent, unsymmetric, intermolecular.

neighboring molecules forming a forked hydrogen bond. This is known as a bifurcated hydrogen bond. The crystals structure of glycine[18] indicates that one of the hydrogen atoms of the $-NH_3^+$ group is attracted almost equally by two oxygen atoms.

The geometric arrangement of the three atoms constituting a hydrogen bond was discussed in the preceeding paragraph, but the position of the hydrogen atom in the bond requires further consideration. In general one would expect only two possible positions for the hydrogen atom, either a symmetric or an unsymmetric location with respect to the two electronegative atoms. For many short hydrogen bonds, however, the pure symmetric case is not well defined. This in effect gives rise to a third case, a statistically symmetric bond.

In the unsymmetric hydrogen bond the hydrogen atom is strongly attached to one atom so that it is located at an appreciable distance from the center of the bond. This case is to be expected for all bonds where the bonding atoms are different, or, if the atoms are the same, where the charge distribution in the molecule changes the effective atomic electronegativity. Examples of unsymmetric hydrogen bonds are very common and are found in both intra- and intermolecular hydrogen bonds, see Figures I - 1(a), 1(b) and 1(c).

In the symmetric hydrogen bond the hydrogen (more correctly the proton) is located at the center of the bond. This case can only exist if the two electronegative atoms are the same and if the bond distance is very short, which is rarely found in molecules. The only instance where this is definitely known is the

bifluoride ion, $\left[F\text{-}H\text{-}F\right]^-$, [19] where the dominating electronic structure is the pure ionic form $F^- H^+ F^-$.

For very short hydrogen bonds where the two electronegative atoms are the same the proton may appear to be at the center of symmetry. If at small distances on both sides of the center of the bond there is a minimum in the potential energy of the system and if the minima are separated by a low energy barrier, then, at normal temperatures, there may be sufficient energy for the proton to oscillate between the two positions. Thus, the proton will appear to be at the center of symmetry of the bond. This type of hydrogen bond will have a center of symmetry, but the proton will not be there. We may classify this as a statistically symmetric hydrogen bond. In crystalline potassium hydrogen bisphenylacetate[20] the intermolecular hydrogen bond may be of this type.

Though there may appear to be a large number of possible types of hydrogen bonds, there are, fortunately, certain restrictions which limit the types to be found. The outline below is a summary of the types of hydrogen bonds,

Intramolecular hydrogen bonds:

linear or straight:	unsymmetric, bonding atoms may be different. symmetric, bonding atoms must be the same.
bent:	unsymmetric, bonding atoms may be different.

Intermolecular hydrogen bonds:

linear or straight:	unsymmetric, bonding atoms may be different. symmetric, (both cases), bonding atoms must be the same.

bent:	unsymmetric, bonding atoms may be different.
bifurcated:	unsymmetric, bonding atoms different, except for the two atoms at the extremes of the fork which are the same.

Methods of Investigation of Hydrogen Bonds:

Over the years a variety of methods have been employed in the investigation of the formation, strength and structure of hydrogen bonds. The methods used may, in an approximate way, be classified as physico-chemical, crystallographic, spectroscopic or theoretical. This section will briefly discuss each of these methods, though the last three are of considerably more interest in regard to the work undertaken in Part II. However, they are all closely linked together in the literature.

Physico-chemical Methods:

The chemical approach involves the study of the thermodynamic properties of liquids, solutions and vapors from which the energy of interaction and the type of association may be derived. The results, though less precise than the other methods, indicate that there is unusually strong interaction between molecules of solute or between molecules of solute and solvent. From the chemical nature of the molecules, molecular association is connected with the presence of hydrogen, usually as part of a hydroxyl, carboxyl or amino group in organic molecules.

Since the hydrogen bond is largely responsible for the interaction between molecules of associated liquids, a comparison of the properties displayed by substances capable of forming hydrogen

bonds with those of closely related compounds in which hydrogen bonding is unlikely or impossilbe affords a qualitative understanding of the bonding. However, it is essential that the distinction between properties of discrete molecules, such as the infrared spectrum, and the properties of the bulk substance, such as melting point, be made. The former will be modified when atoms in the molecule interact with atoms in adjacent molecules. The anomalies in the melting point, boiling point, heats of vaporization and dielectric constant in the isoelectronic sequences of the hydride molecules are familiar examples of the influence of hydrogen bonding on bulk properties.[21]

Quantitative studies give a better insight into the manner of and energy of association, and are, therefore, of more value. In solution association is commonly studied by cryoscopic,[22,23,24] solubility,[22,25,26] heats of mixing,[27,28,29] isopiestic,[30,31] and dielectric constant[32,33,34,35] measurements and by distribution measurements between water and immiscible organic substances.[22] In the vapor phase association is studied by vapor pressure,[36,37,38] vapor density,[39] and heat capacity[40] measurements. Solubility measurements are usefull in differentiating between chelation and association.[25,41,42]

A brief description of the cryoscopic, vapor pressure and vapor density methods is given by Ferguson.[43] A more complete review of earlier chemical aspects of hydrogen bonding has been given by Hunter.[2]

Crystallographic Methods:

X-ray crystallographic studies have revealed interesting and important knowledge with respect to the grouping and arrangement of molecules in crystals. With a complete structural analysis a three dimensional picture of the molecular arrangement in the crystal is obtained. From such an analysis intermolecular contacts may be determined with the same precision as the bond lengths within the molecule itself. In general, such precise information cannot be obtained by any other method for molecules in the solid state.

Organic structures have revealed the presence of two distinct types of interaction between molecules.(44) In the first of these, typical of the hydrocarbons, ordinary packing considerations prevail. The atoms of adjoining molecules are in contact with one another within certain minimum and fairly well-defined limits, the van der Waals distance. These distances are comparatively large and correspond to weak residual attractions between molecules.

Structures which contain strongly electronegative groups together with replaceable hydrogen atoms, such as amino, carboxyl or hydroxyl groups, exhibit an entirely different type of molecular interaction. The structures have a more compact type of molecular grouping, and the distance between the strongly electronegative atoms is appreciably smaller than the sum of the van der Waals radii of the atoms. Evidently an attractive force must be present to be able to overcome to some extent the repulsive force between the atoms. The number and distribution of these short distances can be accounted for by placing a hydrogen atom between

such pairs of atoms. Any interaction which leads to a decrease in the interatomic distance of two electronegative atoms is loosely described as a hydrogen bonded structure.

Because hydrogen bonds play an important role in determining the crystal structure of compounds containing strongly electronegative groups or atoms in addition to hydrogen, a brief examination of the geometry of structures in which this type of bond occurs will be worthwhile. A more complete discussion of this material may be found in Wells,[45] with numerous examples and illustrations.

The atoms between which the hydrogen bonds are formed may be single isolated atoms or they may be part of finite, infinite linear or infinite layer complexes. Long straight chains or layers of atoms have little choice in the way in which to pack in crystals. The former will have their axes parallel and the latter their planes parallel; hydrogen bond formation between atoms of adjacent chains or layers merely affect the packing. For finite complexes the geometric possibilities are far more complicated. When joined by hydrogen bonds the larger aggregates so formed may be (a) finite, (b) infinite chains, (c) infinite layers or (d) infinite three dimensional networks. The simplest cases in each class arise when the finite complexes are all identical. However, the original unit may be a group of atoms so that the number of possible structure types is greatly increased, as shown in Figure I - 2. Still more complex cases arise depending on the shape of the molecules and the position in the molecule of the atoms forming the hydrogen

bond. Several examples of each of the above four classes are given below, while the diagrams of individual structures may be found in Wells[45] and Pauling.[46]

Class (a), finite groups: bifluoride ion, carboxylic acids.

Class (b), infinite chains: bicarbonate ion, β-oxalic acid and diketopiperazine.

Class (c), infinite layers: α-oxalic acid, boric acid and petaerythritol.

Class (d), infinite three dimensional network: ice, resorcinol and dihydrogen phosphate ion.

The distance, type and position of the hydrogen bond in relation to the molecules in the crystal as determined by x-ray measurements has been reviewed by Donohue.[47] Though primarily concerned with the polypeptide structure, there are several important remarks directed at the O-H---O type of hydrogen bond. First of all, for hydrogen bonds of the O-H---O type with an O---O distance greater than 2.54 A, the bond is considered essentially unsymmetric. Secondly, by analogy with the bifluoride ion and the relationship of Pauling between atomic radius and bond type,[48] the probable distance for a symmetric O--H--O bond is about 2.30A. This distance is much shorter than the 2.45 A bond length postulated by Nakamoto, Margoshes and Rundle[49] and by Lippincott and Schroeder.[50]

Carpenter and Donohue[51] have attempted to classify O-H---O type of hydrogen bonds on the basis of the donor oxygen atom and the O---O distance from x-ray measure-

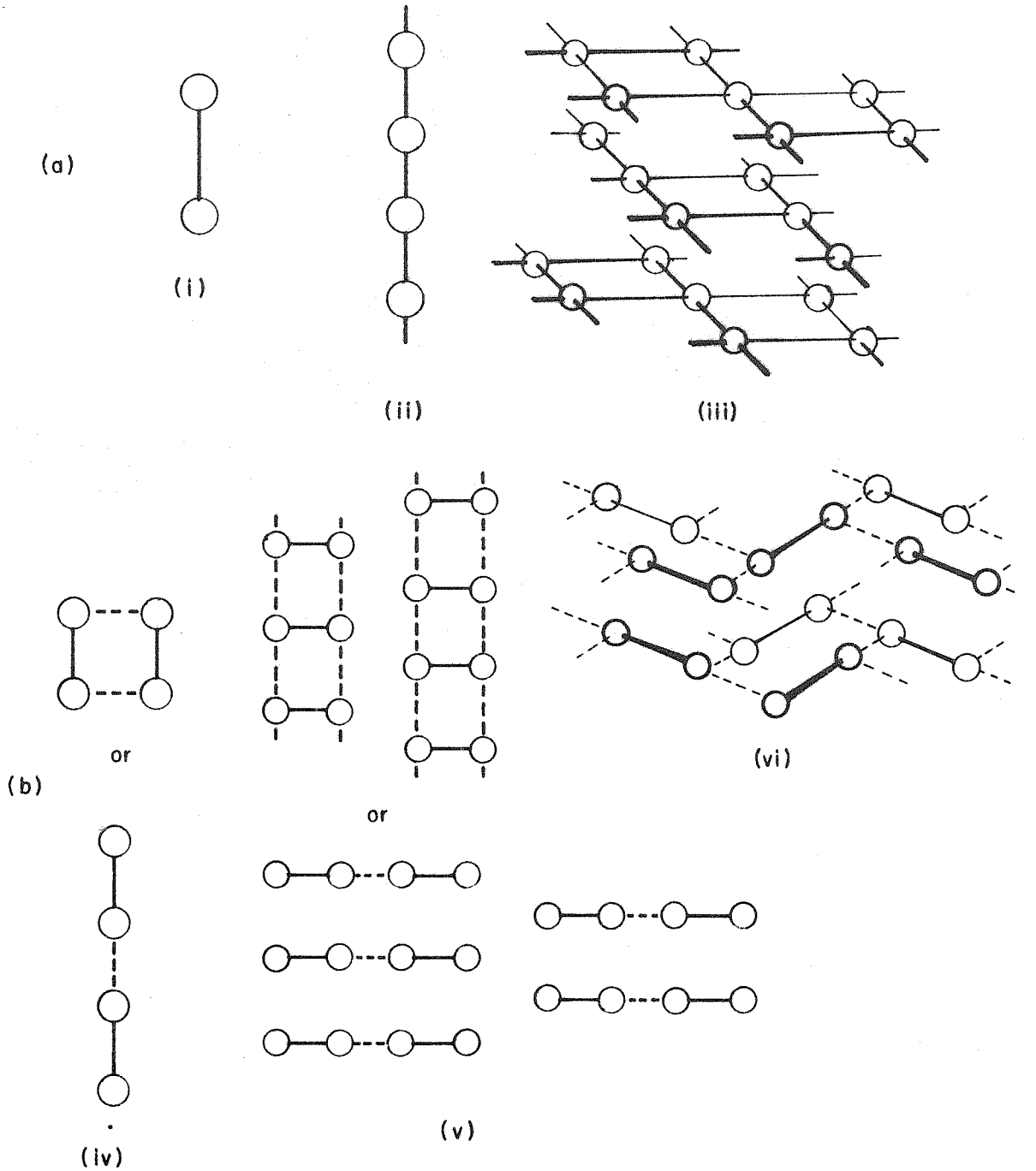

FIGURE I-2

In (a) are shown examples of (i) finite, (ii) infinite 1-dimensional and (iii) infinite 2-dimensional complexes. In (b) Hydrogen Bonds (broken lines) then link the finite complexes (i) into (iv) finite, (v) infinite 1-dimensional, or (vi) infinite 2-dimensional aggregates. (Reproduced from A. F. Wells, STRUCTURAL INORGANIC CHEMISTRY, Oxford, Clarendon Press (1949), Chapter VII, page 256).

ments. The three main types are: (1) those involving a carboxyl group with the acidic hydrogen atom essentially unionized, where the length varies from about 2.50 A in oxalic acid to about 2.65 A in carboxylic acid dimers; (2) those involving hydroxyl groups as alcohols and phenols, where the length varies from about 2.7 to 2.8 A and (3) those involving water molecules, as in ice crystals and certain hydrates, where the length varies from 2.76 to about 2.9 A. There are, of course, uncertainties in such a classification as the O---O distance and not the O-H---O distance has been determined from the x-ray data.

Unfortunately the hydrogen atom is difficult to locate precisely, because it possesses only a single scattering electron and accordingly exerts rather an insignificant effect on the x-ray scattering. Therefore, the existence and location of the hydrogen atom in hydrogen bonds can only be deduced from the observed interatomic distance between two strongly electronegative atoms. Recently, through precise intensity measurements and laborious data refinements, the location of hydrogen atoms from x-ray data has become possible.[16] With neutrons, however, the scattering is by the nuclei of the atoms and it happens that the scattering by a proton, the hydrogen nucleus, is not much below the average of all the elements. As a result it is possible by studying the diffraction of neutrons to produce projections of "neutron scattering density" in which the protons are quite accurately located in relation to the other atoms in the structure.[52] The paper by Bacon contains a

summary of the important hydrogen bonded structures examined by this method,[53] while several more recent neutron diffraction studies on hydrogen bonded crystals are given in the papers of Pepinsky[54] and of Darlow.[55]

From the numerous x-ray measurements on hydrogen bonded O---O distances and the O-H distances obtained from neutron diffraction studies, several correlations have been given for the variation of the O-H distance with the hydrogen bonded O---O distance.[49,50,56,57] Along with the experimentally determined distances, the various graphical correlations are shown in Figure I - 3. It is evident from the data that as the O---O distance decreases the O-H distance increases. Rundle et al[49] suggest that as the O---O distance becomes sufficiently short, the proton will move to the center of the bond just as in the bifluoride ion, with the critical O---O distance of about 2.45 A. Lippincott and Schroeder[50] base their curve on an expression derived from a one dimensional hydrogen bond model which can, however, only be solved by successive approximations. Welsh[56] has used Lippincott and Schroeder's expression though with a different parameter. Due to the uncertainties of the experimental results it is difficult to favor one curve over the other. It is more than probable that the two curves represent a range of possible values for all hydrogen bonded systems. Both curves have a discontinuity at $r_{O-H} = (1/2)\, R_{O---O}$, which is unfortunate. Feilchenfeld[57] has been able to derive a very simple relationship which is in fair agreement with the experimental values and does not have the discontinuity of

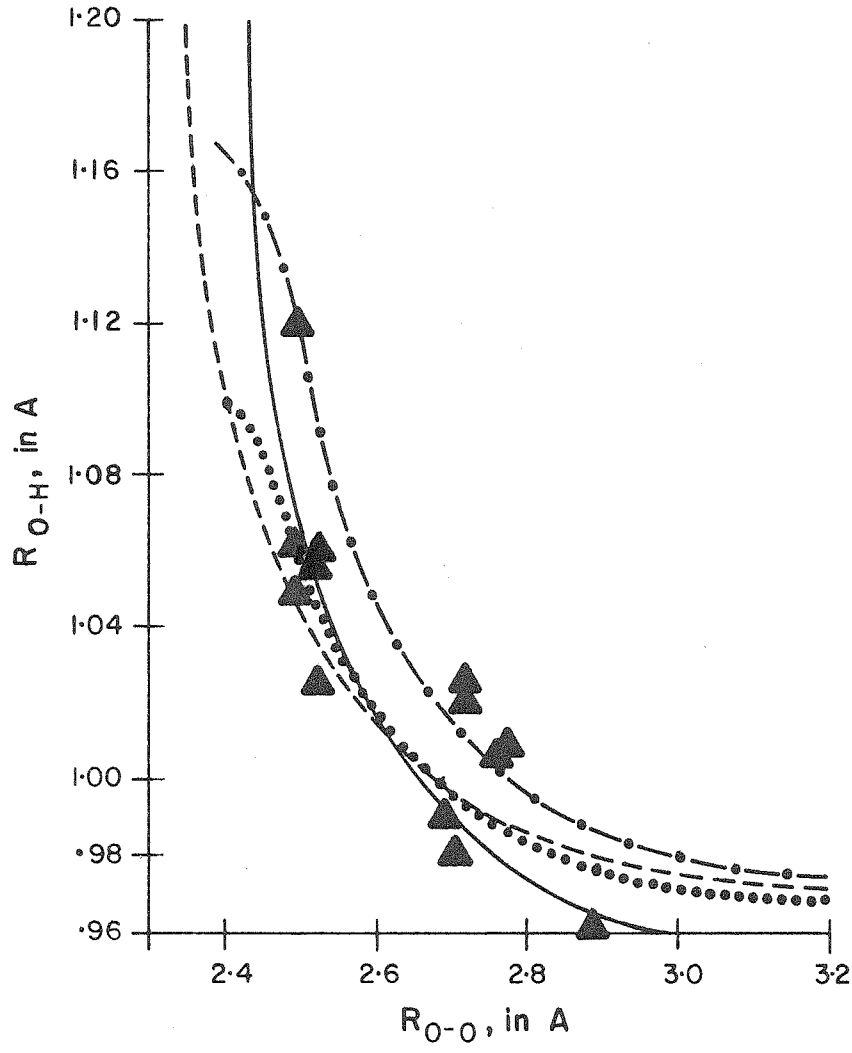

FIGURE I-3

Plot of O-H Bond Length Against O-O Distance for O-H-O Type Hydrogen Bonds

●●●●● , curve due to Welsh (J. Chem. Phys., 26, 710 (1957))

—●—● , curve due to Lippincott and Schroeder (J. Chem. Phys., 23, 1099 (1955))

— — — , curve due to Feilchenfeld (J. Phys. Chem., 62, 117 (1958))

——— , curve due to Nakamoto et al (J. Am. Chem. Soc., 77, 6480 (1955))

▲ , experimental data from Welsh (loc. cit.) and Nakamoto et al (loc. cit.)

Lippincott's and Welsh's curves. A more precise relationship will have to await further theoretical developments.

Spectroscopic Methods:

The spectra of hydrogen bonded molecules exhibit marked differences from the spectra of closely related non-hydrogen bonded molecules. It is, therefore, necessary to consider a general unsymmetric hydrogen bonded system, which may be represented diagramatically by

$$R\text{-}X\text{-}H\text{---}Y\text{-}R'$$

where H is the hydrogen atom concerned in the hydrogen bond formation, X and Y are atoms which are connected by the hydrogen bond (both X and Y are usually electronegative atoms; Y has either a lone-pair or is, more rarely, a group with π electrons) and R and R' represent the remainder of the molecules in which the X-H and Y groups occur.

In the infrared or Raman spectra, where molecular bond stretching and deformation vibrations are active, any variation in the force constant controlling the frequency of the X-H bond by the hydrogen bond force between H and Y will result in a frequency shift. Similarly, the frequency of the Y atom vibration will also be modified. Further, the existence of the hydrogen bond force field will give rise to discrete intermolecular vibrations at low frequencies.

Recently it has been recognized that the lone-pair nonbonding electrons on the Y atom plays an important role in hydrogen bond formation.[58] The electronic absorption

spectra associated with these non-bonding electrons is shifted as a result of hydrogen bonding.[59, 60]

The effects of hydrogen bonding on spectroscopic observations and the region in which they occur may be listed in the following way:[5]

	spectroscopic observation	spectral region
1).	shift in -X-H stretching frequency.	infrared - Raman
2).	broadening of -X-H absorption band.	infrared - Raman
3).	change in -X-H absorption intensity.	infrared - Raman
4).	shift in -X-H deformation frequency.	infrared - Raman
5).	change in intensity and breadth of -X-H deformation band.	infrared - Raman
6).	shift in proton acceptor (Y) bond frequency.	infrared - Raman
7).	change in intensity and breadth of Y-R' absorption band.	infrared - Raman
8).	fine structure of low frequency bands.	Raman
9).	changes in electronic absorption bands ($n \rightarrow \pi^*$)	ultraviolet

The remainder of this section will, therefore, be devoted to each of the spectral regions mentioned above together with their associated spectral observations. A brief paragraph at the end will be devoted to recent developments in nuclear magnetic resonance spectroscopy for studying hydrogen bonding.

Infrared and Raman Spectroscopy:

Perhaps the most used and most versatile of the spectrographic techniques have been in the infrared region. In this region bond stretching and deformation vibrations are active and are readily affected by hydrogen bond formation. The main types of vibrations together with the recommended notation are shown in Table I - 2.[61]

The -X-H Stretching Frequency:

This region of the infrared has been extremely popular for investigation of hydrogen bonded systems. Much of the early work has been covered in the reviews of Davies[1] and Kellner.[2] Studies of the overtone region of the O-H stretching vibration as well as the fundamental have been discussed by Mecke.[62]

Table I - 2

Classification of the Infrared Vibrations for Hydrogen Bonded Systems

Type of Vibration	Description	Notation
$R-\overrightarrow{X-H}---Y-R'$	-X-H stretching	ν XH
$R-X-H---Y-R'$ (↓ on H)	-X-H in-plane bending	δ XH
$R-\overset{\pm}{X-H}---Y-R'$	-X-H out-of-plane bending	γ XH
$(\overrightarrow{RXH})---(\overrightarrow{Y-R'})$	hydrogen bond stretching	ν(XH---Y)
$\downarrow(R-XH)\uparrow---\uparrow(Y-R')\downarrow$	hydrogen bond bending	δ(RXH---YR')
$\downarrow(R-XH)\uparrow---\downarrow(Y-R')\uparrow$	hydrogen bond bending	γ(RXH---YR')

The pioneering work of Wulf, Hendricks, Hilbert and Liddell on the use of near-infrared spectroscopy for the investigation of hydrogen bonding deserves a few lines; for a more complete discussion and list of references to this early work one should read Section 41 in Pauling, The Nature of the Chemical Bond, 2nd. Ed., (1948), pp. 316 327. Working in the first overtone region, near 7000 cm^{-1}, they found that O-H and N-H groups which are involved in strong hydrogen bond formation do not exhibit absorption bands. Instead of a sharp band, the spectrum of these substances show only a weak and diffuse absorption band. This method of investigation provided valuable information regarding the conditions which favor the formation of strong hydrogen bonds.

In the fundamental region, as the strength of the hydrogen bond increases the absorption bands due to the -X-H stretching vibration are (a) shifted to lower frequencies,[62,63,64] (b) broadened in contour,[62,63,64] and (c) changed in intensity.[62,64] Such changes occur in a continuous fashion starting from very slight effects in weakly hydrogen bonded systems.[62,65]

(a) -X-H frequency shift: Qualitative relations between the -X-H frequency shift and the energy of association and the bond length have been realized over the years.[62,63,64] Only recently have fairly precise correlations between -X-H frequency shift and X---Y distance been established.[49,50,56,66,67,68,69,70] Most of the correlations are empirical,[49,66,67,68]

though several are semi-empirical.[50,56,69,70] The semi-empirical treatment by Lippincott and Schroeder for linear[50] and bent[69] hydrogen bonds is by far the most complete. Several of these correlations are shown in Figure I - 4, with the experimental data taken from the papers of Lord and Merrifield[67] and Rundle et al.[49] Lord and Merrifield's curve is essentially a straight line for X---Y distance less than 2.8 A, which fits the experimental data rather well. Pimentel and Sederholm[68] found a linear relation for O-H---O, N-H---O and N-H---N type hydrogen bonds to be valid within the accuracy of the data. Lippincott and Schroeder derived a relationship for frequency shift as a function of the X---Y distance for a number hydrogen bond types.[50,69] Their plot for O-H---O type hydrogen bonds has a maximum frequency shift for an O---O distance of 2.45A. This is the distance considered by Rundle et al[49] to be representative of a symmetric hydrogen bond.

(b) broadening of the absorption band contour: Spectral bands which are associated with the stretching motion of a hydrogen bonded X-H group are very broad. The apparent band width varies considerably, from some tens of wave-numbers as in pyrrole[71] to several hundred wave-numbers in carboxylic acids.[72] In general the bands have a diffuse form, but occasionally, particularly in the vapor and solid state, a distinct but irregular structure is found.[72] Frisch and Vidale[73] calculated a band width of about 30 cm^{-1} on the

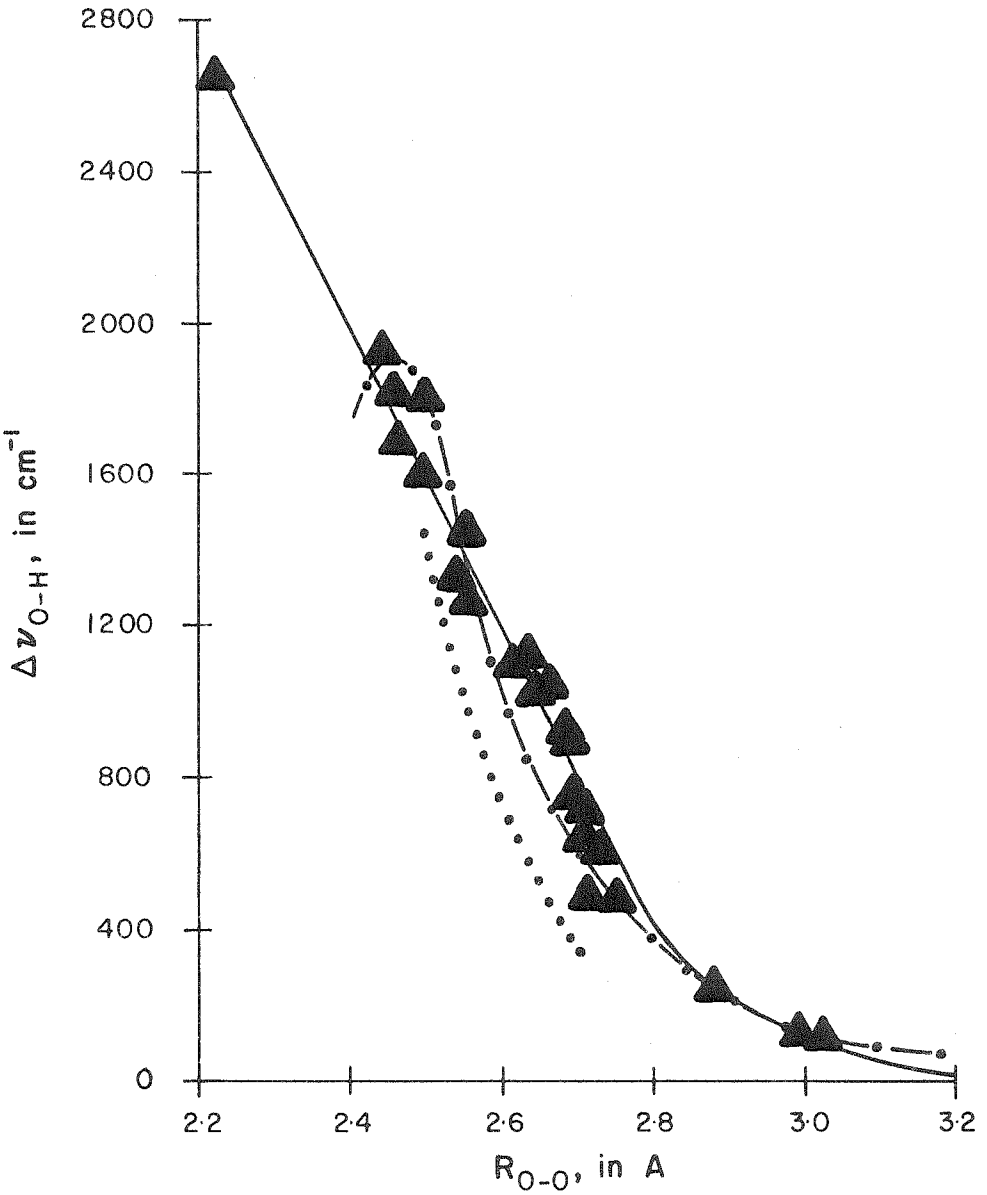

FIGURE I-4

O-H Frequency Shift as a Function of O-O Distance for O-H-O Type Hydrogen Bonds

•••••••, curve from data given by Welsh (J. Chem. Phys., 26, 710 (1957))

•—•—•, curve due to Lippincott and Schroeder (J. Chem. Phys., 23, 1099 (1955))

———, curve due to Lord and Merrifield (J. Chem. Phys., 21, 166 (1953))

▲, experimental data from Lord and Merrifield (loc. cit.) and Nakamoto et al (J. Am. Chem. Soc., 77, 6480 (1955))

assumption that the hydrogen bond force field is anharmonic. Lippincott and Schroeder,[50] however, calculated a band width of 300 - 400 cm^{-1} on the assumption that both the X-H and the (XH---Y) force fields are anharmonic. Several theories have been advanced over the years to account for the breadth and the structure of the bands and are discussed at some length in the papers of Cannon,[5] Sheppard[61] and Bratoz and Hadzi.[74] Sheppard[61] attributes two effects to the band width and band structure; (1) a strong anharmonic interaction between the vibrations approximately described as νXH and ν(XH---Y) and (2) an interaction, through anharmonicity, of the νXH vibration with other overtones and summation bands of similar frequency by Fermi resonance.

(c) change in intensity of the absorption band: Francis[75] studied free and bonded O-H group absorption of n-propyl alcohol in carbon tetrachloride solutions and found the intensity of the bonded hydroxyl band to be about 14 times that of the non-bonded band. Theoretical calculations by Coggeshall[76] on the O-H---O system with Morse functions for the O-H---O bonds, gave satisfactory values for frequency shift and band width, but only a small increase in the band intensity. The integrated intensity of the νOH band for hydrogen bonded alcohols was found by Barrow[77] to increase with the frequency shift and with the acidity of the alcohol and the basicity of the proton acceptor. Huggins and Pimentel[64] also showed a correlation between intensity and frequency shift for a given OH bond in different

acceptor solvents. Tsubomura[78, 79] has done extensive experimental and theoretical work on the intensity of O-H bands of alcohols and phenols. Rundle et al,[49] and recently Reid,[80] state that as the symmetrical configuration is approached, both the broadening and intensity increase are less, and the absorption due to the symmetrical hydrogen bond is sometimes difficult to detect. This is an interesting point as the hydrogen bond distances in solutions for alcohols are relatively long, in the region where an increase in intensity and band width are expected.

The -X-H Deformation Frequency:

In free molecules, the deformation modes, the in-plane and out-of-plane, degenerate into free rotation of the X-H group around the R-X bond. However, when restraints are imposed, such as in hydrogen bonding, the in-plane and out-of-plane deformation modes can be resolved.

In the case of the high frequency in-plane bending vibration the motion of the hydrogen atom is already considerably restricted by the force constant controlling the R-X-H angle. The effect of hydrogen bonding is to restrict further the amplitude of motion, although at the same time making possible the vibration interaction with the low frequency motion of the type δ(RXH---YR'). This latter type of interaction is believed to be the basis of some of the breadth of the δOH vibration of alcohols where hydrogen bonding is not strong.[81] Stuart and Sutherland[81] assigned the δOH band at 1330, 1410 cm^{-1} with a band width of 50 - 100 cm^{-1} for the hydrogen bonded molecules and at 1250 cm^{-1} for the free

molecule. For carboxylic acids the in-plane mode couples with the C-O stretching vibration to give two complex modes absorbing at or near 1300 and 1420 cm^{-1}.[82,83] Two conflicting interpretations have been advanced by various authors for these bands in the spectra of carboxylic acids.[84,85,86,87] Recent work by Hadzi and Pintar[88] on monomeric carboxcylic acids show that if a differentation into a δOH and a ν C-O band can be made at all, the higher frequency band is more liable to be called δOH, whereas the other is the C-O stretching vibration. The shifts of the δOH and νC-O bands arising from association vary considerably with the individual acids, though the average shifts are on the order of 50 to 150 cm^{-1}.

The out-of-plane bending vibration, because of its location has not been investigated as thoroughly as the stretching vibration. There is, nevertheless, sufficient evidence to show that these bands change in frequency, breadth and intensity. They vary in frequency from about 1000 cm^{-1} to 500 cm^{-1} with an increase in band width from about 10 cm^{-1} to several hundred wave-numbers for γ OH bands;[82,83,89] The γNH bands are also broadened.[90,91] Neglecting the different role of the hydrogen bond in the two cases, there is the same general correspondence of the spectroscopic behavior for both the γXH and νXH bands, namely, as the amplitude of the vibration increases the frequency of the absorption band is lowered and its breadth increased.

The Low Frequency Bands:

Very low-frequency vibrations of hydrogen bonded molecules

were first observed over twenty years ago by Gross and Vuks[92] and by Cross, Burnham and Leighton[93] in the Raman spectra of water and ice. Gross and co-workers have recently reinvestigated these low frequency Raman lines in ice, formic acid and crystals of gypsum and magnesium chloride containing water of crystallization.[94] The sharp, closely spaced bands in the region of 150 - 300 cm^{-1} in the spectra of substances containing a hydroxyl group is considered a direct indication of hydrogen bonding and are associated with the vibrations of the hydroxyl group as an entity against the oxygen atom bonded through the hydrogen bond. From the convergence of the lines in the Raman spectra of formic acid, Gross estimated the dissociation energy of the hydrogen bond in the crystalline state to be about 6.2 cal.[94] Reid[80] has found from calculations of the Lippincott-Schroeder type[50,69] that as the O---O distance decreases there is a rapid rise in the hydrogen bond stretching frequency. For example, for an O---O distance of 2.43 A the ν(OH---O) frequency is 850 cm^{-1}, which is in the practical region for infrared spectroscopy.

Ultraviolet Spectroscopy:

In comparison to infrared studies very little detailed work has been carried out in the ultraviolet region on hydrogen bonding. The importance of the lone-pair of electrons on the Y atom for hydrogen bond formation has been proved theoretically[58,95,96] and experimentally.[59,60] On association three electronic structures are possible for a triatomic hydrogen bond, such as

$$X\text{-}H \quad Y \longleftrightarrow X^{-}\text{-}H^{+} \quad Y \longleftrightarrow X^{-}\ H\text{—}Y^{+}$$

where the X-H bond belongs to the proton donor group and Y the proton acceptor atom for the hydrogen bond. Hydrogen bonding results in a blue shift in a class of transitions usually designated as $n \longrightarrow \pi^*$, and is now a method whereby such transitions may be distinguished from the more familiar $\pi \longrightarrow \pi^*$ transitions.

Association band shifts have been studied for α - and β- naphthol with different proton acceptors by Nagakura and Gouterman[97] and for phenolic substances by Burawoy.[98] A more complete account of the influence of hydrogen bond formation on electronic absorption spectra has been presented recently by Lippert.[99]

Nuclear Magnetic Resonance Spectroscopy:

The use of nuclear magnetic resonance for structural determination was first employed by Pake[100] in 1948 on a single crystal of gypsum. Since then a number of simple and complex inorganic structures have been investigated, mainly by the second moment method of Van Vleck.[101] Only in the past few years has this technique been applied to the study of hydrogen bonding in solution. The early work[102,103,104,105] established the general phenomenon of a shift of the proton resonance frequency of the H-X acceptor group with a change in concentration, which is due to the disturbance of the hydrogen bonding equilibrium. Pople has presented a brief discussion of the theory of this technique.[106] Saunders and Hyne[107] have made quantitative measurements on hydrogen bonded systems of hydroxylic groups in carbon tetrachloride. They found t-butanol and phenol to exist as a monomer-trimer system and methanol to exist as a monomer-tetramer system. Though indirect[107,108] this method is sensitive for the

detection of very weak interactions.

Like other techniques presently available, this method cannot solve all problems, but it is an extremely valuable supplementary technique in studying hydrogen bonding.

Theoretical Methods:

From the large amount of experimental data collected over a period of thirty years some of the facts of hydrogen bond formation are fairly well understood. However, what is not clear, nor met with complete agreement, is the interpretation which should be given. The present position of the theory of hydrogen bonding has been reviewed by Coulson[4,109] while Cannon has reviewed the theoretical developments on the interpretation of the spectroscopic observations.[5]

For a proper understanding of the details of hydrogen bond formation, four distinct, though related concepts, have to be considered.[4,109,110] They are

(1) electrostatic interactions

(2) delocalization effects

(3) exchange repulsive forces

(4) dispersion forces

As all of these interactions are essentially electrostatic the separation is in a sense artificial.[109] However, the distinctions implied should be clarified. By the word "electrostatic"

in (1) only such forces as would arise if, in some hypothetical case, the interacting species could be brought together without any deformation of either the charge cloud or by electron exchange. Needless to say this is impossible. Any large-scale, or permanent, distortion of the charge clouds gives rise to the delocalization term (2); the small-scale, or co-ordinate motion of the electrons in the two halves, gives rise to the dispersion force (4); the actual physical overlapping of the charge clouds leads to the essentially quantum effect(3), the repulsive overlap force.[109] Within certain limitations the details of each may be calculated, and some sort of estimate of the hydrogen bond energy made.

The only system for which a satisfactory estimate of the four effects on the hydrogen bond energy have been made is that of ice. The most appropriate values for this system are given in Table I - 3. The agreement is good, and fortunately, the accuracy in calculating most hydrogen bond energy values is considerably greater than for conventional bonds. Therefore, a major part of this section will be devoted to the theoretical contribution of the four effects to the energy of the hydrogen bond.

Table I - 3

Estimated Energy Contributions to Each Separate Hydrogen Bond in Ice [4]

Type of Interaction	Energy (kcal)
Electrostatic	+6
Delocalization	+8
Repulsive overlap	-8.4
Dispersion	+3
Total (theoretical)	+8.6
Experimental (Ref. 110)	+6.1

Electrostatic Interactions:

Since all known hydrogen bonds are between strongly electronegative elements coulombic type interactions were considered responsible for the energy of the hydrogen bond.[111, 112, 113, 114] For a model of the water molecule a formal charge of +q was alloted to each hydrogen atom and a corresponding negative charge of -2q to each oxygen. It was a simple matter to sum all the coulombic interactions between these charges on one water molecule and the corresponding charges on its neighboring molecules. Coggeshall[76] used a simple extension of this model with a Morse potential for the O-H bond, modified by the electrostatic field at the position of the proton due to the other atoms in the system. Reasonable values were calculated for the frequency shift and interaction energy from the energy levels.

The simple model of the water molecule was dealt a fatal blow from the detailed wave-mechanical calculations of Ellison and Shull[115] and the molecular orbital method of Lennard-Jones and Pople,[116, 117] Pople,[118] Duncan and Pople,[119] Burnelle and Coulson[120] and Hamilton.[121] In essence, the total dipole moment in a single water molecule arises partially from the separate O-H bonds and partially from the lone-pair electrons on each oxygen atom. Burnelle and Coulson[120] have estimated that as much as 1.69 Debyes out of the total moment of 1.84 Debyes arises in these lone-pair electrons. Thus, the greater part of the electrostatic interaction is due to the interaction

between a dipole in the O-H bond and a dipole directed from the neighboring oxygen atom in the direction of the lone-pair. Rowlinson[122] has represented each water molecule by an equivalent dipole and quadrupole, and then summed for all neighbors. Thus, the electrostatic interaction is just the sum of terms which may be called dipole-dipole, dipole-quadrupole, etc. A value of 18 kcal per molecule or 9 kcal per hydrogen bond is estimated. Pople[117] has, however, calculated a value of 6 kcal per hydrogen bond, which is considered more reasonable.

Although the true electrostatic energy is still unknown, its value is largely independent of detailed electronic models, about 6 kcal per hydrogen bond. Interestingly, this value appears to be sufficient to account for the whole energy of the hydrogen bond of ice estimated from the heat of sublimation of ice at 0^0K.[110]

Finally, a largely electrostatic hydrogen bond would favor a linear atomic arrangement. This does not, however, exclude a non-linear bond as the variation of electrostatic energy with the angle of non-linearity suggests an approximate cosine type law.[4,109]

Delocalization Effects:

The concept of delocalization can be simplified if the hydrogen bonded region were considered isolated from the rest of the molecule and were to involve only four electrons, of

which the $O_{(1)}$-H---$O_{(2)}$ system will be considered representative of hydrogen bonded systems in general. Two of the electrons are responsible for the $O_{(1)}$-H bond and the other two are one of the lone-pairs. These electrons may be distributed in various ways so that in the complete wave-function, terms corresponding to some or all of the following five valence bond structures may exist:

(i) $-O_{(1)}-H----O_{(2)}$ pure covalent, no charge transfer.

(ii) $-\bar{O}_{(1)}\ \overset{+}{H}---O_{(2)}$ pure ionic, no charge transfer.

(iii) $-\overset{+}{O}_{(1)}\ \bar{H}----O_{(2)}$ pure ionic, no charge transfer.

(iv) $-\bar{O}_{(1)}\ H——\overset{+}{O}_{(2)}$ charge transfer, long H---$O_{(2)}$ bond.

(v) $-O_{(1)}\ \bar{H}\ \overset{+}{O}_{(2)}$ charge transfer, $O_{(1)}$—— $O_{(2)}$ bonding.

Structures (i) - (iii) involve the same pairing possibilities as in an isolated -O-H bond and implies an almost complete electrostatic effect. Structures (iv) and (v) represent the delocalization effect. Unfortunately it is extremely difficult to obtain the correct weighting of these structures so the exact contribution of structures (iv) and (v) is uncertain.

Pauling[123] used an empirical relation between bond order and bond length to estimate the contribution of structures (i), (ii) and (iv). Coulson and Danielsson[124] extended these calculations and found that for a fixed O---O bond distance the location of the

proton in the bond determined the weighted contribution of the three structures, (i), (ii) and (iv). They also demonstrated that the weight of (iv) is sensitive to the nature of the orbitals used on the oxygen atom.

The only serious attempt to include all five structures has been done by Tsubomura.[110] An O-H bond length of 0.96 A and an O---O distance of 2.70 A were used in the calculations, which should be considered representative of a weak hydrogen bond. The estimated weights of structures (i) - (v) are

(i) 70% (ii) 8% (iii) 19% (iv) 1% (v) 1%

The extremely high weight of (iii) is unexpected and unreasonable on purely chemical grounds. Coupled with the orbitals used for the lone-pair of electrons on the oxygen atom the details of the calculations are doubtful.

Overlap-Repulsive Forces:

Both the electrostatic and the delocalization forces would tend to shorten the total length of the hydrogen bond. Therefore, when the atoms approach too close together, a repulsive force would be expected to make a significant contribution to the total energy of the hydrogen bond.

Sokolov[4,109] suggested a repulsive force of up to 60 kcal on the basis of the consistancy of the van der Waals radius of hydrogen. This is impossibly large! Verwey[113,114] estimated an energy of about 8.4 kcal from repulsive energy terms of the form (b/r^n) and $c \cdot \exp(-b/\rho)$.

An interesting point has been brought out by Coulson[4] concerning the non-existence of either lithium or sodium bonds. Although the electronegativities of these two elements is much less than that of hydrogen the analogous bonds have not been established. In hydrogen there are no inner shell electrons so the repulsion will be much smaller than in the case of the other atoms, where the K- and L-shell electrons will begin to repel the oxygen charge cloud at much larger separations. For a more complete discussion of the repulsive force contribution see the reviews of Coulson.[4,109]

Dispersion Forces:

Dispersion forces contribute quite significantly to intermolecular and interatomic potentials of a gas. On the basis of known van der Waals forces between isolated atoms Verwey[113] has estimated a 2.7 kcal contribution to the energy of the hydrogen bond. Recent work by Pitzer[125,126] indicates that these forces may be larger than previously thought. The nuclear magnetic resonance work of Cohen and Reid[102] provides some evidence that dispersion forces due to the high polarizability of the unshared pairs of electrons on both oxygens are important.

Other Theoretical Simplifications:

Any detailed analysis of the hydrogen bond immediately present unmanageable and complex mathematical manipulations. To by-pass this, many simplifications have been introduced, some of which will be briefly mentioned in this paragraph.

The first is the potential function method. Quantum mechanical calculations based on the superposition of Morse potential functions for both X-H and H---Y bonds have been used by Nordman and Lipscomb[127,128] to calculate the vibrational energy levels of the proton, by Kaku[5] to calculate O-H distances, force constants, and barrier height potentials of linear O-H---O bonds, and by Baker[129] in a perturbation calculation for the variation of the O-H frequency with O---O distance. The above treatments are of limited validity.

The most elegant and thorough treatment of hydrogen bonding by the potential function method to date is that of Lippincott and Schroeder for linear O-H---O type bonds.[50] The method has been extended to the general X-H---Y system[69] and the temperature dependence of hydrogen bonding.[130,131] Based on a quantum mechanical model[132] the potential function was found to be more accurate than the conventional Morse function for diatomic molecules.[133] Thus, it has been applied to the X-H and H---Y bonds for a specific hydrogen bond model. The potential function is mainly covalent in nature, though an electrostatic contribution is present as the potential has been used to correlate the properties of fairly polar bonds.[133] Their analysis has been fairly successful in correlating the frequency shift, bond energy and O-H distance as a function of the O---O distance. Also, a complete potential curve for the proton can be derived, from which the potential barrier to proton transfer can be determined and the potential curve for the intermolecular vibrations established. Reid[80] has extended the method by determining the potential surfaces

for both long and short hydrogen bonds. From the apparent success of this method it is possible that the forces making the important contribution to hydrogen bonding are the same as those applicable to ordinary covalent bonds, namely quantum mechanical in origin.

The molecular orbital approach is another method which has been used for a number of years. Recently, two new approaches have been given. Hofaker[134,135] has employed linear combinations of O-H bond orbitals and oxygen lone-pair orbitals, with certain equivalent orbitals deduced from the calculations of Ellison and Shull.[115] No calculations have been given, though it is a general formulation of hydrogen bond formation. Paoloni[136] has introduced excited orbitals of the hydrogen atom, the 2s and 2p, to account for the directional character of many hydrogen bonds. He has only considered a relatively long hydrogen bond, an O---O distance of 2.70 A, in detail, which has given a satisfactory account of the effects of the X-H stretching frequency in the infrared and the dipole moment of the bond. A more general treatment should be made on a short hydrogen bond, about 2.5 A, before a theoretical analysis can be considered complete.

Part II

The Infrared Absorption Spectrum of Several Short Hydrogen-Bonded Molecules

Introduction:

During the past eight years a number of correlations between frequency shift and bond distance have been proposed for hydrogen bonded molecules.[49,50,56,66,67,68,69,70,80] All of the correlations are based on the assignment and determination of the frequency shift of the infrared active X-H stretching vibration, and the determination of the interatomic distance of the hydrogen bonded atoms from X-ray crystallographic, electron diffraction or neutron diffraction studies. Only recently has a semi-theoretical justification been given.[50,69]

The proposed correlations are interesting in two aspects, particularly when applied to an analysis of the infrared spectra of hydrogen bonded molecules. Firstly, for the O-H---O system a maximum frequency shift for the O-H vibration is predicted for an O---O distance of 2.45 A,[50] which is the bond distance for a symmetric hydrogen bond.[49] Secondly, the intensity of the shifted band has been stated to decrease with an increase in frequency shift[49,80] so that for a symmetric hydrogen bond the band may be difficult to locate.[80]

In 1956, Takei[137] determined an O---O distance of 2.40 A from the X-ray crystallographic data of the compound acetamide hemi-hydrochloride. The bond also appeared to be symmetric. Previously, the shortest O---O distance to be found

was in the molecule nickel dimethylglyoxime. It was decided, therefore, that an investigation of the infrared spectrum of this compound should be undertaken to determine (1) from the proposed correlations a band which could be attributed to a shifted O-H band, and (2) the intensity of the band, if found.

At the same time a re-investigation of several selected short hydrogen-bonded molecules was undertaken with the same two objectives in mind. The compounds selected were: nickel dimethylglyoxime, with a very short hydrogen bond, 2.44 A, which is probably symmetric and for which the assigned shifted band is questionable; maleic acid, with a short hydrogen bond, 2.46 A, which is known to be unsymmetric; potassium hydrogen bisphenylacetate, with a hydrogen bond distance on the symmetric-unsymmetric borderline; and finally, potassium hydrogen fluoride, with the shortest known hydrogen bond which is symmetric and with a structure and spectrum which are well-known. Each of the above compounds was studied in a potassium bromide matrix as the hydrogen bonds are destroyed in polar solvents and the compounds are insoluble in non-polar solvents. The spectra and the interpretation thereof are discussed in the following sections, each molecule being treated separately.

Section A: Potassium Hydrogen Fluoride:

At present the shortest known hydrogen bond is exhibited by the bifluoride ion in the compound potassium hydrogen fluoride. The F-H-F hydrogen bond system differs from the more common O-H---O hydrogen bond in two respects: the terminal atoms are different and the bifluoride ion possesses a negative charge. Fortunately the simplicity of the system and wealth of information on its structure,[138,139,140,141] infrared spectrum,[142,143,144,145,146] Raman spectrum,[147,148] hydrogen bond energy,[142,149,150] and bonding character[151,152,153] make it an ideal system for studying hydrogen bonding.

For the reasons given, potassium hydrogen fluoride was selected to investigate the effect of frequency shift on the intensity of the absorption bands and the influence of a potassium bromide matrix on the infrared spectrum of hydrogen bonded molecules. The results would then provide a basis for the interpretation of the infrared spectra of the more complex O-H---O type of hydrogen bond. Also, the feasibility of band intensity measurement in a potassium bromide matrix would be examined. The experimental work was set up with these objectives in mind.

Before commencing with the present work the next two sections will be devoted to a brief review of the structural and spectral aspects of the compound.

Crystal Structure:

Crystalline potassium hydrogen fluoride belongs to space group D_{4h}^{18} - I 4/mcm, with four molecules per unit cell. The dimensions of the tetragonal unit cell are 5.67, 5.67 and 6.81 A, the four potassium atoms located at unit cell positions (0, 0, 1/4), (0, 0, 3/4), (1/2, 1/2, 1/4) and (1/2, 1/2, 3/4). The fluoride atoms are in a dumb-bell shape arrangement with two atoms of each dumb-bell in a plane perpendicular to the tetragonal axis (see Figure II A - 1), like the cesium chloride and ammonium chloride structure. The hydrogen atoms are located in the middle of the dumb-bell,[140,141] forming the bifluoride ion, at unit cell positions (0, 1/2, 0), (1/2, 0, 0), (1/2, 0, 1/2) and (0, 1/2, 1/2). The interatomic distances are determined to be K-F = 2.77 A, K-K = 3.41 and 4.01 A and F-F = 2.26A.

Infrared and Raman Spectra:

Analysis of the infrared spectroscopic data of Rodebush et al[154] by Glockler and Evans[149] led to the adoption of the asymmetric $C_{\infty v}$ model for the bifluoride ion with equivalent potential minima for the proton separated by 0.52 A. Ketelaar[142] calculated a separation of 0.70 A for the same model, though he used different frequencies for the fundamental vibrations. For the $C_{\infty v}$ model Halverson[155] considered the doublet near 3700 cm^{-1} to be the hydrogen frequency, ν_3, of the triatomic $[F\text{-}H\text{-}F]^-$ ion, and the two bands at 1250 and 1430 cm^{-1} found by Ketelaar[142, 143,] to be splitting of the degenerate deformation mode, ν_2.

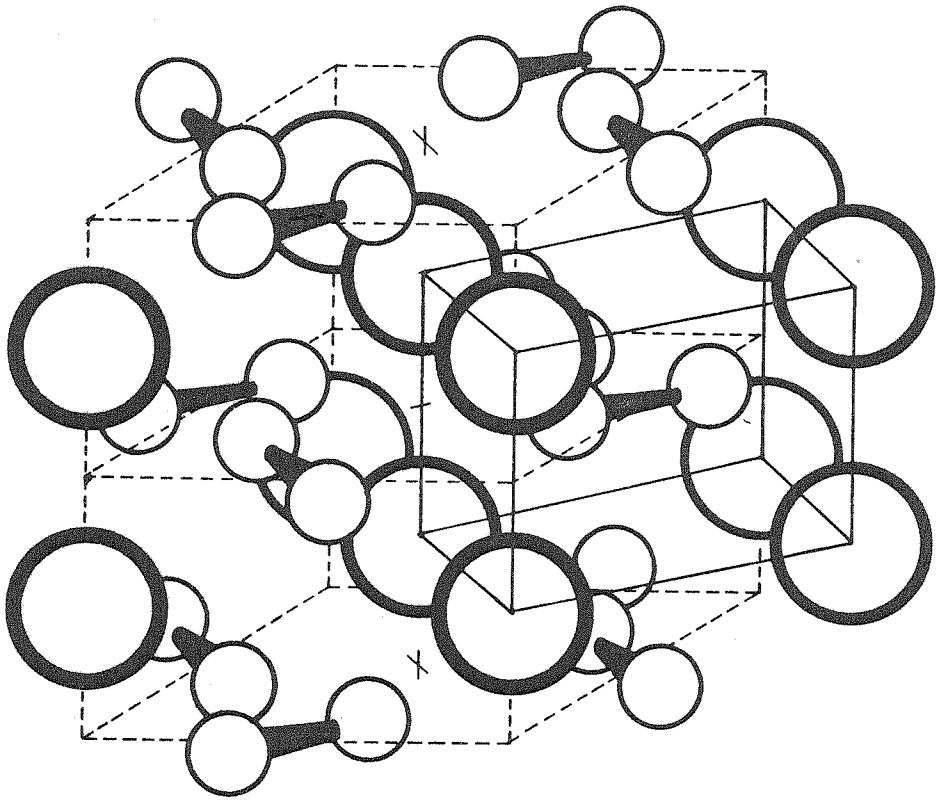

Fluorine

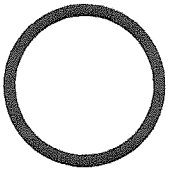

Potassium

FIGURE IIA-1

Crystal Structure of Potassium Hydrogen Fluoride

Dielectric constant measurements by Polder[156] and detailed thermodynamic studies by Westrum and Pitzer[157,158] ascribed symmetry $D_{\infty h}$ to the bifluoride ion. A re-examination of the polarized infrared reflectance spectrum by Ketelaar and Vedder,[144] and the polarized infrared transmission spectrum by Newman and Badger[145] and by Coté and Thompson[146] supported the new model. The bands at 1450 cm^{-1} and 1250 cm^{-1} were assigned the fundamentals ν_3 and ν_2, respectively. Single crystal Raman spectra by Couture and Mathieu[147,148] gave further proof of the symmetric model as only one Raman line was found, at about 600 cm^{-1}, which could be assigned a fundamental; the Raman active symmetric stretching mode, ν_1.

The effect of an alkali halide matrix on the infrared spectrum of the bifluoride ion has been reported by Ketelaar and coworkers.[159,160] When compared with the spectra of the pure crystalline compound, the alkali halide matrix spectra have bands which are much narrower and shifted in frequency. The narrowing is due to the absence of coupling between identical ions, whereas the frequency shift is possibly due to the polarization of the environment by the bifluoride ion.[160]

Experimental Details:

Briefly, the use of potassium hydrogen fluoride was three fold in purpose. First, to devise a method for the preparation of potassium bromide pellets which would give reproducible spectra, both in band position and in band intensity. Second, to

determine the integral band intensity of the infrared active fundamentals in the potassium bromide matrix. Third, to compare the intensity of the absorption bands in the matrix with the intensity of the same bands in the spectrum of the pure crystalline compound.

Commercial samples of KHF_2 (potassium acid fluoride, Merck and Co., Inc. (pure)) were used after recrystallization from aqueous solution in polyethylene and paraffin containers. Samples were first dried for two hours at 120°C, then dried over phosphorous pentoxide at 146°C under reduced pressure (about 1mm of Hg) for 24 hours. All samples were stored in a desiccator over anhydrous magnesium perchlorate until used. Weighed portions of each sample were titrated with standard NaOH to a phenolphthalein end-point, and all titers agreed with the predicted acid content within 1%.

Potassium bromide (potassium bromide, IR grade (250 - 300 mesh), Harshaw Chemical Co.) was used for all pressed pellets without further purification. Five gram portions, however, were dried at 200°C under reduced pressure for 24 hours, then stored in a desiccator over fresh phosphorous pentoxide until used.

Preparation of Potassium Bromide Pressed Discs:

Since the potassium bromide pressed disc technique may affect the infrared spectra of a compound,[161,162] the tech-

niques used will be described in some detail as they were found to give reproducible spectra.

A stock mixture of potassium bromide and potassium bifluoride was prepared from known quantities of the previously dried compounds; the mixture was usually 10% by weight of potassium bifluoride. The substances were ground together in an agate mortar for thirty minutes under an infrared lamp, after which the mixture was further dried for 12 hours over phosphorous pentoxide at 146° C under reduced pressure. The dried mixture was stored over anhydrous magnesium perchlorate until used.

Pellets containing accurately known quantities of potassium bifluoride were prepared from weighed amounts of the mixture to which was added dried potassium bromide to make the total weight about one gram. All weighings were done on a Sartorius "Selecta" semi-micro single-pan balance capable of weighing to within ± 0.05 mgs. The mixture was ground for ten minutes in an agate mortar under an infrared lamp, then dried for 24 hours over phosphorous pentoxide at 146° C under reduced pressure. After drying, the powder was quickly transferred to the pellet die (3/4 in. diameter), evacuated for five minutes with the aid of a mechanical fore-pump, then pressed for 25 minutes under a pressure of 40,000 pounds (about 90,000 lbs per sq. in.). The pellets were mounted in the pellet holders and stored in large weighing bottles over freshly heated silica gel until the spectrum was to be recorded. Potassium bromide blanks were prepared under similar conditions to be used as reference blanks when recording the infrared spectrum of the

potassium bifluoride in the potassium bromide matrix. In Table II A - 1 the data is given for several discs used in this section.

Instrumental Conditions for Recording Spectra:

Spectra were obtained on a Perkin-Elmer Model 21 double-beam recording spectrophotometer equipped with sodium chloride optics. Instrumental conditions used for recording spectra: Slit Program: 955; Response: 1; Gain: 6; Recording Speed: 4 1/2 (0.6 μ/min.); Suppression: 4. Chart settings were such that the spectra were recorded on a linear wavelength basis of two inches per micron and a linear transmittance basis of one inch per 10% transmittance.

Table II A - 1

Data for KHF_2 -KBr Pressed Discs

disc	Stock Mixture* (mgs)	Total Weight (gms)	Disc Weight (gm)	Weight of KHF_2 in Disc (mgs)	Disc Thickness (cm)
h	1.07	1.0014	0.96188	0.135	0.126
g	2.20	0.9944	0.95066	0.276	0.124
i	4.41	1.0102	0.99406	0.569	0.132
j	7.31	1.0233	1.00664	0.942	0.130
l	12.61	1.0412	1.01124	1.605	0.135
blank	----	0.9681	0.96603	----	0.125

* Stock mixture contained 0.1310 mgs of KHF_2 per mg of mixture.

Spectra slit widths were calculated from the equation of Williams[163] assuming the instrumental conditions were such

that $F(s) = 1$ and $\Phi = 0$. For the NaCl prism in the Model 21 the apex angle, α, is 60°, the base of the prism, b, 60 cm and the focal length of the instrument 27 cm. The equation for the spectral slit width, S, in wave-numbers, reduces to

Table II A - 2

Computed Spectral Slit Widths for KHF_2 in KBr Matrix

(for NaCl Optics in Perkin-Elmer Model 21)

ν (cm^{-1})	n_ν	$dn/d\lambda$	s(cm)*	$S(cm^{-1})$
1525	1.51280	$-30.5\ cm^{-1}$	0.0070	13.3
1254	1.50687	$-50.0\ cm^{-1}$	0.0090	7.10

* slit program: 955

$$S(cm^{-1}) = (s\nu^2(4 - n^2)^{1/2})/(108(dn/d\lambda)) + \nu/(120(dn/d\lambda))$$

where s is the slit width in cm, ν the frequency at which the spectral slit width is being calculated in wave-numbers, n_ν the refractive index of sodium chloride at that particular frequency and $dn/d\lambda$ the dispersion of sodium chloride at that particular frequency. Using the refractive index data of Martens for sodium chloride in the infrared region from 1 to 20 μ [164] the computed spectral slit widths at the observed band positions of KHF_2 in KBr matrix are summarized in Table II A - 2.

Methods Used in Integrating Band Intensities:

As all spectra were recorded linear in wave length and transmittance it was necessary to plot the spectra on a scale linear in wave-number and absorbance. The scale used was one inch per 100 cm^{-1} and one inch per 0.1 absorbance unit, defined as $\log(T_o/T)$.

Integrated band intensities were determined by two methods, (a) the peak height - Lorentz band contour method and (b) by weighing cut-out tracings of the band contours, hereafter referred to as "paper integration." The true integrated absorption intensity, A, is defined as

$$A = \int \alpha_\nu \cdot d\nu \qquad \ldots\ldots\ldots(1)$$

where $d\nu$ is in sec^{-1} and α_ν is defined by the absorption law equation

$$I_\nu = I_{0\nu} \cdot \exp(-\alpha_\nu nL) \qquad \ldots\ldots\ldots(2)$$

In (2) n is the concentration in units of molecules per cm^3 and L is the path length of the absorbing medium in cm and α_ν is the molecular absorption coefficient with units of cm^2 molecule $^{-1}$. Substituting equation (2) into (1), the true integrated absorption intensity may be expressed as

$$A = (1/nL) \int \ln(I_0/I)_\nu \, d\nu \qquad \ldots\ldots\ldots(3)$$

If the band contour is assumed to be described by a Lorentz function, that is

$$\ln(I_0/I)_\nu = a/((\nu - \nu_{max})^2 + b^2) \qquad \ldots\ldots\ldots(4)$$

where $(a/b^2) = \ln(I_o/I)_{\nu(max)}$ and $2b = \Delta\nu_{1/2}^{(t)}$, with $\Delta\nu_{1/2}^{(t)}$ being the true band half-width in cm^{-1}, then direct integration (case a) will give the integrated absorption intensity as

$$A = (\pi/2nL) \cdot \ln(I_o/I)_{\nu(max)} \cdot \Delta\nu_{1/2}^{(t)} \qquad \ldots\ldots\ldots(5)$$

However, due to the finite resolution of the instrument, this equation cannot be used directly. Ramsey[165] has shown that for a Lorentz type band the integrated absorption intensity can be evaluated from the experimental curves by the equation

$$A = (K/nL) \cdot \ln(T_o/T)_{\nu\,(max)} \cdot \Delta\nu^{a}_{1/2} \qquad \ldots\ldots\ldots(6)$$

where $\ln(T_o/T)_{\nu(max)}$ is the observed maximum absorbance and $\Delta\nu^{a}_{1/2}$ the apparent band width at half maximum absorbance. The constant K relates the experimental and theoretical band contours, and is determined from the spectral slit-width and the half-width of the band.

By the method of "paper integration" the integral, $\int \log(T_o/T)_\nu \, d\nu$, is evaluated by weighing tracings of the band contours; the integrated absorption intensity then determined by the method of Wilson and Wells.[166] The band contours were traced on paper of fairly uniform texture (Dietzgen Type 197 M Tracing Vellum) on the assumption that the bands were symmetric. The base line (background) was estimated from the absorption on either side of the bands and assumed to be linear under the bands. Band overlap was corrected for by subtraction of the ν_2 band absorption from that of ν_3 band, as the ν_2 band is very sharp, less intense and fairly symmetric. At least five tracings of each absorption band were cut out and weighed. The band area was then computed from the weight of known areas cut from the same sheet of vellum. Calibration areas ranged in size from 1/4 sq. in. to 8 sq. in., so that any variation in the vellum for large and small

band contours would be corrected. A least squares calculation on the calibration data gave the proportionality constant between the mass of the vellum and the area as 39.56 mgs per square inch.

Table II - 3

Calibration Data for Dieztgen Type 197 M Tracing Vellum

Dimensions of Rectangle (in.)	Area (sq.in.)	Number of Rectangles	Average Wgt. of Rectangle (mgs)	Average Wgt. of Paper (mgs/sq.in.)
1/2 x 1/2	0.250	11	9.685	38.74
1/2 x 1	0.500	9	19.47	38.94
1 x 1	1.000	10	39.09	39.09
2 x 1	2.00	10	79.64	39.82
2 x 2	4.00	8	156.62	39.15
2 x 4	8.00	7	317.69	39.81

Results and Discussion:

Spectra of potassium hydrogen fluoride in potassium bromide matrix in varying concentrations are shown in Figure II A - 2 from 4 to 10 microns. For intensity measurements, the curves were plotted on linear wave-number - linear absorbancy scale, as shown in Figure II A - 3, from 2500 cm^{-1} to 1000 cm^{-1}. The frequency of the fundamentals, ν_2 and ν_3, in a potassium bromide matrix were determined to be 1254 cm^{-1} and 1524 cm^{-1}, respectively, from the values of atmospheric water-vapor and thin film polystyrene bands which were recorded on the same chart. The bands, therefore, are believed to be accurate to

within $\pm$ 3 cm^{-1}. These values are in good agreement with those reported by Ketelaar *et al*.[159]

The main obstacle in band intensity measurements, particularly for alkali halide pressed discs, is the determination, or estimation, of background absorption. In Figure II A - 3, the absorbancy of the entire spectrum from 2500 to 1000 cm^{-1} increases as the concentration of potassium bifluoride in the pellet is increased. The effect may be the result of a loss of radiation due to scattering, reflection, absorption, or a combination of these factors. The background absorption, in any case, was measured at 1000 cm^{-1}, 1870 cm^{-1} and 2500 cm^{-1}, see Table II A - 4. A Beer's law plot of the background absorption (or scattering) exhibits departure from a straight line relation at high amounts of potassium bifluoride (see Figure II A - 4), which is an indication of scattering. However, the background values were used to draw the base line under the absorption bands, on the assumption that it was linear over the region of interest.

From the assumed base line, the peak height, defined as $\log(T_o/T)_{\nu\,(max)}$, and band width at half-maximum absorbance were determined for the fundamentals (Table II A - 5). A Beer's law plot for the maximum absorbance of the fundamentals corrected for background absorption (or scattering) exhibit pronounced deviation from a straight line relation for concentrations of potassium bifluoride slightly greater that 0.57 mg per gm pellet, or 15.4 x 10^{17} molecules of KHF_2 per cm^2

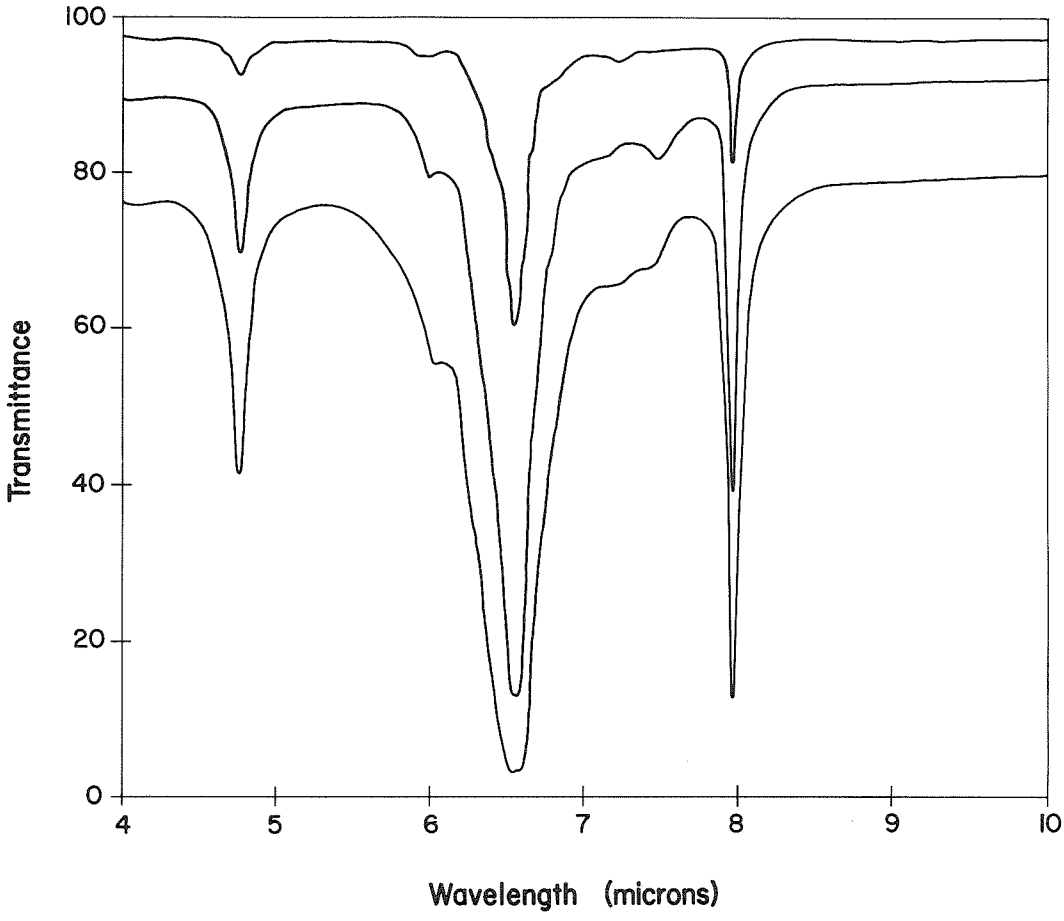

FIGURE II A-2

Infrared Absorption Spectrum of Potassium Hydrogen Fluoride at Several Concentrations in a Potassium Bromide Matrix Between 4 microns and 10 microns

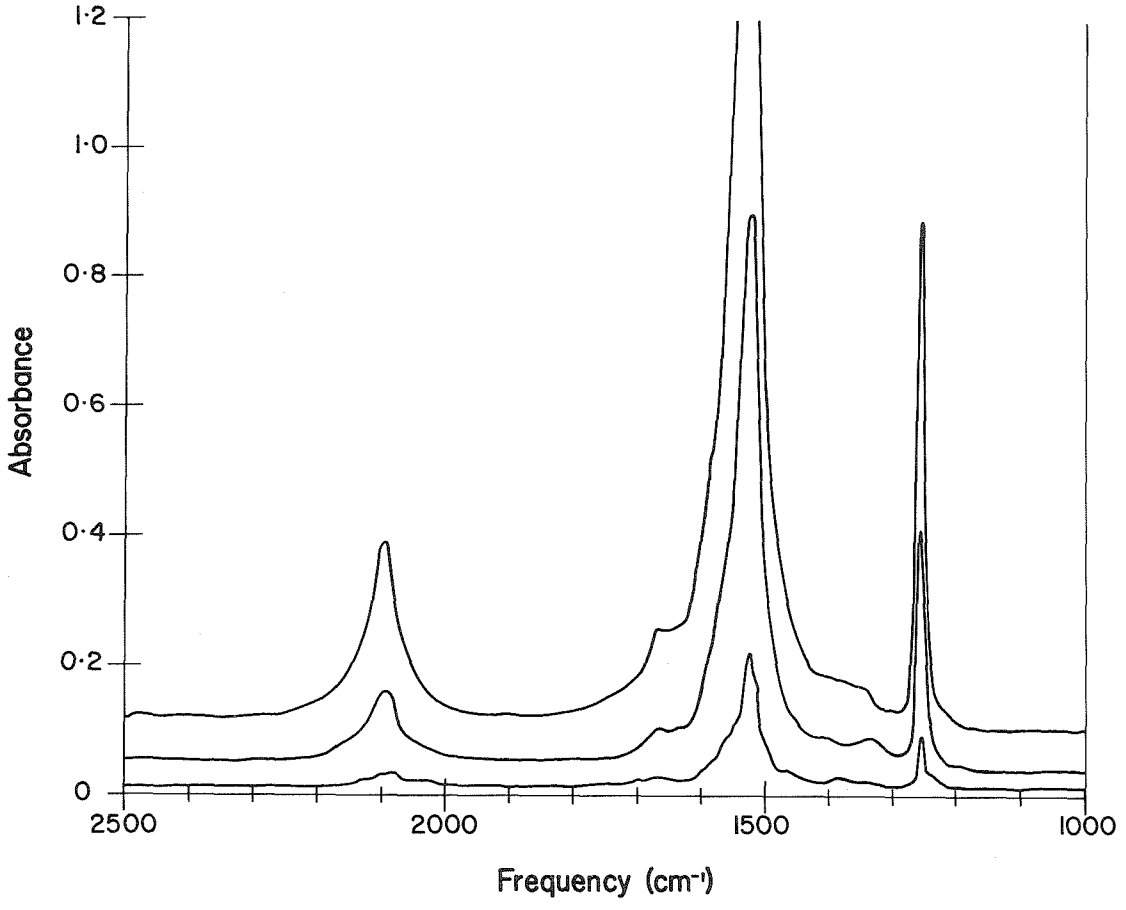

FIGURE II A - 3

Infrared Absorption Spectrum of Potassium Hydrogen Fluoride

at Several Concentrations in a Potassium Bromide Matrix

Between 2500 cm^{-1} and 1000 cm^{-1}

Table II A - 4

Estimated Background Absorption

for KHF_2 -KBr Pressed Discs

Disc	wgt KHF_2 (mgs)	nL (mole. cm^{-1})	Background Absorbancy at 1000cm^{-1}	1870cm^{-1}	2500cm^{-1}
h	0.135	3.65×10^{17}	0.012	0.012	0.012
g	0.276	7.46	0.022	0.037	0.035
i	0.569	15.4	0.038	0.053	0.048
j	0.942	25.5	0.076	0.082	0.082
l	1.605	43.4	0.090	0.122	0.115

Table II A - 5

Data from Spectra of Potassium Hydrogen

Fluoride in a Potassium Bromide Matrix

Disc	wgt KHF_2 (mgs)	ν_2 band ν(max) (cm^{-1})	ν_2 band $\Delta\nu^a_{1/2}$ (cm^{-1})	A [a]	ν_3 band ν(max) (cm^{-1})	ν_3 band $\Delta\nu^a_{1/2}$ (cm^{-1})	A [a]
h	0.135	1253	10.0	0.080	1524	32.0	0.209
g	0.276	1253	14.0	0.166	1524	40.0	0.420
i	0.569	1256	14.0	0.374	1524	45.0	0.855
j	0.942	1255	15.0	0.545	1523	46.0	1.157
l	1.605	1254	13.4	0.789	1524	--	--
Single crystal [b]		1230	30	--	1450	200	--

(a) A is defined as $\log(T_o/T)_{\nu(max)}$

(b) See Ref. (145)

(Figure II A - 4). The shape of the curves is indicative of large particle size[167] which will produce an appreciable amount of scattering. However, it has been assumed that the peaks on the background are due to absorption, and can be treated independently of the background, which is a combination of scattering and absorption. Such a treatment is not proper, but it is difficult to estimate the intensity of the bands otherwise.

The band half-width of the fundamentals are much narrower in the matrix than for a single crystal; for the ν_2 it is about 14 cm^{-1} compared to 30 cm^{-1}, while for ν_3 it is only about 45 cm^{-1} in comparison to almost 200 cm^{-1}.

Although no structure was evident for the ν_3 band even at - 185° C for a single crystal of KHF_2, a narrowing of the band indicated that the breadth is at least in part due to interaction with lattice vibrations.[145] A series of rather weak, ill-defined bands about the wings of the ν_3 band in the potassium bromide matrix is taken as evidence for such interactions. Before any assignments are made it will be instructive to visualize the nature of the local "lattice" vibrations which might couple with internal modes of the bifluoride ion.

In the Raman spectrum of oriented crystals of potassium bifluoride, Couture and Mathieu[147,148] assigned the lines at 90, 100 and 136 cm^{-1} as possible lattice vibrations. Polarization ratios assigned the 136 cm^{-1} line to species a_{1g}, e_g or b_{2g}, the 100 cm^{-1} line to species e_g while the 90 cm^{-1} line was only confirmed.[148] From the crystal structure of potassium bifluoride the "lattice" modes can be classified as to the ions

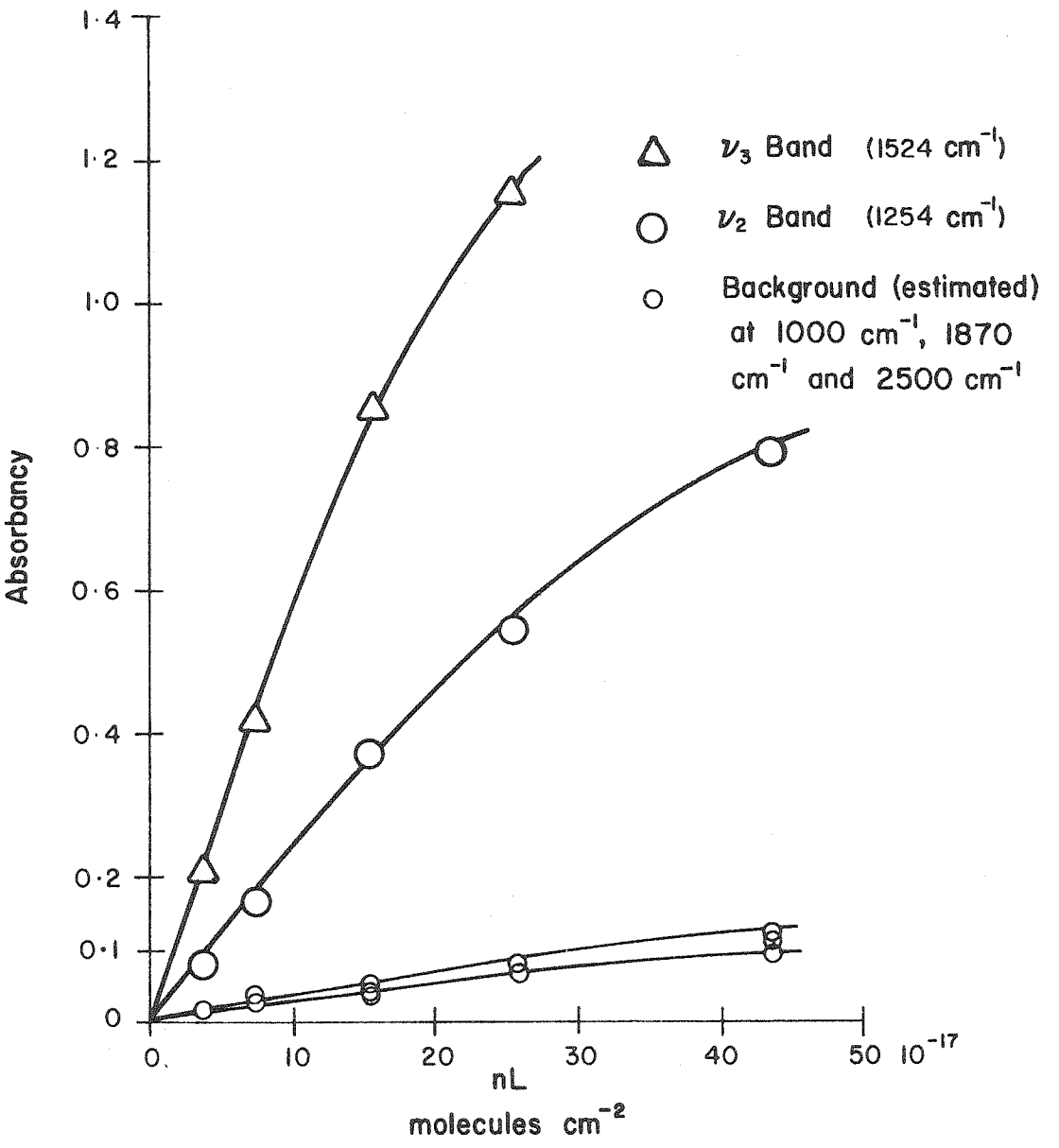

FIGURE II A-4

Plot of Absorbancy of Infrared Active Fundamentals of the Bifluoride Ion in a KBr Matrix
Against Concentration of KHF_2 in a KBr Pressed Disc

involved. The first type would correspond to a motion of the bifluoride ion in some direction and a corresponding motion of the surrounding potassium ions in the opposite direction. There would be two distinct species for this type of vibration; a degenerate mode of species e_g and a non-degenerate mode of species b_{2g}. They would be the highest frequency "lattice" mode and would roughly correspond to the Reststrahlen frequency of potassium bromide.

The second type would be the motion of the potassium ions, a "breathing" type mode, where the bifluoride ion would remain stationary. This mode would be degenerate and belong to species e_g. Also, it would be of relatively high frequency and might couple significantly with the internal vibrations of the bifluoride ion.

A final type of vibrational mode would consist of a number of vibrations of the potassium ions relative to one another. These might be of a lower frequency.

It might be difficult to correlate the lattice frequencies found for potassium bifluoride with the frequencies to be associated with the potassium bromide matrix as the structure of the matrix is not known. Besides, the structure of the host (KBr) and the guest substance (KHF_2) are quite different. Under the rather high pressures needed, about 100,000 lbs per sq. in., for the formation of alkali halide pressed discs it is possible for (1) small crystals of the compound to remain unchanged, but dispersed in the alkali halide; (2) a double displacement reaction to

occur between the compound and the alkali halide to produce small crystals of the new compounds dispersed in the matrix; or (3) a mixed crystal is formed, that is, where the anion of the compound is enclosed in the alkali halide lattice. For the system under investigation, case (2) can be ignored as both matrix material and added compound have the same cation. The infrared spectra rule out case (1); the fundamentals are shifted, which would not occur if the crystals were only dispersed throughout the matrix. Therefore, case (3), the formation of mixed crystals, is the only effect which needs further consideration. For the KHF_2 -KBr system the mixed crystal is defined as the incorporation of the bifluoride ion into the potassium bromide lattice. A more accurate statement of the situation would be solid solution of potassium bifluoride in potassium bromide. Two questions are immediately apparent with regards to the bifluoride ion. First, what is the order of magnitude of the crystal energy of potassium bifluoride and how does it compare with that of potassium bromide, the matrix material? Second, is the size of the bifluoride ion such that it can slip into the KBr lattice without undue distortion? From a consideration of these two questions it is hoped that the use of the KHF_2 single crystal data will be justified.

First, we shall make an estimate of the order of magnitude of the crystal energy of potassium bifluoride. In Figure II A - 1, a sub-unit cell of the KHF_2 unit cell is shown in which each bifluoride ion is surrounded by eight potassium ions, analogous to the cesium cloride structure. To a first approximation, the

crystal energy can be estimated by the equation(168)

$$U_o = (NAe^2Z^2/R_o) \cdot (1 - (1/n))$$

where N is Avogardro's number, A the Madelung constant, Z the charge on the ions, R_o the smallest distance of separation between positive and negative charges and n the Born exponent. For crystalline potassium bifluoride the following numerical values were chosen on the basis of similarity to the cesium chloride structure: for the Madelung constant, $A(R_o) = 1.762670$; for the Born exponent, $n = 10.5$. The value of R_o was calculated from the structural parameters of potassium bifluoride to be 3.309 A, the average distance for the smallest separation between positive and negative charges. The crystal energy, U_o, is calculated to be about 172 kcal/mole, which is greater than that of potassium bromide, 162 kcal/mole. Most likely the potassium bifluoride value is high by 20 to 30 kcal/mole, considering the assumptions used. The exact value is unimportant. Both compounds have moderately high lattice energies of the same order of magnitude, so they should behave the same under the pressure used to form the pressed discs.

The second aspect to consider is the incorporation of the bifluoride ion into the potassium bromide lattice. In Figure II A - 5, a [100] plane of the KBr lattice and a projection of the sub-unit of the KHF_2 unit cell onto a plane perpendicular to the tetragonal axis are shown with two possible orientations of an HF_2^- ion in a KBr lattice, if one assumes a replacement of the Br^- ion. In (A) the bifluoride ion is oriented with its axis along the line joining two potassium ions. In this arrangement there is considerable ion-ion

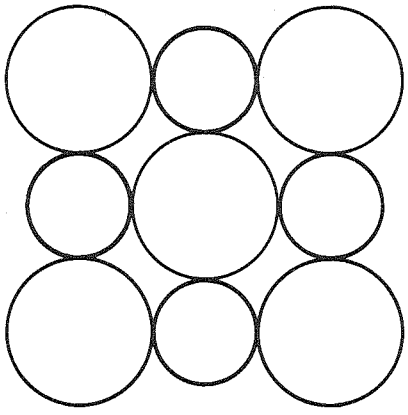

Potassium Bromide
[100] Plane Projection

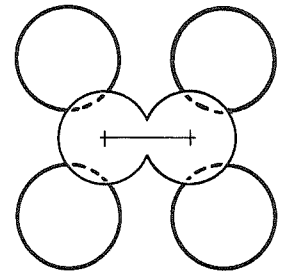

Potassium Bifluoride
Projection on Plane Perpendicular
to Tetragonal Axis

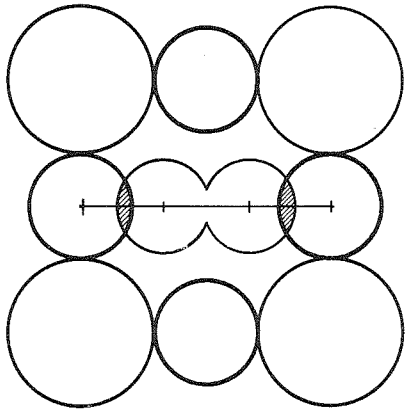

Case A

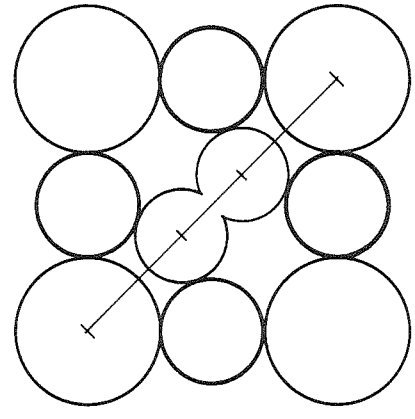

Case B

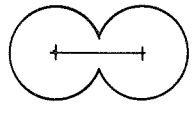

Bifluoride Ion
$r_{F^-} = 1{\cdot}22$ A

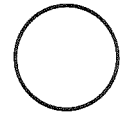

Potassium Ion
$r_{K^+} = 1{\cdot}36$ A

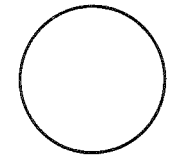

Bromide Ion
$r_{Br^-} = 1{\cdot}95$ A

FIGURE IIA-5

Possible Orientations of a Bifluoride Ion
in a Potassium Bromide Lattice

overlap. An expansion of the KBr lattice by 0.73 A (about 35 kcal of energy) is necessary to have ion-ion contact. In (b), however, the bifluoride ion is oriented along the diagonal, a line joining two bromide ions. Such an arrangement requires no lattice expansion and the bifluoride ion is in contact with four potassium ions. There is, undoubtedly, some lattice expansion due to repulsion between the bifluoride ion and the bromide ions since the closest approach of the HF_2^- - Br^- ions is about 0.35 A in comparison to 0.75 A for Br^- - Br^- ions in potassium bromide. It appears then, that (B) is the most favorable arrangement for solid solution of potassium bifluoride in potassium bromide.

In pure crystalline potassium bifluoride the bifluoride ion is in an axially unsymmetric field which causes a very small splitting of the ν_2 fundamental.[145] As the proposed solid solution model also places the bifluoride ion in a highly unsymmetric field one would expect this mode to be split. No splitting, however, has been observed. It might be pointed out that Ketelaar and co-workers[159,160] did not report any splitting of the ν_2 fundamental in a more complete investigation of the infrared spectra of solid solutions of potassium bifluoride and various alkali halides. The absence of splitting does not invalidate the proposed model though a more thorough investigation will be necessary before it can be completely acceptable.

With a plausible structure for the potassium bromide-potassium bifluoride solid solution it might be well to estimate

the frequency of vibration of the bifluoride ion and the potassium ions, representing the local "lattice" vibrations. If we assume the motion of the ions to be simple harmonic oscillations with the bifluoride ion replacing a bromide ion in a cubic lattice, and the potential constants to be the same, one calculates a frequency shift ratio of 1.35. Reststrahlen measurements have placed the lattice mode of crystalline potassium bromide, designated (K^+-Br^-), at 82.6 microns,[169] which would give a frequency of 165 cm^{-1} for a $K^+-HF_2^-$ vibration. The calculated value is in the region of the observed Raman lines of crystalline potassium bifluoride, so it is quite possible that the local "lattice" modes of the solid solution are about the same as those of the pure crystalline potassium bifluoride. With this in mind the satellites on the ν_3 fundamental will be described.

The most intense satellite on the high frequency side of the ν_3 fundamental is found between 1660 and 1670 cm^{-1}, with a maximum at about 1667 cm^{-1}. This is assigned as $\nu_3 + \nu_{L(136)} = 1660\ cm^{-1}$, an interaction between the asymmetric stretching mode and the local "lattice" mode which may be the relative motion of the bifluoride ion and the potassium ions. A very weak band between 1620 and 1640 cm^{-1} in low concentrations of KHF_2 will be tentatively assigned as $\nu_3 + \nu_{L(100)} = 1624\ cm^{-1}$. A weak band which finally merges into the main band between 1580 and 1610 cm^{-1} will be assigned as $\nu_3 + \nu_{L(90)} = 1614\ cm^{-1}$.

The low frequency side of the ν_3 fundamental is more complex as the appearance and the shape of the bands depends somewhat on

the amount of potassium bifluoride in the disc. However, in the region between 1380 and 1400 cm^{-1} a diffuse band can be tentatively assigned as a difference band, $\nu_3 - \nu_{L(136)} = 1388\ cm^{-1}$. The only other region exhibiting absorption is between 1330 and 1350 cm^{-1}, which can only be assigned the combination $\nu_2 + \nu_{L(90)} = 1344\ cm^{-1}$, even though Newman and Badger were unable to attribute any of the band width of the ν_2 fundamental to lattice vibration interactions. Undoubtedly some of the absorption in this region could be due in part to absorbed water on the KBr powder used to prepare the discs. However, a disc of pure KBr treated under the same conditions as those containing potassium bifluoride showed very weak absorption in the 1600 - 1500 cm^{-1} region.

A well-defined, intense band is found at 2093 cm^{-1} in the KBr matrix spectra. In single crystal spectra an intense band found between 2055 and 2060 cm^{-1} has been assigned the combination band $\nu_3 + \nu_1$.[145,146] If this is the same band then the calculated frequency is 2124 cm^{-1}, on the assumption that $\nu_{1(KBr)} = 600\ cm^{-1}$, a difference of + 31 cm^{-1}. The difference could be the result of a decrease in the convergence constant for the ν_3 and ν_1 vibrations, a decrease in the frequency of the totally symmetric vibration, ν_1, or a combination of these, in going from a single crystal to a potassium bromide matrix.

Evaluation of Integral Absorption Intensity of the ν_2 and ν_3 Band of KHF_2 in a KBr Matrix:

The change in a dipole moment due to the displacement of the atoms of a molecule determines the absorption intensity of a fun-

damental vibration. Consequently, the determination of the intensity of the fundamentals will allow one to study the change in charge distribution in the molecule. In this section the two methods discussed on pages 46 - 49 have been used to estimate the intensity of the two infrared active fundamentals, ν_2 and ν_3, of the bifluoride ion in a potassium bromide matrix.

a). Peak Intensity - Lorentz Band Contour Method:

The first problem associated with this method is whether or not the absorption bands can be described by a Lorentz function. The parameters for a Lorentz band contour have been calculated from the observed bands and have been summarized in Table II A - 6. A comparison of the calculated and observed band contours for the ν_2 and ν_3 fundamentals are shown in Figure II A - 6. The agreement for the ν_2 band is excellent whereas the ν_3 band exhibits considerable deviation about the base and the wings. Still the Lorentz model can be considered a fair representation of the ν_3 band, as the close lying lattice vibration interactions will influence the estimation of the band contour.

Table II B - 6

Data for the Calculation of a Lorentz Type Band Contour

band	ν(max) (cm^{-1})	frequency interval $\Delta\nu$(cm^{-1})	nL (mol. cm^{-2})	$\Delta\nu_{1/2}^{(a)}$ (cm^{-1})	$A(v_m)$	b	a
ν_2	1254	100	43.4×10^{17}	14.1	1.82	7.05	89.2
ν_3	1524	225	15.4×10^{17}	45.0	1.97	22.5	995

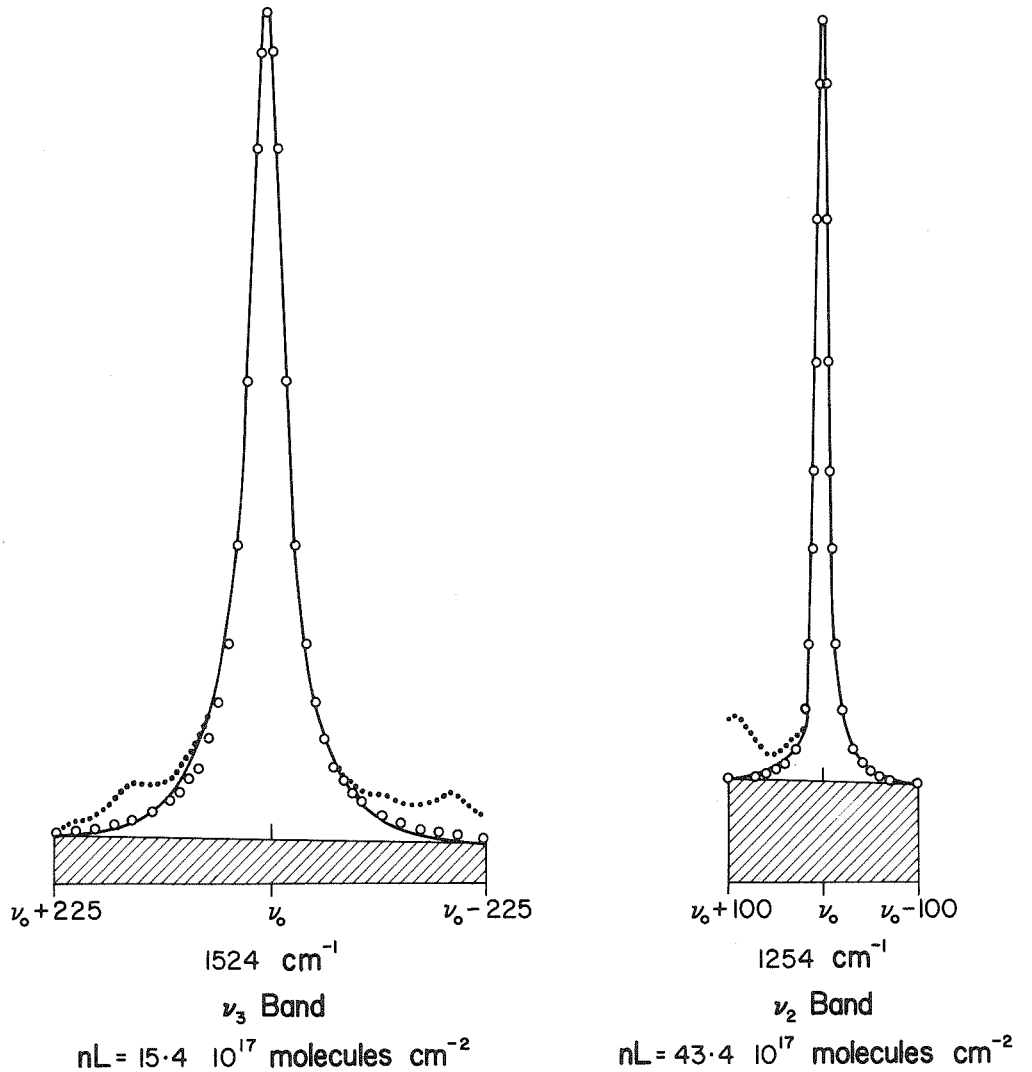

FIGURE IIA-6

Comparison Between Observed and Calculated Band Contours of the Infrared Active Fundamentals of KHF_2 in a KBr Matrix

● ● Observed Band Contour

▬▬ Estimated Band Contour

○ Calculated Lorentz Band Contour

As the observed bands fit the Lorentz model to a good first approximation, the integral absorption intensities were computed from equation (6) with the K values taken from the tables of Ramsey.[165] The necessary data has been summarized in Table II A - 7. The average integral absorption intensities determined by this method are

$$A(\nu_2) = 1.0 \times 10^{-17} \text{ cm}^2 \text{ molecule}^{-1} \text{ cm}^{-1}$$

$$A(\nu_3) = 7.7 \times 10^{-17} \text{ cm}^2 \text{ molecule}^{-1} \text{ cm}^{-1}$$

The values are probably good to within 15 to 20% as the estimation of the peak height intensities and the band width are approximate.

b). "Paper Integration":

The apparent absorption intensities were evaluated by the technique of "paper integration" as described on pages 47 - 49. The data has been summarized in Table II A - 8 for the two infrared active fundamentals. A Wilson-Wells plot for the ν_2 and ν_3 fundamentals of the bifluoride ion in a KBr matrix (Figure II A - 7) yields integral absorption intensities of

$$A(\nu_2) = 0.99 \times 10^{-17} \text{ cm}^2 \text{ molecule}^{-1} \text{ cm}^{-1}$$

$$A(\nu_3) = 7.70 \times 10^{-17} \text{ cm}^2 \text{ molecule}^{-1} \text{ cm}^{-1}$$

The values should be considered reliable to within 20 to 30%. The main problems associated with this method lay in the estimation of the band contour and the intensity of background absorption. The band contour is complicated by overlap between the fundamentals as well as fine structure on the wings, par-

Table II A - 7

Data for the Evaluation of the Integral Absorption Intensity of the Infrared Active Fundamentals of the Bifluoride Ion in a Potassium Bromide Matrix by the Peak Intensity - Lorentz Band Contour Method

Band	ν(max) (cm^{-1})	$\Delta\nu$ (cm^{-1})	S (cm^{-1})	nL ($mol.cm^{-2}$)	$\Delta\nu_1^2/2$ (cm^{-1})	$\ln(T_o/T)^*$	K	$A^{(k)}$ ($cm^2 mol.^{-1} cm^{-1}$)	$\alpha(\nu max)$ ($cm^2 mol.^{-1}$)***
ν_2	1254	±100	7.10	3.65×10^{17}	10.0	0.184	(1.45)**	$(0.73) \times 10^{-17}$	-------
				7.47	14.0	0.382	1.46	1.05	0.63×10^{-18}
				15.4	14.0	0.862	1.51	1.18	0.70
				25.5	15.0	1.26	1.54	1.14	0.59
				43.4	13.4	1.82	1.59	0.90	0.54
ν_3	1524	±225	13.1	3.65×10^{17}	32.0	0.482	1.50	6.74×10^{-17}	1.51×10^{-18}
				7.47	40.0	0.968	1.55	7.78	1.40
				15.4	45.0	1.97	1.57	8.64	1.36
				25.5	46.0	2.67	(1.59)**	7.65	----

* Measured at the center of the band.
** Estimated from the tables of Ramsey, Ref. 165.
*** $\alpha(\nu max)$ is defined as $(2.303/nL) \log(T_o/T)_{\nu(max)}$

Table II A - 8

Data for the Evaluation of the Integral Absorption Intensity of the Infrared Active Fundamentals of the Bifluoride Ion in a Potassium Bromide Matrix by the Wilson-Wells Extrapolation Method

Band	ν(max) (cm^{-1})	$\Delta\nu$ (cm^{-1})	nL ($mol.cm^{-2}$)	$A(\nu_m)$*	Avg. Wgt. Band (mgs)	$\int A(\nu)d\nu$ (cm^{-1})	B** ($cm^2 mol.^{-1} cm^{-1}$)	$\alpha(\nu max)$*** ($cm^2 mol.^{-1}$)
ν_2	1254	±100	3.65×10^{17}	0.080	5.93	1.50	0.946×10^{-17}	0.505×10^{-18}
			7.47	0.166	12.30	3.14	0.968	0.512
			15.4	0.374	32.12	8.22	1.23	0.560
			25.5	0.545	42.87	10.83	0.979	0.493
			43.4	0.789	61.05	15.46	0.820	0.419
ν_3	1524	±225	3.65×10^{17}	0.209	44.54	11.26	7.10×10^{-17}	1.32×10^{-18}
			7.47	0.420	100.1	25.29	7.80	1.30
			15.4	0.855	221.1	55.87	8.35	1.28
			25.5	1.157	301.2	76.12	6.88	1.05

* $A(\nu_m)$ is defined as $\log(T_o/T)_{\nu\,(max)}$

** B is defined by the integral $(2.303/nL)\int A(\nu)d\nu$

*** $\alpha(\nu max)$ is defined by the equation $(2.303/nL)\,A(\nu_m)$

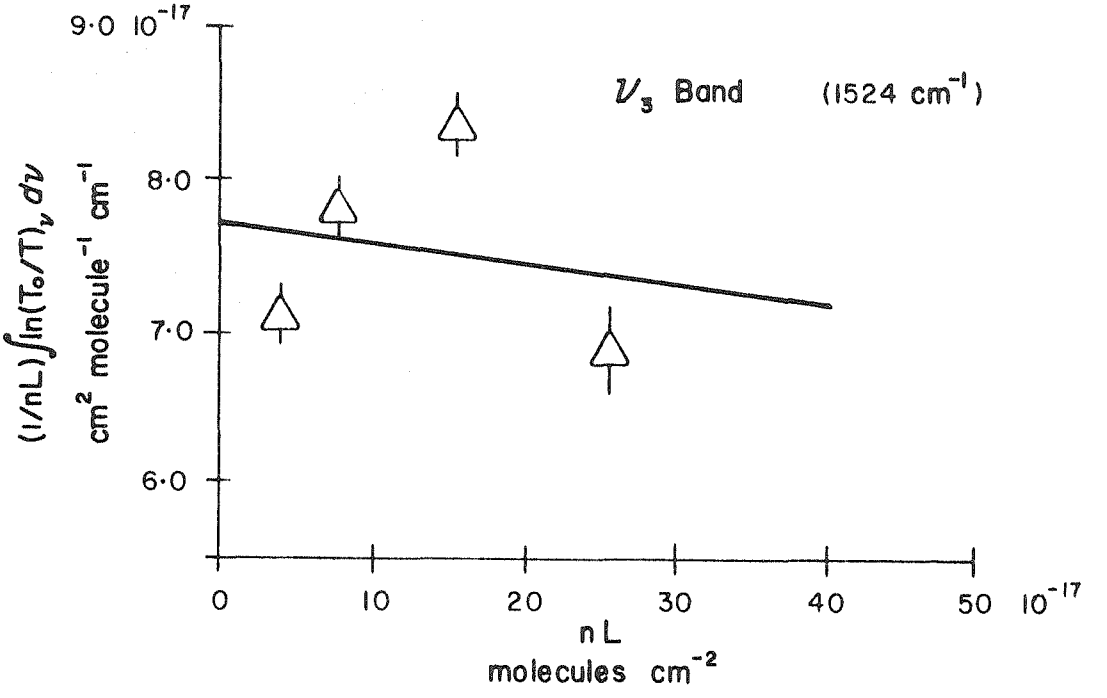

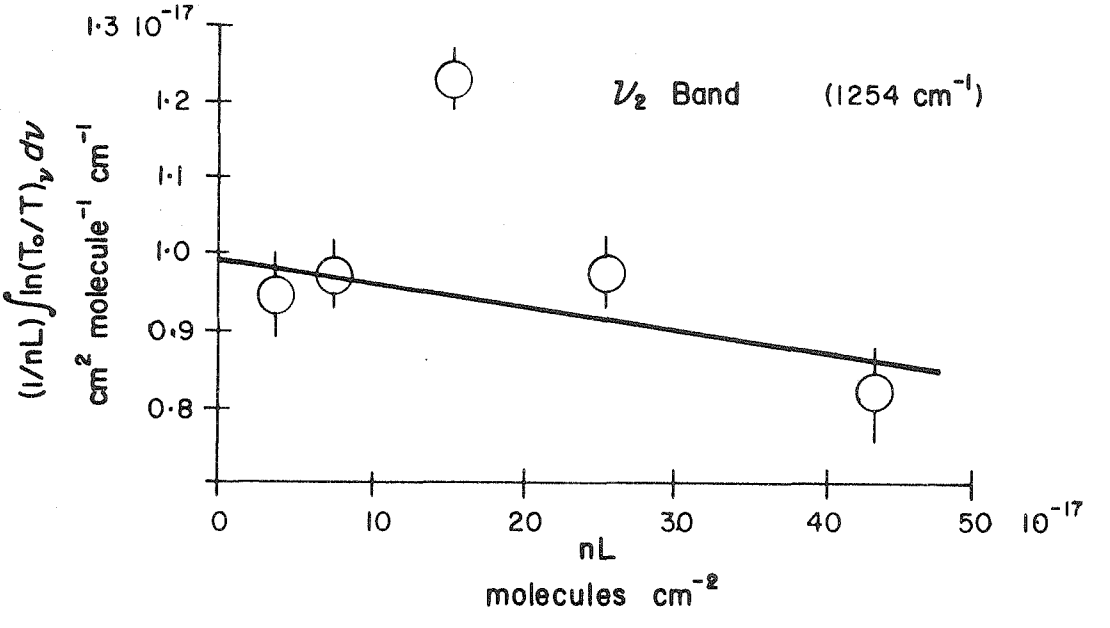

FIGURE IIA-7

Wilson-Wells Plot for ν_2 and ν_3 Bands of KHF_2 in a KBr Matrix

ticularly the ν_3 band. The background is a composite of scattering and absorption, which affects the intensity of superimposed bands. In the present case the area under the bands was assumed to be due entirely to absorption. This is not quite true, but has been used in order to estimate the intensity of the fundamentals in a potassium bromide matrix. Therefore, the excellent agreement between the integral absorption intensities determined by the two methods is fortuitous (Table II A - 9).

Table II A - 9

Integral Absorption Intensities and Absorption Coefficients for Infrared Active Fundamentals of the Bifluoride Ion in a Potassium Bromide Matrix

	ν_2 Band		ν_3 Band	
Method	A*	$\alpha(\nu max)$**	A*	$\alpha(\nu max)$**
Peak Intensity - Lorentz Band Contour	1.0×10^{-17}	0.61×10^{-18}	7.7×10^{-17}	1.42×10^{-18}
Wilson - Wells	0.99	0.54	7.7	1.33

* in units of cm^2 $molecule^{-1}$ cm^{-1}

** in units of cm^2 $molecule^{-1}$

It is immediately apparent that the intensity of the ν_3 fundamental is greater than that of the ν_2 fundamental, over seven times as intense. In single crystal spectra the bands appear of almost comparable intensity due to the fact that it is not practical to obtain very thin crystals and the absorption is almost complete in both cases. Actually ν_3 is more intense. Unfortunately, a direct comparison

of band intensities is not possible, so an exact evaluation of the effect of the potassium bromide matrix on the intensity of the infrared active fundamentals is impossible.

Reid[80] contends that the intensity of the shifted stretching vibration band is very weak for short, symmetric hydrogen bonds. This, however, has not been observed for the ν_3 band of the bifluoride ion. The band is very intense, the frequency greatly shifted from the stretching frequency of monomeric H-F and the hydrogen bond is very short and symmetric. The F-H-F hydrogen bond differs from the O-H---O hydrogen bond system considered by Reid in two respects: the terminal atoms are different and the bifluoride hydrogen bond system is an ion with a negative charge. The effect of the terminal atoms will be on the reduced mass of the hydrogen bonded system and the degree of ionic character associated with the hydrogen bond. The existence of a residual charge will affect the charge distribution on the atoms of the hydrogen bond. Although the exact contribution of each of the above factors on the intensity of the band cannot be readily estimated, the change in charge distribution would be the predominent factor. Any variation in the charge distribution would affect the bond dipole moment, which is in turn associated with the intensity of an infrared absorption band.

Dipole Moment Change with Vibrational Mode:

During the vibrational motion connected with a normal vibration the charge distribution undergoes a periodic charge. This may or may not result in a change in the molecular dipole

moment. If it does, the vibration will be infrared active. Such infrared active vibrations can be treated quantum mechanically in terms of transition probabilities, which can be related to the matrix elements of the dipole moment and the intensity of the absorption band. In the harmonic oscillator approximation, neglecting mechanical and electrical anharmonicity, the integral absorption intensity of the k^{th} fundamental mode, $A^{(k)}$, is related to the rate of change of the total molecular dipole moment, μ, with the i^{th} normal coordinate, Q_i, by the equation

$$A^{(k)} = \int \alpha(\nu) \cdot d\nu = (N\pi/3c^2) \cdot |(\partial\mu/\partial Q_i)|^2 \quad \ldots\ldots\ldots (7)$$

From the intensity of the fundamental vibration the magnitude of $(\partial\mu/\partial Q_k)$ can be determined for each mode, though the sign can not. Since the bifluoride ion possesses sufficient symmetry, it is possible to choose a set of axes so that only one of the dipole moment changes with any normal vibration will be different from zero. Thus, the z-axis has been taken along the bifluoride ion axis and the x- and y-axes at right angles to it. For the non-degenerate ν_3 fundamental, the change in the dipole moment with a change in the bond length, z, is given by

$$(d\mu/dz) = (\partial\mu/\partial Q_3) \cdot (\partial Q_3/\partial z) \quad .$$

As the normal mode, Q_3, is directed along the bond, $(\partial Q_3/\partial z)$ is equal to $(m_r)^{1/2}$, where m_r is the reduced mass of the vibrating system, defined as $(m_H m_F)/(m_H + 2m_F)$ and is equal to 0.8184×10^{-24} gm.

For the doubly degenerate ν_2 fundamental, the change in the dipole moment with normal vibration is given by

$$(\partial\mu/\partial Q_2)^2 = (\partial\mu/\partial Q_{2a})^2 + (\partial\mu/\partial Q_{2b})^2$$

In terms of the cartesian coordinates choosen for the bifluoride ion we shall assume the dipole moment change accompanying a bond bending, for small displacements, x and y, perpendicular to the internuclear axis are given by the relations

$$(d\mu/dx) = (\partial\mu/\partial Q_{2a}) \cdot (\partial Q_{2a}/\partial x)$$

$$(d\mu/dy) = (\partial\mu/\partial Q_{2b}) \cdot (\partial Q_{2b}/\partial y)$$

If the vibration is assumed to be essentially that of a particle of mass m_r, the r educed mass of the bifluoride ion, perpendicular to the ion axis, then for small displacements from the equilibrium configuration, $(\partial Q_{2a}/\partial x) = (\partial Q_{2b}/\partial y)$.

As the vibrations parallel and perpendicular to the ion axis have been attributed to an oscillating particle with the reduced mass of the bifluoride ion, the effective motion of charge responsible for the band intensity can be readily estimated. The effective charge oscillating in the k^{th} vibrational mode along the i^{th} cartesian axis, defined as $f_i^{(k)}$, is the quotient of the change in the dipole moment for the k^{th} vibrational mode along the i^{th} cartesian axis, $\mu_i^{(k)}$, divided by a unit charge is esu units, 4.81 x 10^{-10} esu. The computed values are tabulated in Table II A - 10 for the ν_2 and ν_3 fundamentals of the bifluoride ion in a potassium bromide matrix, together with the calculated values of $(\partial\mu/\partial Q_k)$ and $\mu_i^{(k)}$.

Table II A - 10

Band Intensity and Dipole Moment Derivatives of

Infrared Active Fundamentals of KHF_2 in a KBr Matrix

band	frequency (cm^{-1})	$A^{(k)}$ (cm^2 mol^{-1} cm^{-1})	$\pm(\partial\mu/\partial Q_k)$ ($cm^{3/2}$ sec^{-1})	$\mu_i^{(k)}$ (Debyes/A)	$f_i^{(k)}$
ν_2	1254	1.0×10^{-17}	65.5	0.58	0.12
ν_3	1524	7.7×10^{-17}	269	2.43	0.50
ν_3[a]	1450	----	500	4.50	0.94

(a) Estimated from single crystal data of Ketelaar (Ref. 160)

The intensity of the ν_3 fundamental of the bifluoride ion in a potassium bromide matrix can be attributed to the oscillation of 0.5 unit charge. Ketelaar and van der Elsken[160] have recently determined $(\partial\mu/\partial Q)^2$ for the ν_3 fundamental of the bifluoride ion from reflectence spectra by the method of Hass and Hornig.[170] When reduced to the units employed in this work the intensity of the ν_3 vibration in crystalline potassium bifluoride represents the motion of 0.94 unit charge. This is almost twice that of the bifluoride ion in a potassium bromide matrix. The difference of intensities in the matrix and in the crystal is of interest. Unpublished work of Pullin[171] has shown that in matrix measurements the intensity is considerably underestimated. Recently several authors have shown the intensity of a band in an alkali halide disc will decrease as the particle size of the absorbing species increases.[171 - 175] Experimental evidence seems to indicate that this is the cause of the discrepancy. First, the matrices do not

obey Beer's law, see Figure II A - 4 and the article by Duyckaerts and Bonhomme.[167] Second, an abnormal general scattering exists over the entire spectrum. Third, the apparent band half-width increases significantly with concentration. The apparently large particle size can be produced with the pressure used to form the alkali halide discs. Under pressure diffusion with solid solution formation can occur. Since diffusion is slow, fairly large regions or more or less homogenous solid solution are imbedded in a matrix of almost pure potassium bromide. These regions act like a dispersion of crystals much larger than the original ones. The regions of solid solution differ markedly from the potassium bromide regions due to the abnormally high absorption of the bifluoride ion. Though initially small particles the final pressed disc will contain regions of high concentration of solid solution which act as large particles.

Summary:

Contrary to the hypothesis of Reid[80] the shifted stretching frequency, ν_3, of the bifluoride ion is very intense, in both the crystalline state and in the KBr matrix.

The intensity of the two infrared active fundamentals of the bifluoride ion in a potassium bromide matrix were estimated. The integral absorption intensities are 1.0×10^{-17} and 7.7×10^{-17} cm^2 $molecule^{-1}$ cm^{-1} for ν_2 and ν_3, respectively. The effective motion of charge responsible for the band intensity has been estimated as 0.12 and 0.50 unit charge for ν_2 and ν_3 fundamental, respectively. A descrepancy of a factor of two between the matrix

and the crystal value for the ν_3 fundamental has been found. The difference has been attributed to large regions of solid solution present in the alkali halide pressed disc.

Section B: Acetamide Hemihydrochloride

The recent X-ray crystallographic analysis of acetamide hemihydrochloride by Takei[137] revealed an unusually short intermolecular O---O distance of 2.40 A located on a crystallographic center of symmetry. The short distance has been interpreted on the basis of hydrogen bonding between the oxygen atoms. Unfortunately, X-ray crystallographic techniques were unable to locate precisely the position of hydrogen atoms, so the exact nature of the bond is uncertain. In view of the structure of acetamide hemihydrochloride an examination of the infrared absorption spectrum was undertaken.

Since acetamide hemihydrochloride is a derivative of acetamide an investigation of the infrared spectrum of the parent compound, acetamide, was undertaken at the same time, which would serve as a reference as well as a guide in the frequency assignments of the hemihydrochloride molecule. The infrared spectrum of acetamide has been reported in solution[176 - 178] and in the crystalline state.[178 - 179] The Raman spectrum of crystalline acetamide has been reported by Reitz and Wagner.[180]

Crystal Structures:

Acetamide:

Acetamide crystallizes in two modifications; an unstable orthorhombic form melting at 48.2°C and a stable trigonal or hexagonal form melting at 82°C.[182,183] An X-ray crystallographic investigation on the stable rhombohedral form of acetamide by

Senti and Harker[181] gave unit cell dimensions of a = 1.44 A and c = 13.49 A, with eighteen molecules per unit cell. The crystals belong to space group C_{3v}^6 - R3c. The significant results of the structure analysis are (a) an N-H---O distance which is quite short, only 2.86 A, (b) the acetamide molecule is planar with the N-H bonds in the plane of the molecule, and (c) the molecule exists in the keto form. A simplified diagram of the acetamide structure is shown in Figure II B - 1, where the triangles represent acetamide molecules, the dotted lines the hydrogen bonds between adjacent molecules and the small circles the hydrogen atoms of the NH_2 group. Because the crystal belongs to a non-centrosymmetric space group and because of the limited computational facilities available, the results are not as accurate as might be desired, a probable error of 0.05 A.

Acetamide Hemihydrochloride:

When recrystallized from acetone acetamide hemihydrochloride forms long, flattened needles with a cleavage plane along the needle axis. The crystals belong to space group $P2_1/c$, with two molecules per unit cell. The mono-clinic unit cell has dimensions of a = 6.33 A, b = 8.31 A, c = 8.07 A and $\beta = 111.7^{\circ}$, with the b axis perpendicular to the needle axis which is the [101] plane. The structure may be crudely represented as a highly distorted egg-crate where the planes can be described as composed of chains of the form

----Cl----(H_2HAc)---(AcNH_2)----Cl----(H_2NAc)----

held together by N-H----Cl and O--H--O type hydrogen bonds. The

O--H--O bonds, which are of interest, are parallel to the needle axis in the [101] plane. The chains described above are in both sets of planes. A diagram of the acetamide hemihydrochloride structure is shown in Figure II B - 2. A comparison of the internuclear distances of the acetamide portion of the molecule with those found in crystalline[181] and gaseous[184] acetamide and in the polypeptide unit[185] are given in Table II B - 1. The results of Takei for the acetamide portion of the molecule are closer to the bond distances and bond angles selected by Pauling and Corey[185] for the polypeptide unit than to any of experimentally determined values for acetamide.

Experimental Details:

This section is divided into three parts; the preparation of the materials, the preparation of samples for spectroscopic examination and the instrumental conditions for recording the spectra.

Preparation of Materials:

Acetamide:

Acetamide (labelled Student Preparation from Chemistry Department storeroom) was recrystallized five times from acetone. The long needle-like crystals were dried over phosphorous pentoxide under reduced pressure (about 1 mm of Hg) at room temperature for twelve hours and then sublimed at 80°C under reduced pressure. Small rhombohedral crystals were obtained. The sublimed acetamide was stored in a desiccator over anhydrous magnesium perchlorate until used. Observed melting point (uncorrected under crossed Nicols on a microscope hot-stage was 81.8° - 82.8°C.

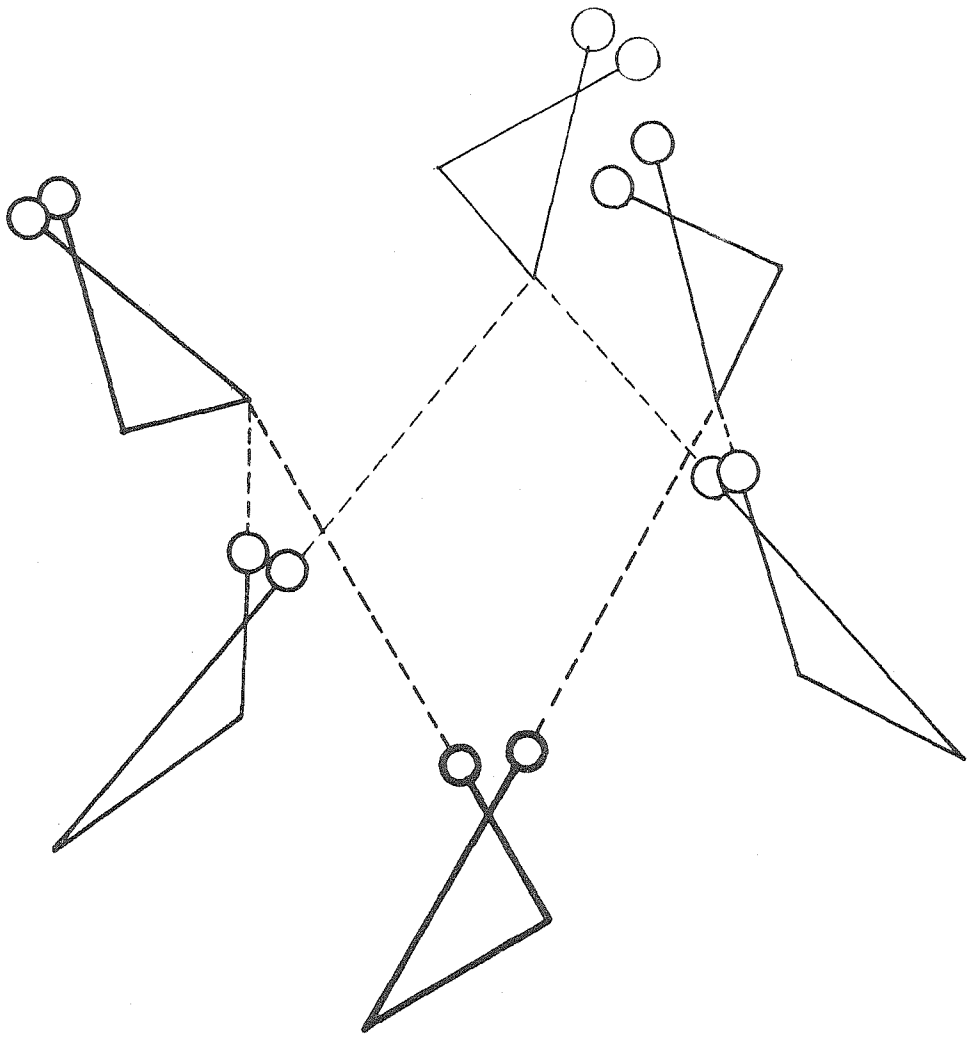

FIGURE II B-1

Packing of Acetamide Molecules in the Crystalline State

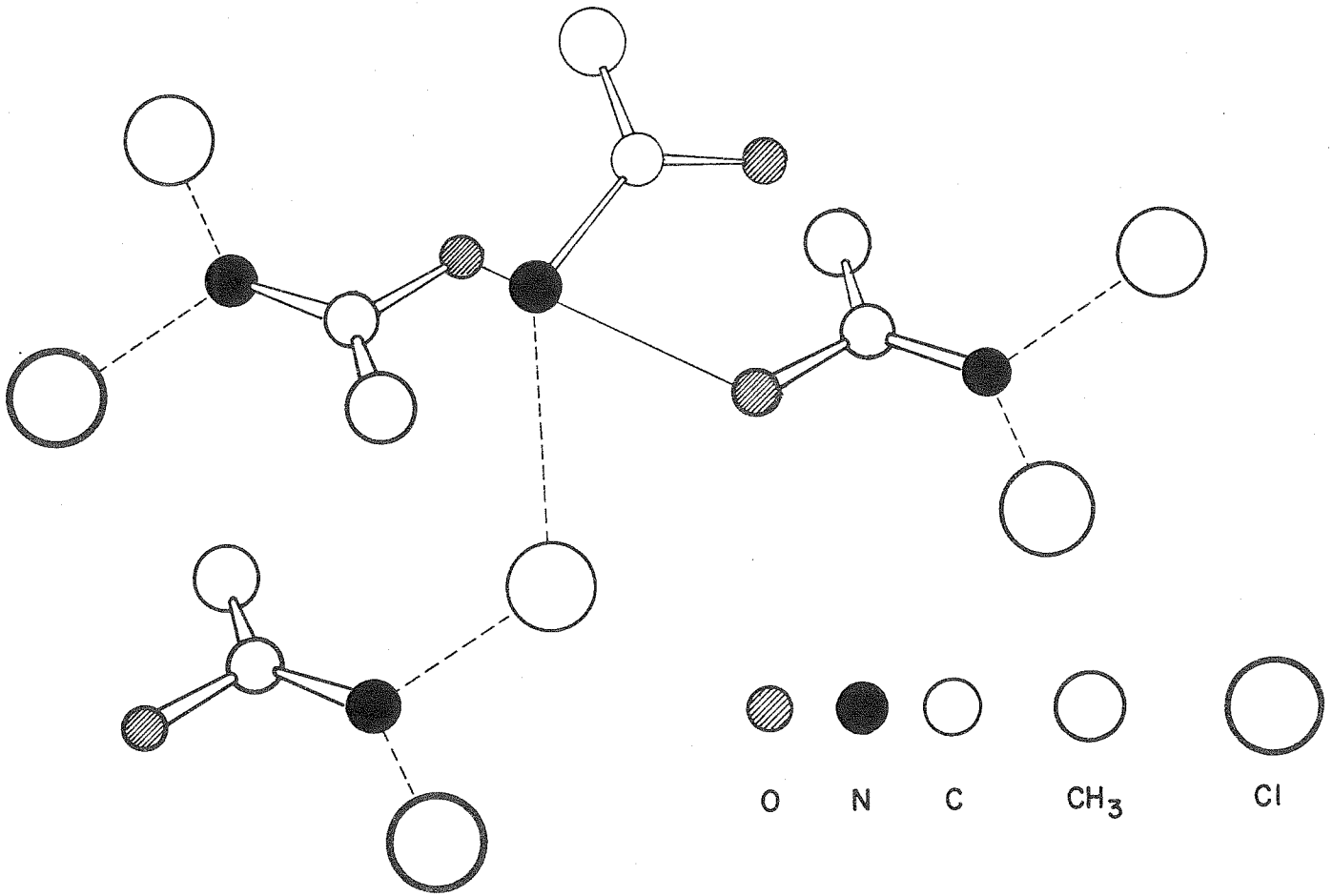

FIGURE II B - 2

Packing of Acetamide Hemihydrochloride Molecules in the Crystalline State

Table II B - 2

Bond Distances and Bond Angles in Acetamide and Acetamide - Like Residues

Substance	Method	Ref.	C-O	C-N	C-C	∠C-C-O	∠C-C-N	∠O-C-N	Hydrogen Bond
Polypeptides	---	185	1.24 A	1.32 A	1.53 A	121°	114°	125°	----
Acetamide	X[a]	181	1.28	1.38	1.51	129°	109°	122°	2.80 A[c]
Acetamide	E.D.[b]	184	1.21	1.36	1.53	122°	113°	125°	----
Acetamide Hemi-hydrochloride	X[a]	137	1.244	1.303	1.507	119°	117°	123°	2.40 A[d] 3.31 A[e] 3.24 A[e]

a). X-ray diffraction
b). Electron diffraction
c). For the N-H---O hydrogen bond
d). For the O---O distance, intermolecular
e). For the N-H---Cl hydrogen bond

Deuterated Acetamide:

Deuterated acetamide was prepared by recrystallization of the sublimed acetamide from heavy water. Three recrystallizations of one gram of acetamide from 1 ml portions of heavy water was sufficient to give almost complete deuteration. The heavy water was removed under reduced pressure with the aid of fresh phosphorous pentoxide. The deuterated material was stored in a sealed container in a desiccator over anhydrous magnesium perchlorate.

Acetamide Hemihydrochloride:

Two methods were used to prepare this compound. The first method is simple and was used by Takei[137] for the preparation of single crystals suitable for X-ray analysis. The second method is more elaborate but has a decided advantage in the preparation of the deuterated compound.

Method A:

Stoichiometric quantities of sublimed acetamide and concentrated aqueous hydrochloric acid were mixed at room temperature. After stirring, the resulting slurry was allowed to stand for about ten minutes. The slurry was then filtered through a medium porous grade sintered glass filter, and washed with cold acetone (about 2°C) until the filtrate was acid free. The crude product was then recrystallized twice from acetone. Long, flattened needles were obtained and were dried over phosphorous pentoxide in a dry nitrogen atmosphere. The crystals were stored in a sealed container in a desiccator over fresh phosphorous pentoxide until used. The melting point (uncorrected) observed under

crossed Nicols on a microscope hot-stage gave a range of 137° - 146°C, which was reproducible, Kahovic and Knollmuller [186] reported the compound to sinter at 123°C and to melt at 131°C. An acidimetric titration and a volumetric chloride analysis [187] indicated the product to be better than 99% pure. Results of the analysis: acid content, as HCl: calculated: 23.60%, found: 23.56%; chloride content: calculated: 22.94%, found: 22.70%.

Method B:

The method of Titherley [188] for the preparation of diacetamide was modified in order to obtain acetamide hemihydrochloride. Details of the procedure are given under the method of preparation of deuterated acetamide hemihydrochloride. The procedure, however, was checked with ordinary acetamide. The product gave the same melting point and infrared spectrum as the product obtained from Method A.

Deuterated Acetamide Hemihydrochloride:

The procedure is a modification of the method of Titherley for the preparation of diacetamide.[188] With this procedure it was possible to carry out the preparation and purification of the deuterated compound with a minimum exposure to the atmosphere. Approximately one gram of sublimed acetmide was placed in the reaction vessel and dissolved in about 1 ml of heavy water by warming slightly. The heavy water was removed under reduced pressure with the aid of a desiccant. This procedure was repeated three times and was considered sufficient to give almost completely deuterated acetamide. To the deutero-acetamide was added 10 - 15 ml of benzene (dried over sodium wire). After

warming to 50°C about 5 ml of a 1:20 acetyl chloride-benzene solution was injected into the reaction vessel. The mixture was heated under reflux with intermittent shaking for two hours on a water bath. The hot benzene solution was then removed and the solid material washed and refluxed with three 5 ml portions of dry benzene. The solid was finally washed with three 2 ml portions of dry acetone. The product was dried over phosphorous pentoxide at room temperature for several hours and then stored in a sealed container in a desiccator over phosphorous pentoxide.

Potassium Bromide (potassium bromide, IR grade (250 - 300 mesh), Harshaw Chemical Co.) was used without further purification. Five gram portions, however, were dried at 200°C under reduced pressure for 24 hours, then stored in a dessiccator over fresh phosphorous pentoxide until used.

Potassium Chloride (potassium chloride, Merck and Co., Inc., (pure)) was precipitated from a saturated solution at room temperature by saturating with hydrogen chloride. The fine crystals were filtered off and washed with a minimum volume of cold(about 2°C) distilled water until the filtrate was neutral to Hydrion paper. The crystals were dried at 125°C for three hours and then under reduced pressure at 200°C for 12 hours. Portions of the recrystallized material were ground in an agate mortar to a particle size of about 250 mesh and then dried under reduced pressure at 200°C for 12 hours. The powder was stored in a desiccator over fresh phosphorous pentoxide until used.

Potassium Iodide (potassium iodide, Merck and Co., Inc., reagent grade, granular) was used without further purification. Small portions were ground in an agate mortar to about 250 mesh and then dried under reduced pressure at 150°C for 12 hours. The powder was stored in a desiccator over fresh phosphorous pentoxide until used.

Preparation of Samples for Spectroscopic Investigation:

The examination of acetamide and acetamide hemihydrochloride was carried out on the crystalline material in the form of mulls, thin crystalline films and in pressed alkali halide discs.

Mulls:

Mulls were prepared by grinding the compound (about 100 mg) with two or three drops of Nujol on a glass plate. Mull spectra were used as a check on the alkali halide pressed disc spectra.

Thin Crystalline Films:

Thin crystalline films between rock salt windows were prepared in the following manner: A small amount of the solid (about 100 mg) was spread over the surface of a polished rock salt plate. A second polished plate was placed over the crystals. The plates were gently heated on an asbestos sheet on a hot plate. As soon as the crystals began to melt the windows were gently pressed together in order to obtain a uniform film. The plates were removed from the hot plate and allowed to cool slowly to room temperature. Examination of the film under polarized light indicated the entire mass was crystalline with some degree of preferred orientation, though crystallization usually occured radially from several sites between the rock salt plates.

Alkali Halide Pressed Discs:

All weighings were done on a Sartorius "Selecta" semi-micro single-pan balance capable of weighing to within ± 0.05 mg. An accurately weighed quantity of the compound, between 0.5 to 5 mg, was mixed with about one gram of the previously dried alkali halide powder in an agate mortar under an infrared lamp for thirty minutes. The mixture was transferred directly to the pellet die (3/4 in. diameter) and evacuated for five minutes with the aid of a mechanical forepump. A pressure of 40,000 pounds was applied and maintained for a time of 20 to 45 minutes. Potassium iodide required a pressing time of 20 minutes, potassium bromide 25 minutes and potassium chloride 45 minutes. The pellets were removed, mounted in holders and stored in large weighing bottles with freshly heated silica gel until the spectrum was to be recorded.

For more accurate work with the potassium bromide discs, a stock mixture of the compound with potassium bromide was prepared, usually 10% by weight. Pellets containing accurately known quantities were then prepared from a weighed amount of the mixture to which was added dried potassium bromide to give a total weight of about one gram. The remainder of the pellet technique was the same as that described in the preceeding paragraph.

Instrumental Conditions for Recording Spectra:

All spectra were obtained using a Perkin-Elmer Model 21 double-beam recording spectrophotometer equipped with sodium chloride and potassium bromide optics. Instrumental conditions used for recording the spectra with sodium chloride optics:

Slit Program: 985; Response: 1:1; Gain: 6-6.2; Recording Speed: 4 (0.6 μ/min); Suppression: 4; Spectral Range: 2 - 15 μ. Instrumental conditions used for recording spectra with potassium bromide optics: Slit Program: 1040; Response: 1:1; Gain: 6.8; Recording Speed: 3 1/2 (0.4 μ/min); Suppression: 1; Spectral Range: 10.5 - 25 μ. Spectra were recorded on a linear wavelength basis of two inches per micron and on a linear transmittance basis of one inch per 10% transmittance.

Spectral slit widths were calculated from the equation of Williams[163] with the refractive index data of Martens for sodium chloride in the region of 1 to 20μ [164] and of Gundlach for potassium bromide in the region of 1.2 to 29 μ [189] (see Table II B - 2).

Table II B - 2

Computed Spectral Slit Widths for Various Optics in Perkin-Elmer Model 21 Spectrophotometer

ν (cm^{-1})	n_ν	$dn/d\lambda$	s(cm)	S (cm^{-1})
2000[a]	1.5270	- 28.0	0.0066	10.68
1500[a]	1.5127	- 38.0	0.0098	6.70
1000[a]	1.4955	- 61.5	0.0173	3.32
667[a]	1.4523	- 70.0	0.0823	6.81
909[b]	1.5233	- 47.5	0.0074	1.38
800[b]	1.5193	- 33.5	0.0086	1.78
500[b]	1.4870	-131.0	0.0355	8.37

(a) all values for NaCl optics, slit program: 985.

(b) all values for KBr optics, slit program: 1040.

Wavelength calibration was carried out by superimposing atmospheric water-vapor, carbon dioxide and thin-film polystyrene bands on each spectrum. The frequencies recommended by Downie et al[190] and the more recent measurements of Plyler et al[191] were used.

Results and Discussion:

For convenience, and for clarity of the discussion, this section is divided into two parts. The first part concerns the frequency assignments of the acetamide molecule in the solid state while the second part deals with the hydrogen bond systems in solid acetamide hemihydrochloride and their role in the interpretation of the infrared spectrum of the compound.

Acetamide:

Mull and thin crystalline film spectra of partially deuterated and undeuterated acetamide are shown in Figure II B - 3. Spectra of acetamide in pressed discs of potassium chloride, bromide and iodide (see Figure II B - 4) are essentially the same as the mull spectrum which indicates the absence of alkali halide-acetamide compound formation under pressure. The infrared spectrum of acetamide and partially deuterated acetamide in the region of 2 to 25 microns (5000 cm^{-1} to 400 cm^{-1}) in a potassium bromide matrix is shown in Figure II B - 5.

The position of the bands (in wave-numbers) of undeuterated and partially deuterated acetamide in the various matrices have been tabulated in Table II B - 3, together with the possible frequency assignments. Most of the wave-number values listed are believed to be accurate to ± 5 cm^{-1} for bands between 400 and 2000 cm^{-1}, to ± 10 cm^{-1}

Figure II B - 3

Infrared Spectra of Acetamide and Partially Deuterated Acetamide as Mulls and as Thin Crystalline Films in the Region of 2 to 15 Microns

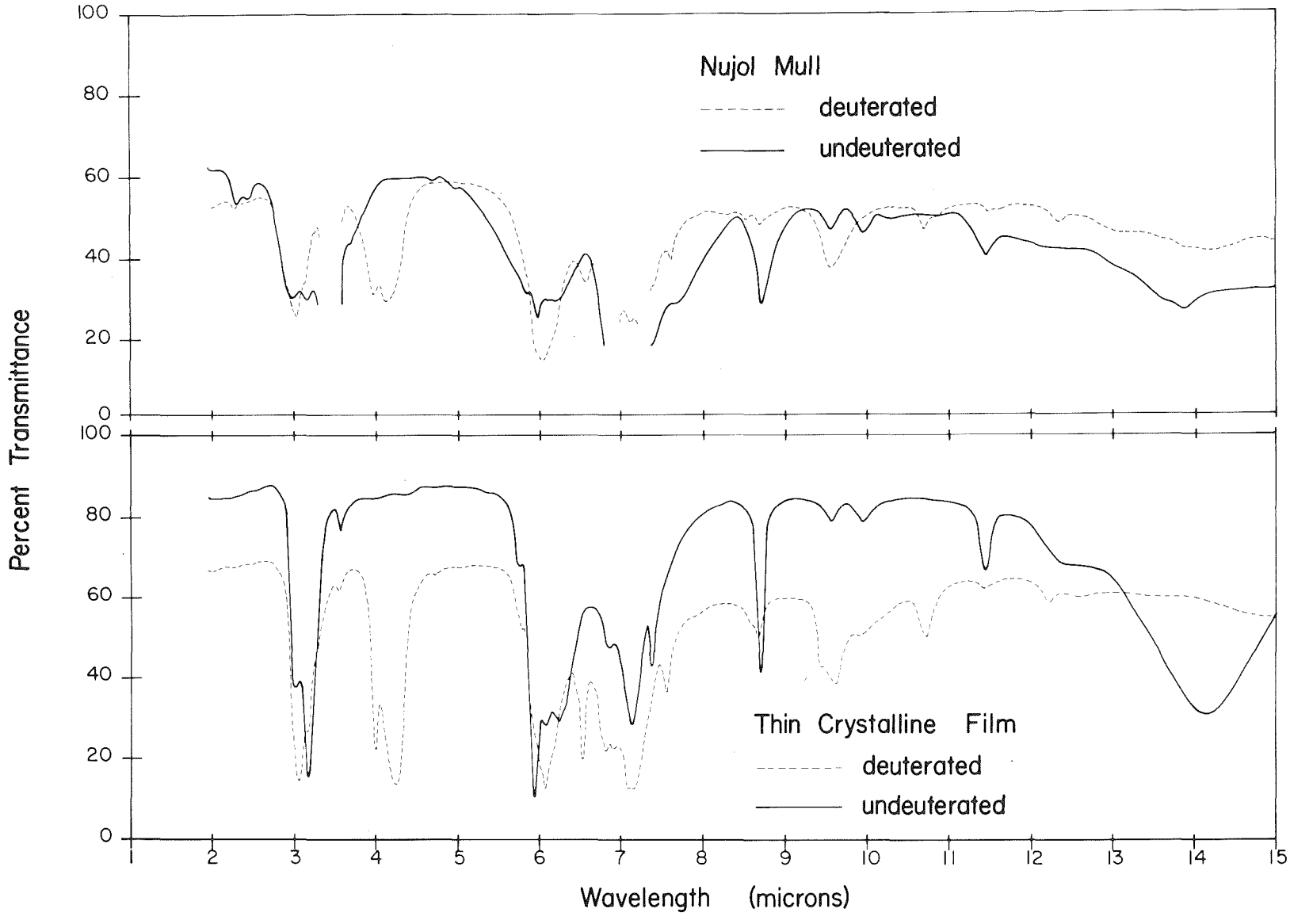
Nujol Mull
deuterated
undeuterated
Thin Crystalline Film
deuterated
undeuterated
Percent Transmittance
Wavelength (microns)
100
80
60
40
20
0
1
2
3
4
5
6
7
8
9
10
11
12
13
14
15

Figure II B - 4

Comparison of the Infrared Spectra of Acetamide in Potassium Chloride, Potassium Bromide and Potassium Iodide Matrices in the Region of 2 to 15 Microns

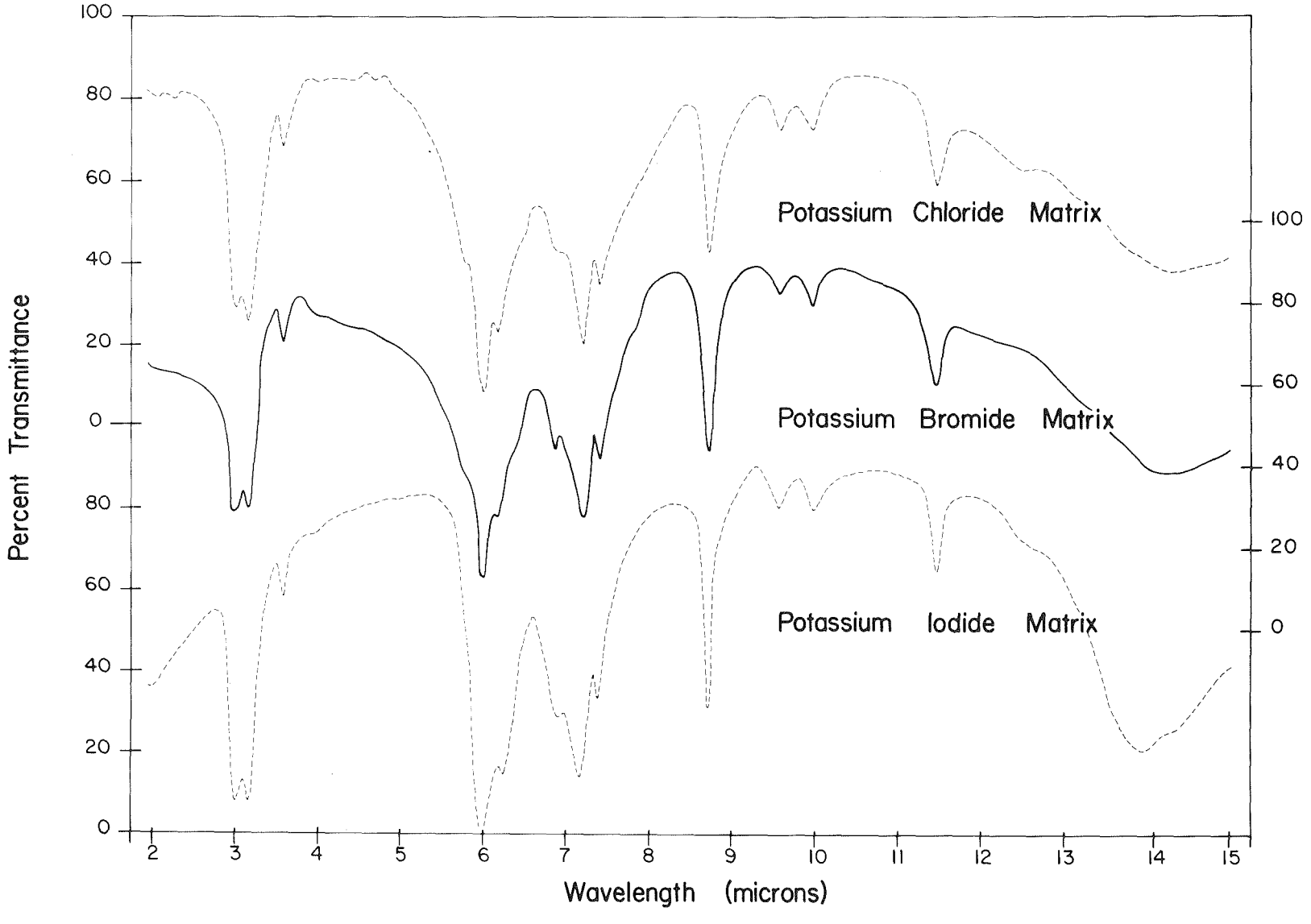
Percent Transmittance
100
80
60
40
20
0
80
60
40
20
0
Potassium Chloride Matrix
Potassium Bromide Matrix
Potassium Iodide Matrix
100
80
60
40
20
0
2
3
4
5
6
7
8
9
10
11
12
13
14
15
Wavelength (microns)

Figure II B - 5

Infrared Spectrum of Acetamide and Partially Deuterated Acetamide in a Potassium Bromide Matrix in the Region of 2 to 25 Microns

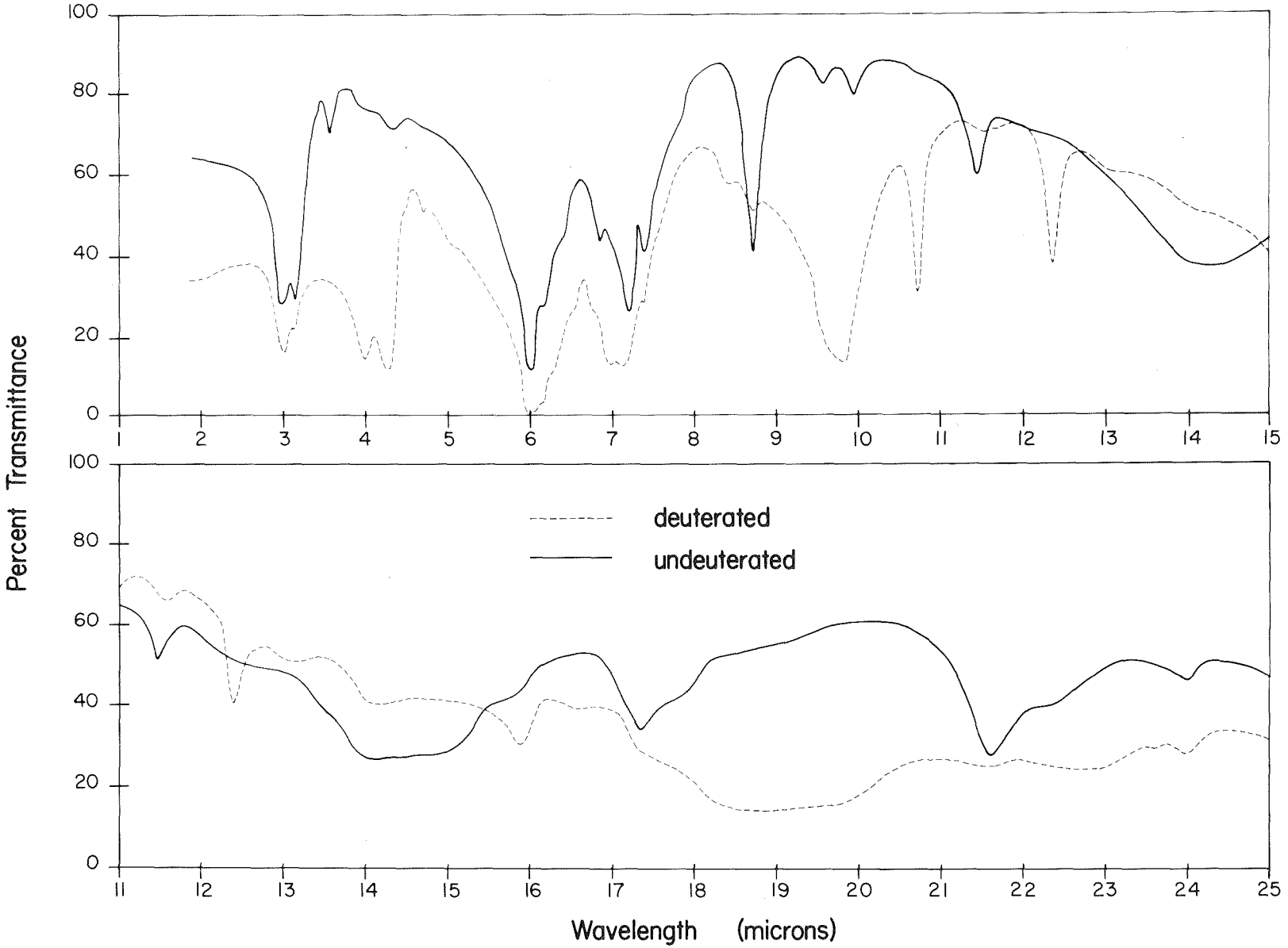
Percent Transmittance
100
80
60
40
20
0
1
2
3
4
5
6
7
8
9
10
11
12
13
14
15
deuterated
undeuterated
11
12
13
14
15
16
17
18
19
20
21
22
23
24
25
Wavelength (microns)

Table II B - 3

Observed Frequencies and Possible Frequency Assignments for Acetamide

Nujol Mull		Thin Crystalline Film		KCl Disc
(undeut'd)	(deut'd)	(undeut'd)	(deut'd)	(undeut'd)
3378 s [a]	3289 s	3300 s	3279 vs	3322 vs
3175 s	----	3155 vs	3175 w(sh)	3165 vs
----	----	----	2899 w	----
----	----	2793 mw	----	2793 ms
----	2525 s	----	2519 vs	----
----	2398 s	----	2361 vs	----
1715 w	----	1733 w(sb)	----	1730 w(sh)
1667 s	1656 vs	1684 vs 1647 s	1650 s	1667 vs
1620 s	1618 w(sh)	1607 s	----	1620 s
----	1522 mw	----	1534 s 1471 ms	----
----	----	1456 m	1449 m	1449 m(sh)
----	1406 s	1403 s	1406 vs	1391 s
----	----	1357 m	----	1351 m
----	1314 w	----	1325 m	----
----	1172 vw	----	1166 vw(sh)	----
1145 ms	1149 vw	1148 s	1148 mw	1145 s
----	----	----	1072 w(sh)	----
1047 m	1045 s	1045 mw	1041 s	1045 mw
1006 m	----	1004 mw	1008 w	1006 mw
---	935 w	----	934 m	---
873 ms	870 vw	875 ms	876 vw	873 m
---	817 w	800 m(sh)	820 w	797 ms(sh)
---	762 w	---	---	---
720 ms(b)	---	705 vs(b)	---	720 m(b)
---	---	---	---	---
---	---	---	---	---
----	---	---	---	---
---	---	---	---	---

(a) All frequencies are given in wave-numbers, cm^{-1}, and the relative intensity scale notation is as follows: s strong; ms moderately strong; m moderate or medium; mw moderately weak; w weak; vw very weak; b broad; vb very broad; sb side band; sh shoulder; sp sharp band and irr irregular.

Table II B - 3

(continued)

KBr Disc (undeut'd)	KBr Disc (deut'd)	KI Disc (undeut'd)	Assignment
3320 s	3320 s	3300 vs	νNH_2 (asym)
3180 s	3205 m(sh)	3155 vs	νNH_2 (sym)
----	----	----	
2775 w	----	2801 m	
----	2519 vs	----	νND_2 (asym)
----	2342 s	----	νND_2 (sym)
----	----	----	
1667 vs	1658 vs	1661 vs	ν C=O (Amide I)
1618 m(sh)	1620 w(sh)	1612 s	δNH_2(sc) (Amide II)
----	----	----	
1445 mw	1449 m	1443 s(sb)	δCH_3 (asym)
1393 s	1387 ms	1395 vs	ν C-CN (asym)
1350 m	1351 w	1357 m	δCH_3 (sym)
----	----	----	
----	1190 s(sb)	----	δND_2 (sc) (Amide II)
1150 s	1147 w	1148 s	γNH_2 (wag)
----	----	----	
1048 w	1040 s(b)	1045 w	ν C-CH_3
1007 mw	----	1004 w	
---	933 ms	---	γND_2 (wag)
873 m	870 w	873 m	γNH_2 (twist)
---	806 ms	815 m	
---	762 w	---	
721 m(b)	710 w	717 vs(b)	δNH_2 (rock)
---	635 w	---	γND_2 (twist)
586 w	---	---	skeletal
---	550-500 s(irr)	---	δND_2 (rock)
469 mw	---	---	skeletal

for bands between 2000 and 2500 cm^{-1} and to $\pm$ 20 cm^{-1} for bands between 2500 and 3500 cm^{-1}. Band intensities were estimated from the relative peak heights when observed in two or more spectra.

An isolated acetamide molecule would have 21 fundamental frequencies, of which six would describe the skeletal modes of the amide residue. However, such a simple system is not encountered, not even in dilute solutions,[177] due to hydrogen bonding between the hydrogens of the $-NH_2$ group and the oxygen of the carbonyl group. In the crystalline state the molecules form a ring structure held together by relatively short, non-linear N-H---O hydrogen bonds. Although the acetamide molecule is planar and in the keto configuration, the actual vibrations are such that the terms often used: carbonyl, C-N and N-H bend vibrations, may be very non-descriptive. The following paragraphs will, therefore, be a brief discussion of the frequency assignments given in Table II B - 3.

The $-NH_2$ Stretching Vibrations:

In the spectrum of undeuterated acetamide two intense bands near 3300 and the 3200 - 3150 cm^{-1} region have been observed. On deuteration the bands diminish in intensity with the appearance of two intense bands at 2500 and 2400 cm^{-1}, which gives a frequency shift factor of 1.32 and 1.33, respectively. These bands have been assigned to the asymmetric and symmetric N-H stretching modes of the $-NH_2$ group. The positions of the bands are in agreement with those reported by Reitz and Wagner for the Raman spectrum of molten acetamide[180] and by Spinner in the infrared spectrum of acetamide in a potassium bromide pressed disc.[178]

Amide I Band (Carbonyl Band):

All spectra recorded exhibit a single strong band near 1667 cm^{-1} with the exception of the thin crystalline film which gives two bands, one at 1684 cm^{-1} and a second at 1647 cm^{-1}. On deuteration the band is shifted about 10 cm^{-1} towards the low frequency end of the spectrum though the intensity remains virtually unchanged. Since the crystal structure shows the molecule to be in the keto form[181] this band is assigned to the C=O stretching mode of the amide group. Although the band is characteristic of the amide linkage it is subject to considerable alteration on change of state in which the N-H---O hydrogen bonds are presumably broken.[177,178,180,192]

Amide II Band:

A moderately strong band near 1620 cm^{-1} in alkali halide pressed disc and mull spectra and at 1607 cm^{-1} in thin crystalline film spectra almost disappears on deuteration. A new band of moderate intensity appears between 1170 - 1190 cm^{-1} in the deuterated spectrum which gives a frequency shift factor of 1.36. Previous workers have assigned this band to the NH_2 scissor mode[176,177,178] although Reitz and Wagner interpreted it as the C=N asymmetric stretching mode of the zwitter ion in solution. A mechanical normal coordinate analysis of the amide linkage by Badger[193] identified the band as being predominantly that of the scissor mode of the $-NH_2$ group. From the behavior of the band on deuteration in the present work it is assigned to the scissor mode, δNH_2 (sc), of the amide group.

1450 cm^{-1} Band:

A band found in the region of 1443 to 1456 cm^{-1} in the spectrum

of undeuterated acetamide appears to be independent of deuteration, but dependent on the matrix material. Previous investigators have assigned the band in the 1450 - 1460 cm^{-1} region to the asymmetric deformation mode of the methyl group[176,178,180] This assignment is used in the present analysis.

1400 cm^{-1} Band:

A relatively strong band apparently unaffected on deuteration is found between 1387 cm^{-1} and 1406 cm^{-1}, depending on the matrix material. Davies and Hallam reported the band at 1379 cm^{-1} with an assignment to that of the C-N stretching mode,[177] though Randall et al[179] suggested it could arise from a skeletal stretching mode. Recent work by Spinner gave the band position as 1402 cm^{-1} in a potassium bromide pressed disc, which is in good agreement with the present work, with the assignment to either the in-plane NH_2 bend or the C-C-N asymmetric stretch.[178] The X-ray analysis of crystalline acetamide by Senti and Harker[181] indicated a C-N bond length of 1.38 A, which is much shorter than the usual covalent bond length of 1.47 A. This suggests a bond strength intermediate between that of a covalent single bond and a normal double bond, which would place the frequency of the "C-N" stretching vibration somewhere between that of the C-N and C=N stretching frequencies. On the other hand, the results of a mechanical normal coordinate analysis of the amide residue, including the NH_2 hydrogens, have shown that interaction of the scissor mode of the NH_2 group with the symmetric O=C-N stretch might give rise to a band between 1303 and 1350 cm^{-1} in the acetamide spectrum. On deuteration the contribution of the symmetric stretch increases with the scissors mode now out-of-phase, so that the change

in intensity due to the interaction may be difficult to interpret.[193] From the present work it is believed that the band near 1400 cm^{-1} is associated with an asymmetric skeletal stretching mode, most probably the asymmetric C-C-N stretch.

1350 cm^{-1} Band:

A moderately strong band between 1350 and 1357 cm^{-1} appears to diminish on deuteration, though the effect may not be real. Davies and Hallam,[177] Randall et al[179] and Spinner[178] have assigned this band to the symmetric deformation mode of the methyl group. Ketones containing an α - methyl group exhibit a displacement of the symmetric methyl bending frequency from 1380 - 1370 cm^{-1} to 1360 - 1355 cm^{-1}.[149] Since the methyl group is in the α - position in acetamide, this frequency is assigned to the symmetric deformation mode of the methyl group.

1150 cm^{-1} Band:

A band of moderate intensity in the vicinity of 1150 cm^{-1} in the spectrum of undeuterated acetamide is found to decrease significantly on deuteration. A new band of comparable intensity appears at 933 cm^{-1}, which gives a frequency shift factor of 1.23. At the same time an increase in the 1040 cm^{-1} band would give a shift factor of 1.1, which may indicate partial deuteration of the NH_2 group. Previous investigators have assigned this band in the spectrum of solid acetamide to the NH_2 bend,[179,180] either the wagging or the rocking mode,[178] to the C-N bend[177] and to the asymmetric C-C-N stretch.[176] The wagging mode of the NH_2 group of methylamine has been assigned to a band in this region[195] so it is possible that the 1150 cm^{-1} band in the acetamide spectrum is also associated with this mode.

1000 cm^{-1} Region:

Two bands of almost equal intensity appear in the 1000 to 1050 cm^{-1} region in the spectrum of undeuterated acetamide, one between 1040 and 1049 cm^{-1} and the other at 1005 cm^{-1}. On deuteration both bands appear to merge into a single broad band at 1040 cm^{-1}, with an increase in the band intensity. The unusual deuteration behavior may be due to a superposition of the 1150 cm^{-1} band slightly shifted as a result of partial deuteration of the NH_2 group and the merging of the 1040 cm^{-1} and 1005 cm^{-1} bands. The appearance of a moderately intense band at 806 cm^{-1} in the deuterated spectrum would give frequency shift ratios of 1.29 and 1.23 for the 1040 cm^{-1} and 1005 cm^{-1} bands, respectively, if they are associated with the NH_2 group.

Previous workers assigned bands at 1045 cm^{-1} and 986 cm^{-1} to the C-C stretch,[177] and the NH_2 bend.[179] In the case of formamide Kahovic and Wassmuth[196] identified the 1000 cm^{-1} Raman line with the asymmetric out-of-plane NH_2 deformation mode. However, the bands in acetamide might well be associated with symmetric skeletal stretching modes of the amide residue, shown schematically as

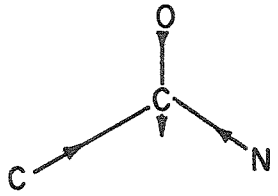

since the $-NH_2$ group and the oxygen atom have the same mass and the C-NH_2 and C=O bond lengths differ only by 0.1 A. In this scheme the 1040 cm^{-1} band may well be the C-C-N symmetric stretch and the 1005 cm^{-1} band the C-C=O symmetric stretch. Both bands are con-

sidered essentially a CH_3-C stretch, and have been designated as such in the present analysis.

875 cm^{-1} Band:

A moderately intense band near 874 cm^{-1} in the undeuterated spectrum almost disappears on deuteration with the appearance of new bands at lower frequencies. The relatively strong band at 806 cm^{-1}, with a shift factor of 1.08, and the relatively weak band at 635 cm^{-1}, with a shift factor of 1.37, in the deuterated spectrum indicates that the 874 cm^{-1} band is associated with the NH_2 group. The 806 cm^{-1} band may arise from the NHD group by partial deuteration and the 635 cm^{-1} band from the ND_2 group on complete deuteration.

Previous workers have assigned the 870 cm^{-1} band to the symmetric skeletal stretch,[176,178] the in-plane C-C-N bend,[180] the O=C-NH_2 bend[177] and the NH_2 torsional mode.[177] Primary amines show broad absorption in the region of 900 to 650 cm^{-1} which alters in shape and frequency with alterations in the degree of hydrogen bonding[197] and may arise from the NH_2 deformation mode.[195] From the behavior of the 875 cm^{-1} band of acetamide in the present work it has been assigned to the NH_2 twisting mode.

720 cm^{-1} Band:

An extremely broad, moderately intense band between 705 and 720 cm^{-1} in the spectrum of undeuterated acetamide almost disappears on deuteration. The appearance of a broad, irregular type band in the region of 550 to 500 cm^{-1} in the deuterated spectrum gives a frequency shift ratio of 1.35. Davies and Hallam suggested the O=C-NH_2 bend or

the NH_2 torsional mode as possible assignments.[177] though Kahovic and Wassmuth assigned the 691 cm^{-1} Raman line of formamide to the NH_2 in-plane asymmetric bend.[196] Since the NH_2 group modes can, to a first approximation, be compared with those of the methylene group, the methylene rocking motion in long chain n-paraffins at 720 cm^{-1} is assumed to describe the motion of the NH_2 group in acetamide for absorption in the same region.

586 cm^{-1} Band:

The relatively weak band at 586 cm^{-1} has been observed only in potassium bromide pressed disc spectra. On deuteration the band either disappears or is swallowed up in the broad, irregular absorption in the 550 - 500 cm^{-1} region. Medium effects are pronounced for this band as it has been reported as high as 585 cm^{-1} in the solid state[178,180] and as low as 537 cm^{-1} in solution.[178] Lecomte and Freyman assigned this band to the asymmetric C-C-N skeletal bend,[176] shown schematically as

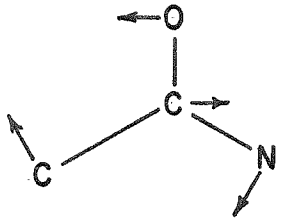

The intensity and postion of the band suggest a skeletal mode, but a detailed description of the skeletal mode is not possible from the present work. The assignment of Lecomte and Freyman is used in the present analysis since deuteration could very well shift the band into the broad absorption of the 550 - 500 cm^{-1} region.

470 cm^{-1} Band:

A relatively weak band at 469 cm^{-1} in the potassium bromide pressed disc spectrum of undeuterated acetamide does not appear in the spectrum of the deuterated material. From previous studies the band between 450 cm^{-1} and 465 cm^{-1} has been assigned to a skeletal mode, possibly the symmetric C-C-N bend.(176) Such an assignment is used in the present analysis.

Acetamide Hemihydrochloride:

Spectra of acetamide hemihydrochloride as a Nujol mull and as a thin crystalline film and in pressed discs of potassium chloride, bromide and iodide are reproduced in Figures II B - 6 and - 7, respectively. Several peculiarities common to all spectra are immediately apparent. First of all the background absorption is extremely broad and very intense, increasing gradually from about 2000 cm^{-1} to a fairly sharp cut-off near 600 cm^{-1} with a maximum in the region of 800 - 900 cm^{-1}. Second of all a very deep "window" suddenly appears in the vicinity of 900 cm^{-1}, almost at the broad background absorption maximum, though two smaller "windows" are found near 1150 cm^{-1} and 1050 cm^{-1}. Finally, deuteration causes a marked decrease in the depth of the "windows" with a noticeable spreading out of the broad, intense background towards lower frequencies (Figure II B - 8). The shape of the "windows" would at first suggest anomalous dispersion sometimes found in mull spectra of organic compounds,(198) but the invariance of the position of the "windows" with matrix material as well as the results of deuteration, makes this simple explanation doubtful. It seems probable that the

Figure II B - 6

Infrared Spectrum of Acetamide Hemihydrochloride as a Mull and as a Thin Crystalline Film in the Region of 2 to 15 Microns

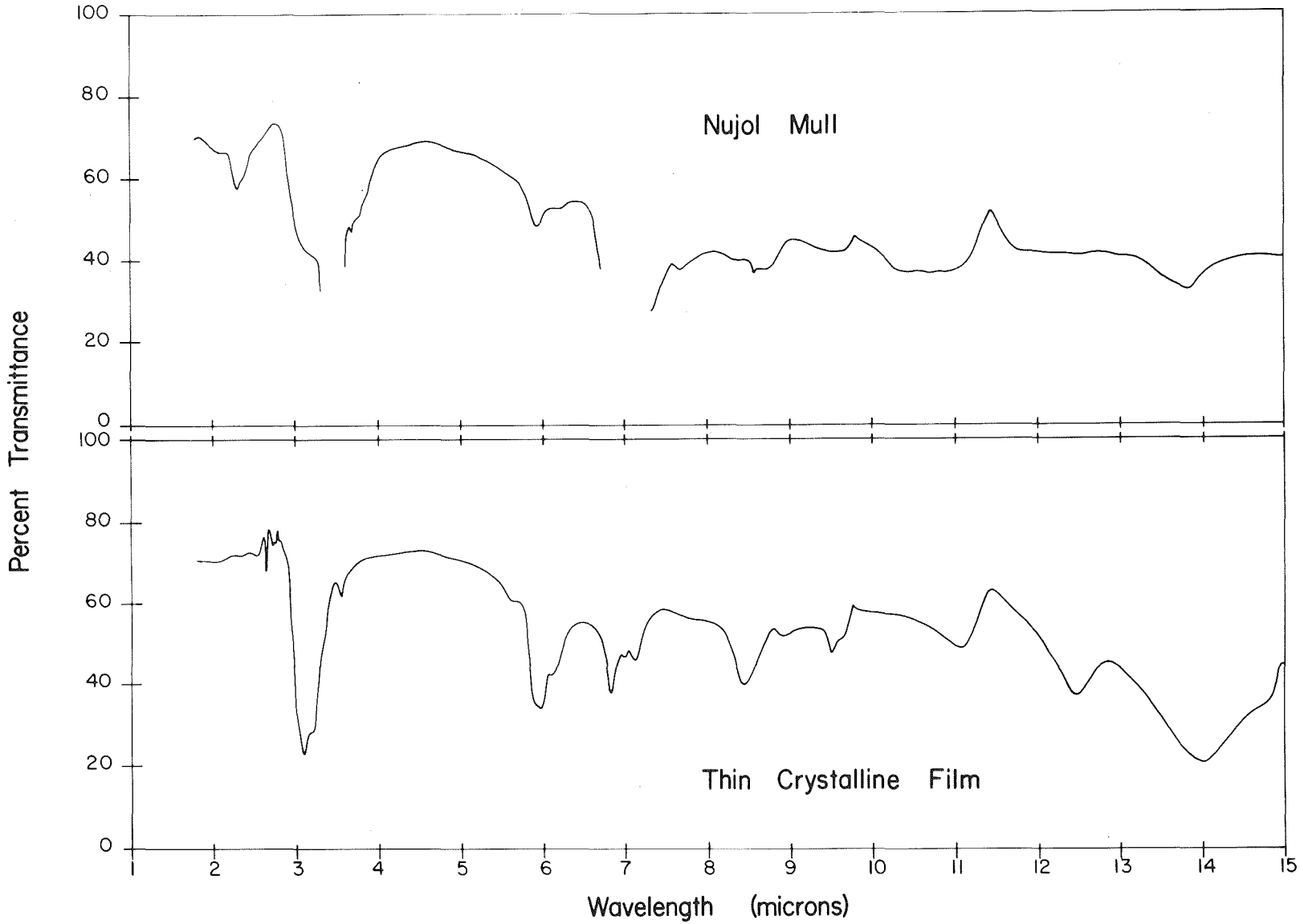
Percent Transmittance
100
80
60
40
20
0
Nujol Mull
100
80
60
40
20
0
Thin Crystalline Film
1
2
3
4
5
6
7
8
9
10
11
12
13
14
15
Wavelength (microns)

Figure II B - 7

Comparison of Infrared Spectra of Acetamide Hemihydrochloride in Potassium Chloride, Potassium Bromide and Potassium Iodide Matrices in the Region of 2 to 15 Microns

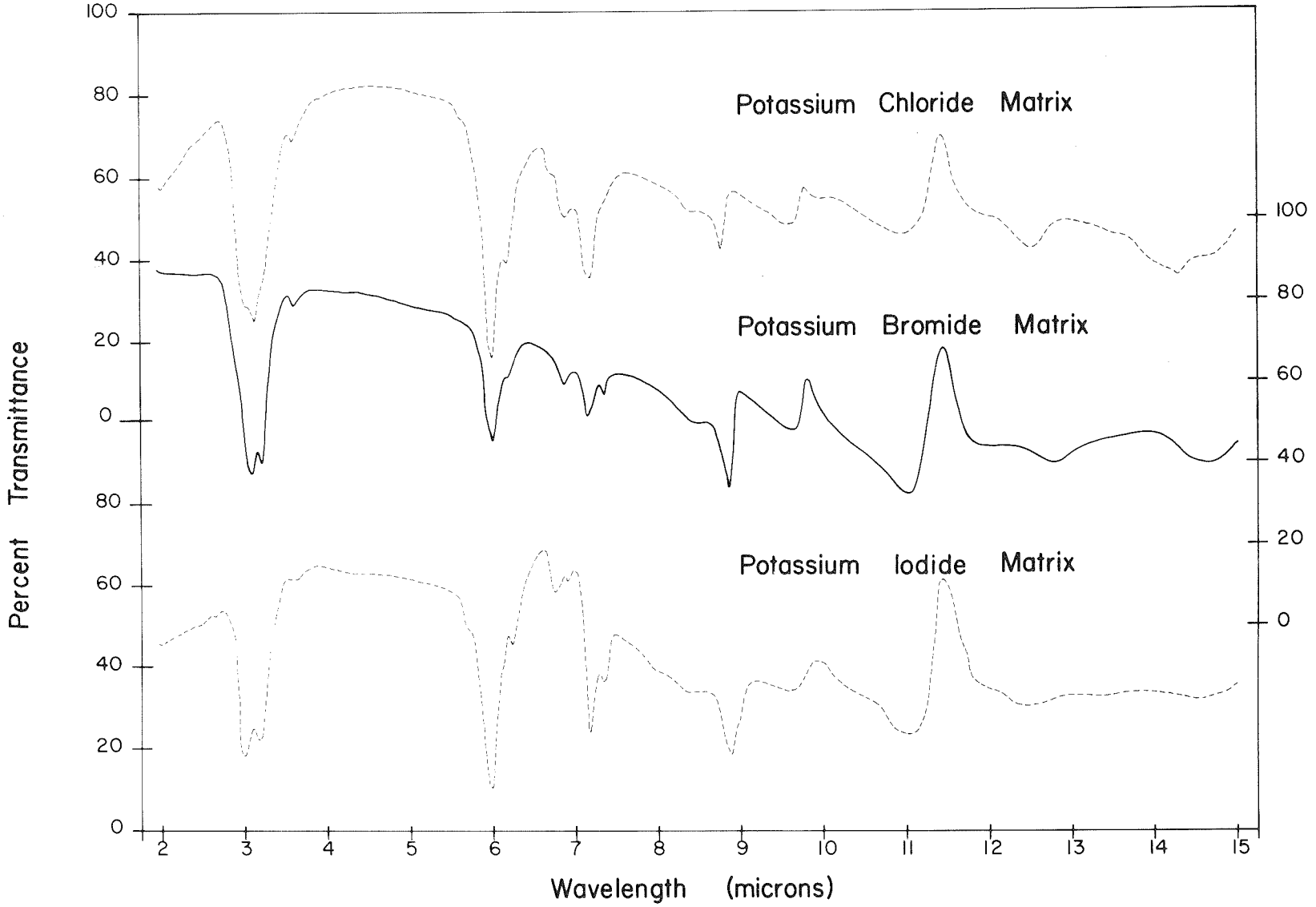
Potassium Chloride Matrix
Potassium Bromide Matrix
Potassium Iodide Matrix
Percent Transmittance
100
80
60
40
20
0
Wavelength (microns)
2
3
4
5
6
7
8
9
10
11
12
13
14
15

Figure II B - 8

The Infrared Spectrum of Acetamide Hemihydrochloride and Partially Deuterated Acetamide Hemihydrochloride in a Potassium Bromide Matrix in the Region of 2 to 25 Microns

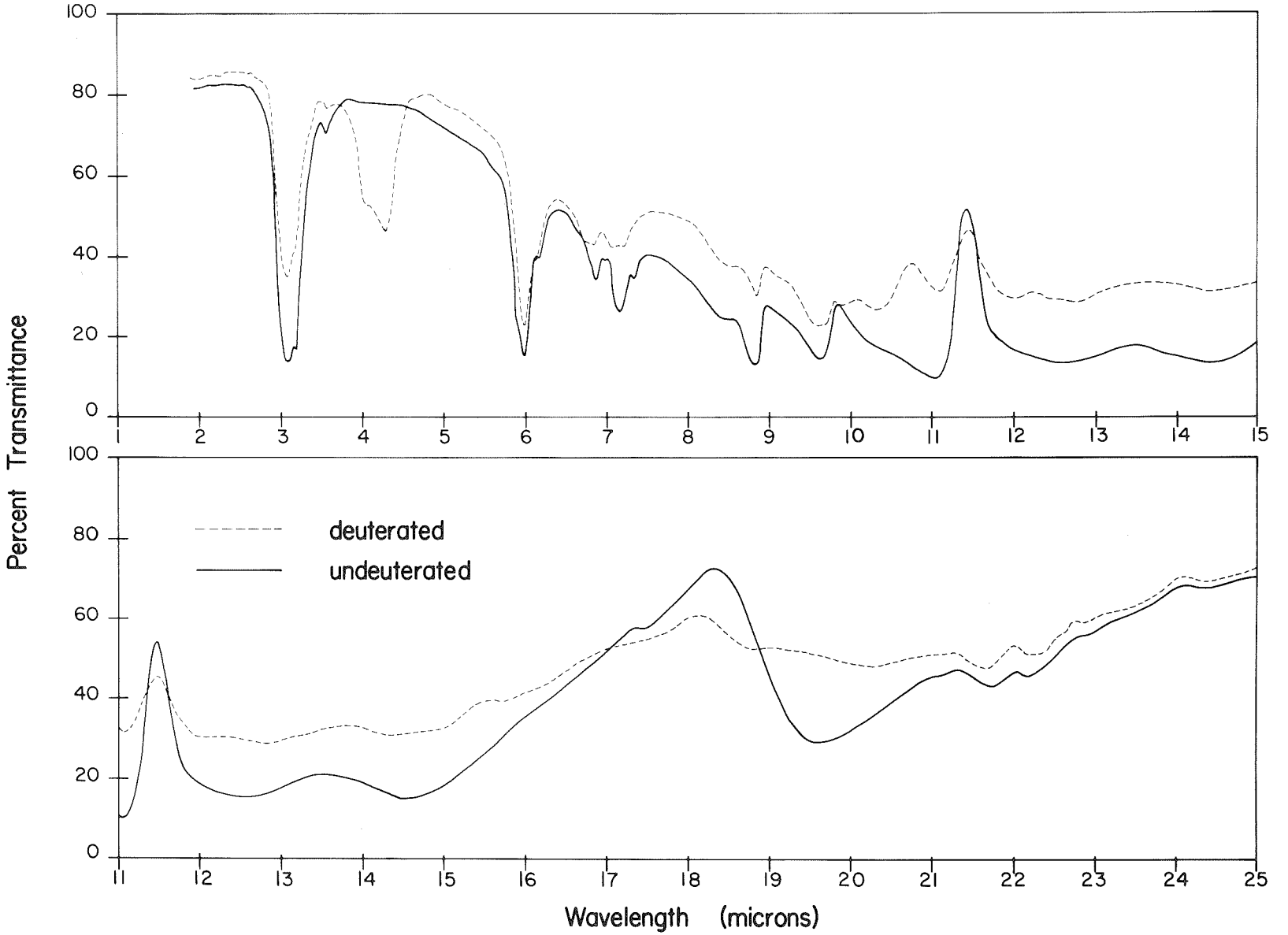
Percent Transmittance
100
80
60
40
20
0
1
2
3
4
5
6
7
8
9
10
11
12
13
14
15
deuterated
undeuterated
11
12
13
14
15
16
17
18
19
20
21
22
23
24
25
Wavelength (microns)

peculiar features are associated with the vibrational modes of the hemihydrochloride molecule. Further justification of this assumption is found in the spectra of N-(t-butyl) - acetamide complexes of hydrohalic acids [199] which exhibit peculiarities very similar to those observed in this work, both in the crystalline state and in chloroform solutions.

A comparison of the spectrum of acetamide hemihydrochloride with that of the parent compound acetamide in a potassium bromide matrix (Figure II B - 9) reveals the "windows" in the hemihydrochloride spectrum coincide with relatively weak absorption bands in the acetamide spectrum. A similar weak absorption band to "window" correspondence is observed in the spectra of the N-(t-butyl) - acetamide hemihydrobromide complex of White.[199] It is very unlikely the correspondence is accidental.

Before discussing the unusual background intensity and the "windows" it will be advantageous to make assignments to as many of the absorption bands as possible in the hemihydrochloride spectrum. The position and relative intensity of the bands and "windows" for the undeuterated and partially deuterated hemihydrochloride in the various matrices have been tabulated in Table II B - 4, along with the possible frequency assignments to be discussed in the following paragraphs.

In making the frequency assignments one is tempted to make a one to one correspondence between the absorption bands of the hemihydrochloride and those of acetamide. Although the structural parameters of the acetamide portion of the hemihydrochloride are almost

Figure II B - 9

A Comparison of the Infrared Spectra of Acetamide and Acetamide Hemihydrochloride in a Potassium Bromide Matrix in the Region of 2 to 25 Microns

Acetamide

Acetamide Hemihydrochloride

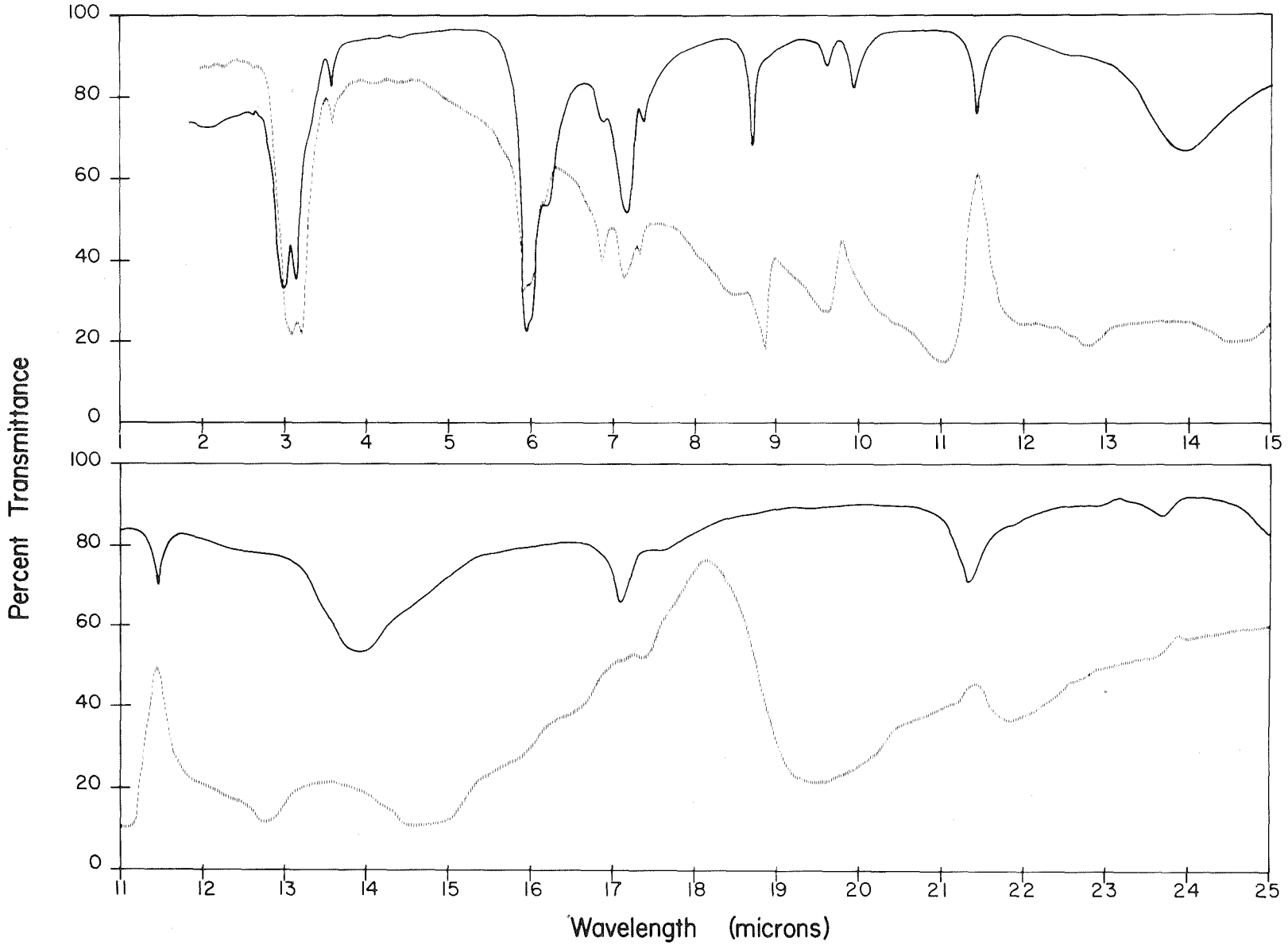
Percent Transmittance
100
80
60
40
20
0
1
2
3
4
5
6
7
8
9
10
11
12
13
14
15
11
12
13
14
15
16
17
18
19
20
21
22
23
24
25
Wavelength (microns)

Table I I B - 4

Observed Frequencies and Possible Frequency Assignments for Acetamide Hemihydrochloride

Nujol Mull (undeut'd)[a]	Crystalline Film (undeut'd)	KCl Disc (undeut'd)	KI Disc (undeut'd)
3300 m(b)	3220 s	3300 vs(sh)	3300 vs
----	3120 m(sb)	3195 vs	3145 vs
2800 w	2800 w	2786 mw	----
----	----	----	----
----	----	----	----
----	----	----	1715 w
1671 ms	1688 w(sb)	1667 vs	1667 vs
	1671 s		
1613 m	1640 w(sh)	1621 m	1605 ms
----	1460 m(sp)	1453 ms	1460 w
----	1435 w	----	----
----	1408 m	1399 s	1389 s
----	----	----	1362 ms
1168 w	1185 s	1190 mw(sh)	1190 m(sh)
1149 mw(b)	----	1148 m	1136 s
	1055 mw		
1042 m(b)	1040 w(sh)	1040 m	1038 ms
1031 m*	----	1028 m*	1009 ms*
---	---	---	---
---	---	---	---
---	905 s(asym)	---	905 s(b)
875 s*	---	876 s*	874 s*
---	802 s(b)	800 ms	---
---	725 vs(vb)	700 vs(vb)	---
---	---	---	---
---	---	---	---
---	---	---	---
---	---	---	---
---	---	---	---

(a) All frequencies reported in wave-numbers; the relative intensity scale notation is as follows: s strong; ms moderately strong; m moderate or medium; mw moderately weak; w weak; vw very weak; b broad; vb very broad; sb side band; sh shoulder; sp sharp band and asym asymmetric band.

(*) Bands so marked appear as "window".

Table II B - 4

(continued)

KBr Disc

(undeut'd)	(deut'd)	Assignment
3247 vs	3215 s	νNH_2
3115 vs	3125 m(sb)	νNH_2
2778 w	----	
----	2469 m(sb)	νND_2
----	2320 s	νND_2
----	----	
1667 vs	1667 s	$\nu C{=}O$ (Amide I)
1618 s(sh)	----	δNH_2 (sc) (Amide II)
1466 m	1475 ms	δCH_3 (asym)
----	----	
1401 ms	1401 m	$\nu O{=}C{-}N$ (asym) or $\nu C{-}C{=}N$ (asym)
1361 m	?	δCH_3 (sym)
1186 m(sh)	1170 m(sh)	skeletal stretch ?
1130 s	1136 m	γNH_2 (wag)
	1124 ms*	
	1052 w	
1040 m	1038 w	$\nu C{-}CH_3$
1022 ms*	1025 w*, 1015 w	" "
---	968 w	γND_2
---	934 m*	
905 s(b)	905 m	?
875 s*	875 ms*	γNH_2 (twist) ?
781 w(b)	800 w(b)	
---	---	
690 s(vb)	---	δNH_2 (rock)
575 w(sb)	---	?
509 s(b)	500 w(b)	skeletal bend
461 w	468 w	?
432 w	448 w	?

identical with those of acetamide, see Table II B - 2, the type of hydrogen bonding responsible for the molecular packing is radically different. In acetamide the molecules are held in a ring structure by relatively short N-H---O hydrogen bonds whereas in the hemihydrochloride the acetamide residues form a distorted egg-crate structure by a series of N-H--Cl--H-N and O--H--O hydrogen bonds. One must, therefore, proceed with caution in making the corresponding frequency assignments.

The NH_2 Stretching Modes:

Two intense bands near 3300 cm^{-1} and 3150 cm^{-1} in the spectrum of the undeuterated hemihydrochloride are reduced in intensity on deuteration. Two strong bands appear at 2470 cm^{-1} and 2300 cm^{-1} in the deuterated spectrum which gives a frequency shift factor of 1.31 and 1.35, respectively. From the NH_2 frequency shift - N---Cl distance correlations for N-H--Cl type hydrogen bonds[49,69] the N---Cl distances of 3.24 A and 3.31 A in the hemihydrochloride should give rise to shifted NH_2 stretching frequencies near 3150 cm^{-1} and 3250 cm^{-1}, respectively. The calculated values from the correlations are in excellent agreement with the observed band positions. Kahovec and Knollmuller[186] assigned only the 3250 cm^{-1} Raman line of acetamide hemihydrochloride to the NH_2 stretch though a moderately strong line was found at 3127 cm^{-1}. It seems certain that the two strong bands in the infrared spectrum of acetamide hemihydrochloride at 3150 cm^{-1} and 3300 cm^{-1} are the NH_2 stretching frequencies shifted as a result of hydrogen bonding with the Cl^- ion.

The NH_2 vibrations are, however, peculiar in that the

intensitites of the bands are about four times those of the same bands in acetamide and are shifted between 50 - 80 cm^{-1} towards lower frequencies although the N---O distance in acetamide is about 0.5 A shorter than the N---Cl distance in the hemihydrochloride. However, the Cl is present in the hemihydrochloride as the Cl^- ion so that the hydrogens of the amine group are displaced from their normal N-H distance of about 0.99 A to a somewhat larger distance. Moreover, the C-N distance of the acetamide residue of the hemihydrochloride is rather short which would indicate possible resonance structures with a positive charge on the N atom. The hydrogens would move into a position nearer the Cl^- ion to accommodate the new charge distribution. If this is true the N-H---Cl^--- hydrogen bond in the hemihydrochloride is stronger than the N-H---O hydrogen bonds of acetamide.

Amide I Band (Carbonyl Stretch):

According to the O---O distance - OH frequency shift correlations for O--H--O type hydrogen bonds[49,50,56,57] the 2.40 A O---O distance in acetamide hemihydrochloride should give a shifted OH stretch absorption band in the region between 2000 cm^{-1} and 1500 cm^{-1}. This assumes the hydrogen is located between the two O atoms of the acetamide residues.* The only defined bands in this

---

* The neutron diffraction study of acetamide hemihydrochloride was recently carried out at Oak Ridge National Laboratory by Dr. S. W. Peterson. His results confirm those of Takei found by X-ray diffraction, but in addition they actually located a hydrogen peak at the center of symmetry between two oxygens. (Private communication from Dr. E. W. Hughes, California Institute of Technology, May, 1959). I have not been able to obtain any further information about the structure of the hydrogen bond, particularly if it is a true symmetric hydrogen bond.

region are the strong band at 1667 cm^{-1} and a moderately weak side band at 1618 cm^{-1}. On deuteration the 1667 cm^{-1} band remains virtually unchanged while the 1618 cm^{-1} side band disappears. The corresponding bands in acetamide have been assigned to the Amide I (Carbonyl Stretch) and the Amide II (NH_2 scissors) modes, respectively. Kahovec and Knollmuller [186] did not report a Raman line in this region, which they interpreted as evidence for a non-carbonyl type structure. The X-ray data indicates that the C-O bonds are of equal length and are about 0.03 A longer than a normal C=O bond.[200] This is a fair indication that the 1667 cm^{-1} band is associated with the stretching mode of the carbonyl group and that the presence of the proton between the two oxygens has little or no bonding with either oxygen to give a C-O structure although recent n. m. r. studies have shown that O-protonation of acetamide occurs in 100 per cent sulfuric acid.[201]

The weak 1618 cm^{-1} band may well correspond to the Amide II mode of acetamide since the band disappears on deuteration. No new band has been observed in the deuterated spectrum which could be assigned to the 1618 cm^{-1} band because of the intense background absorption in the expected region. Thus, any weak deuterated band would be swallowed up in the background absorption.

In passing it should be noted that the integrated intensity under the absorption curve of the hemihydrochloride is almost twice that of acetamide in the 2000 cm^{-1} to 1500 cm^{-1} region. This is an indication of the beginning of the broad, intense background absorption prominent in the acetamide hemihydrochloride spectrum.

1400 cm^{-1} Region:

Three bands are present in the 1550 cm^{-1} to 1300 cm^{-1} region of the spectrum of undeuterated acetamide hemihydrochloride; a moderately strong band near 1460 cm^{-1}, a moderately strong band near 1400 cm^{-1} and a medium band at 1367 cm^{-1}.

The 1460 cm^{-1} band is unaffected by deuteration while the 1360 cm^{-1} band appears to disappear. The disappearance of the 1360 cm^{-1} band may be due to the spreading of the 1400 cm^{-1} band in the deuterated spectrum. The 1460 cm^{-1} and 1360 cm^{-1} bands have corresponding bands in the spectrum of acetamide, which were assigned to the asymmetric and symmetric deformation modes of the methyl group. These assignments have been used in the analysis of the hemihydrochloride spectrum.

The position and intensity of the 1400 cm^{-1} band depends on the matrix material. It is found at 1389 cm^{-1} in a potassium iodide pressed disc and in the crystalline film two bands are found, a moderately intense band at 1408 cm^{-1} and a relatively weak band at 1435 cm^{-1}. A moderately strong Raman line has been reported at 1414 cm^{-1} by Kahovec and Knollmuller.[186] The position of the band compares favorably with the asymmetric C-C-N skeletal stretch of acetamide, but the intensity and deuteration behavior are are different. In the hemihydrochloride the C-N distance is between 0.06 to 0.08 A shorter than the C-N distance in acetamide[181,184] which indicates the C-N bond in the hemihydrochloride is not a normal covalent single bond but nearer that of a C=N bond.[200] The contraction may be due to a large contribution of a $-C=\overset{+}{N}H_2$

structure which would be stabilized by the Cl^- ion nearby. It is possible that this band is associated with either the $O=C=\overset{+}{N}$ asymmetric stretch or the $C-C=\overset{+}{N}$ asymmetric stretch. The former mode would in part account for the bands behavior on deuteration.

1200 - 1100 cm^{-1} Region:

A moderately strong shoulder apparently unaffected by deuteration is found at 1186 cm^{-1}. No corresponding band exists in the acetamide spectrum and Kahovec and Knollmuller [186] did not report a band at this position in the Raman spectrum though they did find a moderately strong line at 1151 cm^{-1}. The only group that could conceivably give rise to absorption in this region would be a -C-N stretch[202] though the C-N distance in the hemihydrochloride makes such an assignment questionable. It may well be a skeletal stretching mode, such as the asymmetric C-C-N stretch, but is unassigned in this work.

A strong band is found at 1136 cm^{-1} in the undeuterated spectrum, which is on the edge of the first "window". The position of the band is, therefore, not very reliable. Kahovec and Knollmuller found a Raman line at 1150 cm^{-1} which was not assigned to any particular mode. On deuteration the 1136 cm^{-1} band in the infrared spectrum is reduced in intensity along with a decrease in the depth of the "window." A moderately weak "window" appears at 934 cm^{-1} with weak side bands at 968 cm^{-1} and 905 cm^{-1} in the deuterated spectrum, which gives a frequency shift factor of 1.17 to 1.26. The behavior of this band is similar to the 1150 cm^{-1} band of acetamide which was assigned to the NH_2 wagging mode. Therefore, the 11 36 cm^{-1} band in the hemihydro-

chloride may be associated with the NH_2 wagging mode.

1000 cm^{-1} Region:

In this region of the spectrum a moderately strong "window" is found at 1022 cm^{-1}. On deuteration the depth of the "window" is reduced considerably and a weak side band appears at 1015 cm^{-1}. The background intensity, however, remains unusually strong. Kahovec and Knollmuller[186] reported a moderately strong Raman line at 1029 cm^{-1}, which is close to the position of the minimum of the "window" observed in the infrared spectrum in the present work. In the acetamide spectrum two relatively weak bands are found at 1040 cm^{-1} and 1007 cm^{-1}, which have been assigned to stretching modes of the $-C-CH_3$ group. Since the $-C-CH_3$ bond length in the hemihydrochloride is the same as that in acetamide, vibrational modes associated with the $-C-CH_3$ group should have approximately the same frequency. Therefore, the "window" at 1022 cm^{-1} is attributed to the stretching mode of the $-C-CH_3$ group. The unusual feature of the "window" is that the vibrational mode is strong in the Raman spectrum but only relatively weak in the infrared spectrum.

900 cm^{-1} Region:

The region between 1000 cm^{-1} and 800 cm^{-1} in the infrared spectrum of the hemihydrochloride is almost structureless with the exception of the deep "window" at 875 cm^{-1} in the middle of the broad, intense background. On deuteration the depth of the "window" is reduced considerably but the surrounding region is still very intense and irregular in structure. The 1000 - 900 cm^{-1} region of the deuter-

ated spectrum is changed by the appearance of a new "window" at 934 cm^{-1} and two weak side bands at 968 cm^{-1} and 905 cm^{-1}. These effects have been attributed to the NH_2 wagging mode shifted to lower frequencies on deuteration. In the Raman spectrum Kahovec and Knollmuller have observed a weak line at 943 cm^{-1} and a strong line at 891 cm^{-1}. In the acetamide spectrum a moderate band is found at 870 cm^{-1}, which has been assigned to the NH_2 twist. The coincidence of the "window" of the hemihydrochloride with the NH_2 twist of acetamide and the appearance of a new "window" in the deuterated spectrum due to a shift in the NH_2 wagging mode suggests some interaction is taking place between the amine groups out-of-plane modes and the broad, intense background absorption. This effect will be discussed more fully in Section F.

700 cm^{-1} Region:

A very broad band superimposed on the intense background is found at 690 cm^{-1}. On deuteration the band is reduced in intensity and is almost swallowed up by the intense background absorption which has been shifted slightly towards lower frequencies. An increase in the intensity of the deuterated spectrum near 510 cm^{-1} might well be due to the shifted 690 cm^{-1} band. This would give a frequency shift ratio of 1.36. Kahovec and Knollmuller found a weak Raman line at 715 cm^{-1} which was not given an assignment. In the acetamide spectrum a broad band in this region was assigned to the rocking mode of the NH_2 group. The behavior of the 690 cm^{-1} band in the hemihydrochloride suggests an NH_2 mode and is, therefore, assigned to the NH_2 rock.

500 cm^{-1} Region:

The only band of significant intensity in this region of the undeuterated hemihydrochloride is the band at 509 cm^{-1}. Two weak bands are also found at 461 cm^{-1} and 432 cm^{-1}. On deuteration the 509 cm^{-1} appears to merge into the broad, intense background which has been shifted towards lower frequencies. The two weak bands are apparently unaffected. Bands with frequencies in this region of the spectrum would be due to skeletal bending modes. Unique assignments of these bands are not possible though it is possible that the 509 cm^{-1} band is associated with an asymmetric skeletal bend involving the NH_2 group because of the apparent deuteration shift.

In the above spectral analysis none of the absorption bands have been attributed to a shifted OH stretching frequency , or to vibrational modes of a symmetric hydrogen bond. In fact, most of the bands could be assigned to corresponding bands in acetamide . This seems to indicate that the hydrogen bond in acetamide hemihydrochloride is symmetric. The broad, intense background absorption is undoubtedly associated with the vibrational modes of this short, symmetric hydrogen bond. Support for this assumption is the comparison of the relative integral absorption intensity of acetamide and acetamide hemihydrochloride and the number of oscillating proton charges responsible for the band intensity.

The infrared absorption spectra of acetamide and acetamide hemihydrochloride in a potassium bromide matrix for the spectral region between 400 cm^{-1} and 2000 cm^{-1} on a linear wave-number - absorbance scale are reproduced in Figure II B - 10. The absorbance is expressed as an absorption coefficient defined as $(1/n) \log (I_o/I)_\nu$, where n is the number of molecules per cm^2. The left hand scale

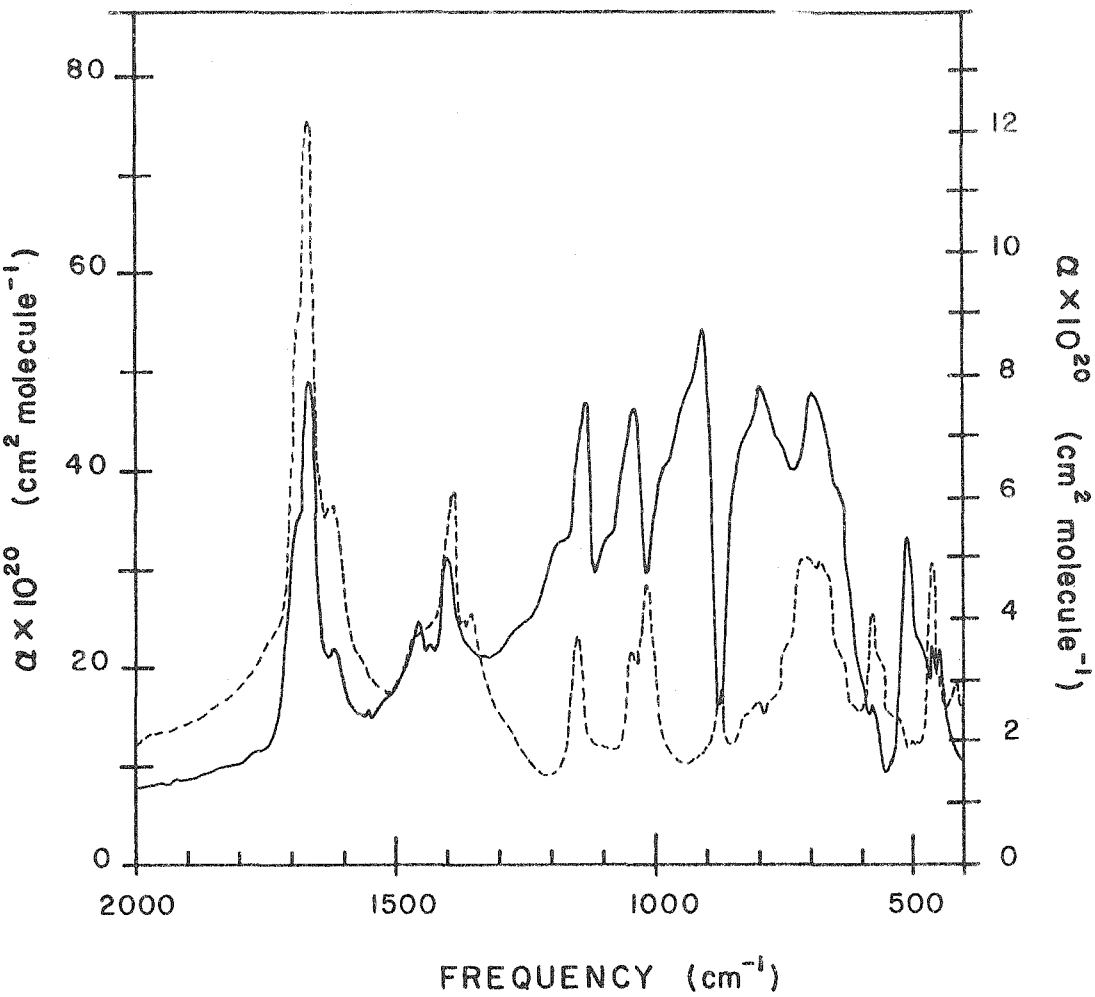

FIGURE IIB-10

Infrared Absorption Spectra of Acetamide (---) and Acetamide Hemihydrochloride (——) Between 400 and 2000 cm^{-1} in a Potassium Bromide Matrix

refers to acetamide hemihydrochloride and the right hand scale to acetamide. Absolute measurements of intense absorption in solids are difficult to make and may not have a simple interpretation in the case of potassium bromide matrices since it is not always easy to distinguish between scattering and true absorption. Therefore, the estimated absorption intensities may be off by almost an order of magnitude as was shown in the case of the intense ν_3 absorption band of the bifluoride ion in a potassium bromide matrix when compared with the single crystal value (see Section A of Part II). Nevertheless, a comparison of the apparent integral absorption intensity of acetamide and acetamide hemihydrochloride in intervals between 2000 cm^{-1} and 400 cm^{-1} reveals rather striking results. The measured values for the two compounds have been tabulated in Table II B - 5. Between 2000 - 1500 cm^{-1} the hemihydrochloride is about 1.6 times as intense and is over 13 times as intense in the interval between 1250 - 700 cm^{-1}. The intensity would be even greater had not the "window" been produced in the overall band contour.

If one naively compares the apparent integral absorption intensities of acetamide and its hemihydrochloride in the 1550 - 550 cm^{-1} region one finds an excess in the latter case which if one assumes that the reduced mass of the vibrating system is that of the proton, suggests the motion of considerably more than one proton charge.** The pertinent data and results have been tabulated in Table II B - 6.

** The equations used in the above calculations and evaluation of the apparent integral absorption intensity from the absorption curves have been derived and discussed in Section A of Part II of this thesis.

Table II B - 5

Comparison of the Integral Absorption Intensity of Acetamide and Acetamide Hemihydrochloride in a Potassium Bromide Matrix in Intervals Between 2000 cm^{-1} and 400 cm^{-1}

	Acetamide Hemihydrochloride			Acetamide			
Interval (cm^{-1})	B* (cm^{-1})	c** (mmol)	$(B/c)_a$	B* (cm^{-1})	c** (mmol)	$(B/c)_b$	$\frac{(B/c)_a}{(B/c)_b}$
2000 - 1500	123	0.0186	6627	222	0.0542	4097	1.62
1500 - 1250	108	0.0186	5805	92	0.0542	1700	3.41
1250 - 700	412	0.0186	22140	91	0.0542	1680	13.2
700 - 400	126	0.0175	7200	178	0.0542	3260	2.2
2000 - 400	---	------	41770	---	------	10740	3.9

* B is defined as $\int \log(I_o/I)_\nu \cdot d\nu$

** c is defined in terms of mmoles of acetamide per gm. KBr.

Table II B - 6

Comparison of the Number of Oscillating Proton Charges in Acetamide and Acetamide Hemihydrochloride in a Potassium Bromide Matrix from the Integral Absorption Intensity in the Region of 1550 cm^{-1} to 550 cm^{-1}

Compound	$(B/n)\times 10^{20}$ (cm^2 $mol.^{-1}$ cm^{-1})	$\mu(k)$ (Debyes/A)	$f(k)$*
Acetamide	2760	3.01	0.63
Acetamide Hemihydrochloride	31370	10.2	2.11

* $f^{(k)}$ is the number of oscillating proton charges.

When one takes into account the number of acetamide residues in the hemihydrochloride the proton charge in excess is found to be about 1.2 to 1.4. This may indicate that the frequencies of two or more of the proton vibrations are nearly coincident, as they are in the bifluoride ion in crystalline potassium bifluoride and in a potassium bromide solid solution. If this is true then the O--H--O hydrogen bond in acetamide hemihydrochloride is probably symmetric.

The "windows" are the last peculiar feature of the hemihydrochloride spectrum to be considered. In making the frequency assignments it was noted that the position of the "windows" coincided with reported medium to strong Raman lines of the hemihydrochloride and relatively wak infrared bands of acetamide. In fact, the weaker the acetamide band the deeper the "window", and the closer the weak band is to the maximum of the broad, intense background the greater the depth of the "window". This implies that the hydrogen bond vibrational modes , particularly those describing the motion of the proton, interact or perturb the vibrational modes of groups with large bond polarizabilities. The "windows" in the hemihydrochloride spectrum have been associated with the stretching of the $-C-CH_3$ bond and the out-of-plane modes of the NH_2 group. These effects, along with the frequency assignments and the structural parameters will be used to discuss the possible resonance structure contributions to the hemihydrochloride molecule in the crystalline state. Several of the possible resonance forms are shown in Figure II B - 11. It should be noted that the unsymmetric structures will have a corresponding structure obtained by inversion through the center of symmetry.

A

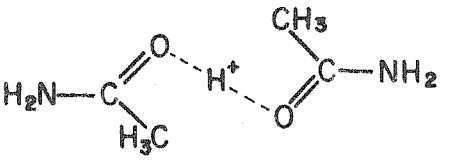

B

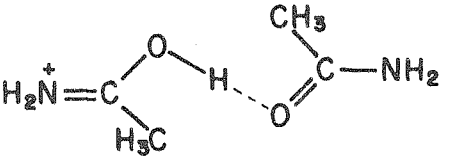

C

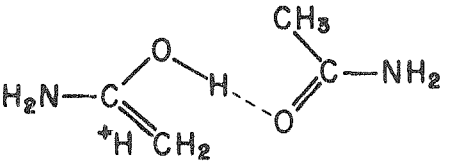

D

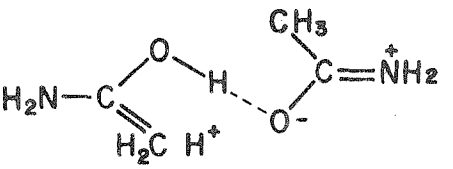

E

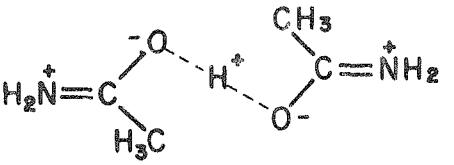

FIGURE II B-11

Possible Resonance Forms of

Acetamide Hemihydrochloride

In structure A the acetamide residues are in the normal keto-configuration with the proton situated midway between the two carbonyl oxygens. This type of structure would account for the 1667 cm^{-1} band assignment to the carbonyl stretch and the intensity of the hydrogen bond vibrational modes. Moreover, the proximity of the $C-CH_3$ group to the hydrogen bond would allow for interaction between the $C-CH_3$ stretch and the in-plane bend of the O--H--O hydrogen bond. The main drawback of this structure is the normal C-N bond, which has been shown not to exist in the crystalline state. This structure will undoubtedly make a large contribution to the final structure, a resonance hybrid.

Structures of type B would have a C=N double bond with the resulting positive charge on the nitrogen stabilized by the presence of the negative chloride ion nearby. This structure accounts for the short C-N distance. Since the proton can be attached to one oxygen or the other, it would oscillate between the two oxygens, giving rise to a double-minimum potential curve for the motion of the hydrogen atom in the hydrogen bond. The slight elongation of the C=O bond may indicate such a contribution.

Resonance structures with a C-C double bond (models C and D) are similar to those used in hyperconjugation. Recent gas phase electron diffraction studies on propylene, isobutene, and cis-2-butene[203] have given a distance of 1.50 A for the C-C single bonds. The $C-CH_3$ distance in acetamide and the hemihydrochloride are identical and about 1.51 A in length. Structure C would contribute single bond character to the C=O bond. Structure D would account for the short C-N bond and give two almost equivalent C-O bonds.

Both structures may make a significant contribution to the final structure because of the stabilizing effect on the partially non-bonded proton due to the proximity of the negative chlorine and oxygen.

Structure E has a large charge distribution which could be stabilized by the presence of the nearby chloride ions and the proton in the hydrogen bond. Such a structure would account for the short C-N bond, the intensity of the hydrogen bond vibrational modes and the crystallographic equivalence of the C-O distances. The difficult with this structure is that the C-O distances should approach the values of a C-O single bond. The slight elongation of the C=O bond suggests such a contribution.

From the possible resonance forms considered above structures A and E would give rise to a symmetric hydrogen bond, while structures B, C, and D would give rise to a statistically symmetric hydrogen bond. Structure A may be the predominent structure, though the others undoubtedly make a significant contribution to the overall structure.

Section C: Nickel Dimethylglyoxime

For a number of years nickel dimethylglyoxime was believed to possess the shortest, and probably symmetric, O-H---O hydrogen bond. To support the symmetric model the disappearance of a relatively weak bond near 1750 cm^{-1} in the infrared spectrum, which was assigned to the hydrogen bond shifted O-H stretching vibration, on deuteration has been cited as evidence.[66,204] It was felt that a thorough re-examination of the infrared spectrum of nickel dimethylglyoxime would provide important information about short, nearly symmetric, hydrogen bonded systems.

As nickel dimethylglyoxime (NiDMG) is a metal chelate complex of dimethylglyoxime (DMG) an examination of the infrared spectrum of the parent compound would be helpful for comparison as well as the assignment of the frequencies. Fortunately, a number of spectral studies on oximes[205-208] and glyoximes[209-212] exist.

Crystal Structures:

Dimethylglyoxime:

Crystals of dimethylglyoxime grown from a 1:1 ethanol - water mixture are triclinic and belong to space group C_i^1 - $P\bar{1}$. There is one molecule per unit cell with unit cell dimensions a = 6.10 A, b = 6.30 A, c = 4.48 A, $\alpha = 122^{\circ}31'$, $\beta = 90^{\circ}6'$ and $\gamma = 79^{\circ}1'$. In Figure II C - 1 is shown a unit cell projection on the (001) plane.[213] The molecules are presumably joined together by a one-dimensional network of hydrogen bonds, as indicated in the figure.

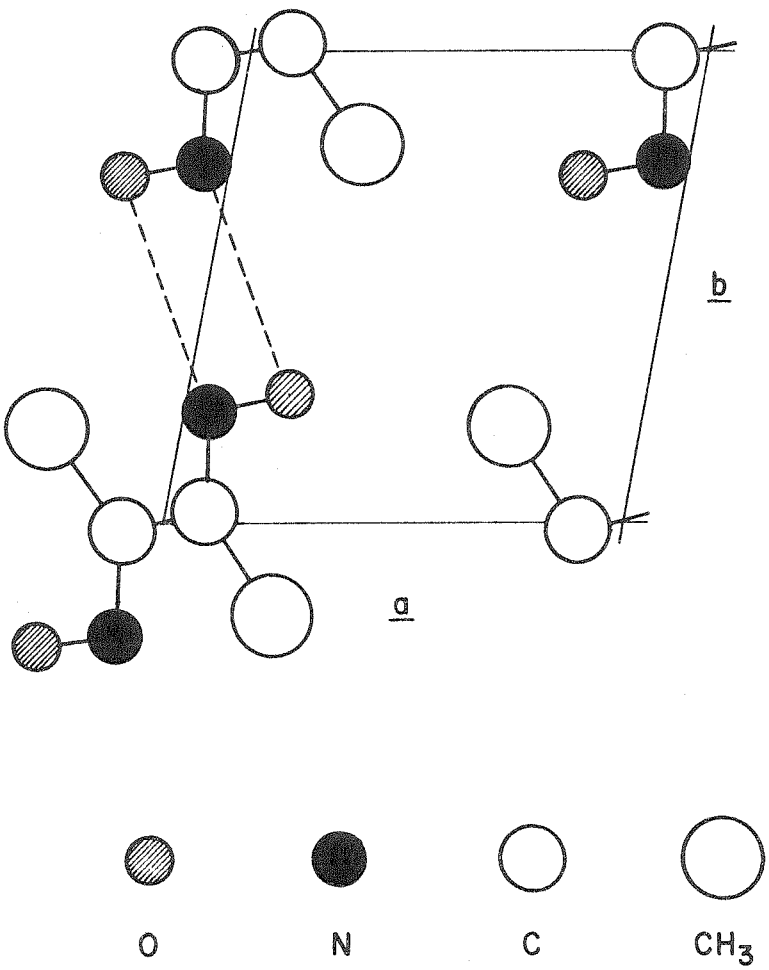

FIGURE II C-1

Crystal Structure of Dimethylglyoxime

Projection on [001] Plane

The molecule is in the trans- configuration and possesses a center of symmetry in the axial C-C bond. The rather short axial C-C distance of 1.44 ± 0.05 A has been interpreted as due to partial double-bond character, about 25%, for this bond. The hydrogen bond formed between a nitrogen of one molecule and an oxygen of another is quite short for an O-H---N bond, 2.83 A. There are four such bonds associated with each molecule in the crystalline state.

Nickel Dimethylglyoxime:

Crystals of nickel dimethylglyoxime are orthorhombic and belong to space group V_h^{26} - I bam. There are four molecules per unit cell with unit cell dimensions a = 16.6 A, b = 10.4 A and c = 6.94 A. The nickel atoms are located at positions (0, 0, 0), (0, 0, 1/2), (1/2, 1/2, 1/2) and (1/2, 1/2, 0).(204, 214)

The molecule is planar with the hydrogen bonded oxygens contained in a five-membered ring system. All molecules are parallel to the (001) plane and are stacked with the nickel atoms directly above each other separated by 3.325 A, or c/2. The methyl groups, however, cause the molecules to be oriented 90° apart in adjacent layers, that is for molecules at (0, 0, 0) and (0, 0, 1/2)

The distance between oxygen atoms of the same molecule is only 2.44 A, which is very short for an O-H--O bond. The hydrogen bonds, if linear, are inclined at an angle of about 44° to the b-axis for Ni(0, 0, 0) and at an angle of about 46° for Ni(0, 0, 1/2).

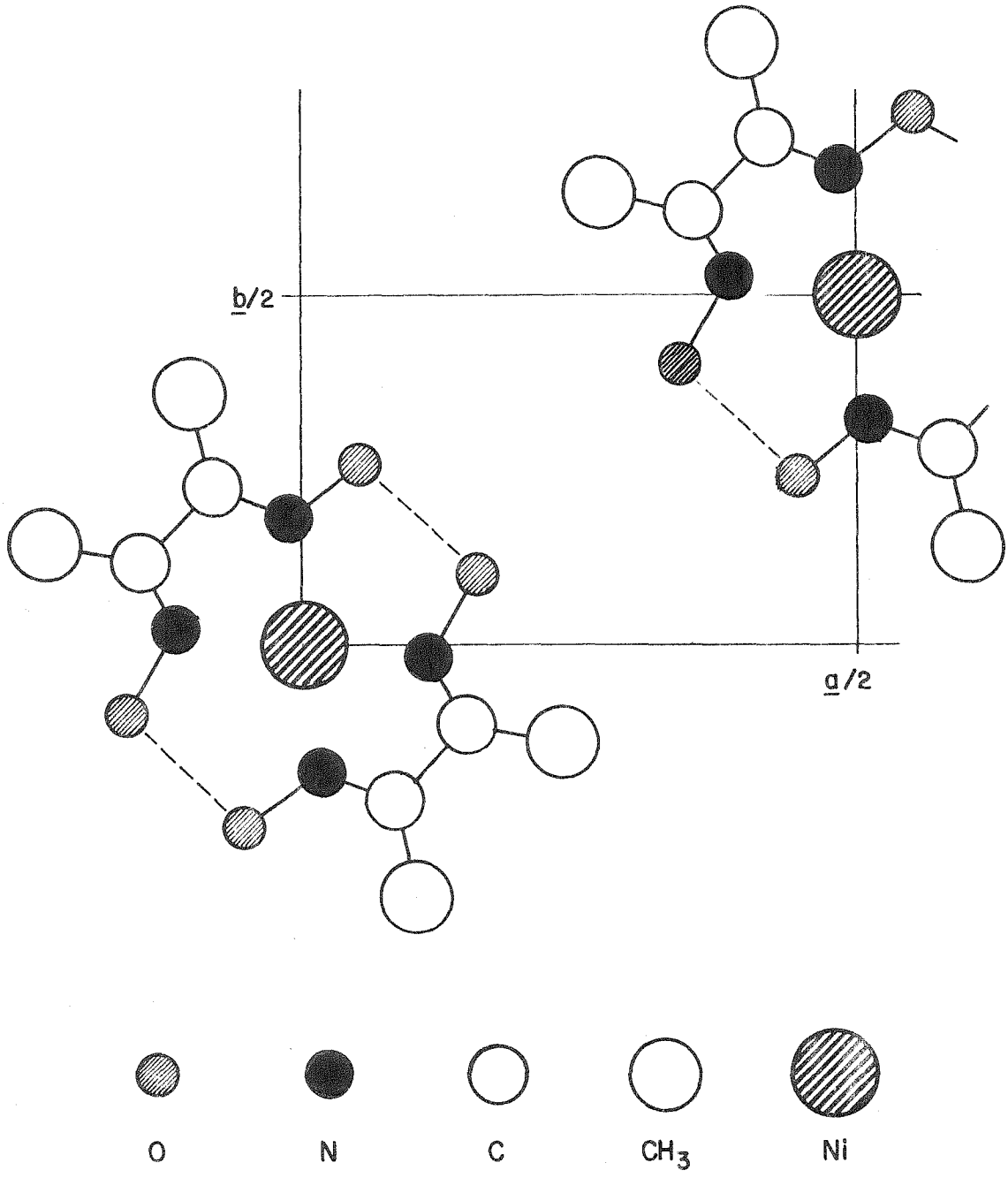

FIGURE II C-2

Crystal Structure of Nickel Dimethylglyoxime

Projection along c-axis on [001] Plane

Dimethylglyoxime:

Dimethylglyoxime (reagent powder, CB 366, Matheson, Coleman and Bell) was recrystallized three times from a 1:1 ethanol (95%) - water mixture. The colorless needles were fried under reduced pressure over phosphorous pentoxide at room temperature for 12 hours, then transferred to a desiccator containing fresh anhydrous magnesium perchlorate.

Deuterated Dimethylglyoxime:

A small quantity of the recrystallized dimethylglyoxime (about 50 mg) was almost completely dissolved in 2 ml of hot heavy water. The aqueous portion was removed while still hot and allowed to cool to room temperature in a stoppered container. When cool, the excess heavy water was removed by evaporation under reduced pressure with the aid of phosphorous pentoxide in a drying tube. The deuterated material was further dried by continued evacuation over phosphorous pentoxide at room temperature for 12 hours, then stored in a sealed container in a desiccator over fresh anhydrous magnesium perchlorate.

Nickel Dimethylglyoxime:

A solution of 2.38 gm of $NiCl_2 \cdot 6H_2O$ (Merck and Co., Inc., reagent grade) in 100 ml of distilled water was heated to 80°C and the acidity adjusted with 1 N acetic acid to about pH 4. With continuous stirring 150 ml of a 1% alcoholic solution of dimethylglyoxime was slowly added, then made slightly alkaline, to about pH 8, by the addition of 2 N ammonium hydroxide. The precipitate and the supernatant liquid were allowed to cool to room temperature where upon the light red precipitate settled out. Most of the supernatant liquid was decanted off, and the remainder, together

with the precipitate, was centrifuged for about five minutes. The precipitate was then washed with three 30 ml portions of 95% ethanol, three 30 ml portions of water and one 30 ml portion of acetone. The red precipitate was dried in an oven at 120°C for one hour. A portion of the material was further recrystallized from nitrobenzene. The deep red needles were dried under reduced pressure for 24 hours at 140° C, then stored in a desiccator over anhydrous magnesium perchlorate.

Deuterated Nickel Dimethylglyoxime:

The following method was devised to prepare deuterated nickel dimethylglyoxime as it was found to be successful in preparing ordinary nickel dimethylglyoxime. About 75 mg of crystalline nickel dimethylglyoxime were dissolved in 1.5 ml of an acid mixture prepared by adding 1 ml of acetyl chloride to 2.5 ml of heavy water. When dissolution was complete, a solution of 1.12 gm of anhydrous potassium carbonate per ml of heavy water was added cautiously until slightly basic; required about 0.8 ml. Ther material was centrifuged in a stoppered tube for two minutes and the supernatant liquid removed. The precipitate was washed with 0.5 ml portions of warm heavy water until the supernatant liquid was neutral to Hydrion paper. The test tube was then transferred to a drying pistol and evacuated. When most of the water was removed the chamber was heated to 140°C and dried with the aid of phosphorous pentoxide for 12 hours. The final product was a deep red-brown in color, unlike the brilliant red of undeuterated nickel dimethylglyoxime.

Preparation of Samples for Spectroscopic Investigation:

The infrared spectra of the above compounds were examined in

form of mulls and potassium bromide pressed discs.

Mulls:

Mulls were prepared by grinding a small quantity of the compound, about 20 to 50 mg, with one or two drops of the mulling agent, which was either Nujol or 1, 3 - hexachlorobutadiene.

Potassium Bromide Pressed Discs:

The techniques used in the preparation of potassium bromide pressed discs have been fully described in the experimental section for acetamide and acetamide hemihydrochloride. In this investigation stock mixtures of dimethylglyoxime - potassium bromide (0.110 mg per mg mixture) and nickel dimethylglyoxime - potassium bromide (0.0538 mg per mg mixture) were used for most of the work. For a rapid comparison of the deuterated and undeuterated compounds in potassium bromide pressed discs a weighed quantity of the compound, on the order of 1 - 2 mg, was ground with one gram of dried potassium bromide in an agate mortar under an infrared lamp for 5 minutes and then quickly transferred to the die. The remainder of the pellet technique was the same.

Instrumental Conditions for Recording Spectra:

Instrumental conditions for recording the spectra were the same as those given in the section for acetamide hemihydrochloride, with the exception of several spectra which were programmed as follows: Optics: NaCl; Slit Program: 927; Response: 1:1; Gain: 6.1; Recording Speed: 4 1/2 (0.84 μ/min); Supperssion: 4; Spectral Range: 2 - 15 μ ; computed spectral slit widths:[163,164] 6.13 cm^{-1} at 2000 cm^{-1}, 3.26 cm^{-1} at 1500 cm^{-1}, 2.06 cm^{-1} at 1000 cm^{-1} and 4.58 cm^{-1} at 667 cm^{-1}.

Results and Discussion:

For convenience this phase of the work is divided into two parts. The first part concerns the infrared spectrum and frequency assignments of the dimethylglyoxime molecule in the solid state while the second part deals with the infrared spectrum and the short intramolecular hydrogen bond of crystalline nickel dimethylglyoxime.

Dimethylglyoxime:

Nujol and hexachlorio-1, 3-butadiene mull spectra of undeuterated and partially deuterated dimethylglyoxime in the region of 2 to 15 microns are shown in Figure II C - 3. The extreme weakness of the deuterated mull spectra may be due to rapid hydrogen - deuterium exchange with atmospheric moisture during the mulling process. Potassium bromide pressed disc spectra of the deuterated material are superior to mull spectra with respect to band intensity and band position (Figure II C - 4). The position of the bands (in wave-numbers) of the undeuterated and partially deuterated dimethylglyoxime in the various matrices have been tabulated in Table II C - 1, together with possible frequency assignments.

The following paragraphs of this part of the discussion will be devoted to the frequency assignments in Table II C - 1, with reference to the structural analysis of dimethylglyoxime and previous infrared studies on oximes and glyoximes.

νO-H Vibration:

Potassium bromide pressed disc spectra of undeuterated dimethylglyoxime exhibit intense absorption at 3200 cm^{-1} superimposed on

Figure II C - 3

Infrared Spectrum of Dimethylglyoxime and Partially Deuterated Dimethylglyoxime as a Mull in the Region Between 2 and 15 Microns

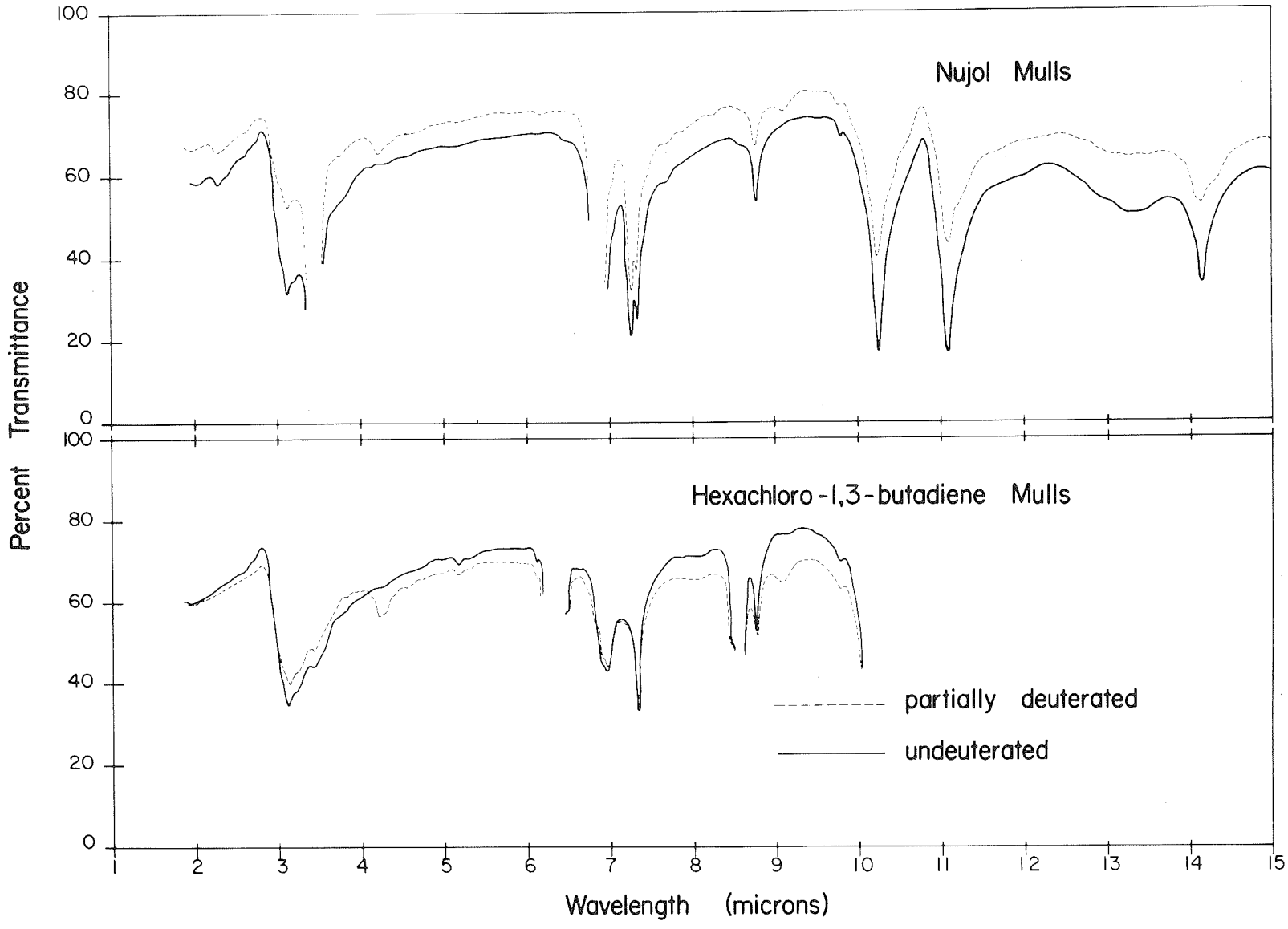
Nujol Mulls
Hexachloro-1,3-butadiene Mulls
partially deuterated
undeuterated
Percent Transmittance
Wavelength (microns)
100
80
60
40
20
0
1
2
3
4
5
6
7
8
9
10
11
12
13
14
15

Figure II C - 4

Infrared Spectrum of Dimethylglyoxime and Partially Deuterated Dimethylglyoxime in a Potassium Bromide Matrix in the Region of 2 to 25 Microns

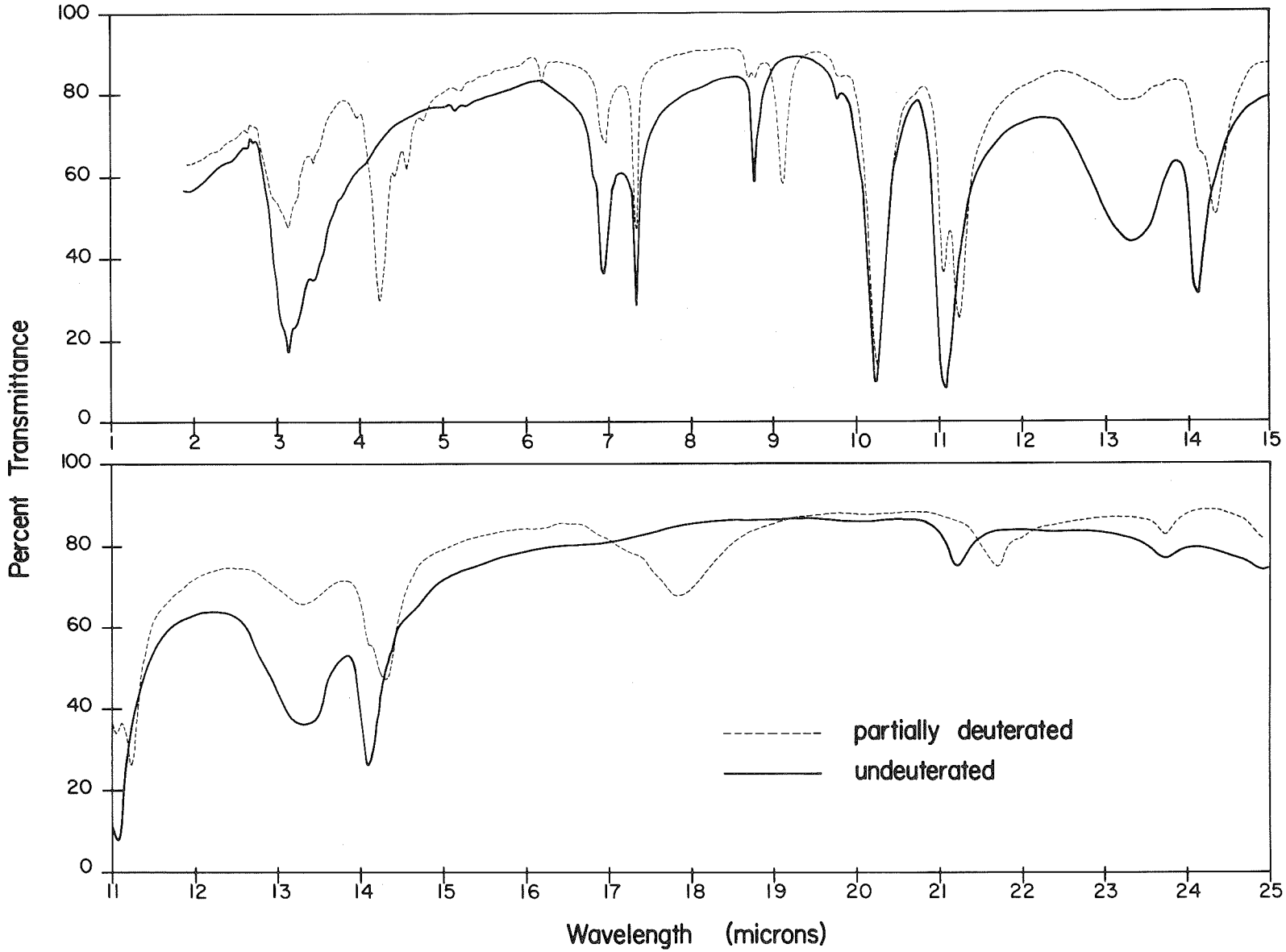
Percent Transmittance
100
80
60
40
20
0
1
2
3
4
5
6
7
8
9
10
11
12
13
14
15
11
12
13
14
15
16
17
18
19
20
21
22
23
24
25
partially deuterated
undeuterated
Wavelength (microns)

Table II C - 1

Observed Frequencies and Possible Assignments for Dimethylglyoxime

Potassium Bromide Disc		Mulls		
undeut'd	deut'd	undeut'd	deut'd	Assignment
3200 s*	3200 s	3200 s	3200 m	ν(O-H)**
3096 m(sh)	3077 w(sh)	3096 m(sh)	3077 mw(sh)	
2946 m	2941 w	2941 m	2945 m	νCH_3
----	2347 s	----	2353 m	ν(O-D)**
----	2278 w	----	----	
----	2179 m	----	2188 vw	
----	2088 w	----	----	
----	1610 w	----	1610 vw	
1435 s	1433 m	1437 s	1437 m	ν(C=N)
1361 s	1361 ms	1362 s	1362 ms	δCH_3
----	1152 w	----	----	
1139 s	1139 w	1139 mw	----	ν(N-O) + δOH
----	1098 m	----	1099 mw	ν(N-O) + δOD
1023 w	1024 w	1023 w	1025 w(sb)	
987 vs	976 vs	978 s	978 s	$\nu(CH_3\text{-}C\text{-})$
904 vs	904 m	905 s	905 ms	ν(N-O(H))
---	891 s	---	---	ν(N-O(D))
751 vs(b)	751 mw(vb)	750 m(b)	755 m(vb)	γOH
709 s	707 w(sh)	708 s	707 ms	δCH_3-C=N-
---	699 s	---	698 ms(sh)	
---	560 s(b)	---	---	γOD
497 m	---	---	---	δ(-C=N-O(H))
---	460 m	---	---	δ(-C=N-O(D))

* All frequencies are given in wave-numbers.

** Group is hydrogen bonded to neighboring oxime nitrogen.

a relatively broad background with a number of weak side bands. On deuteration the band diminishes while a new band appears at 2340 cm^{-1}, which gives a frequency shift ratio of 1.36. From the behavior of the band it is undoubtedly the O-H stretch shifted by about 300 cm^{-1} as a result of N---H-O hydrogen bonding. Previous studies on oximes [205,206,207,208] and glyoximes [211,212] have attributed absorption in this region to the O-H stretching mode.

1435 cm^{-1} Band:

A strong band at 1435 cm^{-1} appears to diminish on deuteration though no new band appears in the dueterated spectrum which could be assigned to this band. In simple oximes, where the C=N linkage is not conjugated, the frequency of the C=N stretching vibration is expected between 1680 and 1650 cm^{-1}. [206,208,215] In the glyoximes, however, conjugation is possible. The structural data of crystalline dimethylglyoxime indicates a short axial C-C distance and a slight elongation of the C=N distances [214] which suggests conjugation between the C-C and C=N groups. If this interpretation is assumed to be true then the "C=N" stretching frequency would lie somewhere between that of the C-N and C=N values. The band would be of moderate intensity since C=N absorption bands are reported to be stronger than C=C bands though not as strong as C=O bands. [216] Therefore, the 1435 cm^{-1} band in the dimethylglyoxime spectrum is assigned to the "C=N" stretch, or possibly, the out-of-phase asymmetric CH_3-C=N- skeletal stretch.

1360 cm^{-1} Band:

A relatively strong band at 1361 cm^{-1} is apparently unaffected by deuteration. The position and intensity of the band is characteristic

of the symmetric deformation mode of the methyl group[217] so this assignment is used in the present analysis. The Raman investigation of acetoxime by Goubeau has the same assignment for the 1372 cm^{-1} line.[205] Borello and Henry[212] reported bands between 1380 cm^{-1} and 1360 cm^{-1} for several glyoximes, however, no assignment was given.

1140 cm^{-1} Band:

A moderately strong, sharp band near 1140 cm^{-1} is almost removed by deuteration. A band of comparable intensity and shape appears at 1098 cm^{-1}, which gives a frequency shift factor of only 1.04. Borello and Henry[212] assigned the 1150 cm^{-1} band of glyoximes to the =N-O stretching mode on the basis of dichoric measurements and deuteration shifts. Although the band position and frequency shift reported by these authors are in agreement with the present work, the assignment is open to question in view of the spectral investigation of Tarte on the cis- and trans- isomers of alkyl nitrite esters.[218, 219] Work by Palm and Werbin[208] on α- and β- oximes has placed the in-plane bending mode of the O-H group at 1300 cm^{-1} and the N-OH stretch at 920 cm^{-1}.

It is possible that the νN-O and δ O-H vibrations couple, similar to the coupling of the ν C-O and δ O-H modes in carboxylic acids,[88] so that the 1140 cm^{-1} band of dimethylglyoxime is not a simple mode. Deuteration would shift the band, with the magnitude of the shift depending on the relative contribution of the respective modes.

980 cm^{-1} Band:

A very strong band in the undeuterated spectrum is found at

978 cm^{-1}, and is unaffected by deuteration. Bands in the neighborhood of 980 cm^{-1} have been reported for glyoximes[209, 212] though no assignments were offered. Since the present work has shown the band to be unaffected by deuteration, it is possible that the band is associated with the CH_3-C stretch, or more likely, the out-of-phase in-plane symmetric CH_3-C=N- stretch.

905 cm^{-1} Band:

A very strong band near 904 cm^{-1} is reduced in intensity on deuteration with the appearance of a strong band at 890 cm^{-1} in the deuterated spectrum. Palm and Werbin have assigned the 920 cm^{-1} band of α- and β- oximes to the N-O(H) stretch[208] and Goubeau gave the same assignment for the 935 cm^{-1} Raman line of acetoxime,[205] though Bernstein places this mode near 812 cm^{-1}.[206] The work of Tarte on alkyl nitrite esters has placed the N-O stretch of the trans- isomer in the vicinity of 814 cm^{-1}.

On the basis of the weak deuteration interaction and the proximity of the band to the N-O stretch of the nitrite esters, it is suggested that this band is associated with the N-O(H) stretch, though it might well be weakly coupled with the δO-H mode.

750 cm^{-1} Band:

On deuteration a strong, though rather broad band at 751 cm^{-1} almost disappears while a new band appears at 560 cm^{-1}, which gives a frequency shift factor of 1.34. This shift factor is very close to the expected value for a hydrogen active mode. Borello and Henry have assigned the in-plane O-H bend to broad bands in this region for glyoximes, which is rather low for such a mode. It is more likely to be the out-of-

plane deformation mode of the O-H group.

710 cm^{-1} Band:

A relatively intense, sharp band at 709 cm^{-1} in the undeuterated material is shifted slightly on deuteration to 699 cm^{-1}. Borello and Henry have reported absorption in this region for glyoximes, though no assignment was made. It is possible that an in-plane skeletal bend of the dimethylglyoxime residue is in this region, in particular the CH_3-C=N- bend. Such an assignment is used in the present analysis as there would be a slight shift on deuteration due to N---H-O hydrogen bonding between adjacent molecules.

500 cm^{-1} Band:

A medium intense band at 497 cm^{-1} disappears on deuteration, though a new band appears at 460 cm^{-1}, which gives a frequency shift factor of 1.07. This band does not appear to represent a hydrogen active mode, though it might well involve the OH group. Tarte has placed the -O-N=O bend of the alkyl nitrite esters in the region of 500 to 600 cm^{-1}[218,219] so it is possible that the 497 cm^{-1} band in dimethylglyoxime represents the in-plane -C=N-O(H) bend. Such a mode would be shifted on deuteration. Therefore, this assignment is used in the present analysis.

Nickel Dimethylglyoxime:

Spectra of undeuterated and partially deuterated nickel dimethylglyoxime as Nujol and hexachloro-1,3-butadiene mulls are shown in Figure II C - 5 for the region between 2 and 15 microns. Potassium bromide pressed disc spectra (Figure II C - 6) were found

Figure II C - 5

Infrared Spectrum of Nickel Dimethylglyoxime and Partially Deuterated Nickel Dimethlyglyoxime as a Mull in the Region Between 2 and 15 Microns

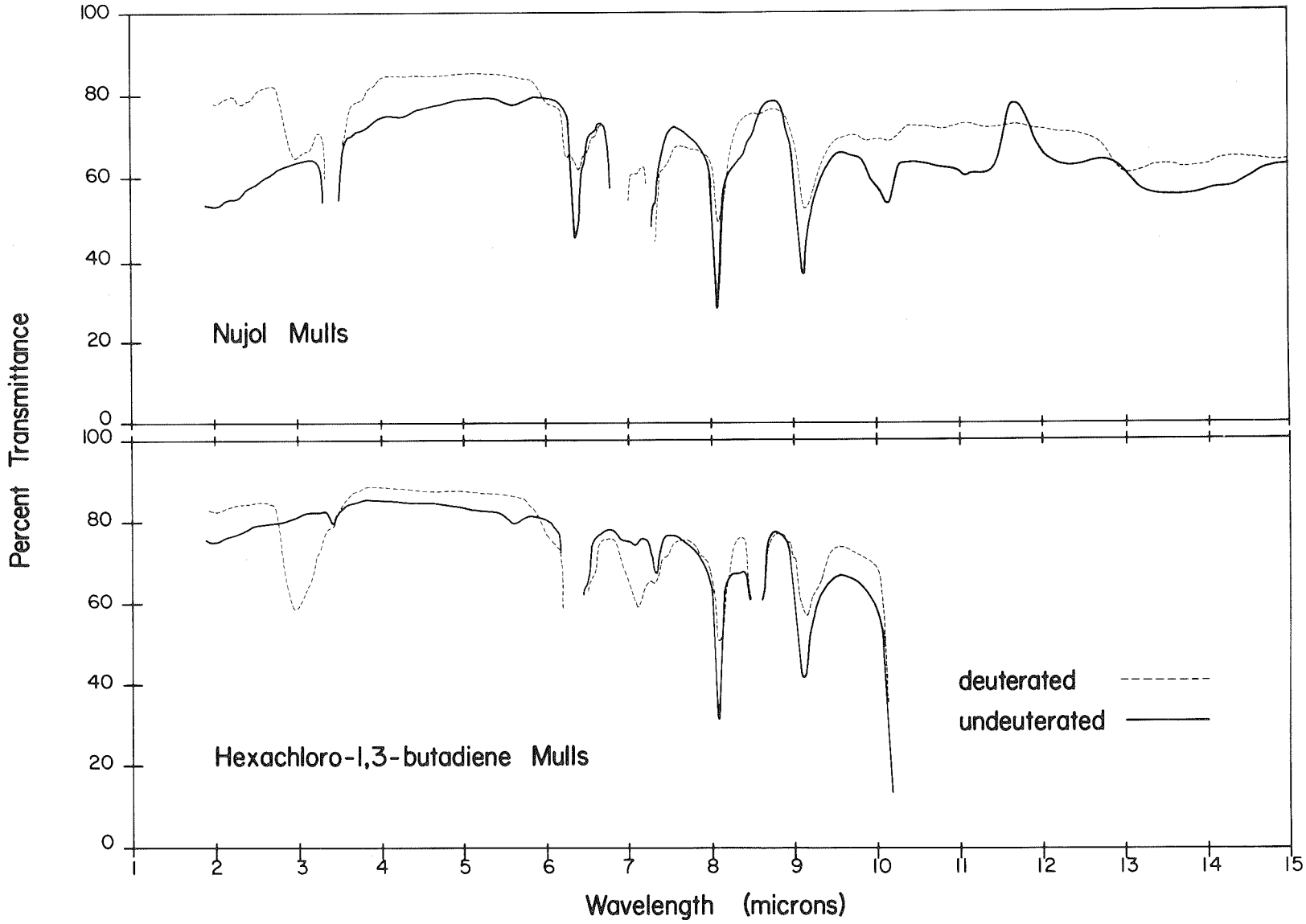
Percent Transmittance
100
80
60
40
20
0
Nujol Mulls
Hexachloro-1,3-butadiene Mulls
deuterated
undeuterated
1
2
3
4
5
6
7
8
9
10
11
12
13
14
15
Wavelength (microns)

Figure II C - 6

Infrared Spectrum of Nickel Dimethylglyoxime and Partially Deuterated Nickel Dimethlyglyoxime in a Potassium Bromide Matrix in the Region of 2 to 25 Microns

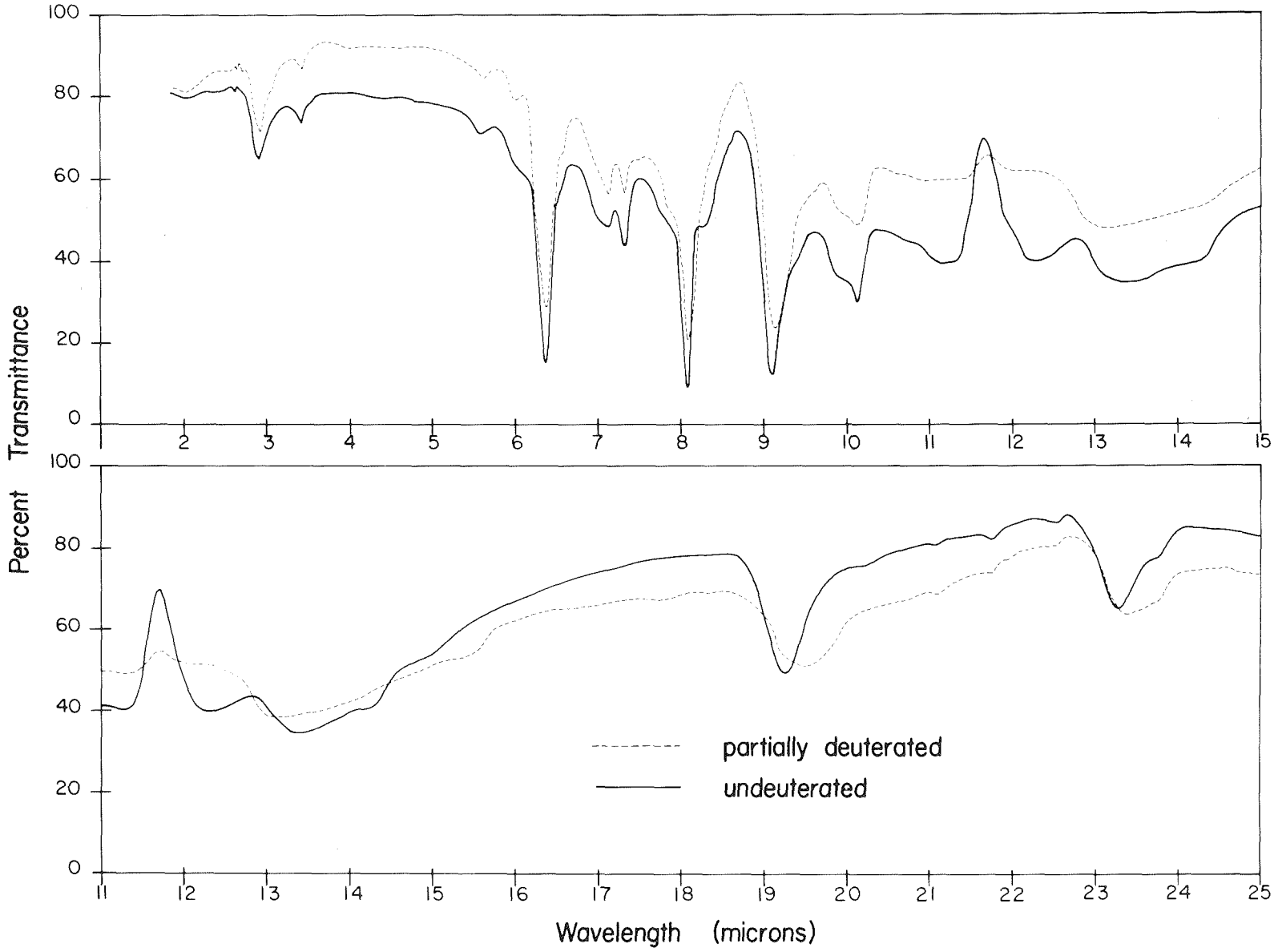
Percent Transmittance
100
80
60
40
20
0
2
3
4
5
6
7
8
9
10
11
12
13
14
15
11
12
13
14
15
16
17
18
19
20
21
22
23
24
25
partially deuterated
undeuterated
Wavelength (microns)

to be identical with the mull spectra in all essential features and were used for the major portion of this work.

Undeuterated nickel dimethylglyoxime spectra exhibit a single deep "window" on an extremely broad, moderately intense background extending from about 1600 cm^{-1} to 600 cm^{-1}. On deuteration the "window" is reduced in depth, though the background absorption remains unusually strong. This leads one to believe that these features are associated with the internal vibrational modes of the nickel dimethylglyoxime complex. The nickel dimethylglyoxime complex is not unique in this respect as spectra of 1,2-bis(vic- dioximo- N,N') Ni(II) complexes exhibit "windows" and unusually intense background absorption in the region between 1000 cm^{-1} and 800 cm^{-1} (220)

A comparison of the spectrum of the nickel complex with that of the parent compound, dimethylglyoxime, in a potassium bromide matrix (Figure II C - 7) shows several distinct and important differences. The "window" of the nickel complex lies on the low frequency side of a strong band of dimethylglyoxime, assigned to the N-O(H) stretching frequency. The background absorption is extremely broad and relatively intense, rising to a maximum in the region between 1000 cm^{-1} and 700 cm^{-1}. Differences in the spectra of the two compounds are expected, but these effects are unusual. Aside from the unusual features of the nickel complex spectrum differences are expected since (a) the dimethylglyoxime residues in the nickel complex are in the cis- configuration whereas the oxime groups in dimethylglyoxime are in the trans- configuration; (b) the types of hydrogen bonding are radically different, an O-H--N type in dimethylglyoxime and an extremely short O--H --O type in

Figure II C - 7

A Comparison of the Infrared Spectra of Dimethylglyoxime and Nickel Dimethylglyoxime in a Potassium Bromide Matrix in the Region of 2 to 25 Microns

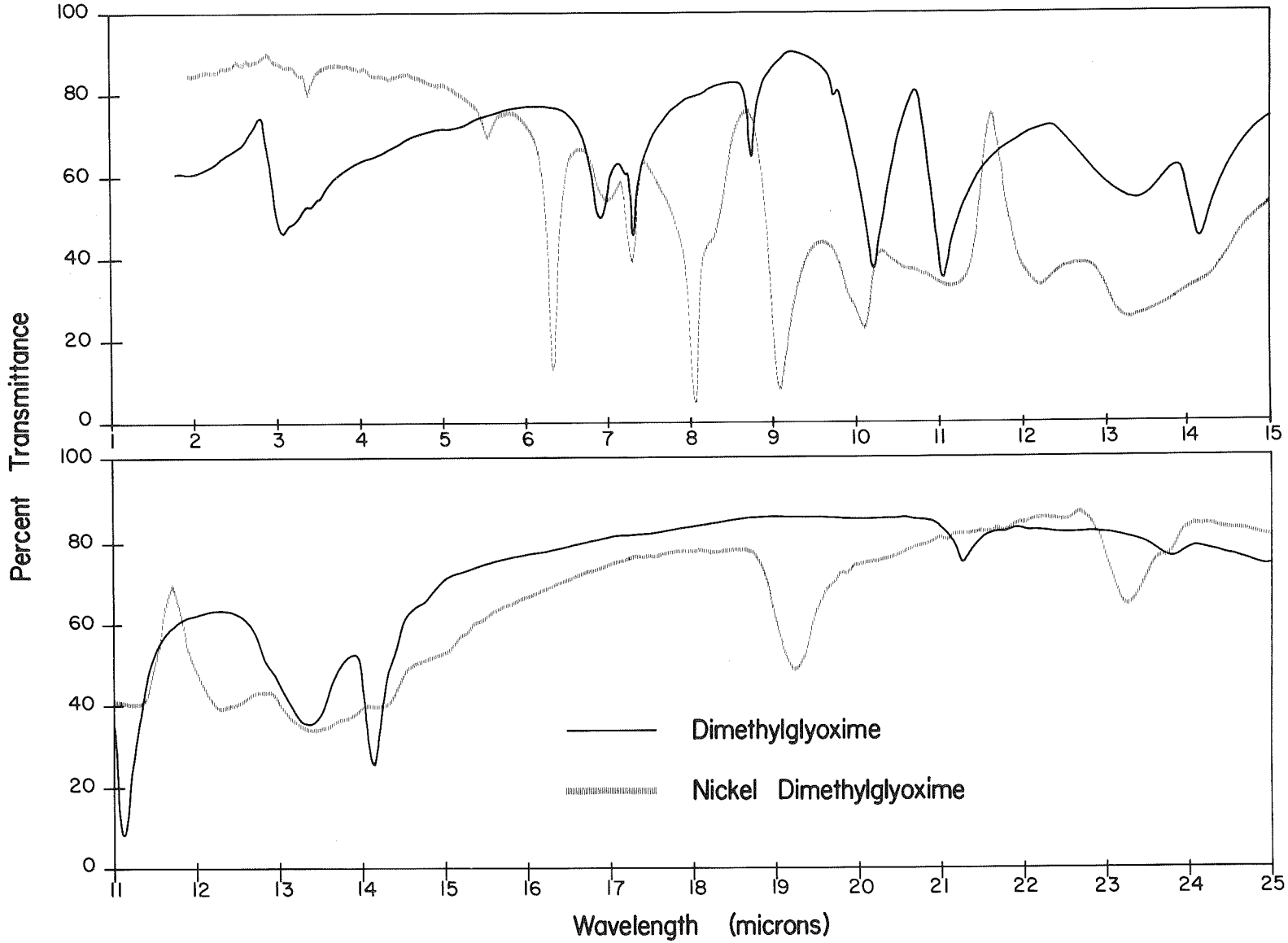
Percent Transmittance
100
80
60
40
20
0
1
2
3
4
5
6
7
8
9
10
11
12
13
14
15
11
12
13
14
15
16
17
18
19
20
21
22
23
24
25
Dimethylglyoxime
Nickel Dimethylglyoxime
Wavelength (microns)

nickel dimethylglyoxime; and (c) the C=N and axial C-C bond lengths in the nickel complex appear to be normal covalent C=N and C-C bonds, but in dimethylglyoxime the axial C-C bond is unusually short which may indicate some double bond character. These structural differences are significant and undoubtedly have a bearing on the unusual features of the nickel dimethylglyoxime spectrum.

The position and relative intensity of the absorption bands of nickel dimethylglyoxime (designated NiDMG) in the various matrices have been tabulated in Table II C - 2 along with the possible frequency assignments. The following paragraphs will discuss these assignments in view of the structural parameters and the molecular symmetry, although the structural data is far from satisfactory.

The C=N Stretching Modes:

Since the C=N and axial C-C bond lengths in crystalline nickel dimethylglyoxime indicate normal covalent C=N and C-C bonds the "C=N" stretching frequency would be shifted towards higher frequency from that of the "C=N" vibration of dimethylglyoxime, into the double bond stretch region between 1600 cm^{-1} and 1500 cm^{-1}. If one considers the symmetry of the NiDMG molecule and the fact that the dimethylglyoxime residues are in the cis- configuration, the C=N bonds form the sides of a five membered ring with a mirror plane perpendicular to the plane of the molecule and bisecting the N - Ni - N angle and the axial C-C bond of the dimethylglyoxime residues (see Figure II C - 2). In each dimethylglyoxime residue the C=N stretching vibrations can vibrate either in-phase or out-of-phase so that in the nickel complex the modes will be symmetric or antisymmetric with respect to a mirror plane which is perpendicular

Table II C - 2

Observed Frequencies and Possible Frequency Assignments for Nickel Dimethylglyoxime

Potassium Bromide Disc		Mulls		
undeut'd	deut'd	undeut'd	deut'd	Assignment
3425 m	----	3378 s	----	
2907 w	----	2915 w	----	νCH_3
----	2882 w	----	----	
1776 w	1774 vw	1779 w	----	
----	1653 mw	----	1650 w	ν(C=N)
----	----	----	1595 m	
1571 s	1563 s(b)	1572 s	1563 ms	ν(C=N)
1425 w(sh)	1429 w(sh)	1418 w	----	δCH_3(asym)
1403 m	1399 m	----	1403 s	ν(C=N) ??
1364 m	1362 m	1364 m	1368 s	δCH_3(sym)
1238 s	1233 s	1237 s	1235 s	ν(N-O)
1208 ms(sh)	1190 w(sh)	1198 mw(sh)	----	δ(O-H-O)
1089 s	1089 s(b)	1094 s	1093 s(b)	ν(N-O)
1009 w(sh)	1005 mw(sh)	1000 w(sh)	1005 vw	ν(C-CH_3)
989 m	987 m(b)	988 w	985 w	ν(C-CH_3)
857 s*	851 w*	855 s*	---	ν(O-H-O) ?
---	763 - 625 m	---	769 mw	
748 mw(b)	---	744 m(vb)	---	γ(O-H-O) ?
701 w(vb)	---	---	---	
517 ms(b)	514 m(b)	---	---	δ(C=N-O)
427 m	429 m(b)	---	---	δ(C-C-CH_3)

* Appears as a "window" in the infrared spectrum.

to the plane of the molecule and the mirror plane of the C=N five membered ring system. The possible modes are shown schematically in diagrams (i) thru (iv), the heavy arrow indicates the direction of the resultant transition moment, if one exists.

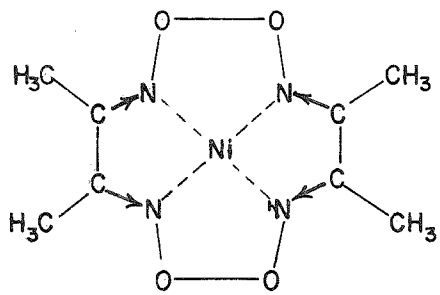

IR in-active

(i)

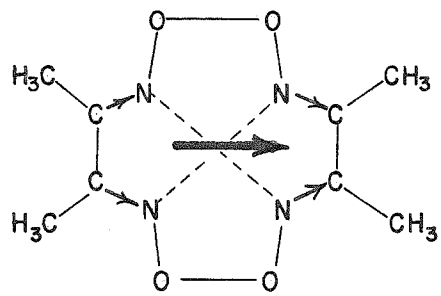

IR active

(ii)

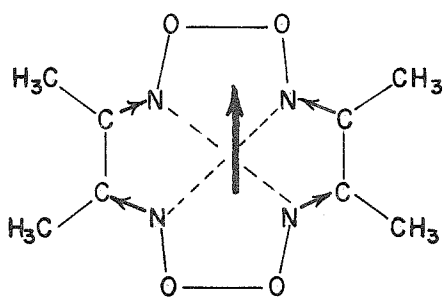

IR active

(iii)

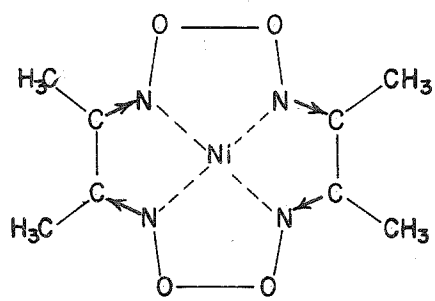

IR in-active

(iv)

The infrared in-active modes (i) and (iv) represent the in-phase symmetric and the out-of-phase antisymmetric C=N stretch coupling modes. Mode (i) is similar to the breathing mode of cyclic

paraffins, which have the breathing frequency in the neighborhood of 1000 cm^{-1} to 700 cm^{-1}.(221) The in-phase antisymmetric mode (ii) has a resultant transition moment in the plane of the molecule in the direction parallel to the hydrogen bond while the out-of-phase symmetric mode (iii) has a resultant transition moment in the plane of the molecule in the direction perpendicular to the hydrogen bond. Mode (iii) would be relatively intense so it is assigned to the strong band at 1571 cm^{-1}. The weak band at 1653 cm^{-1} is assigned to mode (ii), which is near the - C=N- stretching frequency of simple oximes.(208) On deuteration the 1653 cm^{-1} band is enhanced and separated from the side of the strong 1571 cm^{-1} (see Figure II C - 5).

The N-O Stretching Modes:

Coupling between the N-O stretch and the O-H in-plane bend in NiDMG is not likely in view of the short, and probably symmetric, hydrogen bond which may indicate an increase in the O-H distance from 1,07 A to 1,22 A. However, coupling between the N-O stretching vibrations in each dimethylglyoxime residue will give rise to modes similar to those described for the C=N vibrations. In this case the N-O bonds form a five membered ring system containing the short hydrogen bond. Furthermore, the N-O bond distance is about 0.05 A shorter than that of a normal covalent N-O bond and suggests a shift in the N-O stretch towards higher frequencies from that of the N-O stretch in dimethylglyoxime. Shortening of the N-O bond implies that the electron density is greater in the vicinity of the O atom. The O atom may, therefore, have a partial negative charge which would tend to stabilize a symmetric hydrogen bond.

The infrared in-active coupling modes of the N-O groups are described by the in-phase symmetric mode, a pseudo- ring breathing mode which may have a frequency near that of the N-O stretch of the alkyl nitrite esters,[218, 219] and the out-of-phase antisymmetric mode. The out-ofphase symmetric coupling scheme gives rise to a transition moment in the direction perpendicular to the hydrogen bond. This mode is expected to be relatively intense and has been assigned to the strong band at 1238 cm^{-1}. The in-phase antisymmetric mode has a resultant transition moment parallel to the hydrogen bond. Although it would be a lower frequency mode the band should be moderately strong. Therefore, this mode has been assigned to the 1089 cm^{-1} band.

The $C-CH_3$ Stretching Modes:

The carbon-carbon stretching frequency will be associated with the $-C-CH_3$ group, however, the actual mode will undoubtedly involve the entire cis- $H_3C-C-C-CH_3$ system. With the cis- arrangement of the methyl groups the phase relationship and the symmetry of the residue modes will give rise to infrared active and infrared in-active vibrational modes similar to those described for the C=N stretching modes.

The infrared in-active mode is the in-phase symmetric $-C-CH_3$ stretch couple. Such a mode would probably have a frequency of about 800 cm^{-1} if one were to compare it with the symmetric skeletal stretch of cyclobutane.[221] More important are the infrared active modes. The out-of-phase symmetric couple would have a resultant transition moment in a direction perpendicular to the hydrogen bond whereas the in-phase antisymmetric couple would

give rise to a transition moment in the direction parallel to the hydrogen bond. The former mode would be the higher frequency mode and the latter mode would be at a slightly lower frequency, though more intense. On this basis the moderately strong shoulder at 1009 cm^{-1} is assigned to the out-of-phase symmetric stretch coupling mode and the strong band at 987 cm^{-1} is assigned to the in-phase antisymmetric stretch coupling mode.

The O--H--O Modes:

Previous investigations of the infrared spectrum of NiDMG were restricted to the high frequency portion of the spectrum as the primary concern was in the location of the hydrogen bond shifted OH stretching frequency. The extremely short O----O distance hints at a possible symmetric hydrogen bond, which would require the O-H bond length to increase from 1,07 A in the unsymmetric model to about 1.22 A in the symmetric model. Presumably the position and intensity of the shifted OH stretching frequency would differentiate between the symmetric and unsymmetric model. Rundle and co-workers [66,204] attributed a relatively weak band near 1780 cm^{-1} to the hydrogen bond shifted OH stretch since deuteration caused the band to disappear. The large shift in frequency was interpreted as a possible symmetric hydrogen bond. However, the weakness of the band as well as the "normal" appearance of the background absorption in this region makes one skeptical of the assignment. In the present investigation the band has been found at 1776 cm^{-1}, in agreement with the reported position, in mull and potassium bromide pressed disc spectra, see Figures II C - 5 and - 6. On deuteration the band appears to be reduced in intensity

(disappeared in the mull spectrum). The deuteration effect alone does not prove, or disprove, that the band is the shifted OH stretch since overtones and summation bands of the low frequency modes of the glyoxime system could give rise to absorption is this region.

In this investigation the spectrum of NiDMG has been examined down to 400 cm^{-1} and has revealed the presence of several moderately strong low frequency bands. It is conceivable that some of these bands are associated with the bending modes of the oximes portion of the dimethylglyoxime residues and could couple with a higher frequency stretching mode to give a band at 1776 cm^{-1}. Of the several possible summation bands the (517 + 1238) is considered the most likely one since both bands have modes of the same symmetry species, are relatively strong and could be considered to describe a mode ofthe hydrogen bonded system. The 1238 cm^{-1} band has been assigned to the out-of-phase N-O stretch couple, which would resemble an O--H--O in-plane bend, and the 517 cm^{-1} band has been assigned to the out-of-phase symmetric -C=N-O bend, which also resembles an O--H--O in-plane bend. This type of summation band would account for the deuteration effect if the hydrogen bond is symmetric and if there is weak interaction between the in-plane bend of the hydrogen bond and the N-O groups modes just mentioned. Therefore, it is possible to account for the weak band at 1776 cm^{-1} without reference to a shifted OH stretch. Moreover, this implies that the hydrogen bond in NiDMG is probably symmetric. If the assignment of the summation band is correct then the correlations between O---O distance and OH frequency shift are not reliable for extremely short, symmetric hydrogen bonds.

The effects of deuteration on the NiDMG spectrum are subtle, with the exception of the disappearance of a moderately strong shoulder at 1208 cm^{-1} and the reduction of the intensity of the "window" at 851 cm^{-1}. The bands at 748 cm^{-1} and 701 cm^{-1} may be affected by deuteration though it is very difficult to evaluate since the deuterated spectrum background is very broad, moderately intense and highly irregular in this region.

The moderately strong shoulder at 1208 cm^{-1} may be associated with the in-plane bend of the O--H--O system since it is near the out-of-phase symmetric N-O stretch, which has been stated resembles the in-plane bend of the O--H--O system. Deuteration casues the shoulder to disappear. However, no new band has been observed in the deuterated spectrum in the expected region of 880 cm^{-1}. Part of the difficulty in detecting a shifted band in this region of the deuterated spectrum is due to the irregular shape of the "window" side bands in the deuterated spectrum.

Of extreme interest is the broad, relatively intense background absorption in the 1000 - 700 cm^{-1} region and the deep "window" at 857 cm^{-1}. The only clues to the nature of this region are the reduction in the depth of the "window" and a spreading out of the broad background absorption towards lower frequencies on deuteration. It is highly probable that the background absorption is associated with the vibrational modes of the hydrogen bond system, such as the asymmetric stretching mode and the deformation modes. Deuteration would broaden the background, extending it towards lower frequencies. Since the NiDMG was not completely deuterated the spectrum would be the superposition of the deuterated and undeuterated species.

The OH---O stretching frequency of unsymmetric hydrogen bonded systems is very low, in the vicinity of 300 - 200 cm^{-1}, (92 - 94) outside the accessible region of ordinary infrared spectrophotometers. Recently Reid (80) has predicted that as the O---O distance becomes smaller the OH---O frequency increases rapidly so that for an O---O distance of 2.43 - 2.45 A (as found in NiDMG) the stretching frequency should lie in the 850 - 750 cm^{-1} region, which is readily accessible with the infrared spectrophotometer used in this investigation. However, such a mode would be infrared active only in the case of an unsymmetric hydrogen bond. It is doubtful that this mode can be considered as part of the broad, strong background as the hydrogen bond in NiDMG is most probably symmetric.

The "window" at 857 cm^{-1} is the peculiar feature of the Ni-DMG spectrum, though not unique to the dimethylglyoxime complex of nickel. The invariance of the position of the "window" with the matrix material as well as the decrease in depth on deuteration leads one to conclude it is associated with the internal vibrational modes of the NiDMG molecule. It is possible that the O--H--O modes (the broad background) interact or perturb weak infrared active modes not observed or infrared in-active modes, such as the in-phse symmetric N-O stretch couple, in the same molecule or in neighboring molecules. The intra- molecular interaction or perturbation is more likely since the planar NiDMG molecules in adjacent layers are oriented 90° with respect to one another and separated by a distance of about 3.25 A. Therefore, any interaction between the O--H--O deformation modes in one molecule with the highly polarizable $H_3C-C-C-CH_3$ cis - system in an adjacent plane would be relatively weak. The "window"

effect will be discussed more fully in Section F in conjunction with the unusual breadth and intensity of the low frequency region of the spectra of short hydrogen bonded compounds.

Section D: Potassium Hydrogen Bis-Phenylacetate

Crystalline potassium hydrogen bis-phenylacetate exhibits an interesting type of hydrogen bond. Crystallographically the hydrogen atom is situated on a center of symmetry,[222] though the oxygen - oxygen distances places the system on the border-line of the symmetric - asymmetric type hydrogen bond.[47] Unfortunately, the neutron diffraction study of Bacon and Curry[223] did not resolve this problem, though the earlier X-ray crystal structure analysis was confirmed.

An early examination of the infrared spectrum of this molecule by Davies and Orville Thomas[224] supported the asymmetric model of the hydrogen bond. However, Hadzi and Novak,[225] in a later investigation, concluded that the hydrogen bond is symmetric. In view of the conflicting interpretations of the infrared spectrum as well as the unusual type of hydrogen bond it was felt that further study of the infrared spectrum of this compound was warranted.

For comparison the spectrum of the acid and its neutral salt were examined under identical conditions. A direct comparison with the acid, however, is not entirely satisfactory since it exists as a dimer in the crystalline state. The neutral salt, on the other hand, does not dimerize. Crystallographic data for both of these compounds is lacking so that a structural comparison with the acid salt is impossible.

Crystal Structure:

Crystals of potassium hydrogen bis-phenylacetate are monoclinic and belong to space group C_s^4 - Bb or C_{2h}^4 - P 2/b. There

are four molecules per unit cell with unit cell dimensions a = 28.4 A, b = 4.50 A, c = 11.97 A and β = 90.4°. Part of the unit cell is shown in Figure II D - 1 for a projection on the (010) plane.[222, 223]

Every potassium atom is situated at a center of an octahedron of oxygen atoms with four at a distance of 2.88 A and two at a distance of 2.75 A. To each pair of phenylacetate residues there corresponds an acidic hydrogen atom, located between oxygen atoms of adjacent molecules separated by a distance of 2.54 A. The proton appears to be located on a center of symmetry. Whether a statistical center or a true single-minimum potential center exists still remains to be solved. The hydrogen bonds lie in the (010) plane, at about an angle of 29° to the a-axis. Neutron diffraction results indicate that the hydrogen motion is unsymmetric, with a slight preference in a direction perpendicular to the hydrogen bond.

Phenylacetic Acid:

Commercial phenylacetic acid (Eastman No. 574) was recrystallized three times from water. The colorless leaflets were dried under reduced pressure over phosphorous pentoxide at room temperature for 12 hours, then stored in a desiccator over fresh anhydrous magnesium perchlorate until used. Melting range (uncorrected) observed under crossed Nicols on a microscope hot-stage was 75.8°-77.4° C; literature value:[226] 76.7°C. Titration with standard sodium hydroxide solution gave a neutralization equivalent of 136.5; calculated value: 136.1.

Potassium Phenylacetate:

A 10 ml aliquot of a 0.1 gm per ml alcoholic solution of phenyl-

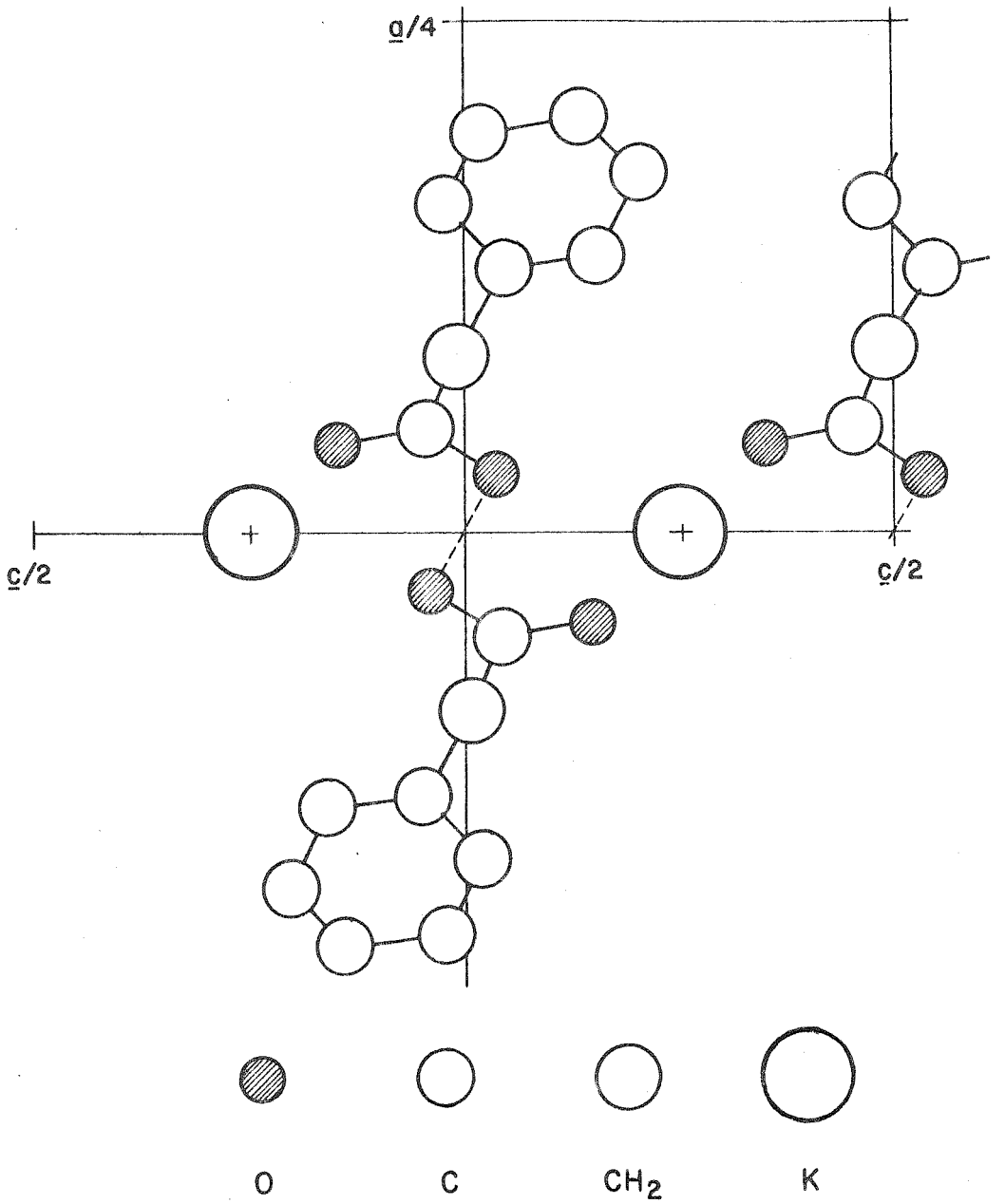

FIGURE II D - I

Crystal Structure of Potassium Hydrogen Bis-Phenylacetate

Projection along [010] Plane

acetic acid was neutralized with 4.12 ml of a 0.1 gm per ml alcoholic potassium hydroxide solution. The volume was reduced by evaporation to about 3 ml, then chilled overnight in a refrigerator at 5°C. The fine crystalline mass was filtered off and recrystallized from an ethanol - benzene solution. Short, white prismatic clusters formed on slow evaporation of the solvent. The crystals were dried under reduced pressure over phosphorous pentoxide at room temperature for a period of 12 hours. The material was stored in a desiccator over fresh anhydrous magnesium perchlorate. Crystals of this compound did not melt when heated to 200°C. Titration with standard hydrochloric acid solution gave a neutralization equivalent of 173.8; calculated value: 175.1.

Potassium Hydrogen Bis-Phenylacetate:

The procedure of Smith and Speakman[227] was modified slightly for the preparation of small quantities of this compound. A 10 ml aliquot of an alcoholic solution of phenylacetic acid (0.1 gm per ml solution) was half neutralized by the addition of 2.06 ml of alcoholic potassium hydroxide (0.1 gm per ml solution). The volume was reduced by evaporation to about 5 ml, then chilled overnight in a refrigerator at 5°C. The fine needle-like crystalline mass was recrystallized from a minimum volume of absolute ethanol. The resultant crystals were relatively long needles. They were dried under reduced pressure over phosphorous pentoxide at room temperature for 12 hours. Melting range (uncorrected) observed under crossed Nicols on a microscope hot-stage was 141.2° - 143.3°C; reported value:[222] 142°C. Titration with standard sodium hydroxide solution gave a neutralization equivalent of 312; calculated value: 311.1.

Attempts to Prepare Deuterated Potassium Hydrogen Bis-Phenylacetate:

Attempts to prepare the deuterated species of this compound by recrystallization from heavy water were unsuccessful. A mixture of phenylacetic acid and potassium phenylacetate was always obtained, as determined by microscopic examination and melting point determination under crossed Nicols.

Preparation of Samples for Spectroscopic Examination:

The infrared spectrum of each of the above compounds was determined in the form of a mull and a potassium bromide pressed disc.

Mulls:

Mulls were prepared by grinding a small quantity of the compound, about 20 - 50 mg, with one or two drops of the mulling agent, such as Nujol.

Potassium Bromide Pressed Discs:

The techniques used in the preparation of potassium bromide pressed discs have been fully described in the section on acetamide and acetamide hemihydrochloride. In this phase of the work stock mixtures of phenylacetic acid - potassium bromide (0.0917 mg per mg mixture), potassium phenylacetate - potassium bromide (0.0335 mg per mg mixture) and potassium hydrogen bis-phenylacetate - potassium bromide (0.0849 mg per mg mixture) were used.

Instrumental Conditions for Recording Spectra:

Instrumental conditions for recording the spectra were the same as those described previously.

Results and Discussion:

Nujol mull spectra of phenylacetic acid, potassium phenylacetate and potassium hydrogen bis-phenylacetate are shown in Figure II D - 2. Spectra of the compounds in a potassium bromide matrix (Figure II D - 3) are identical with the mull spectra, but the quality of the spectra are superior to those of the mulls in regards to band shape and band intensity. Moreover, the potassium bromide matrix extends the spectral range to 25 microns so that a number of low frequency vibrations have been observed. The position and relative intensity of the bands have been tabulated in Table II D - 1 for the three compounds examined as a mull and in a potassium bromide matrix.

Before discussing the peculiarities of the infrared spectrum of the acid salt, it will be necessary to consider the spectrum and frequency assignments of the acid and the neutral salt. Therefore, the discussion is divided into three parts. The first two parts deal with the frequency assignments of phenylacetic acid and potassium phenylacetate while the third part concerns the structure of the hydrogen bond of the acid salt in view of the frequency assignments of potassium hydrogen bis-phenylacetate.

Phenylacetic Acid:

The solid line curve in Figures II D - 2 and - 3 is the spectrum of phenylacetic acid. The band positions of the acid salt in a potassium bromide matrix and the possible frequency assignments have been tabulated in Table II D - 2, together with the values and assignments reported by Davies and Thomas[224] for comparison.

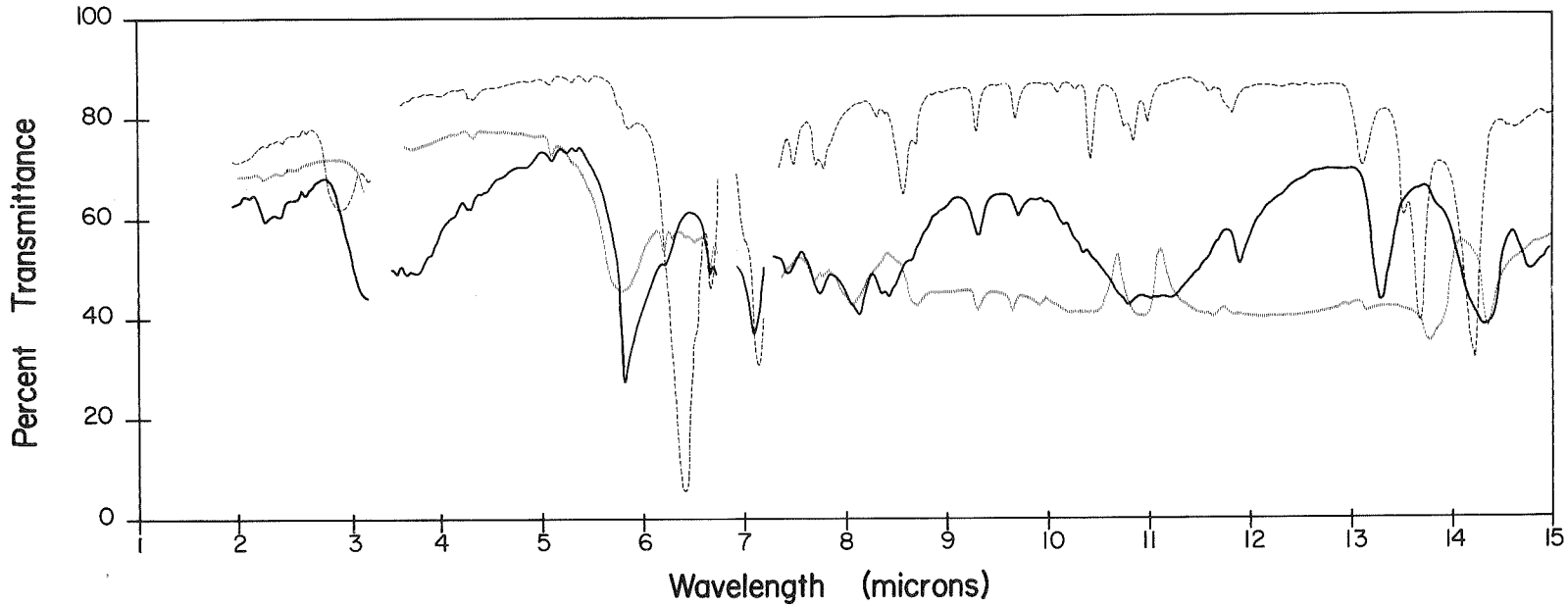

FIGURE II D-2

Infrared Spectrum of Phenylacetic Acid (——), Potassium Phenylacetate (------), and Potassium Hydrogen Bis-Phenylacetate (▒▒▒▒▒▒▒▒) as a Nujol Mull Between 2 and 15 Microns

Figure II D - 3

The Infrared Spectrum of Phenylacetic Acid (——), Potassium Phenylacetate (- - -) and Potassium Hydrogen Bis-Phenylacetate(⫼⫼⫼) in a Potassium Bromide Matrix in the Region of 2 to 25 Microns

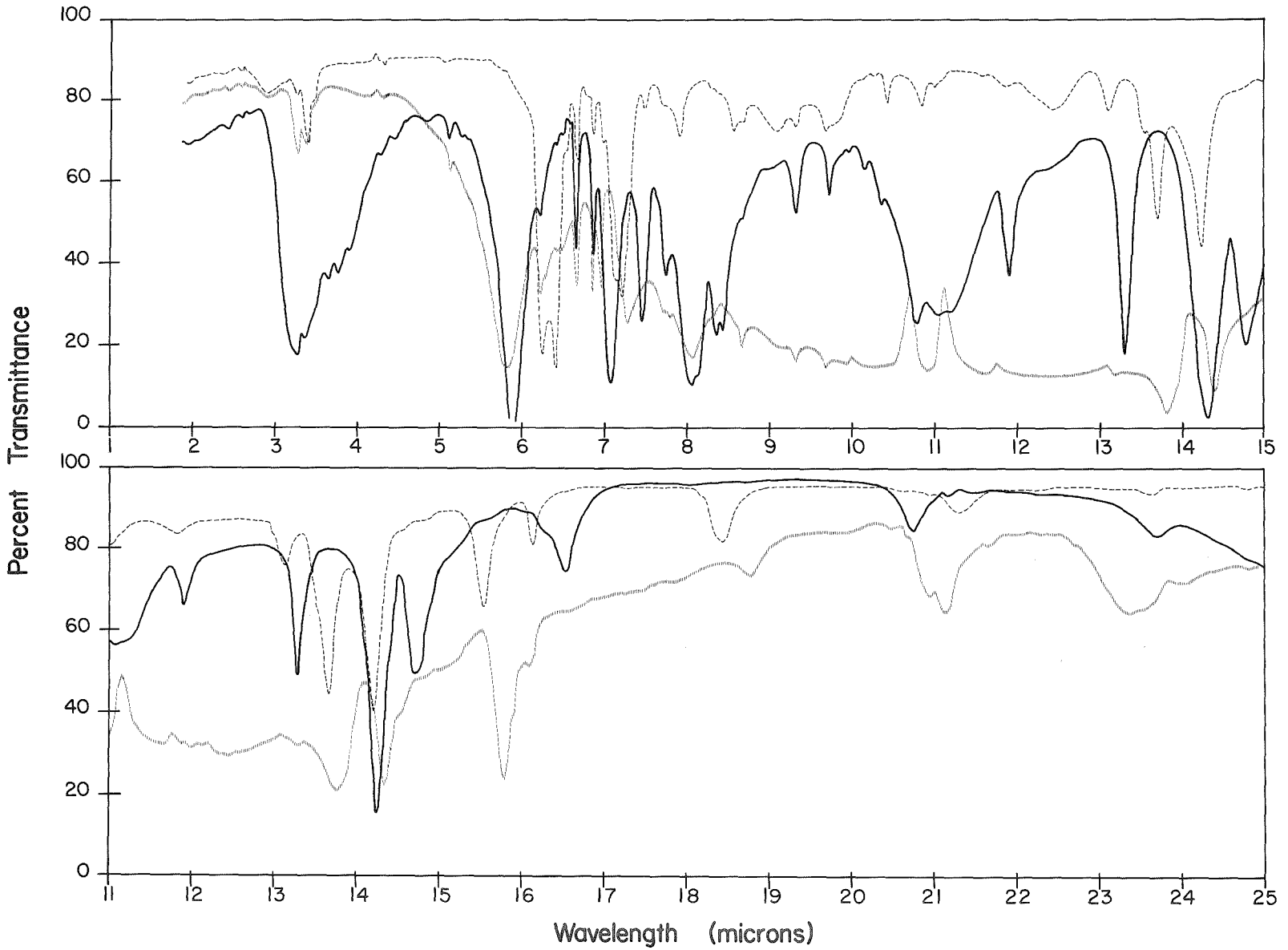
Percent Transmittance
100
80
60
40
20
0
1
2
3
4
5
6
7
8
9
10
11
12
13
14
15
11
12
13
14
15
16
17
18
19
20
21
22
23
24
25
Wavelength (microns)

Table II D - 1

Observed Frequencies for Phenylacetic Acid, Potassium Phenylacetate and Potassium Hydrogen Bis-Phenylacetate

Phenylacetic Acid		Potassium Phenylacetate		Potassium Hydrogen Bis-Phenylacetate	
Mull	KBr Disc	Mull	KBr Disc	Mull	KBr Disc
----	3030	----	3049 vw	----	3040 w
----	2959 w	----	2942 w	----	2976 w
----	----	----	2857 w	----	2857 w
2732 w	2740 w	----	2730 vw	2725 vw	2725 w
2660 w	2653 w	----	----	----	----
----	2545 vw	----	----	----	----
----	2273 vw	----	----	----	----
----	2053 w	----	----	----	----
1953 w	1951 vw	----	----	1949 vw	1949 vw
1715 s	1695 vs	----	----	1724 s	1730 vs
1608 w	1603 w	----	1597 ms	1605 s	1600 ms
----	----	1555 s	1558 s	----	1560 w
----	1501 m	1499 w	1499 w	----	1488 m
----	1456 m	----	----	----	1456 m
----	----	----	----	----	1435 m
1408 s	1408 s	1395 m	1395 m	----	1370 s
1351 mw	1349 ms	1332 w	1332 w	----	----
1290 m	1287 m	1294 w	1294 w	----	1294 m
----	----	1282 w	1278 w	----	1282 w
----	1241 s	----	----	----	1238 s
1230 m	1229 ms	----	----	----	----
1196 w	1196 w	----	----	----	----
1186 w	1183 w	----	----	----	----
----	----	1166 w	1166 w	----	----
----	----	1148 w	1152 w	----	1156 s
1073 m	1072 w	1073 w	1073 w	1073 w	1071 vw
1030 w	1029 w	1032 w	1031 w	1032 vw	1034 w

Table II D - 1
(continued)

Observed Frequencies for Phenylacetic Acid, Potassium Phenylacetate and Potassium Hydrogen Bis-Phenylacetate

Phenylacetic Acid		Potassium Phenylacetate		Potassium Hydrogen Bis-Phenylacetate	
Mull	KBr Disc	Mull	KBr Disc	Mull	KBr Disc
985 w	986 vw	---	---	---	---
965 vw	965 vw	958 w	958 w	---	---
---	---	---	---	934 m*	934 m*
923 ms	923 m	---	920 w	---	---
904 m	904 m	908 w	910 mw	---	---
892 m	893 m	---	---	898 s*	898 s*
---	---	862 vw	860 vw	858 w**	858 w**
840 m	840 m	844 vw	843 vw	---	---
751 s	756 ms	760 m	762 w	763 mw**	763 mw***
---	---	---	754 mw	---	---
---	---	737 mw	737 w	---	---
---	---	---	732 m	---	---
701 s	702 s	704 s	704 s	694 s	694 ms
---	673 ms	---	---	---	---
---	---	---	644 m	---	636 s
---	624 w	---	620 mw	---	621 w
---	605 mw	---	---	---	---
---	---	---	543 m (b)	---	533 w
---	482 w	---	474 w (b)	---	478 m
---	---	---	---	---	473 m
---	---	---	---	---	429 m (b)

* Appears as " window" in spectrum.

** Appears as "window" in spectrum, but very weak.

*** Resembles Christiansen effect in NaCl region, KBr region diffuse.

The region between 3000 cm^{-1} and 2500 cm^{-1} is characteristic of dimeric carboxylic acids[228-230] so that the phenylacetic acid molecule is dimerized in the solid state and in the potassium bromide matrix. If the intermolecular hydrogen bond distance of the acid dimer is in the range of 2.65 to 2.75 A, the shifted OH stretching frequency of the hydroxyl group of the carboxylic acid group would appear in the region of 2600 - 3100 cm^{-1}. The moderately strong band at 3030 cm^{-1} might well be the hydrogen bond shifted OH stretch, which would imply a hydrogen bond distance of 2.75 A. This is rather long for an acid dimer hydrogen bond.

The very strong band at 1695 cm^{-1} is undoubtedly due to the C=O stretch of the carboxylic acid group as dimeric aromatic carboxylic acids have strong absorption in the neighborhood of 1685 cm^{-1} [228,231] whereas the monomeric species has the absorption shifted to about 1720 cm^{-1}.[228] Davies and Thomas[224] have assigned the C=O stretch to a band at 1710 cm^{-1} while Hadzi and Novak[225] have reported the same band as high as 1750 cm^{-1}. Flett[228] has reported a band at 1697 cm^{-1} for solid phenylacetic acid and a band at 1730 cm^{-1} for solutions of phenylacetic acid in dioxane.

Moderately strong bands at 1408 cm^{-1} and 1241 cm^{-1} are assigned to the coupled $\nu C\text{-}O + \delta OH$ mode of carboxylic acid dimers.[232,233] Flett[228] has found bands at these positions in 45 out of 60 carboxylic acids, one of which was phenylacetic acid.

A rather broad, moderately intense band with peaks at 904 cm^{-1} and 893 cm^{-1} is found in the spectrum of phenylacetic acid in a potassium bromide matrix. Work by Davies and Sutherland[234] and Hadzi and Sheppard[232] have confirmed the assignment of bands

Table II D - 2

Band Positions and Frequency Assignments of Phenylacetic Acid

Davies - Orville Thomas		This Work	
Position (cm^{-1})	Assignment	Position (cm^{-1})	Assignment
3058 s		3030 m s	
----		2959 w	
2710 m		2740 w	
2618 m		2653 w	
----		2545 vw	
----		2273 vw	
----		2053 w	
----		1951 vw	
1710 s	νC=O	1695 vs	νC=O
----		1603 w	
1505 m	R	1501 m(sp)	R
1458 m		1456 m	R
1410 s		1408 s	δOH + νC-O
----		1349 ms	R
1295 s	R	1287 m	R
----		1241 s	δOH + νC-O
1237 m	νC - O	1229 ms(sh)	
1195 m	R	1196 w	R
----		1170 w(sh)	R
1155 m	R	1155 m	R
1074 m	R	1072 w	R
1030 m	R	1028 w	R
----		1003 vw	
985 w		986 vw	
965 m	R	965 vw	R
927 s	R	923 m	R
906 s		904 m	γ OH
893 s		893 m(b)	
840 m	R	840 m(b)	R
755 s	R	756 m	δ(O=C-OH)
701 s	R	702 s	R
680 m		673 ms(b)	δ(O=C-OH)
		624 w	
		605 mw	R
		482 w	

in the vicinity of 935 cm^{-1} to the hydroxyl out-of-plane deformation mode. Flett[228] has reported strong bands at 928 cm^{-1} and 904 cm^{-1} for phenylacetic acid. Hadzi and Novak[225] have assigned the γ OH frequency to a band at 950 cm^{-1}. Davies and Thomas[224] have reported strong bands at 927 cm^{-1}, 906 cm^{-1} and 893 cm^{-1} with the 927 cm^{-1} band being assigned to the residue, $C_6H_5CH_2$-, and the other two bands left unassigned. In this work the bands at 904 cm^{-1} and 893 cm^{-1} are assigned to the γ OH mode as they are absent from the spectrum of the neutral salt.

Hadzi and Sheppard[232] have suggested that the in-plane deformation mode of the carboxylic acid group of dimeric acids may occur in the vicinity of 679 cm^{-1}. In the present work the moderately strong band at 673 cm^{-1} is assigned to such a mode. It is possible that the moderately strong band at 756 cm^{-1} is also associated with the carboxlic acid group since the neutral salt has a band of comparable intensity in the neighborhood of 732 cm^{-1}, which is associated with the in-plane deformation mode of the carboxylate ion. Davies and Thomas have not given an assignment for the band at 680 cm^{-1} but have assigned the 755 cm^{-1} band to a residue mode.

A complete analysis of the phenylacetic acid spectrum has not been undertaken as the carboxylic acid group modes were of immediate interest. The bands designated by the letter R are attributed to modes of the $C_6H_5CH_2$- residue. In general, the position of the bands of phenylacetic acid are in agreement with the values reported by Davies and Thomas (see Table II D - 2), although there is a difference of opinion on the frequency assignments.

Potassium Phenylacetate:

The spectrum of potassium phenylacetate is indicated by the dashed line in Figures II D - 2 and - 3. The position of the bands of the neutral salt in a potassium bromide matrix have been tabulated in Table II D - 3, with the frequency assignments of this investigation as well as those of Davies and Thomas.

The neutral salt is of particular interest for the location and assignment of the vibrational modes of the carboxylate ion, in which resonance between the two C-O bonds is possible. Lecomte and co-workers have made a very extensive study of the infrared spectra of the salts of organic acids[235] and have found two characteristic bands between 1610 - 1550 cm^{-1} and between 1400 - 1300 cm^{-1}, which corresponds to the asymmetric and symmetric modes of the COO^- structure. In the solid state the two frequencies show minor variations with the nature of the metallic ion and also with the nature of the group to which the ionized carboxyl group is attached.[236] In the present study the strong absorption at 1597 cm^{-1} and 1558 cm^{-1} has been assigned to the asymmetric stretch of the COO^- ion, and the moderately strong band at 1395 cm^{-1} has been assigned to the symmetric stretch of the COO^- ion. Hadzi and Novak[225] assigned the symmetric stretch to a band at 1395 cm^{-1}, which is in agreement with the present work. Davies and Thomas[224] reported the band as high as 1410 cm^{-1} for the same assignment.

The in-plane deformation mode of the carboxylate ion was assigned by Davies and Thomas to a strong band at 735 cm^{-1}. In the present work a moderately strong band has been found at 732 cm^{-1},

Table II D - 3

Band Positions and Frequency Assignments of Potassium Phenylacetate

Davies - Orville Thomas		This Work	
Position (cm^{-1})	Assignment	Position (cm^{-1})	Assignment
3049 s		3049 vw	R
2915 s		2912 vw	R
----		2857 vw	
----		1704 vw	
1600 s	$\nu_a(COO^-)$	1597 ms(sh) }	$\nu_a(COO^-)$
----		1558 }	
1500 m	R	1499 w	R
1460 m		----	
1410 s	δOH or $\nu_s(COO^-)$	1395 m	$\nu_s(COO^-)$
----		1332 w	
1290 s	R	1294 w	R
----		1274 w	
----		1203 w	
1190 m	R	1190 vw	R
----		1166 w	
1158 s	R	1152 w	R
1073 m	R	1073 w	R
1037 s	R	1031 w	R
----		1018 w	
985 w		---	
970 w	R	958 w	R
940 s		---	
930 s		920 w(b)	R
907 m		910 mw	R
855 m		860 vw(sh)	
840 m	R	843 vw	R
---		762 w	
---		754 w	
735 s	$\delta(COO^-)$	737 w }	$\delta(COO^-)$
---		732 m }	
707 s	R	704 s	R
688 m		644 m	$\delta(COO^-)$
---		620 w	R
---		543 m(b)	
---		471 w(b)	R(bend)

which is assigned to the asymmetric bending mode of the carboxylate ion. The symmetric bend is assigned to a medium intense band at 644 cm^{-1}. The symmetric mode of the carboxylate ion is shifted by about 29 cm^{-1} on going from the acid to the neutral salt.

The remaining low frequency bands have been left unassigned due to an incomplete analysis of the spectrum. The bands designated by the letter R are attributed to modes of the residue, $C_6H_5CH_2$-.

Potassium Hydrogen Bis-Phenylacetate:

Spectra of the acid salt of phenylacetic acid are indicated by the vertical dashed lines in Figures II D - 2 and - 3. It is evident that the acid salt spectrum has a number of bands in common with both the acid and the neutral salt, however, there are several major differences so that the acid salt spectrum is not a superposition of the spectra of the acid and the neutral salt. The particular distinguishing feature is the broad, relatively intense background extending from about 2000 to 500 cm^{-1} with two strong "windows" appearing in the region of 1000 to 750 cm^{-1}. Hadzi and Novak[225] presented spectra which are very similar, though the relative intensity of the background and the "windows" was difficult to estimate. In the present investigation potassium bromide pressed discs were found to give a more reliable spectrum, though all the features of interest were found in the mull spectrum.

The position and relative intensities of the bands of the acid salt have been tabulated in Table II D - 4, along with the frequency assignments for the hydrogen bonded system and the

Table II D - 4

Band Positions and Possible Frequency Assignments for Potassium Hydrogen Bis - Phenylacetate

Davies - Orville Thomas		This Work	
Position (cm^{-1})	Assignment	Position (cm^{-1})	Assignment
3042 s		3040 w	
2976 s		2976 w	
----		2857 w	
1946 w		1949 vw	
1755 s	νC=O	1730 vs(b)	νC=O
1570 s	$\nu_a(COO^-)$	1600 ms	$\nu_a(COO^-)$ or ν_aO-H-O
----		1560 w	
----		1538 w	
1500 m	R	1488 m	R
----		1456 m	R
1460 m		1435 m	
1375 s	δOH or $\nu(COO^-)$	1370 s(b)	δO-H-O
1290 s	R	1294 m(sb)	R
----		1282 w	
1245 m	νC-O	1238 s	νC-O or δO-H-O
1206 m	R	1202 w(sh)	
1155 s	R	1156 s	R
1073 m		1073 w	
1036 w		1034 w	
985 w		----	
965 m	R	----	
945 m		----	γ O-H-O or γOH
----		934 s*	
925 m	R	---	
890 s		898 s*	473+429 = 902 (?)
860 s		858 w	
841 s	R	851 w	
763 m	R	763 ms	$\delta(COO^- H^+)$
728 m	δCOO^-	724 s	
695 s	R	694 ms	
---		688 w	
---		636 s	$\delta(COO^- H^+)$
---		621 w	R
---		553 w	
---		478 m	
---		473 m	
---		429 m(b)	

* Appear as "windows" in the spectrum.

pseudo-carboxylic acid group. The band positions and assignments of Davies and Thomas have been included in the table for comparison.

The 3000 to 2700 cm^{-1} region of the spectrum of the acid salt is very similar to that of the neutral salt. This is a good indication that the material under investigation is not a mixture of the acid and the neutral salt, but a distinct compound. Since bands in this region are mainly associated with the carbon-hydrogen stretching modes, as well as overtones, no assignments will be given.

The region between 2500 and 1800 cm^{-1} is of more interest in that a hydrogen bonded OH group with an O----O distance of 2.54 A should give rise to a shifted OH stretching frequency between 2200 and 2000 cm^{-1}. In the spectrum of the acid salt no absorption is found in this region with the exception of a weak band at 1949 cm^{-1}. This weak band is also found in the spectrum of phenylacetic acid. Hadzi and Novak were unable to associate any absorption in this region to a shifted OH stretching frequency and concluded that the hydrogen bond must be symmetric. The present work supports the symmetric model, though a more complete discussion of the pseudo-carboxylic acid modes is necessary before any model of the system is established.

A strong band is found at 1730 cm^{-1} and is in the region of the C=O stretching frequency of monomeric carboxylic acids.(228) Due to the symmetry about the hydrogen bond in the acid salt, this band must be due to an out-of-phase stretching mode of the C=O groups on neighboring phenylacetate residues. The existence of the C=O groups is born out by the neutron diffraction in-

vestigation of the acid salt by Bacon and Curry,[223] who found the C-O and C=O distances of 1.30 and 1.22 A, respectively, which are in agreement with calculated distances for normal covalent single and double C-O bonds.[201] Hadzi and Novak and Davies and Thomas have reported the band nearer 1750 cm^{-1}, with the assignment to that of the C=O stretch. Therefore, the acid salt has a free carbonyl group, similar to monomeric carboxylic acids.

Davies and Thomas have interpreted the earlier X-ray structure and the appearance of bands at 1570 cm^{-1} and 1375 cm^{-1} in the infrared spectrum of the acid salt as evidence for the existence of the carboxylate ion. Hadzi and Novak on the other hand have attributed absorption in the 1580 - 1560 cm^{-1} as due to the asymmetric stretch of the symmetric hydrogen bond. To support their assignment deuteration caused the band to disappear, though no shifted band was reported. In the present work a strong band is found at 1600 cm^{-1} with a relatively weak band at 1560 cm^{-1}. Since the recent structural investigation[223] does not indicate a carboxylate ion, or unusual C-O distances, the assignment of Davies and Thomas is questionable. If this band is associated with the motion of the hydrogen atom in the hydrogen bond it might well describe the oscillation of the hydrogen atom, or possibly a proton, in a broad, anharmoic potential minimum. Furthermore, this would imply that the empirical relationships between O---O hydrogen bond distance and O-H frequency shift fail for short, symmetric hydrogen bonds.

In monomeric acids the coupled ν C-O + δ OH mode gives rise to absorption in the 1280-1380 cm^{-1} and 1070-1200 cm^{-1} re-

gions while the dimeric species has absorption in the 1400 cm^{-1} and 1300 cm^{-1} regions.(88) For both species of carboxylic acids the higher frequency band is more liable to be designated as the δOH mode. In the acid salt the 1370 cm^{-1} band may well be a pseudo-νC-O + δO--H mode, which would correspond to an in-plane bend of the hydrogen bond, with a relatively long O-H distance (about 1.27 A in comparison to the normal distance of 1.07 A).

A strong band in the 1240 cm^{-1} region has been assigned by Davies and Thomas to the C-O stretch, whereas Hadzi and Novak have attributed the band in this region to the deformation mode of the hydrogen bond system on the basis of deuteration of the acid salt. The deuteration effect mentioned by Hadzi and Novak is difficult to discern in their spectrum, so the assignment is open to question. Esters and lactomes exhibit absorption in the 1250 cm^{-1} region which has been assigned to the C-O stretch.(237) The C-O stretching component of the coupled νC-O + δOH mode in monomeric and dimeric carboxylic acids is found in this region. The 1238 cm^{-1} band of the acid salt might well be associated with the C-O stretch. From the symmetry of the hydrogen bonded system the out-of-phase C-O stretch would be equivalent to an in-plane O--H--O bend, which may account for the observed deuteration effect and frequency assignment of Hadzi and Novak.

The region between 1000 cm^{-1} and 850 cm^{-1} is of unusual interest in that very few absorption bands are found on the broad, intense background, with the exception of two strong "windows" at 934 cm^{-1} and 898 cm^{-1}. Davies and Thomas did not report unusual absorption or band anomalies in the acid salt spectrum. On the other hand mull spectra of Hadzi and Novak were

found to exhibit the effects noted in the present work, though their background was difficult to estimate. In the acid spectrum a relatively broad, intense band with several well-defined absorption peaks found in the vicinity of 900 cm^{-1} has been attributed to the out-of-plane deformation mode of the OH group of the carboxylic acid groups as well as possible residue modes, either C-C stretching or C-H bending modes. The neutral salt spectrum, however, has only a few relatively weak bands in this region, those due to the residue modes. The position of the "windows" in the spectrum of the acid salt with respect to the γ OH frequency of phenylacetic acid is more than a chance occurance. It is likely that in a symmetric hydrogen bond absorption in this region is associated with the out-of-plane deformation mode of the O--H--O system. Further discussion of the "windows" and the broad background absorption associated with short hydrogen bonded systems will be given in Section F.

Of the low frequency bands in the acid salt spectrum those at 763 cm^{-1}, 724 cm^{-1}, and 636 cm^{-1} will be compared with the bands found in phenylacetic acid and potassium phenylacetate spectra. In the neutral salt bands at 732 cm^{-1} and 644 cm^{-1} have been assigned to the asymmetric and symmetric deformation modes of the carboxylate ion, respectively, whereas the bands at 756 cm^{-1} and 673 cm^{-1} in the acid spectrum have been assigned to the in-plane deformation mode of the carboxylic acid group. If the 724 cm^{-1} and 636 cm^{-1} bands in the acid salt are associated with the pseudo-carboxylic acid group, it would indicate that the structure of the group is more like the carboxylate ion. But, if the two higher frequency bands are associated with the group, it would imply a carboxylic acid group. The neutron diffraction structural analysis

does not support the carboxylate ion while the infrared spectrum does not support a carboxylic acid group. The actual configuration is somewhere between these two extremes.

This problem leads directly into the question of possible structures for the hydrogen bond system in potassium hydrogen bisphenylacetate. In view of the spectroscopic and crystallographic data several possible structures are shown schematically in diagrams (i) thru (iv). Structure (i) was proposed by Davies and Thomas from their infrared investigation of the acid salt. This structure supposes that the acid salt is

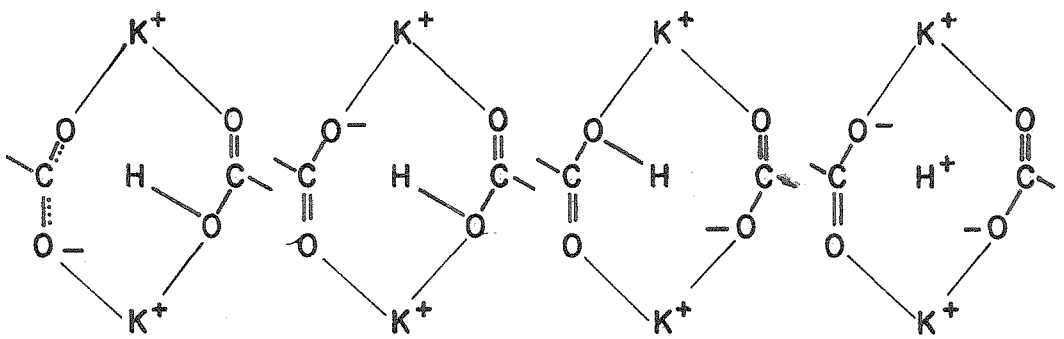

(i) (ii) (iii) (iv)

the neutral salt and the acid joined by an unsymmetric hydrogen bond, the hydrogen atom being associated with the hydroxyl group of the carboxylic acid group. The absence of a hydrogen bond shifted OH stretching vibration and the out-of-plane deformation mode of the carboxylic acid hydroxyl group as well as the recent structural analysis which indicates normal C-O and C=O bond lengths, makes this model questionable. Structures (ii) and (iii) were first proposed by Speakman to account for the short C-O and C=O bond distances in his crystal structure

analysis.(222) Such structures support the mesohydric tautomerism concept proposed by Hunter.(2) Coulson(4) rejects this concept on the grounds that the resonance energy is not large enough unless the proton is centrally located and the energy necessary to expand a normal O-H bond to the required distance is too great. Nevertheless, structures (ii) and (iii) are not unreasonable in that the hydrogen bond in the acid salt is probably symmetric, at least, statistically symmetric, and the spectroscopic and crystallographic data would fit such models. An alternative model is proposed and is represented by structure (iv). In this model the hydrogen bond is considered to be symmetric and electrostatic in nature, similar to the hydrogen bond in the bifluoride ion. If the proton oscillates in a potential curve with a broad minimum it would appear to give structures similar to (ii) and (iii), but there would be no bond formed between the O atoms and the proton. The proton oscillation would be highly anharmonic. Such a model is consistent with the spectral work and the structural data for the C-O bonds, and would account for the intensity of the hydrogen bond vibrational modes. Thus, the structure of the acid salt may be described as an infinite layer of potassium ions and protons situated between layers of phenylacetate residues, the carboxyl group residues being linked together strongly by protons and on either side weakly by the potassium ions. The protons are situated mid-way between two oxygens forming a symmetric hydrogen bond.

Section E: Maleic Acid

In hydrogen bonds the hydrogen atom is usually closer to one of the atoms it connects. As the distance decreases there is the possibility that the hydrogen atom will become equidistant from the end atoms of the hydrogen bond. For the O-H---O system a symmetric configuration has been estimated for an O---O distance of 2.45 A.[49] Maleic acid possesses an intramolecular hydrogen bond with an O---O distance of 2.46 A.[238]* The bond, however, is not symmetric. It was felt that a study of the infrared spectrum of maleic acid might provide worthwhile information with regards to the structure of very short hydrogen bonds.

Crystal Structure:

Crystals of maleic acid are monoclinic and belong to space group $P 2_1/c$ with four molecules per asymmetric unit cell. The unit cell has dimensions $a = 7.47$ A, $b = 10.5$ A, $c = 7.65$ A and $\beta = 123.5^{\circ}$. In Figure II E - 1 is shown a projection of the unit cell along the z axis at $z = 1/4$. The molecules are presumably joined together by a two dimensional network of hydrogen bonds, as indicated by the dashed lines in the figure.

The molecule is in the cis- configuration and almost planar with nearly equivalent C - C bonds of length 1.45 A. The C-C distances are peculiar in that the "double bond" distance seems very long for a conjugated system. More precise data now available on conjugated systems shows a distinct difference between predominantly single and predominantly double C-C bonds.[239] The C=O

* Recalculation of the internuclear distances from Shahat's data (Structure Reports for 1952, A.J.C. Wilson, General Editor, Vol. 16, pp. 431 - 432, Oosthock, Utrecht (1959)) gives an O---O distance of 2.43 A, though the probable limits of error are ±0.05 A.

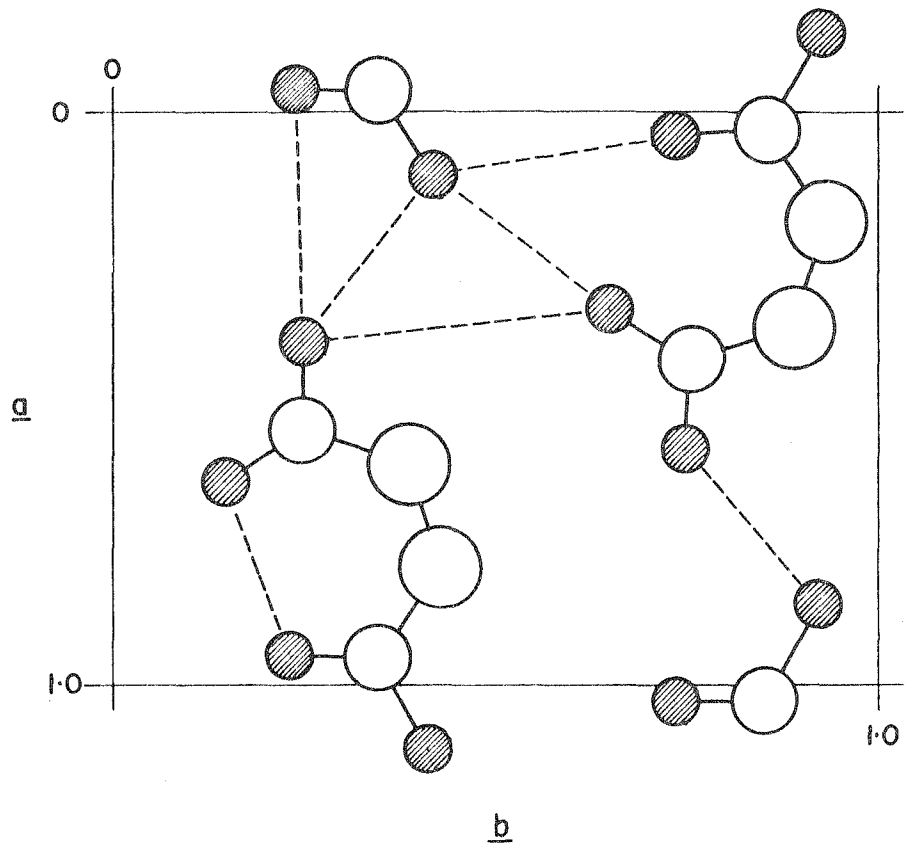

FIGURE II E - I

Crystal Structure of Maleic Acid

Projection along c - axis at z = 1/4

and C-O(H) bonds are reported to be 1.20 A and 1.27(5) A, respectively, with a non-planar configuration for the carboxyl group. Recalculated values[240] for a planar carboxyl group give C=O and C-O(H) distances of 1.16 A and 1.32 A, respectively, which are normal for carboxylic acids.[15,16]

The hydrogen bond formed between oxygen atoms of the carboxyl groups of the same molecule is 2.46 A, which is one of the shortest bonding distances of the O-H---O type. On the other hand, the bonds formed between an oxygen of one molecule and an oxygen of another is rather long for an O-H---O bond, 2.75 A.

Experimental Details:

Maleic Acid:

Maleic acid (Eastman T 690) was recrystallized twice from acetone and then sublimed under reduced pressure at 80°C. The sublimed material was stored in a desiccator over fresh anhydrous magnesium perchlorate. Melting range (uncorrected) observed under crossed Nicols on a microscope hot-stage was 130.2° 131.5°C; literature value:[226] 130.5°C. Titration with standard sodium hydroxide solution gave a neutralization equivalent of 115.9; calculated value: 116.1.

Deuterated Maleic Acid:

Deuterated maleic acid was prepared by repeated recrystallization from heavy water. Two recrystallizations of a one gram quantity from 1 ml portions of heavy water was sufficient to give almost complete deuteration. The excess heavy water was removed under reduced pressure with the aid of phosphorous pentoxide,

and finally dried at 56°C under reduced pressure over phosphorous pentoxide. The crystals were stored in a sealed container in a desicator over fresh anhydrous magnesium perchlorate.

Preparation of Samples for Spectroscopic Investigation:

The infrared spectrum of maleic acid and deutero-maleic acid was examined on the crystalline material in the form of mulls and potassium bromide pressed discs.

Mulls:

Mulls were prepared by grinding the compound, usually 50 mg, with one or two drops of the mulling agent, which was either Nujol (liquid paraffin) or hexachloro - 1, 3 - butadiene.

Potassium Bromide Pressed Discs:

The techniques used in the preparation of potassium bromide pressed discs have been fully described on pages 43 - 45 . In this part of the work a stock mixture of maleic acid - potassium bromide (0.0996 mg per mg mixture) was used for most of the work. For a rapid comparison of the deuterated and undeuterated compounds in potassium bromide discs a weighed quantity of the compound, on the order of 1 to 2 mg, was ground with one gram of dried potassium bromide in an agate mortar under an infrared lamp for 5 minutes and then quickly transferred to the die. The remainder of the disc technique was the same.

Instrumental Conditions for Recording Spectra:

Instrumental conditions for recording the spectra were the same as those described in the previous sections.

Results and Discussion:

Infrared spectra were observed for maleic acid and partially deuterated maleic acid in a potassium bromide matrix and as a mull. Mull spectra of the deuterated and undeuterated material are shown in Figure II E - 2. In Figure II E - 3 are shown the infrared spectra of deuterated and undeuterated maleic acid in a potassium bormide matrix in the region between 2 and 25 microns. In general the infrared spectrum of maleic acid appears to be well-behaved, unlike the complex spectra of the previously discussed short hydrogen bonded molecules. The quality of the mull spectra compare quite favorably with those obtained as a potassium bromide matrix with respect to band positions and band intensities.

The frequencies observed for both the deuterated and undeuterated species of maleic acid as a mull and in a potassium bromide matrix have been tabulated in Table II E - 1 together with possible frequency assignments. Most of the wave-number values listed are believed to be accurate to ± 5 cm^{-1} for bands between 1000 and 2000 cm^{-1}, to ± 10 cm^{-1} for bands between 2000 and 2500 cm^{-1} and to ± 20 cm^{-1} for bands between 2500 and 3000 cm^{-1}. Band intensities were estimated from relative peak heights when observed in two or more spectra, The symbols used in Table II E - 1 following the frequency values are defined as: vw very weak; w weak; mw moderately weak; m medium; ms moderately strong; s strong; vs very strong; b broad band; sp sharp band; sh shoulder; and bk background absorption.

A major portion of this section will be devoted to a discussion of the frequency assignments given in Table II E - 1. In maleic acid vibrational modes associated with the hydroxyl group of the carboxyl

Figure II E - 2

Infrared Spectra of Maleic Acid and Deuterated Maleic Acid as Mulls in the Region of 2 to 15 Microns

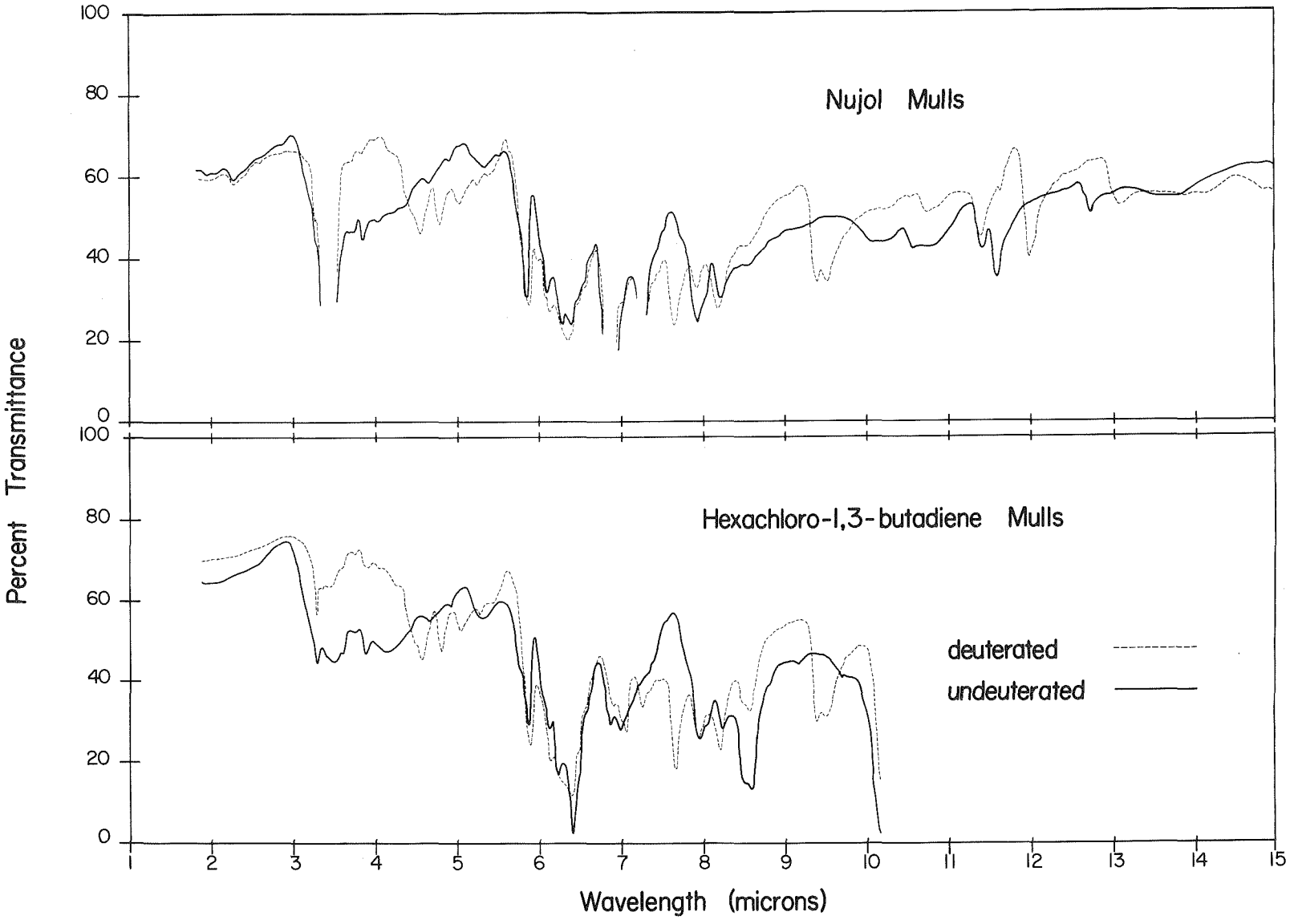
Percent Transmittance
100
80
60
40
20
0
Nujol Mulls
Hexachloro-1,3-butadiene Mulls
deuterated
undeuterated
1
2
3
4
5
6
7
8
9
10
11
12
13
14
15
Wavelength (microns)

Figure II E - 3

Infrared Spectrum of Maleic Acid and Deuterated Maleic Acid in a Potassium Bromide Matrix in the Region of 2 to 25 Microns

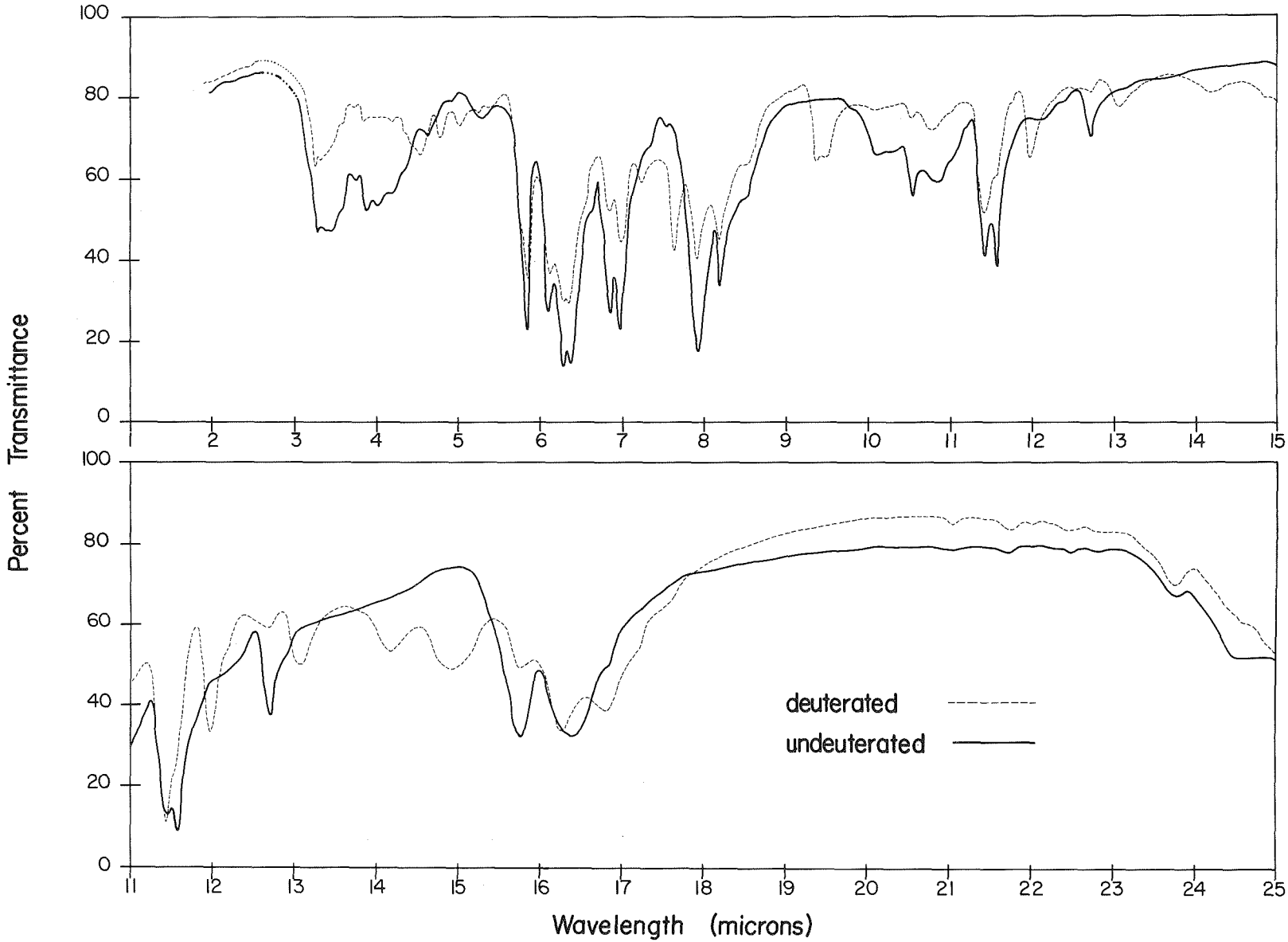
Percent Transmittance
100
80
60
40
20
0
1
2
3
4
5
6
7
8
9
10
11
12
13
14
15
11
12
13
14
15
16
17
18
19
20
21
22
23
24
25
deuterated
undeuterated
Wavelength (microns)

Table II E - 1

Observed Frequencies and Possible Assignments for Maleic Acid

KBr Disc		Mulls		
(undeut'd)	(deut'd)	(undeut'd)	(deut'd)	Assignment
3030 w(bbk)	3030 m(sp)	3049 m(sp)	3049 m(sp)	νCH
----	2924 m(b)	2924 m	2941 m(b)	
2857 m(b)	----	----	----	
----	----	2778 w	----	
2667 w(bbk)	2660 w	2667 vw	2667 vw	
2571 w(bbk)	2577 vw	2584 m	2577 w	
2483 w(bbk)	2483 vw	2481 w	2481 vw(bbk)	
----	----	2439 m(b)	----	
2392 w(bbk)	2358 vw	----	2358 vw	
----	2203 m	----	2193 m(bsh)	νOD(inter)
2160 w	----	2151 w	----	
2114 w	----	2128 w	----	
----	2089 m	----	2083 m	νOD(inter)
2033 vw(sh)	----	2033 vw	----	
----	1988 m	----	1984 m	
----	----	----	1934 m	
1880 mw(b)	----	1880 mw(b)	----	νOH(intra)
1706 ms	1708 s	1704 s	1704 s	νC=O
1637 s	1637 s	1637 s	1629 s	νC=C
1591 vs(b)	1590 vs(b)	1587 s(b)	1587 s(b)	νC=C ?
1567 vs(b)	1572 vs(b)	1565 s(b)	----	νC=C ?
1460 s	1460 m	1460 ms	1449	δOH + νC-O + δCH
1435 s	1432 ms	1433 ms	1418 ms	
----	1383 m	----	1379 m	νOD(intra)
1361 w(sh)	----	----	----	
1323 w	----	----	----	
----	1309 m	----	1305 ms	δOD + νC-O + δCH
1263 vs	1263 m	1258 ms	1259 m	δOH + νC-O + δCH
1217 s	1221 m	1217 m	1219 s	δOH + νC-O + δCH
1174 w(sh)	1172 w(sh)	1168 w(sh)	1170 w(sh)	νC-C(OOH) ?
----	1062 m	----	1064 ms	
----	1052 ms	----	1052 ms	δOD
986 w(b)	984 w(b)	985 w(b)	----	γCH(in-phase)
946 m	950 vw	935 m(b)	930 w	γOH(intra)
921 m(b)	923 w(b)	---	---	γOH(inter)
875 ms	875 s	875 m	875 m	(skeletal) ?
863 ms	865 m(sh)	864 mw	858 w	δ(O=C-O(H))
---	831 m	---	831 s	δ(O=C-O(D))
786 m(b)	786 vw	---	785 w	ν(OH--O)
---	766 mw	---	---	ν(OD--O)
---	705 w(b)	---	---	γOD(intra)
---	668 w(b)	---	---	γOD(inter)
634 ms	631 w	---	---	δ(O=C-O(H)) intra
---	614 mw(b)	---	---	δ(O=C-O(D)) intra
609 m(b)	---	---	---	δ(O=C-O(H)) inter
---	594 mw(b)	---	---	δ(O=C-O(D)) inter

group and the carboxyl group proper with respect to hydrogen bonding are of particular interest. Therefore, the discussion of the spectrum will center around these vibrational modes.

Hydroxyl Vibrational Modes of the Carboxyl Group:

The prime interest in the infrared spectrum of maleic acid lies in the influence of hydrogen bond formation on the hydroxyl vibrational modes of the carboxyl group, which may be classified as the hydroxyl stretching mode, ν(O-H), the out-of-plane deformation mode, γ(O-H), and the in-plane deformation mode, δ(O-H). Each of these modes will be discussed in the next few paragraphs.

ν(O-H) Bands:

In the liquid or solid state carboxylic acids exist as dimers or higher polymers.[228,229] A series of weak bands superimposed on a broad background between 2700 and 2500 cm^{-1} is characteristic of carboxylic acid dimers and higher polymers.[230] In maleic acid the long, intermolecular hydrogen bond of 2.75 A results in the formation of an essentially infinite one-dimensional chain of molecules. Flett[228] observed two bands in this region at 2600 and 2510 cm^{-1}, while in the present work they are found at 2577 and 2483 cm^{-1}, respectively. Both of these bands are in some manner concerned with the O-H vibrational modes as on deuteration two new bands are found at 1988 and 1934 cm^{-1}. Bratoz, Hadzi and Sheppard[230] have explained these bands as combinations of lower frequency vibrations involving the COOH group, the intensity being enhanced by Fermi resonance with the O-H fundamental.

If the more or less unique relationships between O---O distance and the O-H frequency shift[49,50,56,66-70] are applied to the long,

intermolecular hydrogen bond of maleic acid, an absorption band should exist in the region between 3000 and 3150 cm^{-1}. This region, unfortunately, is very poorly defined with sodium chloride optics, both in the undeuterated and deuterated maleic acid spectrum. In the spectrum of the deuterated species, however, two bands of moderate intensity appear at 2203 and 2089 cm^{-1}, which, if due to the O-D stretching vibration would have their respective O-H bands in the 3000 to 3100 cm^{-1} region. This is just the region predicted for the weak, intermolecular hydrogen bond, which suggests that maleic acid exists as a dimer or a higher polymer in the potassium bromide pressed discs.

Of more importance is the very short intramolecular hydrogen bond. Lord and Merrifield[67] have assigned a band at 2000 cm^{-1} to the shifted O-H stretching vibration whereas Nakamoto et al[49] have placed this vibration in the vicinity of 1800 cm^{-1}. A simple calculation using the relationship of Pimentel and Sederholm[68] would place it near 1880 cm^{-1}. In the present work undeuterated maleic acid exhibits a moderately weak though rather broad band at 1880 cm^{-1}. On deuteration the band disappears while a band of medium intensity appears at 1383 cm^{-1}. As this band exhibits the expected frequency shift on deuteration it has been assigned the hydroxyl stretching mode, ν(O-H), of the short intramolecular hydrogen bonded carboxyl group.

γ(O-H) Bands:

Two medium intensity bands are found at 946 and 921 cm^{-1} in the potassium bromide matrix spectrum and a single medium intensity band at 935 cm^{-1} in the Nujol mull spectrum. On deuteration the bands are shifted to 705 and 668 cm^{-1}, respectively, with an (H)/(D) ratio of

1.34 for both bands. Davies and Sutherland have suggested that in lower fatty acids the out-of-plane deformation mode of the hydroxyl of the carboxyl group may arise near 935 cm^{-1}.[234] This has been subsequently confirmed by Flett,[228] Shreve et al[229] and Hadzi and Sheppard.[232] Hadzi and Sheppard[232] have also shown that the hydroxyl out-of-plane deformation mode exhibits the expected shift on deuteration to 675 ± 15 cm^{-1}. Therefore, the bands found at 946 and 921 cm^{-1} in the potassium bromide matrix spectrum are assigned to the out-of-plane deformation mode of the hydroxyl of the carboxyl groups. The higher frequency one for the intramolecular hydrogen bonded carboxyl group and the lower frequency band to the intermolecular hydrogen bonded carboxyl group.

δ(O-H) Bands:

The higher frequency in-plane deformation mode of the hydroxyl hydrogen has not been as thoroughly investigated as the two previously discussed vibrational modes. The motion of the hydrogen atom is considerably restricted by the force constant controlling the R-O-H angle coupled with the effect of hydrogen bonding. Work by Flett,[228] Corish and Chapman[233] and particularly Hadzi and Sheppard[232] have attributed a moderately strong band near 1430 cm^{-1} in carboxylic acid dimers to a C-O stretching vibration coupled with an O-H in-plane deformation vibration. Recent work by Hadzi and Pintar[88] on monomeric carboxylic acids have shown that if differentation into δ O-H and ν C-O bands is to be made, the high frequency band near 1430 cm^{-1} is more reasonably called δ O-H. This would also be true of the dimeric species. Flett[228] has observed a single intense band at 1437 cm^{-1} in the spectrum of maleic acid, whereas in this work two strong bands at 1460 and 1435 cm^{-1} have been observed. On deuteration the intensity of both bands diminishes,

though they are still moderately intense. Furthermore, in the deuterated spectrum two moderately strong bands are found at 1062 and 1052 cm^{-1}, which would give an (H)/(D) frequency shift ratio of 1.360 and 1.365, respectively. This is further supported by the two strong bands at 1263 and 1217 cm^{-1} in the undeuterated spectrum. Deuteration causes a decrease in the band intensities with a shift of the 1263 cm^{-1} band to 1309 cm^{-1}. In carboxylic acids bands of this frequency are attributed to the ν (C-O) mode of the δ(O-H) + ν(C-O) coupled vibration.(88)

Compounds of the type RHC=CHR' have two in-plane deformation modes with frequencies in the region between 1460 and 1200 cm^{-1}.(241) Maleic acid possesses α, β -unsaturation, though the molecule is in the cis- configuration. As these modes are planar coupling with the δ(O-H) + ν(C-O) mode, which is also planar, is possible. Thus, the vibrational mode will be of the type δ(O-H) + ν(C-O) + δ(C-H). On deuteration the hydroxyl hydrogen is readily replaced with deuterium, which will shift the δ(O-H) component by the expected ratio. The ν(C-O) vibration, which is really a ν(C-O(H)) vibration, will also be affected. The δ(C-H) vibration will, however, remain essentially unchanged, though coupled with the new frequency. Farmer(161) has found four bands in the spectrum of dimeric cinnamic acid and three bands in crotonic acid which could be attributed to a coupling scheme of this type. Therefore, the four intense bands at 1460, 1435, 1263 and 1217 cm^{-1} have been assigned the planar coupled mode δ(O-H) + ν(C-O(H)) + δ(C-H).

Vibrational modes attributed to the hydroxyl group are: intra- ν(O-H) = 1880 cm^{-1}; inter- ν(O-H) = 3000 - 3100 cm^{-1} (estimated); intra- γ(O-H) = 946 cm^{-1}; inter- γ(O-H) = 921 cm^{-1}; pseudo δ(O-H) = 1460 cm^{-1} and 1435 cm^{-1}.

Carboxyl Group Vibrational Modes:

The recalculated structural data[240] indicates the C=O and C-O(H) bond distances are almost normal C=O and C-O(H) bonds for a carboxylic acid,[15,16] therefore, in this section we will be concerned with the vibrational modes associated with the carboxyl group. Specific groups under consideration are the C=O stretching mode, ν(C=O), the C-O(H) stretching mode, ν(C-O(H)), and the in-plane deformation mode, δ(O=C-O(H)). Evidence is given for the existence of the hydrogen bond stretching mode, ν(OH--O), associated with the short intramolecular hydrogen bond.

ν(C=O) Band:

Flett[228] has reported the C=O stretching vibration of α,β-unsaturated acids to be near 1700 cm^{-1}. Because of α,β-unsaturation coupling between the C=O and C=C bond vibrations may displace the C=O absorption band by about 30 cm^{-1} to lower frequency.[242] Therefore, the intense band at 1706 cm^{-1}, which is unaffected by deuteration, is assigned to the C=O stretching mode.

ν(C-O(H)) Band:

The assignment of this mode has been briefly discussed in conjunction with the in-plane hydroxyl deformation mode. Two moderately strong bands in the undeuterated species are found at 1263 and 1217 cm^{-1}. On deuteration, the 1263 cm^{-1} is shifted to 1309 cm^{-1}, an increase of +46 cm^{-1}. Hadzi and Pintar[88] have shown that bands associated with the δ(O-H) + ν(C-O(H)) mode are displaced between +50 and +150 cm^{-1} to the high frequency side. So if differentiation into a δ(O-H) and a ν(C-O(H)) mode is made, the band at 1263 cm^{-1} could be assigned to the

C-O(H) stretching mode. This is an oversimplification as the band is really a composite of the in-plane hydroxyl deformation modes. The band at 1217 cm^{-1} appears to be predominantly the δ(C-H) deformation frequency.

δ(O C-O(H)) Bands:

Hadzi and Sheppard[232] have suggested that the O C-O(H) deformation mode of the carboxyl group of dimeric acids may occur near 679 cm^{-1}. In the present work a moderately strong band appears at 634 cm^{-1} with a second relatively broad band near 609 cm^{-1}. On deuteration broad bands of moderately weak intensity appear at 614 and 594 cm^{-1}. These bands are assigned to the carboxyl in-plane deformation modes of the two carboxyl groups, one involved in intramolecular hydrogen bonding and the other intermolecular hydrogen bonding.

ν(OH---O) Band:

The O---O motion of two hydrogen bonded oxygen atoms has been much less thoroughly investigated than the hydroxyl stretching mode, because it lies in a more difficult accessible region of the spectrum, and may be easily confused with other low-frequency modes, particularly in the spectra of hydrogen bonded solids. Sharp, closely spaced bands in the 150 to 300 cm^{-1} region of the Raman spectra of substances containing a hydroxyl group is considered a direct indication of hydrogen bonding with the hydroxyl group as an entity vibrating against the oxygen atom.[94] Reid[80] has recently proposed from a semiempirical treatment of the hydrogen bond that as the O---O distance decreases there is a rapid rise in the hydrogen bond stretching frequency.

Interpolation among Reid's values for a hydrogen bond distance of 2.46 A, such as that found in for the intramolecular hydrogen bond in maleic acid, would be expected to give rise to an absorption band between 730 and 790 cm^{-1}. In this work a moderately intense band has been observed in the spectrum of undeuterated maleic acid at 786 cm^{-1}. On deuteration a moderately weak band appears at 766 cm^{-1}, which, if associated with the hydrogen bond stretching mode has an (H):(D) ratio of 1.028. This is in agreement with the theoretical shift ratio of 1.033 for an OH---O system. If the deuterated band is associated with an O-D motion it would have an O-H band near 1050 cm^{-1}, a region where no bands have been observed for undeuterated maleic acid. The band at 786 cm^{-1} is therefore, assigned to the hydrogen bond stretching vibration of the intramolecular hydrogen bond.

A moderately strong band at 863 cm^{-1} appears to be related to the carboxyl group since on deuteration the band diminishes while a new band of moderate intensity appears at 831 cm^{-1}. The frequency shift ratio of 1.035 compares favorable with the theoretical value for a carboxyl type vibration. If the 831 cm^{-1} band in the deuterated spectrum were due to a hydroxyl type vibrational mode it would have its origin in the region of 1130 - 1140 cm^{-1}. No bands are found in this region so for that reason it has been classified with the carboxyl group vibrations. A possible assignment is that of an asymmetric stretching mode of the O C-O(H) group.

Vibrational modes attributed to the carboxyl group are: intra- and inter- ν(C=O) = 1706 cm^{-1}; pseudo ν (C-O(H)) = 1263 cm^{-1} and

1217 cm^{-1}; intra- δ(O C-O(H)) = 634 cm^{-1} and inter- δ(OC-O(H)) = 609 cm^{-1}; intra- ν(OH---O) = 786 cm^{-1}; and an unassigned carboxyl band at 863 cm^{-1}.

Skeletal Vibrational Modes:

The last group of frequency assignments to be considered are those of the skeletal vibrational modes such as the C-H vibrations, the C=C vibration and the C-C type vibration.

In cis- disubstituted ethylenes the C-H stretching mode is near 3030 cm^{-1} and in conjugated dienes and α,β - unsaturated ketones the band may be quite strong.(243) A medium intense, sharp band at 3030 cm^{-1} in the spectrum of deuterated and undeuterated maleic acid is, therefore, assigned to the ν(C-H) vibration.

The frequency of the out-of plane C-H deformation mode of cis- RHC=CHR' type ethylenes is still uncertain though Sheppard and Sutherland(244) originally placed it between 980 and 965 cm^{-1}, in the same range as the trans- system. Spectra of several cis- isomers suggest that the absorption peak due to this vibration lies near 690 cm^{-1},(245) though substitution at the α position results in a marked shift to higher frequencies. Conjugation with carbonyl groups has a very marked effect, and the group -CH=CHOOR (cis) absorbs near 820 cm^{-1}.(245) It is possible that the very weak band near 826 cm^{-1} might be associated with this vibrational mode, though the weak band at 986 cm^{-1} is assigned to the C-H out-of-plane, in-phase bending vibration. It is unaffected on deuteration whereas the 826 cm^{-1} disappears.

The weak in-plane C-H deformation vibration of cis- RHC=CHR' type ethylenes occurs between 1420 and 1400 cm^{-1}.(246) In the α,β - un-

saturated carboxylic acids several strong bands have been observed in the 1340 to 1220 cm^{-1} region,[161] which are attributed to coupling of the in-plane C-H deformation vibration with the $\delta(O-H) + \nu(C-O(H))$ mode of the carboxylic acid dimer. The two pair of strong bands at 1460 and 1435 cm^{-1} and 1263 and 1217 cm^{-1} in maleic acid are attributed to this type of coupling, which has been discussed previously in the sections on the in-plane O-H deformation mode and the C-O(H) stretching mode. If a band is to be assigned to a C-H in-plane deformation mode the band at 1217 cm^{-1} would be selected. Deuteration produces very little change in the intensity of the band and no shift towards higher frequencies has been observed as with the 1263 cm^{-1} band.

Conjugation of a double bond with a carbonyl group results in a low frequency shift of the C=C absorption band.[247,248] In α,β-unsaturated acids the shift is considered slight as Freeman[249] quotes 1653 to 1631 cm^{-1} for a series of 2-hexenoic acids. Flett[228] assigned such a mode to a band at 1635 cm^{-1} in maleic acid. Therefore, the 1637 cm^{-1} band of the present work is assigned to the C=C stretching vibration, which implies the existence of a C-C "double-bond" in crystalline maleic acid. Two intense bands at 1591 and 1567 cm^{-1} may be taken as further support as the C=C stretching vibration may be displaced down to 1550 cm^{-1} if the ethylenic hydrogens are replaced by halogen or other polar groups.[250] Such bands seem to suggest large asymmetry which might well arise from an asymmetric type of intra- and inter- molecular hydrogen bonding between carboxylic acid groups.

The weak band at 1174 cm^{-1} is assigned to the C-C(OOH) stretching vibration on the basis of weak bands found in this region in iso-propyl and tert-butyl structures.[251]

Only the intense band at 875 cm^{-1} has been unassigned. From its behavior on deuteration the band might well be associated with a skeletal in-plane deformation vibration, such as $\delta(C{=}C\text{-}C)$, though it is a rather high frequency for such a vibration.

Summary:

The maleic acid spectrum appears to be normal and "well-behaved" for a molecule possessing an extremely short O---O distance, or more commonly referred to as a hydrogen bond. The background absorption in the low frequency region is "normal", i.e., there is no unusually broad overall absorption. The results of this investigation indicates that there is something more fundamental than a short hydrogen bond in order to account for the unusual absorption of low frequency infrared radiation by molecules possessing short hydrogen bonds.

The present investigation supports the asymmetric structure of the short, intramolecular hydrogen bond in crystalline maleic acid. The carbonyl absorption band position is normal (1706 cm^{-1}) and the assignment of the 1637, 1591 and 1567 cm^{-1} bands to C=C stretching vibrations are indicative of an asymmetric hydrogen bond. The hydrogen bond shifted O-H stretching vibration has been found at 1880 cm^{-1}. The band at 786 cm^{-1} has been assigned to the hydrogen bond stretching vibration, $\nu(OH\text{--}O)$, in the region suggested by Reid.[80] This mode represents the motion of the carboxyl groups as an entity, though one could consider it as a bending of a $=C\text{-}C\text{-}O(H)$ group and a $=C\text{-}C{=}O$ group.

Although the maleic acid spectrum is rather simple, coupling between the various in-plane deformation and stretching modes makes a unique assignment of the frequencies almost impossible.

Section F: Infrared Absorption Associated with Strong Hydrogen Bonds.

In this section we will attempt to tie together the results of the individual hydrogen bonded system investigations (Sections A thru E) into a plausible relationship between the structure of strong hydrogen bonds and the absorption in the infrared. Therefore, a brief resumé of the structural features of the hydrogen bonded systems and their infrared absorption spectra will be instructive.

In potassium hydrogen fluoride the bifluoride ion is the hydrogen bonded system. This is perhaps the simplest system known. Evidence from neutron diffraction [140] and nuclear magnetic resonance studies [141] supports a symmetric hydrogen bond so the bifluoride ion may be considered a symmetric linear triatomic molecule. Thus, a simple infrared spectrum would be expected for the bifluoride ion. Although the infrared active modes give relatively broad and intense bands in the crystalline state [142,145,146] and in potassium bromide pressed discs (Section A) the observed spectrum is "normal" and well-behaved.

The short intramolecular O---O distance in maleic acid has been attributed to hydrogen bond formation between the hydroxyl group and the carbonyl group of the carboxylic acid groups. This short hydrogen bond is not symmetric, and most likely, non-linear. Although the molecular system involved in the hydrogen bond formation is more complex than that of the bifluoride ion the infrared spectrum is "normal" and fairly simple (Section E).

In acetamide hemihydrochloride, nickel dimethylglyoxime and

potassium hydrogen bis-phenylacetate the O---O distance joining two complex molecular systems falls in the region of possibly symmetric hydrogen bonds.[47] The infrared spectra of all three compounds are unusual in that an extremely broad, intense background absorption with deep "windows" always appears in the low frequency region of the spectrum. The striking similarity in the shape and location of these features (Figure II F - 1) strongly suggests that the hydrogen bond vibrational modes may be associated with the unusual spectral behavior. From the limited number of systems examined it appears that the broad background absorption and "windows" will result only if the hydrogen bond is symmetric (or statistically symmetric) and joins two complex molecular systems.

The remaining portion of this section will be devoted to a discussion of the unusual spectral behavior of short, symmetric hydrogen bonded systems. For convenience the discussion is divided into three parts. The first part is a normal vibrational analysis of an isolated symmetric hydrogen bonded system, the second part deals with the breadth and intensity of the low frequency absorption and the third part concerns the origin of the "windows" in the broad background.

Normal Vibrational Analysis of an Isolated Symmetric Hydrogen Bonded System:

To simplify the normal vibrational analysis we will consider the hydrogen bonded system as an isolated five atom molecule of the form C O-H-O C with the hydrogen atom located at the center of the line joining the two oxygen atoms. If we restrict the system to planar symmetric configurations three structures are possible; a

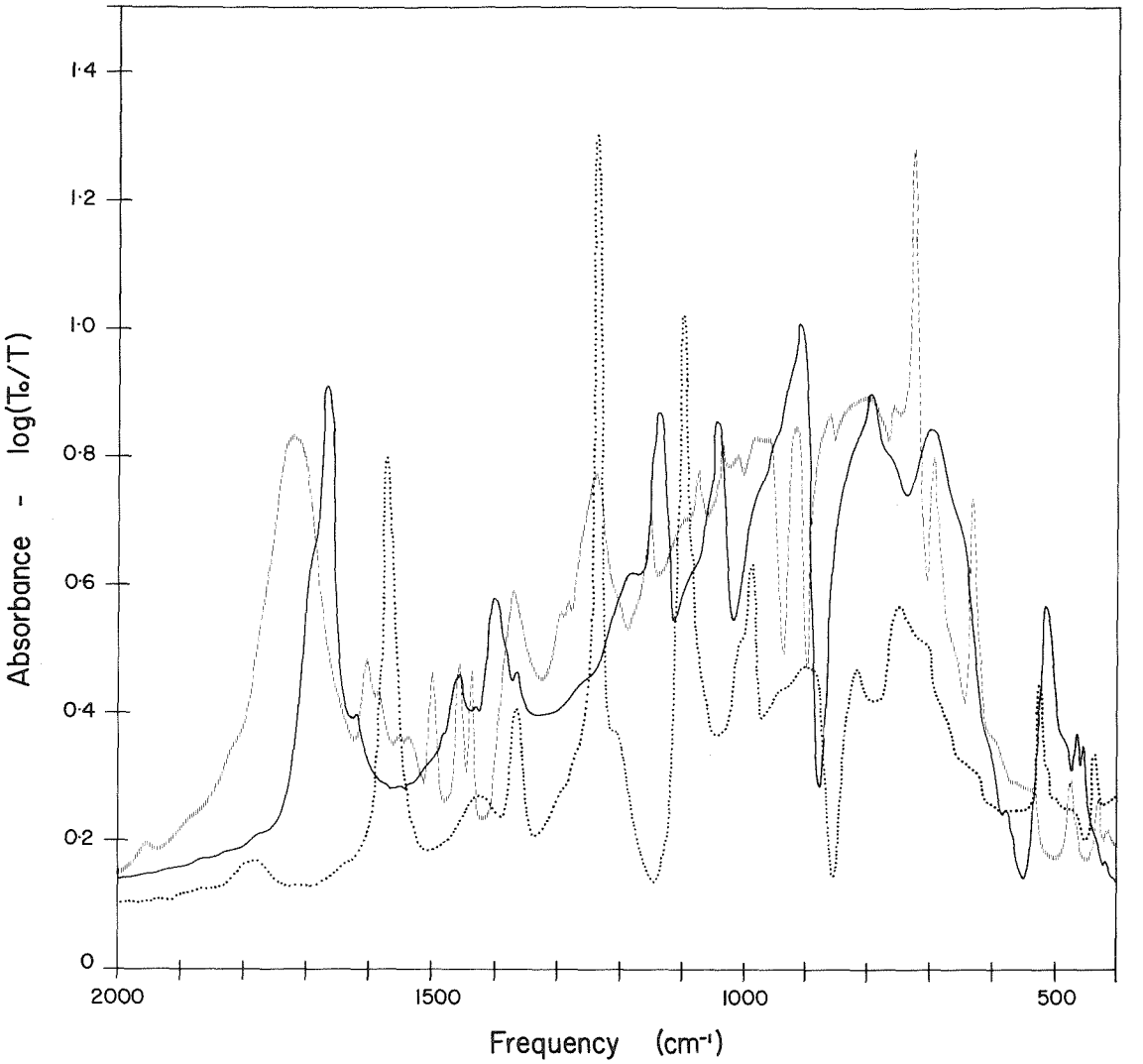

FIGURE II F-1

Comparison of the Infrared Spectrum of Acetamide Hemihydrochloride (——), Nickel Dimethylglyoxime (·····) and Potassium Hydrogen Bis-Phenylacetate (▒▒▒▒▒▒) in a Potassium Bromide Matrix Between 2000 and 400 cm⁻¹

linear arrangement belonging to point group symmetry $D_{\infty h}$, a cis- arrangement of the two carbon atoms belonging to point group symmetry C_{2v}, and a trans- arrangement of the two carbon atoms belonging to point group symmetry C_{2h}. In the present normal vibrational analysis we will consider the hydrogen bond system having C_{2h} symmetry as it describes the hydrogen bond system in acetamide hemihydrochloride and potassium hydrogen bis-phenylacetate.

The representation of the five atom hydrogen bond system of C_{2h} point group symmetry in terms of the irreducible components gives three type A_g modes, four type B_u modes and two type A_u modes.[252, 253] Selection rules permit the type A_g vibrations in the Raman spectrum only and the type B_u vibrations in the infrared and Raman spectra. The idealized normal modes of the hydrogen bond system for the allowed symmetry species are shown in Figure II F - 2 and can be described in terms of bond-bending and bond-stretching modes. For the totally symmetric A_g modes S_1 represents the in-phase C=O stretch, S_2 the symmetric CO--OC stretch (or the symmetric hydrogen bond stretch) and S_3 the in-phase COH in-plane bend. For the in-plane asymmetric type B_u modes S_4 represents the out-of-phase C=O stretch, S_5 the asymmetric hydrogen bond stretch (the hydrogen mode), S_6 the out-of-phase COH in-plane bend and S_7 the in-plane hydrogen bond bend. The out-of-plane type A_u modes represent the hydrogen bond bend, S_8, and the C=O bend (or torsional mode), S_9.

A potential function of the quadratic type containing interaction terms involving bond-stretching with bond-bending motion and bond-stretching with adjacent bond-stretching motion has been assumed.

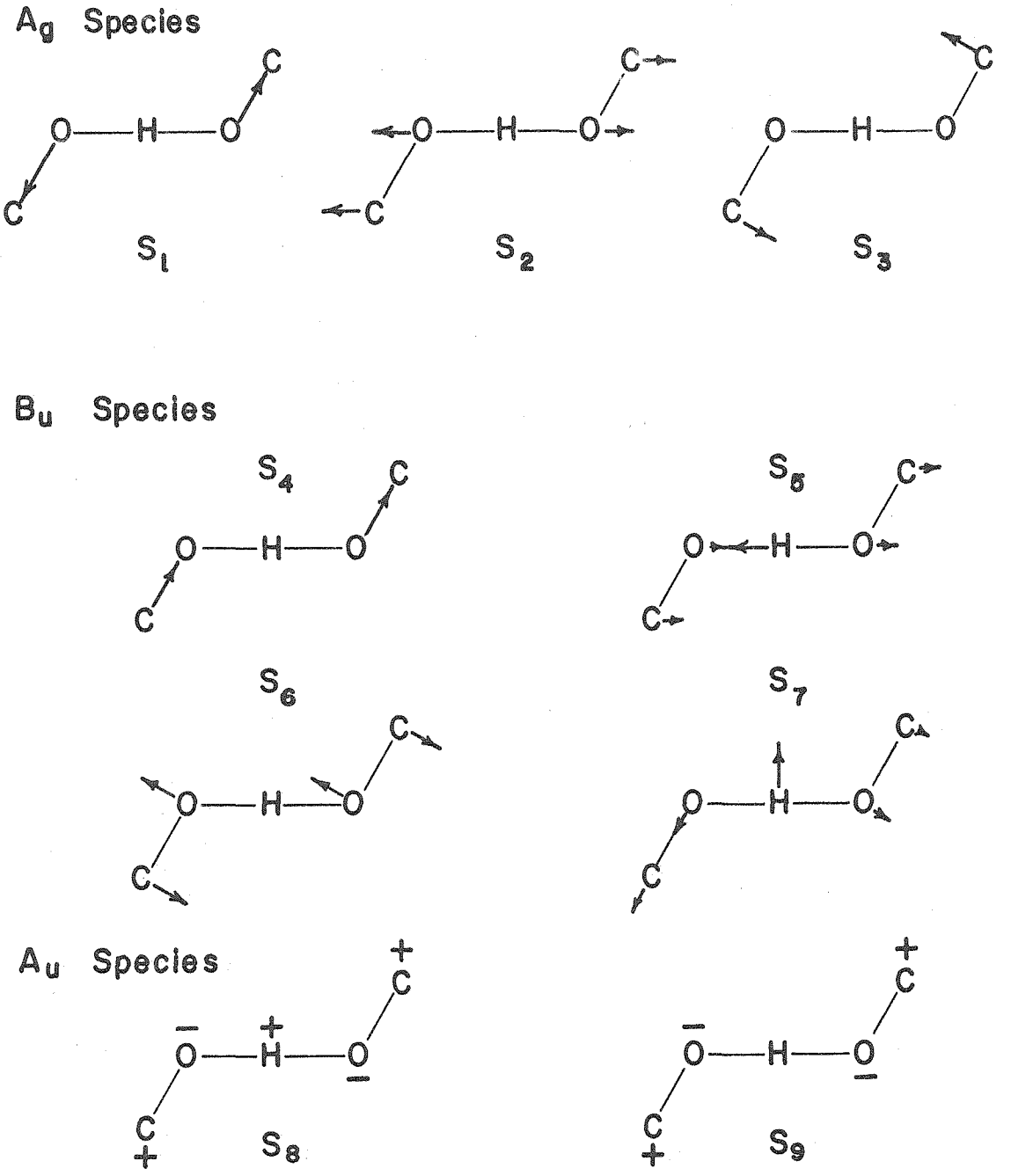

FIGURE II F-2

Possible Normal Modes of a Five Atom Hydrogen Bond with C_{2h} Symmetry

The quadratic potential function used is

$$
\begin{aligned}
2V = {} & f_r\left[(\Delta r_1)^2 + (\Delta r_2)^2\right] + 2f_d(\Delta d)^2 + f_{rd}\left[\Delta r_1 \Delta d_1 + \Delta r_2 \Delta d_2\right] \\
& + 2f_{dd}(\Delta d_1 \Delta d_2) + f_\alpha(rd)\left[(\Delta \alpha_1)^2 + (\Delta \alpha_2)^2\right] \\
& + f_\beta(d\Delta\beta)^2 + f_{r\alpha}(\Delta r)\left[r_1(\Delta \alpha_1) + r_2(\Delta \alpha_2)\right] \\
& + f_{d\alpha}(\Delta d)\left[d_1(\Delta \alpha_1) + d_2(\Delta \alpha_2)\right] + f_{d\beta}(\Delta d)(d\Delta\beta) \\
& + f_\gamma(\Delta d)\left[(\Delta \gamma_1)^2 + (\Delta \gamma_2)^2\right] + f_\delta(d\Delta\delta)^2
\end{aligned}
$$

where the internal coordinates have been defined as the changes in bond length and bond angles; r_i and d_i the equilibrium C=O and O-H bond distances, α_i and β the equilibrium COH and O-H-O in-plane bond angles and γ_i and δ the equilibrium COH and O-H-O out-of-plane bond angles. The force constants, f_r, f_d, f_α, f_β, f_{rd}, f_{dd}, $f_{r\alpha}$, $f_{d\alpha}$, $f_{d\beta}$, f_γ and f_δ, are defined by the bond and angle displacements associated with them in the above expression.

From the assumed symmetry of the hydrogen bond system internal symmetry coordinates, S_i, were constructed from the internal coordinates, s_i, in the usual manner[254] and have been tabulated in Table II F - 1. The use of symmetry coordinates allows one to factor the secular equations for the normal vibrations into equations for A_g, B_u and A_u symmetry species. Since the secular equations can be derived simply by the Wilson method[255,256,257] from the corresponding F and G matrices, the matrices will be presented rather than the expanded equations. The F matrices for the A_g, B_u and A_u symmetry species are given in Table II F - 2. Since the matrices are symmetric with respect to the main diagonal

TABLE II F- I

Symmetry Coordinates for Hydrogen Bond System

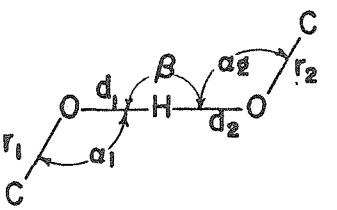

In Terms of the Internal Coordinates

A_g Species

$$S_1 = (1/\sqrt{2})(\Delta r_1 + \Delta r_2)$$
$$S_2 = (1/\sqrt{2})(\Delta d_1 + \Delta d_2)$$
$$S_3 = (1/\sqrt{2})(\Delta \alpha_1 + \Delta \alpha_2)$$

B_u Species

$$S_4 = (1/\sqrt{2})(\Delta r_1 - \Delta r_2)$$
$$S_5 = (1/\sqrt{2})(\Delta d_1 - \Delta d_2)$$
$$S_6 = (1/\sqrt{2})(\Delta \alpha_1 - \Delta \alpha_2)$$
$$S_7 = \Delta \beta$$

A_u Species

$$S_8 = (1/\sqrt{2})\,\Delta \gamma$$
$$S_9 = \Delta \delta$$

TABLE II F - 2

Table of F Matrix Elements for C_{2h} Hydrogen Bond System

A_g Species

	S_1	S_2	S_3
S_1	f_r	f_{rd}	$f_{r\alpha}$
S_2		$f_d + f_{dd}$	$f_{d\alpha}$
S_3			f_α

B_u Species

	S_4	S_5	S_6	S_7
S_4	f_r	f_{rd}	$f_{r\alpha}$	0
S_5		$f_d - f_{dd}$	$f_{d\alpha}$	$-\sqrt{2}\, f_{d\beta}$
S_6			f_α	0
S_7				f_β

A_u Species

	S_8	S_9
S_8	f_γ	0
S_9		f_δ

TABLE II F-3

Table of G Matrix Elements for C_{2h} Hydrogen Bond System

A_g Species

$$G_{11} = \mu_C + \mu_O$$
$$G_{22} = \mu_O$$
$$G_{33} = \rho_d^2 \mu_H + \rho_r^2 \mu_C + (\rho_d^2 + \rho_r^2 - 2\rho_d \rho_r \cos\alpha) \cdot \mu_O$$
$$G_{12} = \mu_O \cos\alpha$$
$$G_{13} = -\rho_d \mu_O \sin\alpha$$
$$G_{23} = -\rho_r \mu_O \sin\alpha$$

B_u Species

$$G_{44} = \mu_C + \mu_O$$
$$G_{55} = \mu_O + 2\mu_H$$
$$G_{66} = \rho_d^2 \mu_H + \rho_r^2 \mu_C + (\rho_d^2 + \rho_r^2 - 2\rho_d \rho_r \cos\alpha)\mu_O$$
$$G_{77} = 2\rho_d^2 (\mu_O + 2\mu_H)$$
$$G_{45} = \mu_O \cos\alpha$$
$$G_{46} = -\rho_r \mu_O \sin\alpha$$
$$G_{47} = G_{57} = 0$$
$$G_{56} = -\rho_d \mu_O \sin\alpha$$
$$G_{67} = -\rho_d [2\rho_d \mu_H + (\rho_d - \rho_r \cos\alpha)\mu_O]$$

A_u Species

$$G_{88} = 2\rho_d^2 (\mu_O + 2\mu_H)$$
$$G_{99} = -\rho_d^2 (2\mu_H + \mu_O) - \rho_d \rho_r \mu_O$$

only the off-diagonal elements on the upper side of the main diagonal need be given. The G matrix elements were constructed from the generalized method of Decius[258,259] and have been tabulated in Table II F - 3.

In evaluating the normal frequencies of the COHOC hydrogen bond system the force constants and interaction constants of the water molecule and the carbon dioxide molecule [260] and those of the hydrogen bond system of the formic acid dimer [261] were modified for the present symmetric hydrogen bond calculations. The force constant values used, in units of 10^5 dynes per centimeter, are: $f_r = 11.0$, $f_d = 0.90$, $f_\alpha = f_\gamma = 0.30$, $f_\beta = f_\delta = 0.05$, $f_{rd} = 0.01$, $f_{dd} = 0.05$, $f_{r\alpha} = 0.02$, $f_{d\alpha} = 0.01$ and $f_{d\beta} = 0.01$. The observed value of 1.244 A for the C O distance and 117° for the COH in-plane angle in acetamide hemihydrochloride[137] were used in all calculations. The O-H distance was assumed to be one-half of the observed O---O distance of 2.40 A in the hemihydrochloride molecule and the in-plane O-H-O angle β, the out-of-plane O-H-O angle δ, and the out-of-plane COH angle γ, were all assumed to be 180° in all calculations.

The calculated frequencies for the modes of the allowed symmetry species and the approximate assignments are given in Table II F - 4. Further refinements of the frequencies were not carried out since the exact location of the hydrogen bond vibrational modes are not known for the systems examined. The calculated values are only approximate and are probably higher than the true values; for example, the infrared active C=O stretch was calculated to be 1768 cm^{-1}, in

Table II F - 4

Calculated Normal Frequencies and Frequency Assignments for a Five-Atom Hydrogen Bond System of C_{2h} Symmetry

Symmetry Type	Frequency (cm^{-1})	Mode	Assignment
A_g	1712	S_1	C=O (in-phase) stretch
	1076	S_2	OHO sym. stretch
	387	S_3	COH (in-phase) bend
B_u	1768	S_4	C=O (out-of-phase) stretch
	1670	S_5	OHO asym. stretch
	1155	S_7	OHO in-plane bend
	405	S_6	COH (out-of-phase) bend
A_u	497	S_8	OHO out-of-plane bend

the hemihydrochloride spectrum the band at 1670 cm^{-1} was assigned to this mode. Moreover, changes in the interaction constants $f_{r\alpha}$ and $f_{d\alpha}$ were found to have a significant effect on the in-plane hydrogen bond modes; an increase in these interaction constants by a factor of 10 shifts the symmetric stretch and the in-plane bend of the hydrogen bond system about 350 cm^{-1} towards higher frequencies and the asymmetric hydrogen bond stretch by about 50 cm^{-1} towards lower frequencies. It is interesting to note that the symmetric stretch of the hydrogen bond system considered is a relatively high frequency mode, near 1076 cm^{-1}. Reid[80] has estimated the vibrational frequency of the (OH)--O stretch as a function of the O---O distance, and for a hydrogen bond distance of 2.40 A the stretching frequency would fall in the region between 850 cm^{-1} and 950 cm^{-1}.

Although this simple normal vibrational analysis is far from complete it does support the interpretation of the intensity of the

broad background absorption in the acetamide hemihydrochloride spectrum in terms of the near coincidence of two or more proton vibrational modes.

Breadth of Hydrogen Bond Vibrational Bands:

Although the hydrogen bond systems investigated are extremely short it will be advantageous to briefly examine several of the mechanisms which have been advanced to explain the breadth of the OH stretching frequency in weak hydrogen bonds. The mechanisms considered are the anharmonic coupling of the νOH and ν(OH---O) vibrations, Fermi resonance of the νOH with overtones and summation bands and the proton transfer in an O-H--O system, in the order given.

Anharmonic Coupling: On hydrogen bond formation the OH bond length has been observed to increase in length as the O---O distance contracts.[49] This implies that the force constant of the OH bond is reduced while that of the hydrogen bond O---O is increased. Thus, the modes of vibration which can be described as νOH and ν(OH--O) are strongly and anharmonically coupled together. In the same manner that a considerable reduction in the O---O distance on hydrogen bond formation causes a marked lowering of the mean OH stretching frequency, so the range of values of O---O caused by thermal vibrations of the relatively weak hydrogen bond gives rise to a range of OH frequencies, and hence, to a broad absorption band.[61,63] A more precise classical interpretation would involve the coupling of the high frequency OH vibration with the low frequency hydrogen bond stretch, so the broad band would actually consist of a

series of sub-bands of frequency νOH $\pm$ nν(OH---O). These simple classical mechanisms are not correct since the hydrogen bonded molecules execute quantized intermolecular vibrations. Although the consequences of a quantum mechanical energy level scheme parallel closely those of the classical theories there is, however, an important difference between the two viewpoints, namely, that transitions from the lowest level of the ground vibrational state can occur to several levels in a vibrationally excited state. This means that even at low temperatures when all molecules are initially in the lowest energy levels of the ground state a band of considerable breadth with frequencies νOH + nν(OH--O) will persist.

Fermi Resonance: If the frequency of the anharmonic fundamental stretching vibration of the OH group is coincident with combination frequencies of the same symmetry species Fermi resonance can occur. In addition to the anharmonic coupled frequencies described above, other interacting summation frequencies might, for example, involve overtones of the δOH vibration, or combinations of these with ν(OH--O) vibrations. Since most of the hydrogen bonded systems that can conveniently be studied are part of complex molecules, many types of summation bands can often occur in the shifted OH region. Such a mechanism will cause an intensity decrease in the OH band and give rise to a series of sub-bands.

Proton Transfer: Cannon[5] has proposed a mechanism whereby the hydrogen atom of an O-H--O system is vibrating in a double minimum potential curve. If the first excited state of the νOH vibration occurs above the central maximum, then the appropriate

absorption band will be broadened. Broadening is the result of a rapid proton transfer from one potential well to the other, and hence, the proton will have a short life-time in the original state. This concept is not true. Such an occurrence would lead not to a broadening but to a wide splitting of the upper energy levels. Thus, it would give rise to two separate νOH bands, both of which may be broadened. Recently, Blinc and Hadzi[262] have shown that for a proton in an unsymmetric double-minimum potential with a low energy barrier tunnelling of the proton becomes perceptible with appreciable splitting of the two infrared active frequencies. The simple proton transfer mechanism is, therefore, not able to explain the unusual breadth of the OH stretching frequencies.

The breadth of the OH shifted absorption bands of weak hydrogen bonded systems can be satisfactorly described in terms of a strong anharmonic interaction between the vibrations νOH and ν(OH---O) and an interaction through anharmonicity of the νOH vibrations with overtones and summation bands of similar frequency by Fermi resonance. Taken together these two mechanisms are more effective than either one alone; both require broad bands made up of a number of sub-bands. For strong hydrogen bonded systems it is necessary to re-examine the broadening mechanisms since the OH stretch frequency decreases while that of the OH---O stretch increases. Moreover, in weak hydrogen bonds the hydrogen atom is attached to one of the oxygen atoms while in strong hydrogen bonds the hydrogen atom may be situated mid-way between the two oxygens or it may oscillate between two equilibrium

positions on either side of the center of the hydrogen bond. We will consider both cases in discussing the breadth of the low frequency region of the spectrum of a strong hydrogen bonded system.

Single - Minimum Potential: For true symmetric hydrogen bonds the energy of the system can be described by the potential surface contour lines shown in Figure II F - 3.* The

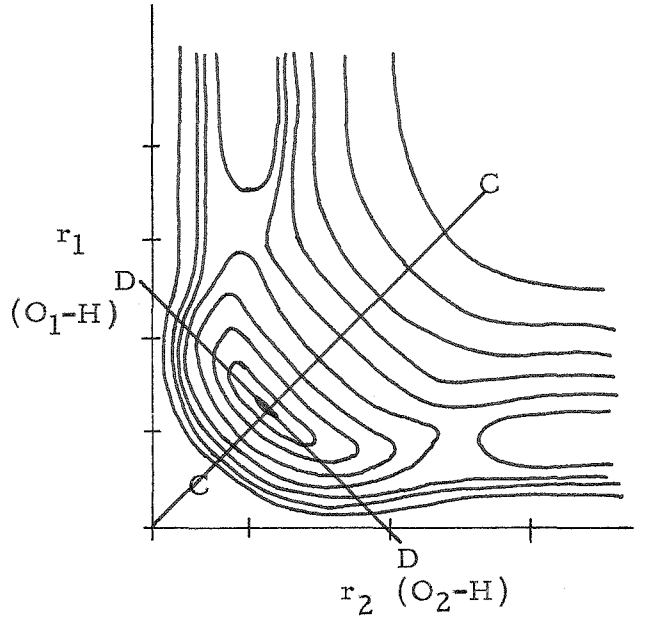

FIGURE II F - 3

Potential Surface for O - H - O Hydrogen Bond System

distance r_1 is defined by the O_1 - H distance and the distance r_2 is defined by the O_2 - H distance. The surface has a deep minimum at the point r_1 equal to r_2 corresponding to the equilibrium position

* This is the same potential surface given in Herzberg, Infrared and Raman Spectra , D. Van Nostrand Company, Inc., New York, 1945, pp. 203, for the ground electronic state of the CO_2 molecule.

of the hydrogen bonded system. The plateau region corresponds to the energy of the $O_1 + H + O_2$ atoms at great distances from one another. From the minimum the potential energy increases in all directions, that is for any change of r_1 or r_2 or both. A cross section of the potential surface along the line CC represents the potential energy curve for the O---O motion at a fixed O-H distance, the symmetric stretch of the hydrogen bond. A cross section of the potential surface along the line DD represents the potential energy curve for the hydrogen atom motion at a fixed O---O distance; the asymmetric stretch of the hydrogen bond. The O---O potential curve resembles that of the vibrational scheme for the electronic states of a diatomic molecule, while the O-H-O potential curve has a broad, almost flat potential minimum. Each potential curve will have its own energy levels describing the quantized vibrational levels of the hydrogen bond system. In the normal vibrational analysis carried out in an earlier part of this section the separation between the ground vibrational level and the first vibrationally excited state of the symmetric stretch was found to be about 1076 cm^{-1} and that of the asymmetric stretch was found to be near 1670 cm^{-1}. If these frequencies are near correct then coupling between them would not give rise to a band progression in the region of interest. However, coupling of these modes with other low frequency modes is possible, such as bending and torsional modes as well as lattice type modes.

If we are to assume low frequency lattice interaction each vibrational level of the different vibrational modes can be described

by a potential surface similar to Figure II F - 3 where the r's now correspond to the RO-H distances and the potential energy curves represent the quantized lattice vibration. Thus, each hydrogen bond vibrational transition can take place to several of the lattice vibrational levels so that the hydrogen vibrational band will be composed of a series of sub-bands. The allowed transitions and intensities of the sub-bands will depend on the shape of the potential surfaces in the ground vibrational state and the excited vibrational states. For the interaction of the asymmetric hydrogen bond stretch with the symmetric stretch of the hydrogen bonded molecules a possible energy level scheme and possible spectrum are shown in Figure II F - 4. Like the hydrogen bond stretching modes

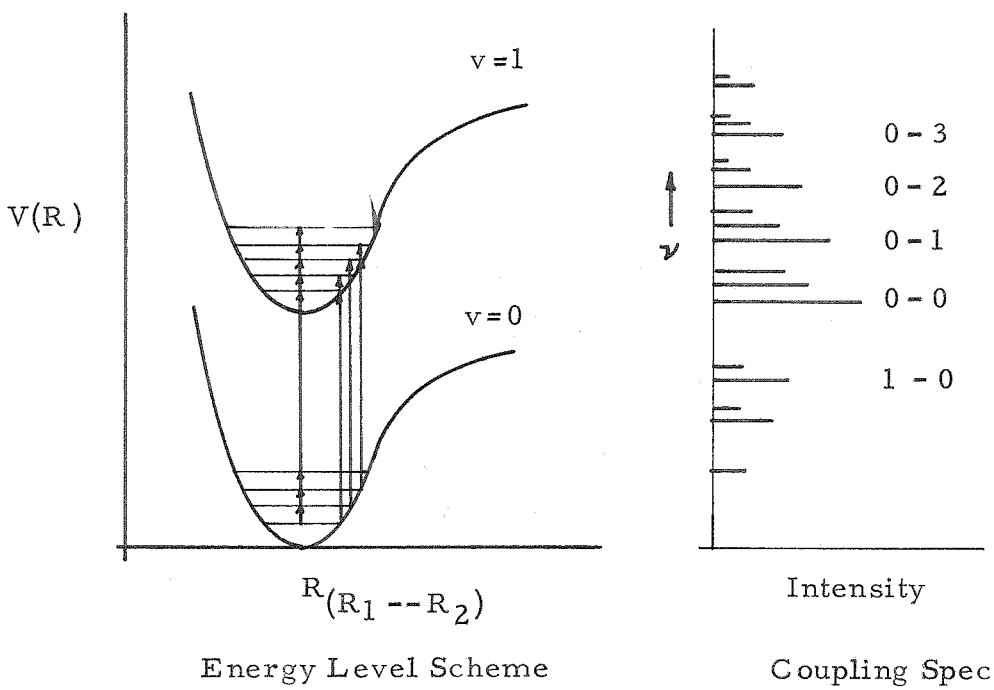

FIGURE II F - 4

Energy Level Scheme for Interaction of Hydrogen Bond Modes With Low Frequency Lattice Vibrations and a Schematic Spectrum Showing Possible Coupled Frequencies

the hydrogen bond bending modes, the in-plane and out-of-plane modes, may also couple with the various lattice modes to give rise to similar types of band progressions. Moreover, the normal vibrational analysis of the short hydrogen bonded system placed the in-plane hydrogen bond bend frequency near 1055 cm^{-1} so that the coupled hydrogen bond bend - lattice modes may be involved in Fermi resonance with some of the hydrogen bond stretch - lattice modes to smooth out the absorption in the low frequency region of the spectrum.

Double - Minimum Potential: For short hydrogen bond distances the motion of the hydrogen atom may be oscillating between two potential minima of equal depth separated by a low potential barrier. The symmetric double-minimum problem has been extensively studied by a number of authors[263-267] in conjunction with the splitting of the vibrational levels of the NH_3 molecule. Recently, Blinc and Hadzi[268] have extended the Wall-Glockler method[267] to hydrogen bonded systems in conjunction with the Lippincott - Schroeder relationship[50] between OH frequency shift and O---O distance in order to estimate the splitting of the infrared active levels.

In the Wall - Glockler approach the potential energy curve consists of two parabolas defined by the expression

$$V = (k/2)\cdot(|x| - 1)^2$$

where 2l equals the distance between the two minima and k is the force constant of the oscillator. This function is only a rough approximation in hydrogen bonded system since the oxygen atoms

vibrate and hence, l is not fixed. However, vibrational energy level expressions can be obtained by solving the wave-equation in which the Wall-Glockler potential function and suitably combined harmonic oscillator wave-function have been inserted. A plot of the energy levels for the symmetric and antisymmetric states of the ground vibrational state and the first vibrationally excited state are shown in Figure II F - 5. as a function of the dimensionless parameter q. The parameter q is given by the expression

$$q^2 = (4\pi m \nu_o / h)\ l^2$$

where m is the mass of the proton, ν_o the average fundamental frequency and l the distance from the center of the hydrogen bond to the potential minimum. For large q values the symmetric and

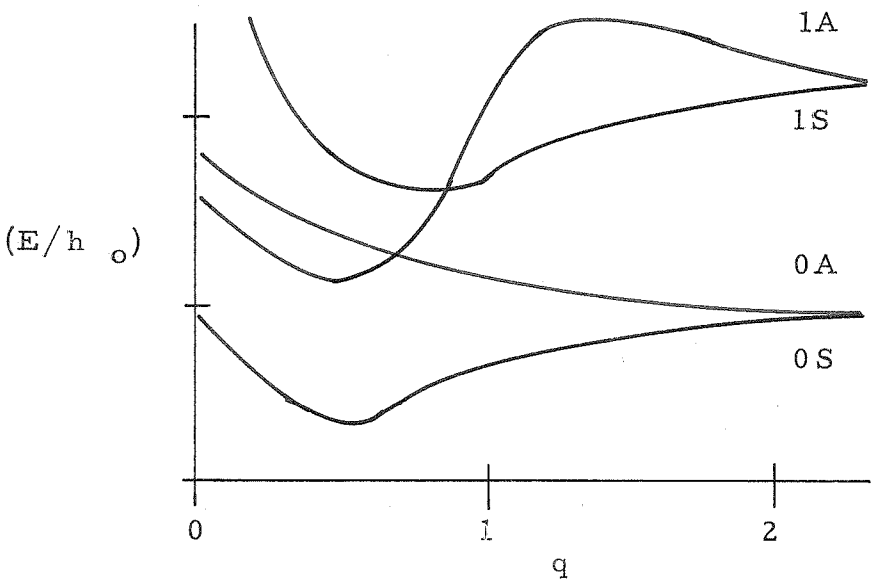

FIGURE II F - 5

Splitting of Energy Levels as a Function of Parameter q

antisymmetric levels are degenerate. As q becomes smaller the levels are split, with the separation increasing with decreasing q. When q becomes less then unity the 1A level crosses the 1S level so that the energy of the 1A level is less than that of the 1S level. Finally, for very small q values the 1A level crosses the OA level! This unusual behavior may be due to the approximate wavefunctions used by Wall and Glockler in solving for the energy levels. Therefore, for systems with q less than unity the results will not be valid. This is unfortunate as the hydrogen bond systems under consideration have q values less than unity. Blinc and Hadzi[268] have estimated a q value of 0.3 for an O---O distance of 2.40 A, which gives a separation of the potential minima of about 0.04 A and a potential barrier of about 0.4 kcal/mole. This is the hydrogen bond distance in acetamide hemihydrochloride. In the present study approximate calculations were made for q's of 0.2 and 0.3 using the energy level expressions given by Wall and Glockler.[267] Although the numerical values obtained are not reliable they do show that the splitting of the symmetric and the antisymmetric levels is appreciable so that transitions between the symmetric and antisymmetric levels in the same vibrational state can give rise to an infrared absorption band in the neighborhood of 500 - 1000 cm^{-1}. Such transitions are not unreasonable as Costain and Dowling[269] have only recently reported a splitting of about 300 cm^{-1} between the symmetric and antisymmetric levels of the inversion - wagging mode of the NH_2 group in ground state level in formamide.

For small potential barriers and small potential minima separation each vibrational level is split into a symmetric and anti-

symmetric level, and for each of these levels coupling with low frequency lattice levels is possible to give rise to a series of broad bands. If these broad bands overlap it will result in an extremely broad band extending for several hundred or more wave-numbers. A possible energy level scheme and possible spectrum are shown below.

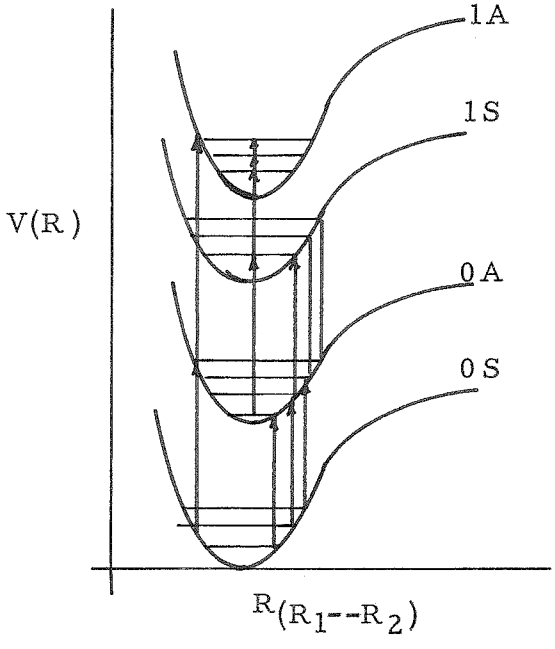

Energy Level Scheme

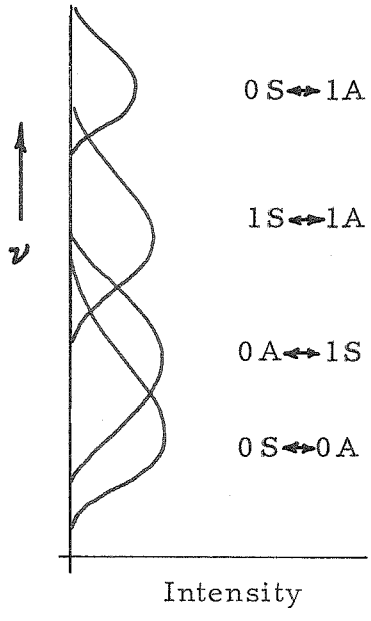

Possible Spectrum

We cannot at present distinguish between these two potential energy systems for short hydrogen bonds. Both would give rise to an intense broad background absorption in the low frequency region of the spectrum. The double-minimum potential system is attractive as it offers an explanation to the apparent decrease in intensity of the hydrogen bond shifted OH stretch frequency with decreasing hydrogen bond distance.(80)

"Window" Effect Associated with Short Hydrogen Bonded Systems:

A number of years ago Price and Tetlow[198] reported "anomalous dispersion" effects in the region of 600 to 1100 cm^{-1} in mulls of organic crystals. These authors implied that there is a relation between the "anomalous dispersion" phenomenon and the polarizabilities which are responsible for the Raman effect. In some cases it might be that bands which give rise to the effect are also strong in the Raman effect due to the fact that the polarizibility is a fairly strong function of the normal coordinate in question. This explanation is not believed to be the origin of the "windows" in the short hydrogen bonded systems investigated for several reasons. First of all, the intensity and shape of the "window" does not resemble that of the usual anomalous dispersion band which exhibits abnormally high transmission on the higher frequency side and abnormally low transmission on the lower frequency side. Second of all, the position and shape of the "window" is not effected by the matrix. Third of all, and perhaps most significant, spectra of N-(t-butyl)-acetamide hemihydrochloride complexes in chloroform solutions were found to exhibit deep "windows" in the region of interest.[197]

Although the "windows" have been observed in spectra of nickel dimethylglyoxime and potassium hydrogen bis-phenylacetate, only the acetamide hemihydrochloride molecule offers enough information to develop a plausible explanation. The following observations relating the spectra of acetamide and the hemihydrochloride to the "window" effect are (a) the 875 cm^{-1} band in the infrared spectrum of acetamide is relatively weak whereas the

Raman line is very intense;[180] (b) an intense Raman line is found at 873 cm^{-1} in the spectrum of the hemihydrochloride;[186] and (c) the deep "window" in the infrared spectrum of the hemihydrochloride at 875 cm^{-1} is in the band envelope of the hydrogen bond vibrational modes. If the acetamide residue in the hemihydrochloride has a weak band at 875 cm^{-1} the "window" effect may be explained in terms of a highly selective perturbation of an energy level giving rise to the 875 cm^{-1} absorption band by certain energy levels of the complex hydrogen bond vibrational modes.

The great breadth of the absorption band of the hydrogen bond vibrational mode has been ascribed to coupling of the hydrogen modes with low frequency "lattice" modes, which means a number of discrete energy levels will exist for each hydrogen bond mode in the ground state and in vibrationally excited states. As the spacing between sub-levels in each vibrational state is not equal a broad energy distribution will result. Therefore, only a small fraction of the total molecules present will have at any instant a hydrogen bond vibrational mode with a frequency of 875 cm^{-1}. If a vibrational mode, designated mode A, not associated with the hydrogen bond modes, though coupled with the low frequency "lattice" modes, has a narrow energy distribution at 875 cm^{-1} and has an energy level of the first vibrational state coincident with an energy level of the first vibrational state of a hydrogen bond mode, interaction between the two levels may occur. The conditions for interaction are presumably analogous to those of Fermi resonance, which means mode A must be of the same symmetry species as the hydrogen bond mode.

As a result of the perturbation, the small fraction of the molecules with the proper energy levels are removed from this region in

the hemihydrochloride system. This will result in a "window" in the infrared spectrum only if the transition moment for the transition from the ground state to the first vibrational state of mode A is small in the unperturbed molecules.* The remaining large fraction of the unperturbed molecules will not contribute significantly to the absorption in the "window" region. Since the Raman line of the hemihydrochloride is very intense and apparently not shifted from the position of the corresponding Raman line in acetamide the perturbation energy must be weak between the hydrogen bond vibrational level and the mode A level of the acetamide residue. Unfortunately, the shape of the Raman line is not known so that further evaluation of the interaction will not be possible.

The appearance of small peaks on either side of the "window" are undoubtedly produced by transitions between the ground level and the mixed energy states described by wave-functions which are mixtures of the zero-order approximation wave-functions of the hydrogen bond vibrational modes and mode A. The Raman line would be expected to show some broadening about the base, which may be symmetric or unsymmetric depending on the magnitude of the perturbation energy.

A schematic representation of the "window" effect in terms of the energy levels for the hydrogen bond modes and the acetamide residue mode A is shown in Figure II F - 6. In the energy level scheme an energy level of one of the hydrogen bond modes, which is

---

* The weak band in acetamide at 875 cm^{-1} is assumed to describe the same mode in the acetamide residue of the hemihydrochloride. For nickel dimethylglyoxime and potassium hydrogen bis-phenylacetate, the spectra of the comparison compounds are not directly helpful as the frequencies in question are, for the most part, shifted somewhat from those which presumably exist in the compounds of interest.

Figure II F - 6

Energy Level Scheme and Possible Band Contours
for Perturbation Mechanism

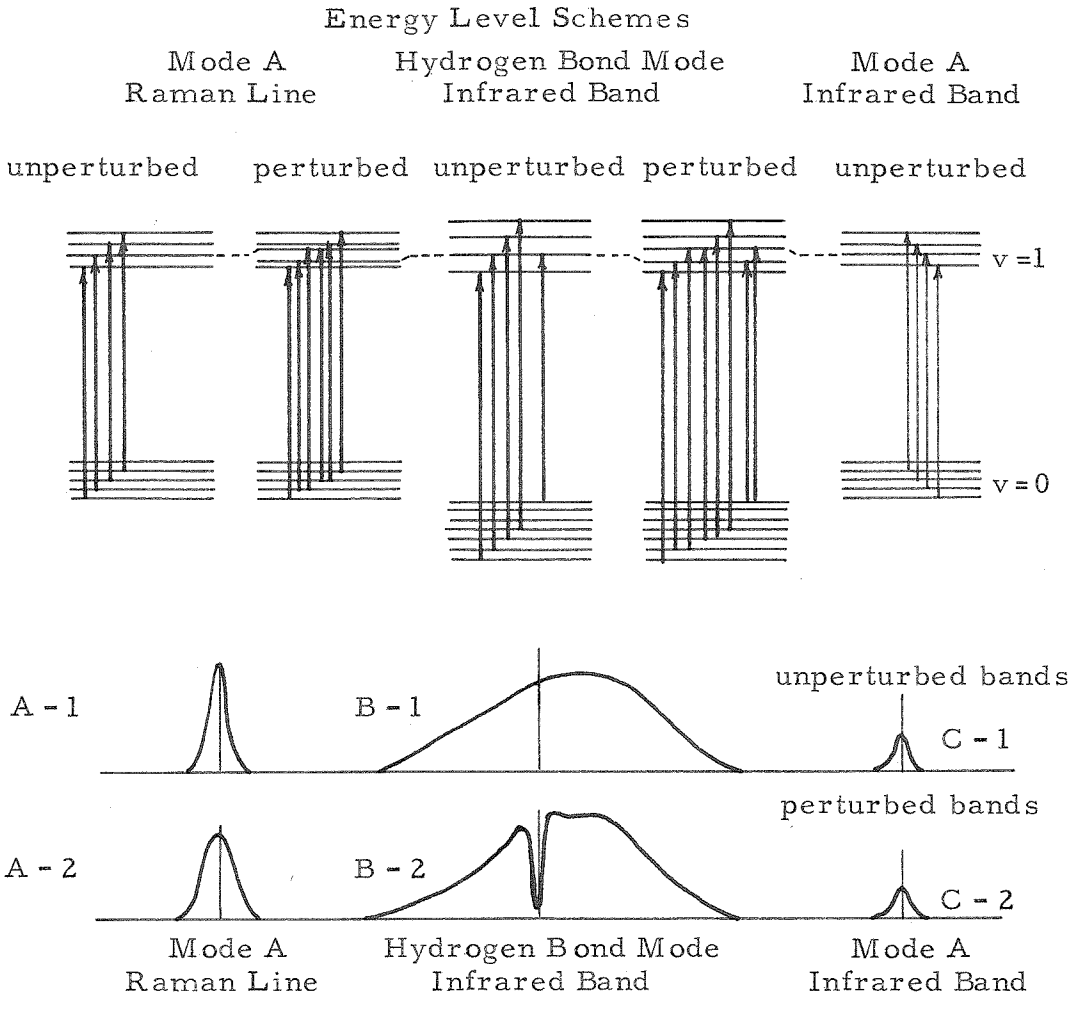

---

an upper level of a strong transition with a large transition moment, is coincident with an energy level of mode A, which is an upper level of a weak transition with a small transition moment. Since the sub-level spacing of the coupled hydrogen bond mode vibrational states are not equal a broad energy distribution, or band contour (curve B - 1) results. Removal of this level in the upper vibrational state of the hydrogen bond mode will give rise to a hole in the transitions

from the ground state levels, hence a "window" will appear in the infrared spectrum (curve B - 2). On the other hand, the energy level spacings in the vibrational states of mode A are such that all transitions give rise to a very narrow energy distribution.(curves A - 1 and C - 1). Removal of an energy level from the upper state of mode A by the perturbation will affect only a small fraction of the total transitions from the ground state to the first vibrational state. Therefore, the Raman line (curve A - 2) will appear unaffected, i.e., will be intense, and the contribution of the infrared absorption of mode A to the infrared spectrum in the "window" region will be very small.

For the "window" effect to appear in the infrared spectrum of short hydrogen bonded compounds the following requirements must be satisifed: (1) the hydrogen bond must be short and symmetric, or statistically symmetric; (2) the hydrogen bond must join two complex molecular systems; (3) two vibrational energy levels must be available to interact, one of which is associated with a hydrogen bond vibrational mode; (4) the hydrogen bond vibrational energy distribution should be broad and the interacting level should be the upper level of a strong transition with a large transition moment; and (5)the other interacting level should have a narrow vibrational energy distribution and be the upper level of a weak transition with a small transition moment. Thus, the broad background absorption in the low frequency region of the infrared spectrum and the "window" effect may be a method of distinguishing between short, symmetric hydrogen bonds and short, unsymmetric hydrogen bonds.

References

1. M. M. Davies, Ann. Repts. Chem. Soc., London, 43, 1 - 29 (1946).
2. L. Hunter, ibid, 43, 141 - 155 (1946).
3. L. Kellner, Repts. Progr. Phys., 15, 1 - 23 (1952).
4. C. A. Coulson, Research 10, 149 - 159 (1957).
5. C. G. Cannon, Spectrochim. Acta 10, 341 - 368 (1958).
6. Hydrogen Bonding, D. Hadzi (Editor), Pergamon Press, London (1959).
7. L. Pauling, Nature of the Chemical Bond, 2nd Ed., Cornell University Press, Ithica, New York (1948), Chap. IX pp. 284 - 289.
8. H. O. Pritchard and H. A. Skinner, Chem. Rev., 55, 745 - 786 (1955).
9. W. Gordy, J. Chem. Phys., 7, 163 - 166 (1939).
10. L. H. Jones and R. M. Badger, J. Am. Chem. Soc., 73, 3132 - 3134 (1951).
11. R. C. Lord, B. Nolin and H. D. Stidham, J. Am. Chem. Soc., 77, 1365 - 1368 (1955).
12. L. Pauling, The Nature of the Chemical Bond, 2nd Ed., Cornell University Press, Ithica, New York (1948), Chap. IX, p. 333.
13. J. A. A. Ketelaar, Chemical Constitution, Elsiver Publishing Company, Amsterdam (1953), Chap. V, p. 381.
14. L. N. Ferguson, Electron Structures of Organic Molecules, Prentice-Hall, Inc., New York (1952), Chap. 2, p. 57.
15. J. D. Morrison and J. M. Robertson, J. Chem. Soc., 1949, 980 - 986.
16. W. Cochran, Acta Cryst., 6, 260 - 26 (1953).
17. G. E. Bacon and N. A. Curry, Prod. Roy Soc., (London), A 235, 552 - 5 (1956).
18. R. E. Marsh, Acta Cryst., 10, 654 - 663 (1958).

19. S. W. Peterson and H. A. Levy, J. Chem. Phys., 20, 704 - 707 (1952).

20. G. E. Bacon and N. A. Curry, Acta Cryst., 10, 524 - 528 (1957).

21. L. Pauling, The Nature of the Chemical Bond, 2nd. Ed., Cornell University Press, Ithica, New York (1948), Chap. IX, pp. 290 - 296.

22. E. N. Lassettre, Chem. Rev., 20, 259 - 303 (1937).

23. L. Hunter et al, J. Chem. Soc., 1945, 806 - 809.

24. L. Hunter and N. Reynolds, ibid, 1950, 2857 - 2864.

25. N. V. Sidgwick, The Electronic Theory of Valency, Oxford University Press (1937), pp. 138 - 151.

26. M. J. Copley, C. S. Marvel and co-workers, J. Am. Chem. Soc., 63, 1609 (1941) and earlier papers.

27. G. von Elbe, J. Chem. Phys., 2, 73 - 81 (1934).

28. M. J. Copley, C. S. Marvel and co-workers, J. Am. Chem. Soc., 62, 3263 - 3264 (1940) and earlier papers.

29. L. F. Audrieth and R. Steinman, ibid, 63, 2115 - 2116 (1941).

30. F. T. Wall and P. E. Rouse, ibid, 63, 3002 - 3005 (1941).

31. _____ and F. W. Barnes, ibid, 67, 898 - 899 (1945).

32. H. A. Phol, M. E. Hobbs and P. M. Gross, J. Chem. Phys., 9, 408 (1941).

33. _____, ibid, 9, 415 (1941).

34. A. A. Maryott, M. E. Hobbs and P. M. Gross, J. Am. Chem. Soc., 71, 1671 - 16 (1949).

35. See papers by M. Magat (pp. 309 - 320), L. Sobczyk (pp. 323 - 329), and T. Gaumann and J. Hoigne (pp. 331) in Hydrogen Bonding, D. Hadzi (Editor), Pergamon Press, London (1959).

36. R. C. Herman and R. Hofstader, J. Chem. Phys., 6, 534 - 540 (1938).

37. R. C. Herman, Ibid, 8, 256 - 258 (1940).

38. M. D. Taylor, J. Am. Chem. Soc., 73, 315 - 317 (1951).

39. E. W. Johnson and L. K. Nash, ibid, 72, 547 - 556 (1950).

40. W. Weltner, Jr. and K. S. Pitzer, ibid, 73, 2606 - 2610 (1951).

41. W. Baker et al, J. Chem. Soc., 1937, 479 - 483, and earlier papers.

42. H. O. Chaplin and L. Hunter, ibid, 1939, 484 - 489 and earlier papers.

43. L. N. Ferguson, Electron Structures of Organic Molecules, Prentice-Hall, Inc., New York (1952), Chap. 2, pp. 59 - 68.

44. J. M. Robertson, Organic Crystals and Molecules, Cornell University Press, Ithica, New York (1953), pp. 219 - 225.

45. A. F. Wells, Structural Inorganic Chemistry, Oxford, Clarendon Press, (1949), pp. 249 - 266.

46. L. Pauling, The Nature of the Chemical Bond, 2nd. Ed., Cornell University Press, Ithica, New York (1948), Chap. IX, pp. 296 - 315.

47. J. Donohue, J. Phys. Chem., 56, 502 - 510 (1952).

48. L. Pauling, J. Am. Chem. Soc., 69, 542 - 553 (1947).

49. K. Nakamoto, M. Margoshes and R. E. Rundle, J. Am. Chem. Soc., 77, 6480 - 6486 (1955).

50. E. R. Lippincott and R. Schroeder, J. Chem. Phys., 23, 1099 - 1106 (1955).

51. G. B. Carpenter and J. Donohue, J. Am. Chem. Soc., 72, 2315 - 2328 (1950).

52. G. E. Bacon, Neutron Diffraction, Oxford, Clarendon Press (1955), Chap. I - VII, pp. 1 - 196.

53. Paper by G. E. Bacon in Hydrogen Bonding, D. Hadzi (Editor), Pergamon Press, London (1959), pp. 23 - 32.

54. R. Pepinsky, ibid, pp. 33 - 34.

55. S. Darlow, ibid, pp. 37 - 44.

56. H. K. Welsh, J. Chem. Phys., 26, 710 (1957).

57. H. Feilchenfeld, J. Phys. Chem., 62, 117 - 118 (1958).

58. W. S. Fyfe, J. Chem. Phys., 21, 2 - 4 (1953).

59. G. J. Brealey and M. Kasha, J. Am. Chem. Soc., 77, 4462 - 4468 (1955).

60. G. C. Pimentel, ibid, 79, 3323 - 3326 (1957).

61. N. Sheppard, Hydrogen Bonding, D. Hadzi (Editor), Pergamon Press, London, (1959), pp. 85 - 104.

62. R. Mecke, Disc. Faraday Soc., 9, 151 - 177 (1950).

63. R. M. Badger and S. H. Bauer, J. Chem. Phys., 5, 839 - 851 (1937).

64. C. M. Huggins and G. C. Pimentel, J. Phys. Chem., 60, 1615 - 1619 (1950).

65. R. S. McDonald, J. Am. Chem. Soc., 79, 850 - 854 (1957).

66. R. E. Rundle and M. Parsol, J. Chem. Phys., 20, 1487 (1952).

67. R. C. Lord and R. E. Merrifield, J. Chem.Phys., 21, 166 - 167 (1953).

68. G. C. Pimentel and C. H. Sederholm, J. Chem. Phys., 24, 639 - 641 (1956).

69. R. Schroeder and E. R. Lippincott, J. Phys. Chem., 61, 921 - 928 (1957).

70. H. Feilchenfeld, Spectrochim, Acta, 12, 280 - 283 (1958).

71. M. L. Josien and N. Fuson, J. Chem. Phys., 22, 1169 - 1177 (1954).

72. S. Bratoz, D. Hadzi and N. Sheppard, Spectrochim. Acta, 8, 249 - 261 (1956).

73. H. L. Frisch and G. L. Vidale, J. Chem.Phys., 25, 982 - 986 (1956).

74. S. Bratoz and D. Hadzi, J. Chem. Phys., 27, 991 - 997 (1957).

75. S. A. Francis, J. Chem. Phys., 19, 505 - 506 (1951).

76. N. D. Coggeshall, J. Chem. Phys., 18, 978 - 983 (1950).

77. G. M. Barrow, J. Phys. Chem., 59, 1129 - 1132 (1955).

78. H. Tsubomura, J. Chem. Phys., 23, 2130 - 2133 (1955).

79. _____, ibid, 24, 927 - 931 (1955).

80. C. Reid, J. Chem. Phys., 30, 182 - 190 (1959).

81. A. V. Stuart and G. B. B. M. Sutherland, J. Chem. Phys., 24, 559 - 570 (1956).

82. D. Hadzi and N. Sheppard, Proc. Roy. Soc. (London), A 216, 247 - 266 (1953).

83. _____, Trans. Faraday Soc., 50, 911 - 918 (1954).

84. O. Thomas, Disc. Faraday Soc., 9, 339 - 345 (1950).

85. J. K. Wilmshurst, J. Chem. Phys., 25, 478 - 480 (1956).

86. _____, ibid, 25, 1171 - 1173 (1956).

87. R. E. Kagarise, ibid, 27, 519 - 522 (1957).

88. D. Hadzi and M. Pintar, Spectrochim. Acta, 12, 162 - 168 (1958).

89. A. V. Stuart and G. B. B. M. Sutherland, J. Chem. Phys., 20, 1977 (1952).

90. H. K. Kessler and G. B. B. M. Sutherland, ibid, 21, 570 (1953).

91. N. Sheppard, S. Mizushima et al, Trans. Faraday Soc., 53, 589 - 600 (1957).

92. E. Gross and M. Vuks, J. Phys. Radium, 7, 113 (1936).

93. P. C. Cross, J. Burnham and P. A. Leighton, J. Am. Chem. Soc., 59, 1134 - 1147 (1937).

94. See paper by E. Gross in Hydrogen Bonding, D. Hadzi (Editor), Pergamon Press, London, (1959), pp. 203 - 210.

95. J. A. Pople and J. Lennard-Jones, Proc. Roy. Soc. (London), A 205, 155, 163 (1951).

96. W. G. Schneider, J. Chem. Phys., 23, 26 - 30 (1955).

97. S. Nagakura and M. Gouterman, J. Chem. Phys., 26, 881 - 886 (1957).

98. Paper by A. Burawoy in Hydrogen Bonding, D. Hadzi (Editor), Pergamon Press, London (1959), pp. 259 - 275.

99. See paper by E. Lippert in Hydrogen Bonding, D. Hadzi (Editor), Pergamon Press, London (1959), pp. 217 - 257.

100. G. E. Pake, J. Chem. Phys., 16, 327 - 337 (1948).

101. See E. R. Andrew, Nuclear Magnetic Resonance, Cambridge University Press (1956), Chap. 6, pp. 152 - 165.

102. A. D. Cohen and C. Reid, J. Chem. Phys., 25, 790 (1956).

103. C. M. Huggins, G. C. Pimentel and J. N. Shoolery, J. Phys. Chem., 60, 1311 - 1314 (1956).

104. E. Becker, U. Liddel and J. N. Shoolery, J. Mol. Spectroscopy, 2, 1 - 8 (1958).

105. Review paper by W. G. Schneider in Hydrogen Bonding, D. Hadzi (Editor), Pergamon Press, London (1959), pp. 55 - 69.

106. See paper by J. A. Pople in Hydrogen Bonding, D. Hadzi (Editor), Pergamon Press, London (1959), pp. 71 - 76.

107. M. Saunders and J. B. Hyne, J. Chem. Phys., 29, 1319 - 1323 (1958).

108. Paper by C. Reid and T. M. Conner in Hydrogen Bonding, D. Hadzi (Editor), Pergamon Press, London (1959), pp. 77 - 83.

109. Paper by C. A. Coulson in Hydrogen Bonding, D. Hadzi (Editor), Pergamon Press, London (1959), pp. 339 - 360.

110. H. Tsubomura, Bull. Chem. Soc. Japan, 27, 445 - 450 (1954).

111. J. D. Bernal and R. H. Fowler, J. Chem. Phys., 1, 515 - 548 (1933).

112. M. Magat, Ann de Phys., 6, 108 (1936).

113. E. J. W. Verwey, Rec. trav. chim., 60, 887 - 896 (1940).

114. _____, ibid, 62, 127 - 142 (1942).

115. F. O. Ellison and H. Shull, J. Chem. Phys., 23, 2348 - 2357 (1955).

116. J. Lennard-Jones and J. A. Pople, Proc. Roy. Soc. (London), A 202, 166, 323 (1950).

117. _____, ibid, A 205, 151, 163 (1951).

118. J. A. Pople, J. Chem. Phys., 21, 2234 - 2235 (1953).

119. A. B. F. Duncan and J. A. Pople, Trans. Faraday Soc., 49, 217 - 224 (1953).

120. L. Burnelle and C. A. Coulson, ibid, 53, 403 - 405 (1957).

121. W. Hamilton, J. Chem. Phys., 26, 345 - 351 (1957).

122. J. S. Rowlinson, Trans. Faraday Soc., 47, 120 - 129 (1957).

123. L. Pauling, J. Chem Phys., 46, 435 (1949).

124. C. A. Coulson and U. Danielsson, Arkiv. Fys., 8, 239 (1954).

125. K. S. Pitzer, J. Chem. Phys., 23, 1735 (1955).

126. K. S. Pitzer and E. Catalano, J. Am. Chem. Soc., 78, 4844 - 4846 (1956).

127. C. E. Nordman and W. N. Lipscomb, J. Chem. Phys., 19, 1422 (1951).

128. _____, ibid, 21, 2077 - 2078 (1953).

129. A. N. Baker, J. Chem. Phys., 22, 1625 - 1626 (1954).

130. J. N. Finch and E. R. Lippincott, J. Phys. Chem., 61, 894 - 902 (1957).

131. Paper by E. R. Lippincott, J. N. Finch and R. Schroeder in Hydrogen Bonding, D. Hadzi (Editor), Pergamon Press, London (1959), pp. 361 - 374.

132. E. R. Lippincott, J. Chem. Phys., 26, 1678 - 1685 (1957).

133. E. R. Lippincott and R. Schroeder, J. Am. Chem. Soc., 78, 5171 - 5178 (1956).

134. L. Hofaker, Z. Electrochem., 61, 1048 - 1053 (1957).

135. Paper by L. Hofaker in Hydrogen Bonding, D. Hadzi (Editor), Pergamon Press, London (1955), pp. 375 - 383).

136. L. Paoloni, J. Chem. Phys., 30, 1045 - 1058 (1959).

137. W. J. Takei, Ph.D. Thesis, California Institute of Technology, 1957, pp. 2 - 31.

138. J. M. Bozorth, J. Am. Chem. Soc., 45, 2128 - 2132 (1923).

139. L. Helmholz and M. T. Rogers, ibid, 61, 2590 - 2592 (1939).

140. S. W. Peterson and H. A. Levy, J. Chem. Phys., 20, 704 - 707, (1952).

141. J. S. Waugh, F. B. Humphrey and D. M. Yost, J. Phys. Chem., 57, 486 - 490 (1957).

142. J. A. A. Ketelaar, Rec. Trav. Chim., 60, 523 - 555 (1941).

143. _____, J. Chem Phys., 9, 775 - 776 (1941).

144. _____ and W. Vedder, ibid, 19, 654 - 655 (1951).

145. R. Newman and R. M. Badger, ibid, 19, 1207 - 1208 (1951).

146. G. L. Coté and H. W. Thompson, Proc. Roy. Soc. (London), A 210, 206 - 216 (1951 - 1952).

147. L. Couture and J. P. Mathieu, Compt. rend., 228, 555 - 557, (1949).

148. J. P. Mathieu and L. Couture-Mathieu, Compt. rend., 230, 1054 - 1056 (1950).

149. G. Glockler and G. E. Evans, J. Chem Phys., 10, 607 - 609, (1942).

150. M. Davies, ibid, 15, 739 - 741 (1947).

151. L. Pauling, The Nature of the Chemical Bond, 2nd Ed., Cornell University Press, Ithica, New York (1948), pp. 297 - 298.

152. H. Hamano, Bull. Chem. Soc., Japan, 30, 741 - 745 (1957).

153. M. Karplus, quoted in paper by C. A. Coulson, Ref.(4), p. 150.

154. A. M. Buswell, R. L. Maycock and W. H. Rodebush, J. Chem. Phys., 8, 362 - 365 (1940).

155. F. Halverson, Rev. Mod. Phys., 19, 111 - 113 (1947).

156. D. Polder, Nature 160, 870 (1947).

157. K. S. Pitzer and E. F. Westrum, J. Chem. Phys., 15, 526 (1947).

158. E. F. Westrum and K. S. Pitzer, J. Am. Chem. Soc., 71, 1940 - 1949 (1949).

159. J. A. A. Ketelaar, C. Haas and J. van der Elsken, J. Chem.Phys., 24, 624 - 625 (1956).

160. J. A. A. Ketelaar and J. van der Elsken, J. Chem. Phys., 30, 336 - 337 (1959).

161. V. C. Farmer, Spectrochem. Acta, 8, 374 - 389 (1957).

162. A. W. Baker, J. Phys. Chem., 61, 450 - 458 (1957).

163. V. Z. Williams, Rev. Sci. Instr., 19, 135 - 178 (1948).

164. F. F. Martens, Ann. Phys., 6, 603 - 640 (1901).

165. D. A. Ramsey, J. Am.Chem. Soc., 74, 72 - 80 (1952).

166. E. B. Wilson, Jr., and A. J. Wells, J. Chem. Phys., 14, 578 - 580 (1946).

167. J. Bonhomme and G. Duyckaerts, Compt. rend. 27 congr. intern. chim. ind., Brussels, (1954); Industrie Chim. Belge, 20, Spec. No., 145 - 150 (1955).

168. L. Pauling, The Nature of the Chemical Bond, 2nd Ed., Cornell University Press, Ithica, New York(1948), Chap. X, pp. 339 - 363.

169. M. Born and K. Huang, Dynamical Theory of Crystal Lattices, (1st Ed., corr.), Oxford, Clarendon Press (1956), p. 123.

170. C. Hass and D. F. Hornig, J. Chem. Phys., 26, 707 (1957).

171. Comment by Prof. R. M. Badger on some published work of A. D. E. Pullin.

172. G. Duyckaerts, Spectrochim. Acta, 7, 25 - 31 (1955).

173. J. Bonhomme, ibid, 7, 32 - 44 (1955).

174. J. W. Otvos, H. Stone and W. R. Harp, Jr., ibid, 9, 148 - 156 (1957).

175. W. D. Hobey and R. M. Badger, Reports for the Year 1958 - 1959 on Research Activities of the Division of Chemistry and Chemical Engineering at the California Institute of Technology, Pasadena, p. 39, P 50.

176. J. Lecomte and R. Freyman, Bull. Soc. Chim. France, 8, 601 - 602 (1941).

177 M. Davies and H. E. Hallam, Trans. Faraday Soc., 47, 1170 - 1176 (1951).

178. E. Spinner, Spectrochim. Acta, 1959, 95 - 109.

179. H. M. Randall, R. G. Fowler, N. Fuson and J. R. Dangl, Infrared Determination of Organic Structures, D. van Nostrand Co., Inc., New York, 1949, pp. 12, 39 - 40, 125.

180. A. W. Reitz and J. Wagner, Z. physik, chem., B 43, 339 - 354 (1939).

181. F. Senti and D. Harker, J. Am. Chem. Soc., 62, 2008 - 2019 (1940).

182. P. Groth, Chemische Krystallographie, Band III, J. Springer, Stuttgart (1910), p. 108.

183. M. W. Porter and R. C. Spiller, Barker Index of Crystals, Vol. I, Part 2, H. 346 and O. 691.

184. M. Kimura and M. Aoki, Bull. Chem. Soc. Japan, 26, 429 - 433 (1953).

185. L. Pauling and R. Corey, Proc. Roy, Soc., (London), B 141, 10 - 20 (1953).

186. L. Kahovic and K. Knollmuller, Z. physik. Chem., B 51, 49 (1943).

187. E. H. Swift, G. M. Arcand, R. Lutwack and D. J. Meier, Anal. Chem., 22, 306 - 308 (1950).

188. A. W. Titherley, J. Chem. Soc., 1900, 411 - 413.

189. E. Gundlach, Z. physik, 66, 775 - 783 (1930).

190. A. R. Downie, M. C. Magoon, T. Purcell and B. Crawford, Jr., J. Opt. Soc. Am., 43, 941 - 951 (1953).

191. E. K. Plyler, L. R. Blaine and M. Nowak, J. Res. Nat. Bureau Stnd., 58, 195 - 200 (1957).

192. R. E. Richards and H. W. Thompson, J. Chem. Soc., 1947, 1248.

193. R. M. Badger, Office of Naval Research Contract N 6ori-102, Task Order VI, Project NR-055-o19, Technical Report No. 8, October 31, 1954, pp. 3 - 19.

194. W. West (Editor), Chemical Applications of Spectroscopy, Vol. IX, Techniques of Organic Chemistry, Interscience Publishers, Inc., New York, 1956, p. 501.

195. ibid, pp. 519 - 520.

196. L. Kahovec and H. Wassmuth, Z. physik. Chem., B 48, 70 (1940)

197. L. J. Bellamy, The Infrared Spectra of Complex Molecules, 2nd. ed., Methuen, London, 1958, p.256.

198. W. C. Price and K. S. Tetlow, J. Chem. Phys., 16, 1157 - 1162 (1948)

199. E. H. White, J. Am. Chem. Soc., 77, 6215 (1955)

200. L. Pauling, The Nature of the Chemical Bond, 3rd. ed., Cornell University Press, Ithica, New York, 1960, p.229.

201. G. Fraenkel and C. Niemann, Proc. Nat. Acad. Sci,, 44, 688 - 691 (1958).

202. Ref. 194, p. 531.

203. J. P. McHugh, Ph. D. thesis, California Institute of Technology, 1957.

204. L. E. Godycki, R. E. Rundle, R. C. Voter and C. V. Banks, J. Chem. Phys., 19, 1205 - 1206 (1951).

205. J. Goubeau, Z. physik. Chem., B 36, 45 - 84 (1937)

206. H. J. Berstein, J. Chem. Phys., 6, 718 - 721 (1938).

207. A. M. Buswell, W. H. Rodebush and M. F. Ray., J. Am. Chem. Soc., 60, 2444 - 2449 (1938).

208. A. Palm and H. Werbin, Can. J. Chem., 31, 1004 - 1008 (1953)

209. H. Boer and J. A. Goedkoop, Rec. trav. chim., 69, 1196 - 1206 (1950).

210. G. Duyckarets, Bull. Soc. Roy. Sci., Liege, 21, 196 - 206 (1952).

211. M. Milone and E. Borello, Gazz. chim. ital., 85, 500 - 509 (1955).

212. E. Borello and L. Henry, Compt. rend., 241, 1280 - 1281 (1955).

213. L. L. Merritt and E. Lanterman, Acta Cryst., 5, 811 - 817 (1952).

214. L. E. Godycki and R. E. Rundle, Acta Cryst., 6, 487 - 495 (1953).

215. L. J. Bellamy, The Infrared Spectra of Complex Molecules, 2nd. ed., Methuen, London, 1958, p. 269.

216. Ref. 194, p. 532.

217. Ref. 194, pp. 348 - 350.

218. P. Tarte, Bull. soc. chim. Belges, 60, 227 (1951).

219. P. Tarte, Bull Soc. Roy. Sci., Liege, 20, 16 - 19 (1951).

220. R. C. Voter, C. V.Banks, V. A. Fassel and P. W. Kehres, Anal. Chem., 23, 1730 - 1735 (1951).

221. Ref. 194, p. 365.

222. J. C. Speakman, J. Chem. Soc., 1949, 3357.

223. G. E. Bacon and N. A. Curry, Acta Cryst., 10, 524 - 528 (1957).

224. M. Davies and W. J. Orville Thomas, J. Chem. Soc., 1951, 2858.

225. D. Hadzi and A. Novak, Nuovo Cimento, 10, 3rd. Supplement, 715 - 726 (1955).

226. Handbook of Chemistry and Physics, 31st ed., Chemical Rubber Publishing Co., Cleveland, 1949.

227. N. Smith and J. C. Speakman, Trans. Faraday Soc., 44, 1031 - 1036 (1948).

228. M. St. C. Flett, J. Chem. Soc., 1951, 962 - 967.

229. O. D. Shreve, M. R. Heather, H. B. Knight and D. Swern, Anal. Chem., 22, 1498 - 1503 (1950).

230. S. Bartoz, D. Hadzi and N. Sheppard, Spectrochim. Acta, 8, 249 - 255 (1956).

231. J. F. Grove and H. A. Willis, J. Chem. Soc., 1951, 877.

232. D. Hadzi and N. Sheppard, Proc. Roy. Soc. (London), A 216, 247 (1953).

233. P. J. Corish and D. Chapman, J. Chem. Soc., 1957, 1746.

234. M. Davies and G. B. B. M. Sutherland, J. Chem. Phys., 6, 755 (1938).

235. See references quotated in L. J. Bellamy, The Infrared Spectra of Complex Molecules, 2nd. ed., Methuen, 1958, p. 174.

236. M. M. Stimpson, J. Chem. Phys., 22, 1942 (1954).

237. Ref. 215, pp. 188 - 191.

238. M. Shahat, Acta Cryst., 5, 763 - 768 (1952).

239. L. Pauling, The Nature of the Chemical Bond, 3rd. ed., Cornell University Press, Ithica, New York, 1960, pp. 232 - 240.

240. A. J. C. Wilson (General Editor), Structure Reports for 1952, Vol. 16, Oosthoek, Utrecht, 1959, pp. 431 - 432.

241. J. Guy, Bull. Soc. chim. France, 1955, 2818.

242. Ref. 194, p. 375.

243. Ref. 194, p. 378.

244. N. Sheppard and G. B. B. M. Sutherland, Proc. Roy. Soc. (London), A 196, 195 (1949).

245. Ref. 215, p. 48.

246. Ref. 194, pp. 382 - 383.

247. Ref. 194, pp. 373 - 375.

248. Ref. 215, pp. 39 - 42.

249. N. K. Freeman, J. Am. Chem. Soc., 75, 1859 - 1861 (1953).

250. Ref. 194, pp. 368 - 373.

251. Ref. 215, pp. 25 - 27.

252. G. Herzberg, Molecular Spectra and Molecular Structure, II. Infrared and Raman Spectra of Polyatomic Molecules, D. Van Nostrand Company, Inc., New York, 1945, p. 106.

253. E. B. Wilson, Jr., J. C. Decius and P. C. Cross, Molecular Vibrations, McGraw-Hill, New York, 1955, p. 326.

254. ibid, pp. 117 - 125.

255. E. B. Wilson, Jr., J. Chem.,Phys., 7, 1047 (1939)

256. E. B. Wilson, Jr., ibid, 9, 76 (1941)

257. Ref. 253, pp. 127 - 145.

258. J. C. Decius, J. Chem. Phys., 16, 1025 (1948)

259. J. C. Decius, ibid, 20, 511 (1952)

260. Ref. 253, p. 175, p. 178.

261. T. Miyazawa and K. S. Pitzer, J. Am. Chem. Soc., 81, 74-79 (1959).

262. R. Blinc and D. Hadzi, Molecular Physics, 1, 391 (1958)

263. D. M. Dennison and G. E. Uhlenbeck, Phys. Rev., 41, 313 (1931)

264. P. M. Morse and P. Stueckelberg, Helv. Phys. Acta, 4, 337 (1931).

265. N. Rosen and P. M. Morse, Phys. Rev., 42, 210 (1932).

266. M. F. Manning. J. Chem. Phys., 3, 136(1935).

267. F. T. Wall and G. Glockler, ibid, 5, 314 (1937).

268. R. Blinc and D. Hadzi, Hydrogen Bonding, D. Hadzi (Editor), Pergamon Press, London (1959), pp. 141 - 153.

269. C. C. Costain and J. M. Dowling, J. Chem. Phys., 32, 158-165 (1960).

PROPOSITIONS

Proposition 1.

In an effort to elucidate the structure and mechanism of bioluminescence a number of workers have investigated the simpler chemiluminescent systems. In particular, the chemiluminescent oxidation of 2,3-dihydrophthalazine-1,4-diones, (I), designated DPD, have been extensively investigated.

(I) 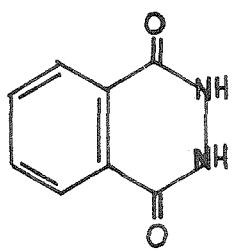

The nature of the DPD molecule has been studied by Drew and coworkers (1-4) and the conditions for oxidation have been examined and reviewed by a number of authors (5-8). However, the mechanism and the species responsible for the luminescence are still not known, though several have been proposed.

Drew and Garwood (9) isolated a peroxide addition compound of DPD, (II), which on further oxidation gave the typical chemiluminescence,

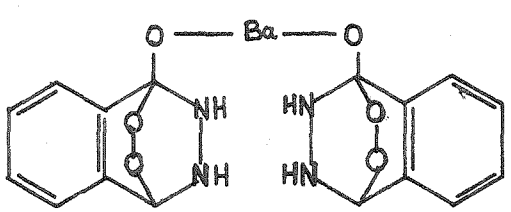 (II)

with some original DPD remaining, and some phthalic acid produced. Wilhelmsen et al. (8) used Drew and Garwood's intermediate, but assumed an activated hemiphthalate radical was responsible for the luminescence. Johnson et al. (7) had earlier proposed a mechanism with the distribution of the peroxide and the DPD, the peroxide acting to induce a quinone type electronic structure in the phenyl ring.

The mechanisms may be summarized as:

Drew and Garwood:

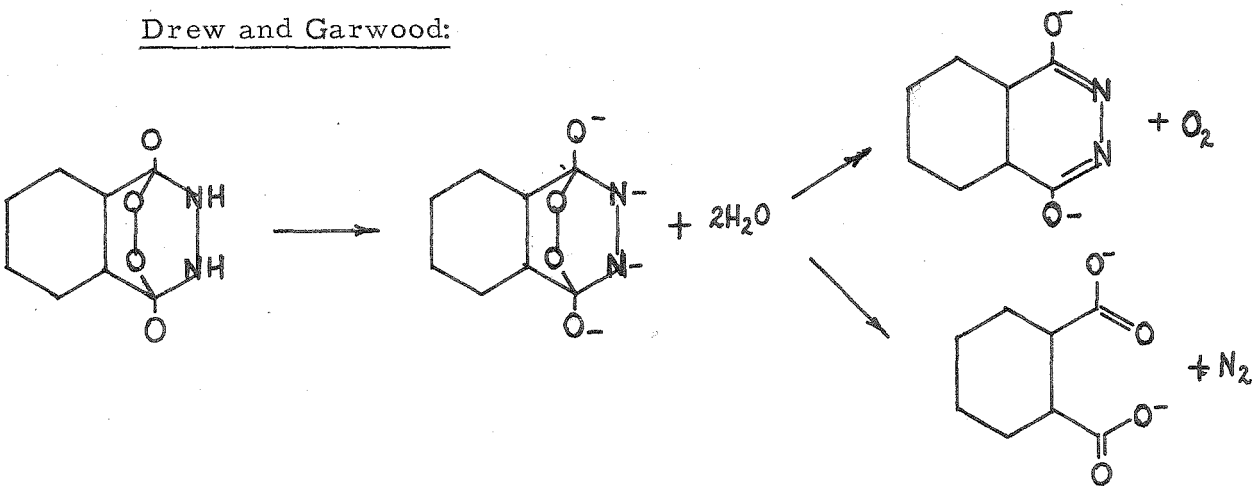

Wilhelmsen et al.:

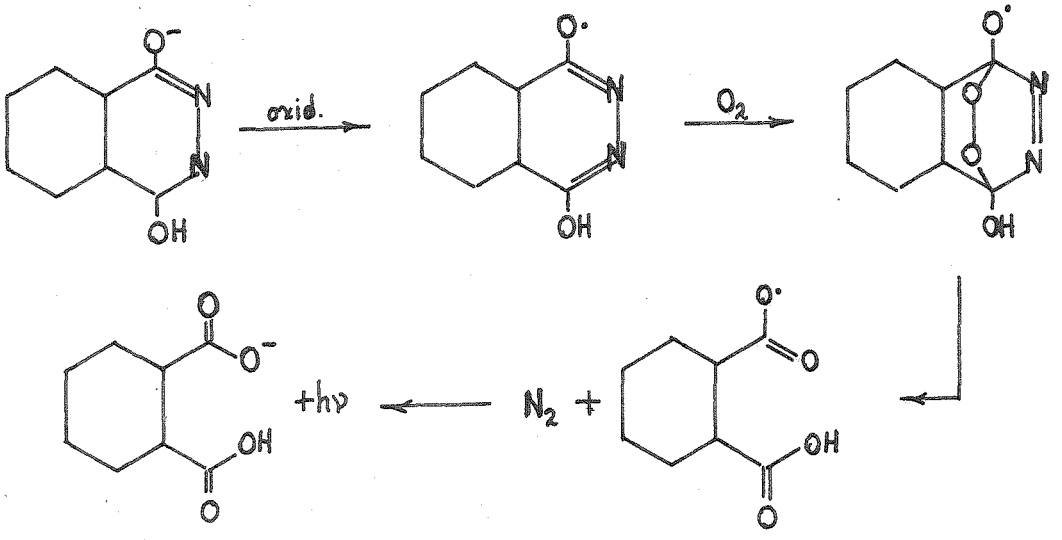

Johnson et al. (only species of interest are shown):

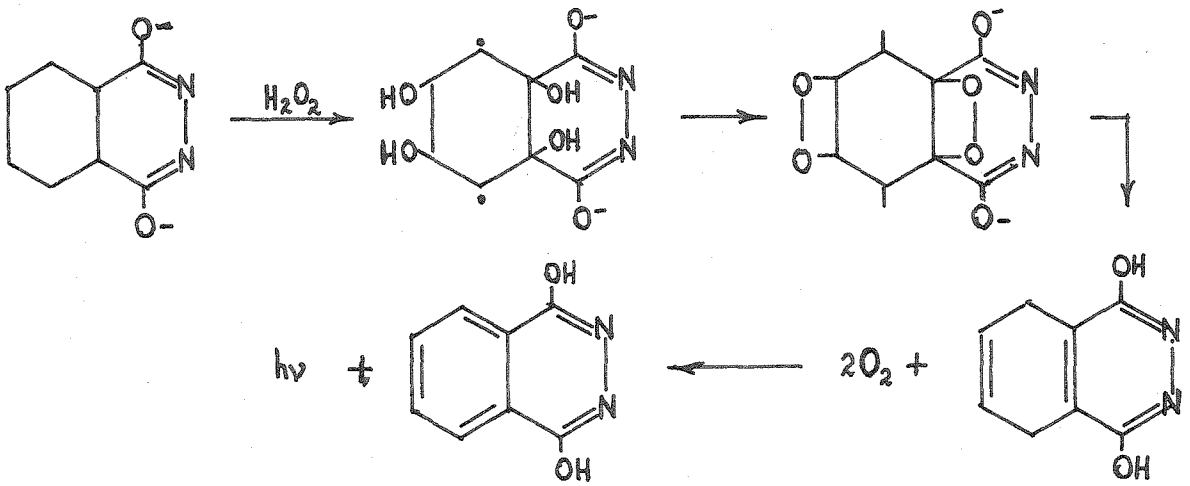

Several methods are proposed which will reduce the number of mechanisms and possibly solve the question of species responsible for luminescence.

Johnson's mechanism can be eliminated by blocking the reactive sites. Two compounds readily prepared are shown below:

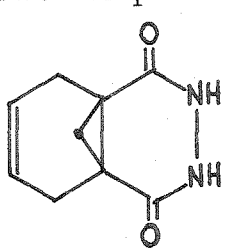

and

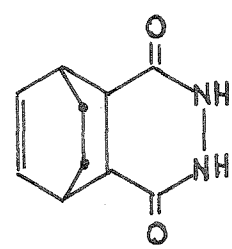

No luminescence would occur if Johnson's mechanism were correct. To differentiate between Wilhelmsen's (8) and Drew's (9) it is suggested that the N^{15} DPD compound be prepared, and O^{18} enriched H_2O_2 be used as the oxidizing agent. According to Wilhelmsen's mechanism, each mole of DPD will give 1 mole of N_2 gas, and the O^{18} should end up in the phthalic acid. Starting with the peroxide complex of Drew and

Garwood (9), which has been prepared with O^{18} enriched H_2O_2, subsequent oxidation with $H_2O_2{}^{18}$, give H_2O^{18}, and, depending on predominant radiative step, will give $O_2{}^{18}$ and $N_2{}^{15}$ in varying amounts, besides having the unoxidized DPD and the phthalic acid with O^{18}. Analysis for the ratio of O^{18}/N^{15} should tell, since it is assumed that the intensity of luminescence is proportional to the number of decaying species.

References

1. H. D. K. Drew and H. H. Hatt, J. Chem. Soc. 1937, 16.

2. H. D. K. Drew and F. H. Pearman, ibid., 1937, 26.

3. H. D. K. Drew and F. A. Hobart, ibid., 1937, 33.

4. H. D. K. Drew and F. H. Pearman, ibid., 1937, 586.

5. A. Bernanose, T. Bremer and P. Goldfigner, Bull. soc. chim. Belges, 56, 269 (1947).

6. T. Bremer, ibid., 62, 569-610 (1953).

7. F. H. Johnson, H. Eyring and M. J. Polissar, Kinetic Basis of Molecular Biology, John Wiley and Sons, New York, 1954; pp. 164-168.

8. P. C. Wilhelmsen, R. Lumry and H. Eyring, Luminescence of Biological Systems (F. Johnson, Editor), Am. Assoc. Advance. Sci., Washington, D. C., 1955, pp. 75-98.

9. H. D. K. Drew and R. F. Garwood, J. Chem. Soc., 1938, 791.

Proposition 2.

In the last decade there has been a revived interest in the structure of the unstable oxides of nitrogen as well as the stable oxides. In 1956, Smith and Hedberg (1) determined the N-N distance in N_2O_4 to be 1.75 A, a rather long bond distance for a chemical bond. The more unstable oxide, N_2O_3, has not been worked on as thoroughly until the past few years.

Two structures have been proposed for the N_2O_3 molecule; a Y-type structure with an N-N bond and a W-type structure with N-O bonds. Of these two structures, the Y-structure has received the most support by infrared spectroscopic studies (2,3), though Crawford et al. (3) did report evidence for the unstable W-form. Recently, Mason (4) investigated the ultraviolet spectrum of the liquid N_2O_3 and Hisatsune and Devlin (5) the Raman spectrum of N_2O_3 dissolved in $C_2H_2Cl_2$ at -30°C. The latter authors have attempted to deduce a suitable structure by comparing the calculated entropy with the entropy values estimated from equilibria data for a structure with an N-N distance of 2.08 A and the angle between the N-N bond and the N-O group of about 100°. The N-N distance seems unusually long, and the angle too small, particularly since these authors claim the rotation is free about the N-N bond.

For several years I have been interested in the structure of this molecule, particularly with reference to the N-N bond length. It is suggested that the gas phase infrared be re-examined, this time by the double-beam method and at a sufficiently low temperature to reduce the

degree of dissociation of N_2O_3 into NO and NO_2 (or N_2O_4). Also, if it should ever become available, an attempt at the gas phase electron diffraction will be strongly recommended. This last technique is, however, not without a number of technical difficulties, the most important being the superposition of the diffraction patterns of NO and $NO_2(N_2O_4)$ and that of N_2O_3. The dissociation could be reduced by using an excess of NO, as it will give a simple diffraction pattern but creates an overall fogging. However, it is felt that this will yield more reliable data than is presently available from spectroscopic observations alone.

References

1. D. W. Smith and K. Hedberg, J. Chem. Phys., 25, 1282 (1956).

2. L. D'Or and P. Tarte, Bull. Soc. Roy. Sci. Liege, 22, 276-284 (1953).

3. W. B. Fateley, H. A. Bent and B. C. Crawford, J. Chem. Phys., 31, 204-217 (1959).

4. J. Mason, J. Chem. Soc., 1959, 1288.

5. I. C. Hisatsune and Devlin, Spectrochim. Acta, 16, 40 (1960).

Proposition 3.

It has been proposed in Section F (Part II) of this thesis that the unusual spectral behavior of short hydrogen bonded compounds may be associated with the high degree of symmetry of the hydrogen bond and the complexity of the molecular system joined by the hydrogen bond. Thus, it is a method whereby one can distinguish between short symmetric and short unsymmetric hydrogen bonds.

The number of compounds investigated, which fulfill the requirements, were limited, so that a firm conclusion was not arrived at. It is, therefore, proposed that this investigation be expanded to include several more hydrogen bond systems to see if the effect is still present. For the compounds to be selected, the acid salts of carboxylic acid seem the most profitable. As an example, the hydrogen maleate ion has been shown to have an extremely short O---O distance of about 2.44 A(1, 2), with the hydrogen situated at the center of the O---O bridge (2). Partial spectral studies (1) have indicated the effects described in this thesis are also present.

It is also proposed that the investigations be carried out at low temperatures, in order to verify the broadening mechanism and the "window" effect associated with the hydrogen bonds. At low temperatures, the broad background should be noticeably reduced, though a residual band width will still be present. Similarly, the "windows" should be reduced in depth as the fraction of the molecules in the perturbing energy level will be correspondingly reduced.

References

1. H. M. E. Cardwell, J. D. Dunitz and L. E. Orgel, J. Chem. Soc., 1953, 3740.

2. S. W. Peterson and H. A. Levy, J. Chem. Phys., 29, 948 (1958).

Proposition 4.

In recent years, an interest in clathrate compounds has been revived (1, 2). A clathrate may be described as a single-phase solid consisting of two distinct components, the host and the guest; the guest is retained in closed cavities or cages provided by the crystalline structure of the host, so the cage and enclosed molecules are taken as a unit. The structure of clathrates has been extensively investigated by Powell and Palin (3-6) in England. For the SO_2 clathrate of hydroquinone these authors reported the SO_2 molecule to be in a cavity of about 4 A in diameter. A molecule thus enclosed will have lost its translational energy, some rotational energy and maybe some vibrational energy; but a clathrate of a molecular gas affords a convenient opportunity for studying the free molecular properties of the gas in the absence of superimposed effects of intermolecular interactions. However, weak interactions between the guest and the surrounding cage may exist, similar to those found in physical adsorption, since the host component is usually

characterized by one or more permanent molecular dipoles and a distorted structure.

Several years ago Hexter and Goldfarb (5) reported an infrared investigation of clathrates of HCl, CO_2, H_2S, and SO_2 in the β-hydroquinone structure in KBr pressed discs. Their results were inconclusive, even with regard to the presence of the guest molecule in the substances examined, although the CO_2 clathrate did show a weak band contour near 667 cm^{-1}, which was interpreted in terms of a restricted rotator (8). The poor quality of their results is not surprising as the clathrates are not stable at elevated temperatures or pressures (3), both of which occur during the pelleting process. Also, the molecules used by these authors are fairly heavy so the rotational spacing is small.

In the near future I am planning to re-investigate the infrared spectra of clathrates in order to determine if (a) there is any strong interaction between the guest and the host, and (b) the rotation of the guest molecules is restricted. In order to accomplish this, several new approaches will be used. First of all, lighter guest molecules will be introduced into the host, such as HCN and C_2H_2, as the rotational spacing will be larger and more readily determined. Second of all, single crystals of the clathrates will be used; this will in effect avoid the loss of the guest molecule by decomposition.

References

1. F. D. Cramer, Rev. Pure and Applied Chem., 5, 413 (1955).

2. L. Mendelcorn, Chem. Rev., 59, 827 (1959).

3. D. E. Palin and H. M. Powell, J. Chem. Soc., 1947, 208-210.

4. D. E. Palin and H. M. Powell, ibid., 1948, 571.

5. D. E. Palin and H. M. Powell, ibid., 1948, 815.

6. H. M. Powell, ibid., 1948, 61.

7. R. M. Hexter and T. D. Goldfarb, J. Inorg. and Nuclear Chem., 4, 171-178 (1957).

8. H. H. Nielsen, J. Chem. Phys., 3, 189 (1935).

Proposition 5.

Solutions of thiocyanic acid have been reported to decompose on standing to give a new substance having the empirical formula $C_2H_2N_2S_2$ (1, 2). Johnson and co-workers (3) prepared a compound of the same empirical formula by refluxing NH_4SCN with acetic anhydride.

Fleisher (4) and Hantzsch and Wolvenkamp (5) prepared a compound of the same composition as Johnson's from the alkaline degradation of isoperthiocyanic acid, $C_2H_2N_2S_3$. This material was shown (7) to be potassium cyanodithiocarbamate (I), and not the supposed potassium dithiocyanate (II) (6).

I

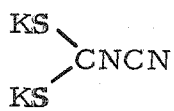

II

No work has been reported to confirm the structure of Johnson's compound, or that the thiocyanic acid polymerization product is the dimer of HNCS or the cyanodithiocarbamate. From the method of synthesis, it is suggested that Johnson's product is the acid dimer (III), with the thioketo-structure. Compound (III) is similar to the dimer of isocyanic acid, of which the phenyl isocyanate dimer has been shown to be in the keto configuration (7) (IV). If structure III is that of the

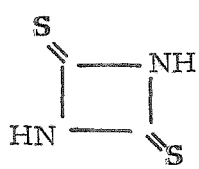

III

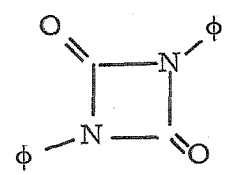

IV

isothiocyanic acid dimer, the mechanism of Johnson's reaction may be

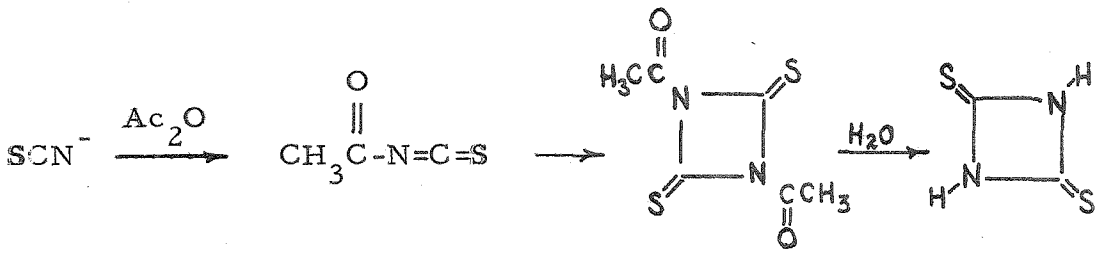

This could be checked out by dimerizing some $CH_3\overset{O}{\overset{\|}{C}}N=C=S$ with a pyridine catalyst, as is done to make the dimer of phenylisocyanate (7).

References

1. P. Klason, J. prakt. Chem., 38, 383 (1888).
2. H. N. Stokes and J. P. Cain, J. Am. Chem. Soc., 29, 443 (1907).
3. T. B. Johnson, A. J. Hill and B. H. Bailey, J. Am. Chem. Soc., 37, 2406 (1915).
4. A. Fleisher, Ann., 179, 204 (1875).
5. A. Hantzsch and M. Wolvenkamp, Ann., 331, 265 (1904).
6. P. Klason, J. prakt. Chem., 38, 366 (1888).
7. J. C. Brown, J. Chem. Soc., 1955, 2931.

Proposition 6.

The dipole derivative of the ν_3 fundamental of the bifluoride ion in a KBr matrix was found to be about one-half the value obtained from single-crystal reflectance measurements (1). Ferriso and Hornig (2) have recently published dipole derivatives for the infrared active fundamentals of the ammonium ion in several alkali halide matrices, which exhibited a wide variation for the matrix material and from the single-crystal value. Although the effects of scattering and reflection make it difficult to obtain reliable measurements of the integral absorption intensities, the reported deviations are greater than the experimental error.

The influence of the solvent upon the frequencies of the solute has been considered in terms of the polarization of the environment by the ion (3), though the short range repulsive forces are probably essential in determining the frequency shifts (4).

Since no systematic examination of these effects has been considered on the intensity of the infrared bands, it is proposed that the intensity and dipole derivative of infrared bands be examined in solid solutions. Simple diatomic ions, such as the cyanide ion, the hydroxide ion, hydrosulfide ion, are suggested as suitable solutes, with the alkali halides as the solvents, as several theoretical treatments have recently been advanced on the solvent effect of infrared bands (5, 6). Buckingham's paper (5) is more complete as it includes the effect of the solvent on the frequency, intensity and width of the infrared bands of diatomic molecules.

References

1. See Section A, Part II of this thesis, pp. 62 - 74.
2. C. C. Ferriso and D. F. Hornig, J. Chem. Phys., 32, 1240 (1960).
3. J. A. A. Ketelaar and J. van der Elsken, ibid, 30,336 (1959).
4. A. Maki and J. C. Decius, ibid ., 31, 772 (1959).
5. A. D. Buckingham, Trans. Faraday Soc., 56, 753 (1960).
6. A. D. E. Pullin, Spectrochim. Acta, 13, 125 (1958).

Proposition 7.

White has proposed an ionic dimer for the hemihydrohalide complexes of N-(t-butyl)-acetamide (1), which are similar to the structure of carboxylic acid dimers; that is, the acetamide residues are held together by O---H-N hydrogen bridges. The spectrum published by the author for chloroform solution of the compound is very similar to that of the hemihydrochloride of acetamide (see Section B, Part II of this thesis), so it is believed that White's structure is wrong. Presumably the dimer would be held together by a relatively short O--H--O hydrogen bond.

Because of the importance of these compounds in regard to the structure of the hydrogen bond and the "window" effect in acetamide hemihydrochloride (Section B, Part II), several points of White's work need clarification. First of all, the size of the molecular unit in solution has to be determined, that is whether the complex exists as a polymer or an ion. This can be readily determined

from the molecular weight of the substance in solution, which could best be determined from the vapor pressure lowering by the transpiration method of Washburn and Heuse (2). Second of all, it is suggested that the nature of the species in solution be determined from conductivity measurements. An ionic species would support a proton type hydrogen bond.

Further work is also suggested on the investigation of the hemihydrohalide complexes of other N-substituted amides in order to determine the group, or groups, responsible for the "windows."

References

1. E. H. White, J. Am. Chem. Soc., 77, 6215 (1955).

2. E. W. Washburn and E. W. Heuse, ibid., 37, 309 (1915).

Proposition 8.

A number of years ago a study was initiated (1) to determine the relative strength of Lewis acids using a series of Hammett weak base indicators (2,3) in an aprotic solvent. The first problem was the evaluation of the equilibrium between the Lewis acid and the weak base indicator by standard spectrophotometric methods. The absorption curves of the weak base indicator indicated acid-base interaction, though no new absorption peaks were found. Calculated equilibrium constants showed a pronounced increase with increasing acid concentration. This is illustrated by the following data for the Lewis and stannic chloride and the

weak base indicator p-nitroaniline in benzene solvent (assuming an acid to base ratio of 1:2):

Base Conc. (10^4M)	Acid Conc. (10^4M)	K(1:2)
9.06	8.57	0.13×10^{-8}
9.06	17.14	0.30
4.81	34.3	0.71
9.06	85.7	1.79
4.81	171.4	2.11

It is suggested that the increasing values are due to trace quantities of water in the solvent, benzene, since stannic chloride, on contact with moist air, will produce HCl. Thus, the mixed acid HCl + $SnCl_4$ is probably a stronger acid than either acid alone. This explanation can be justified by studying the acid-base reaction under rigorously anhydrous conditions, with HCl, $SnCl_4$, and various mixtures of HCl in benzene.

References

1. N. E. Albert, unpublished work, at the Polytechnic Institute of Brooklyn, 1954.

2. L. P. Hammett and A. J. Deyrup, J. Am. Chem. Soc., 54, 2721, 4239 (1932).

3. L. P. Hammett and M. A. Paul, ibid., 56, 827 (1934).

Proposition 9.

At times it is necessary to estimate the bending force constant for an asymmetric group, from analogous molecules, or to make extrapolations based on some property of the bond. A simple relationship has

been worked out which gives moderate success in estimating the bending force constant of an asymmetric group, i-j-k, in terms of the force constants of the symmetric groups i-j-i and k-j-k. The relationship is

$$f_{ijk} = (f_{iji} \cdot f_{kjk})^{1/2} - 0.1/(x_i + x_k)$$

where f_{iji} is the force constant for the group i-j-i, f_{kjk} is the force constant for the group k-j-k, and x_i and x_k are the electronegativities of atoms i and k. The usefulness of this relationship is illustrated for the HCX bending force constant, where the f's are in units of 10^5 md / A. The values of the force constants were taken from Table 8-2 of Wilson, Decius and Cross, Molecular Vibrations, p. 176.

	Atom			
Force Constant	F	Cl	Br	I
f(HCX) - cal.	0.56	0.37	0.31	-
f(HCX) - obs.	0.57	0.36	0.30	0.23